146

STUDIES ON SOME INTRACELLULAR PARASITES OF THE MARINE BIVALVE, TELLINA TENUIS (DA COSTA)

Volume Two

Studies on a coccidian parasite of the ovary and a mycoplasma-like organism with an associated virus in the digestive gland of the marine bivalve, *Tellina tenuis* (da Costa)

J.S.Buchanan B.Sc. (Wales) M.I.Biol.

Unit of Aquatic Pathobiology

University of Stirling

November 1976

Ph.D. awarded / conferred } March 1977

LIST OF PLATES

LIST OF PLATES

LIST OF PLATES

---oo0oo---

Abbreviations used in the accompanying plates

AC	Absorptive cell
AM	Amylopectin
AS	Amorphous material
B	Basal body
C	Conoid
CHR	Chromatin
CW	Cyst wall
DB	Dense body
DC	Dead cell
DPO	Ductules of paired organelles
DV	Vesicles with thick walls
DWF	Developing wall-forming bodies
GER	Granular endoplasmic reticulum
G	Gut
GO	Golgi apparatus
GR	Granular bodies
HC	Host cell
HL	Heterolytic vacuole
HP	Heterophagic vacuole
IL	Inner layer of oocyst wall
IM	Inner layer of the pellicle
L	Lipid
LC	Lacuna
LU	Lumen of the tubule
LM 1-3	Limiting membranes of parasites
LT	Leucocyte
LS	Longitudinal section
M	Membrane
MC	Mucous layer
MG	Microgamont

Abbreviations used in the accompanying plates

MI	Mitochondrion
MT	Microtubules
MV	Microvesicles
N	Nucleus
NS	Nucleolus
OL	Outer layer
OW	Outer wall
PG	Pale granules
PO	Paired organelles
RER	Rough Endoplasmic reticulum
SC	Sporocyst
SER	Smooth endoplasmic reticulum
SM	Sporocyst membrane
SZ	Sporozoite
V	Virus

Principle collecting areas

Plate 1.

West sands, St. Andrews, Fife.
samples were collected at the
line of surf nearest the rocks.

Plate 2

The bathing station, by West sands,
St. Andrews, where samples of Tellina
tenuis, Cardium edule and Donax
vittatus were collected.

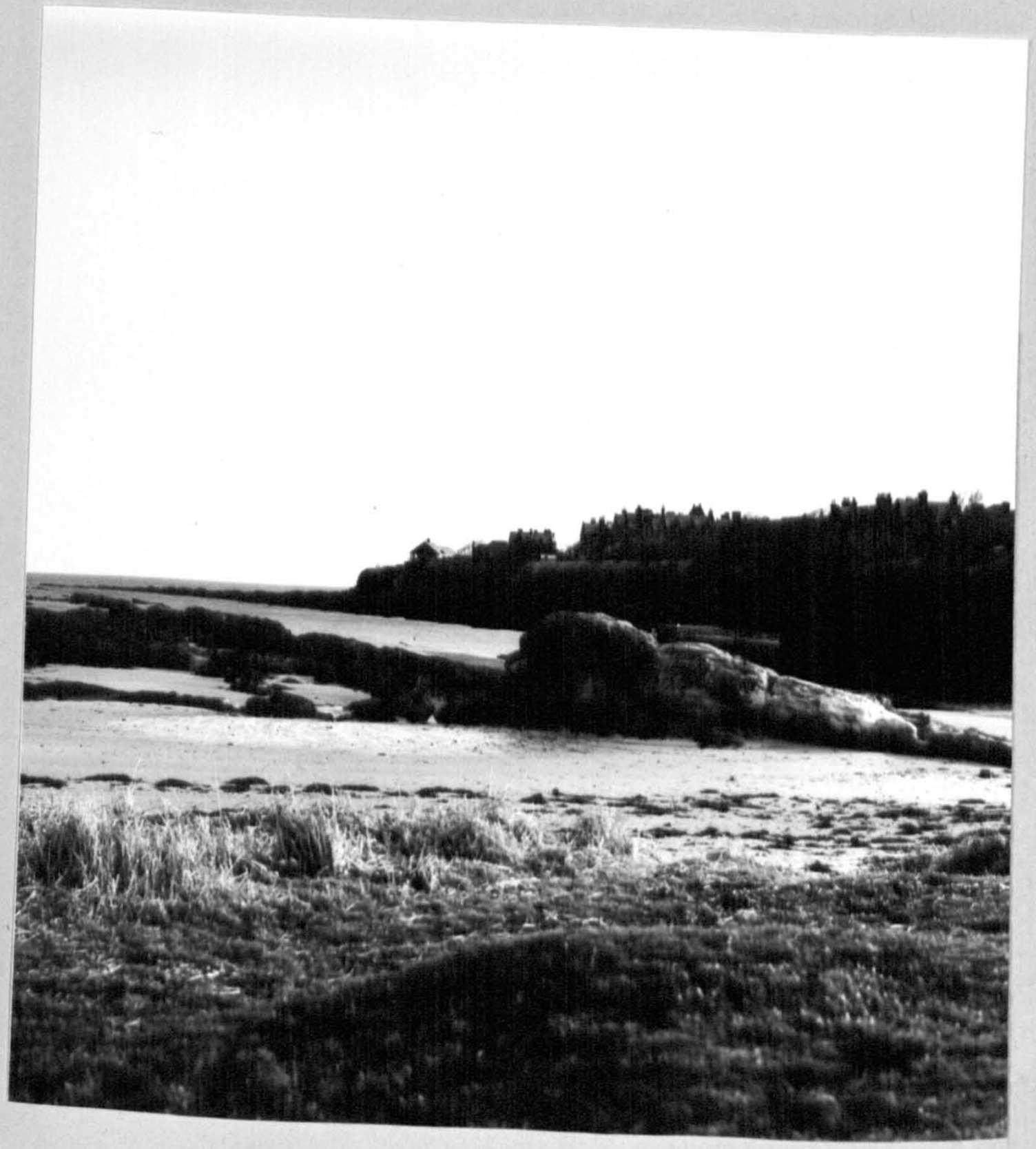

Principle collecting areas

Plate 3.

Aultbea, Loch Ewe at MLWN.

Tellina were collected at the centre of the bay at the water's edge.

Plate 4.

Kames Bay, Millport, Isle of Cumbrae. Butcher's rock, corresponding with MLWN tide level (station 3) is at the extreme left. The well marked strand line at centre corresponds with station 1 of this survey.

SECTION TWO

Macroscopic appearance of Tellina heavily parasitized by a coccidian

Plate 5

A light to medium infestation. Areas of oocyst accumulations within the gonad are arrowed.

Magnification x 10

Plate 6

Whole animal removed from the shell. The branching gonadal tubules are packed with coccidian oocysts to the exclusion of all ova of the host.

Magn. x 5

Plate 7

Detail from the above. Magnification x 40.

Macroscopic appearance of Tellina parasitized by a coccidium

Plate 8

Heavily parasitized female. The ovary is packed with masses of coccidian oocysts

Magn. x 20

Plate 9

Detail from the above. Note the gills (1) and labial palps (2) turned back to show the gonadal tubules packed with oocyst of 30 um average diameter

Magn. x 60

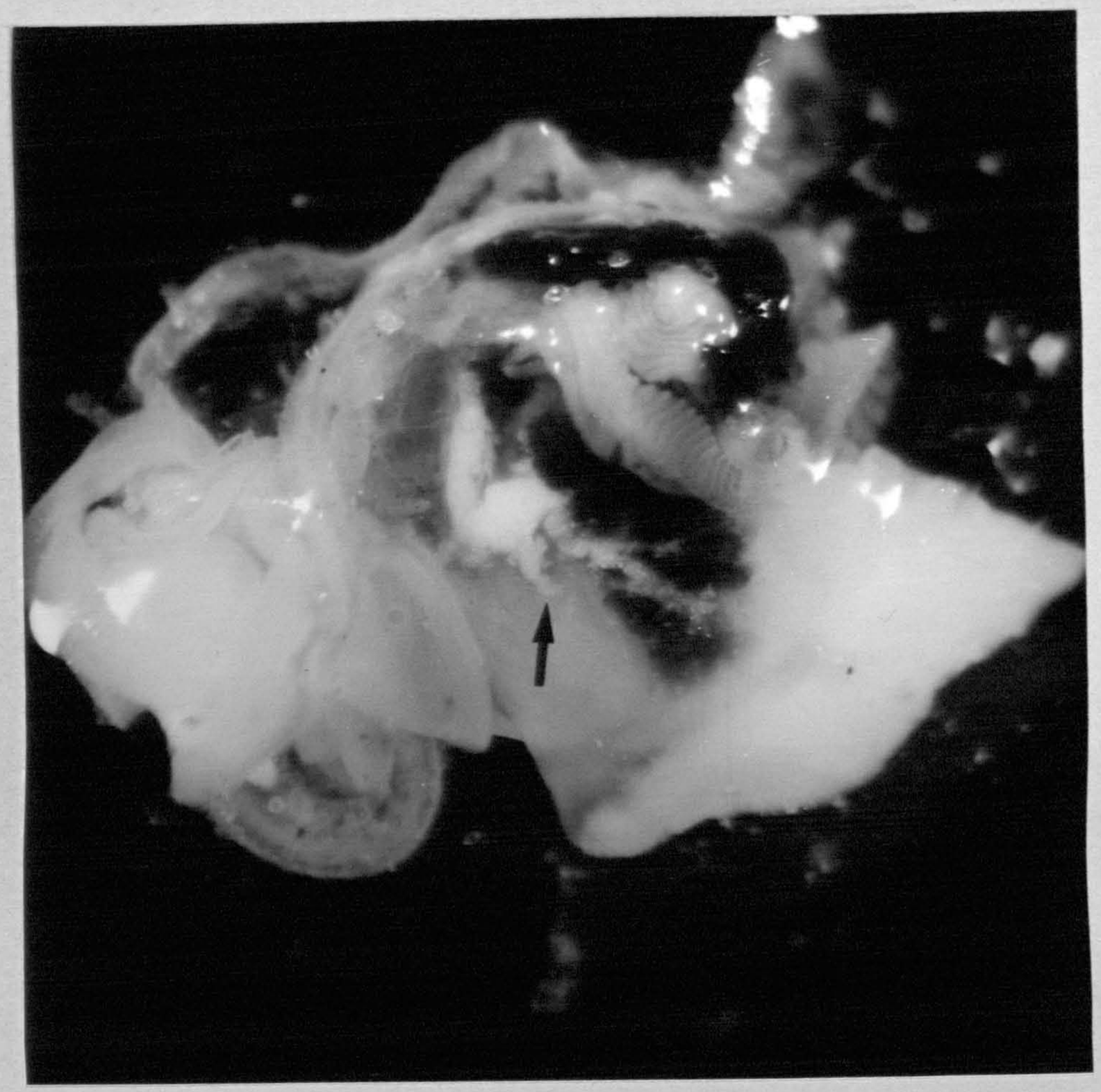

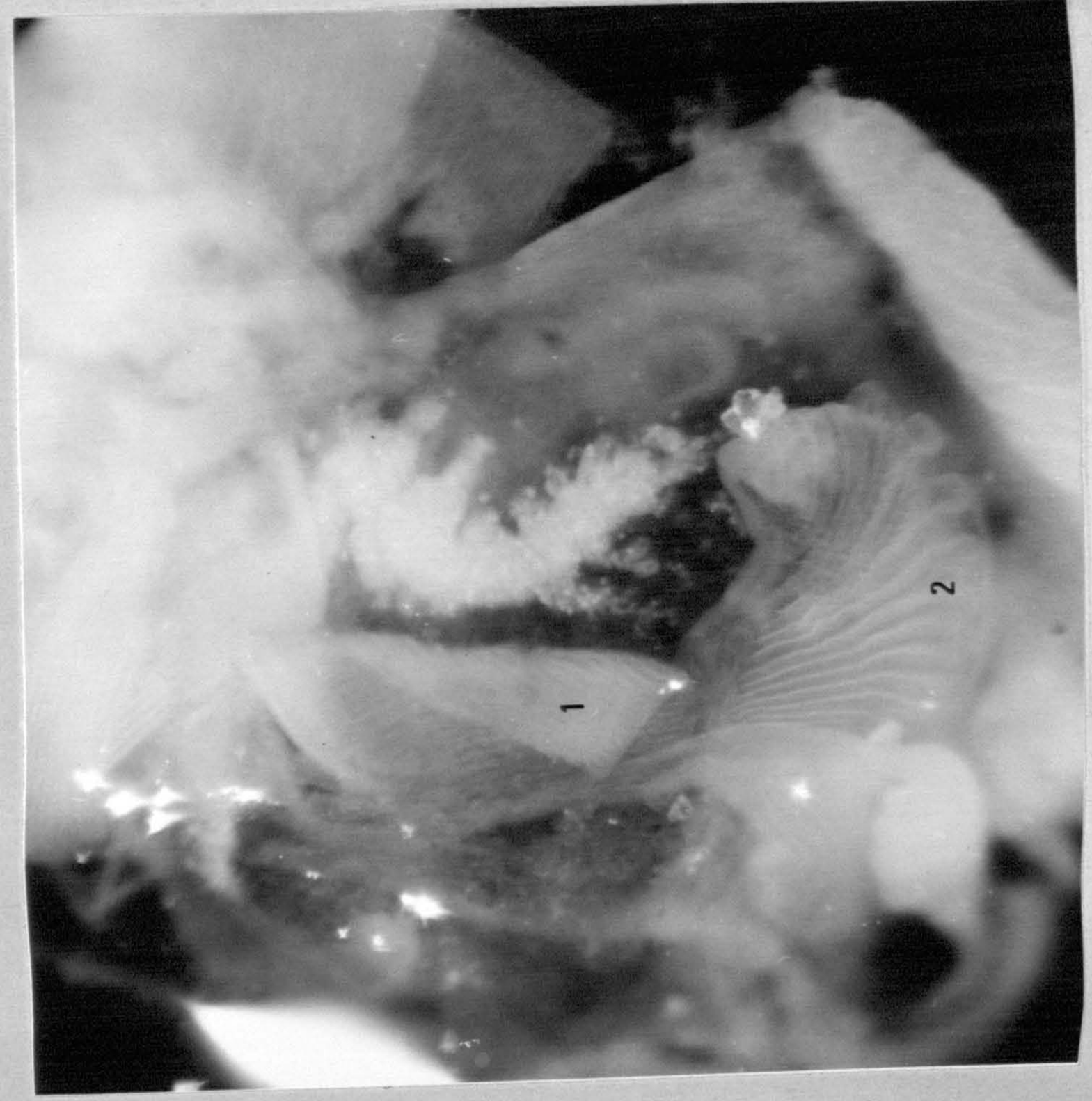
1
2

Plate 10.

Nomarski Interference contrast photomicrograph of developing oocyst stages of Merocystis tellinovum.

Magnification X 100

Plate 11.

Detail of the above X 250. Individual sporozoites and precleavage sporocysts have been released from the oocyst envelope in this squash preparation.

Plate 12.

Sporocyst formation within the oocyst well. Sporocysts can be seen forming by condensation of the sporoplasm at the perimeter. A mass of granular and agranular amoebocytes are clustered at the centre of this photomicrograph.

Magnification X 400.

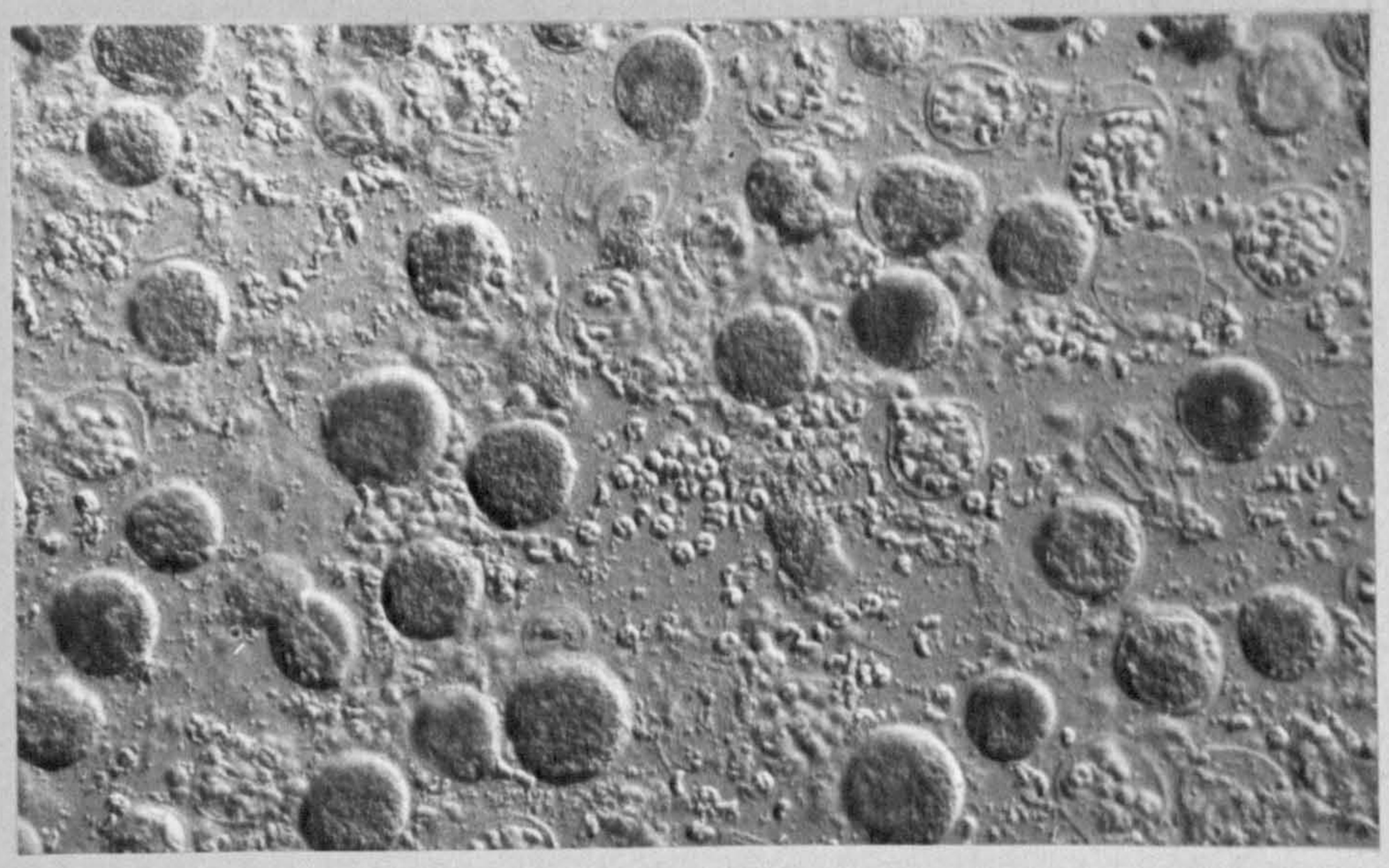

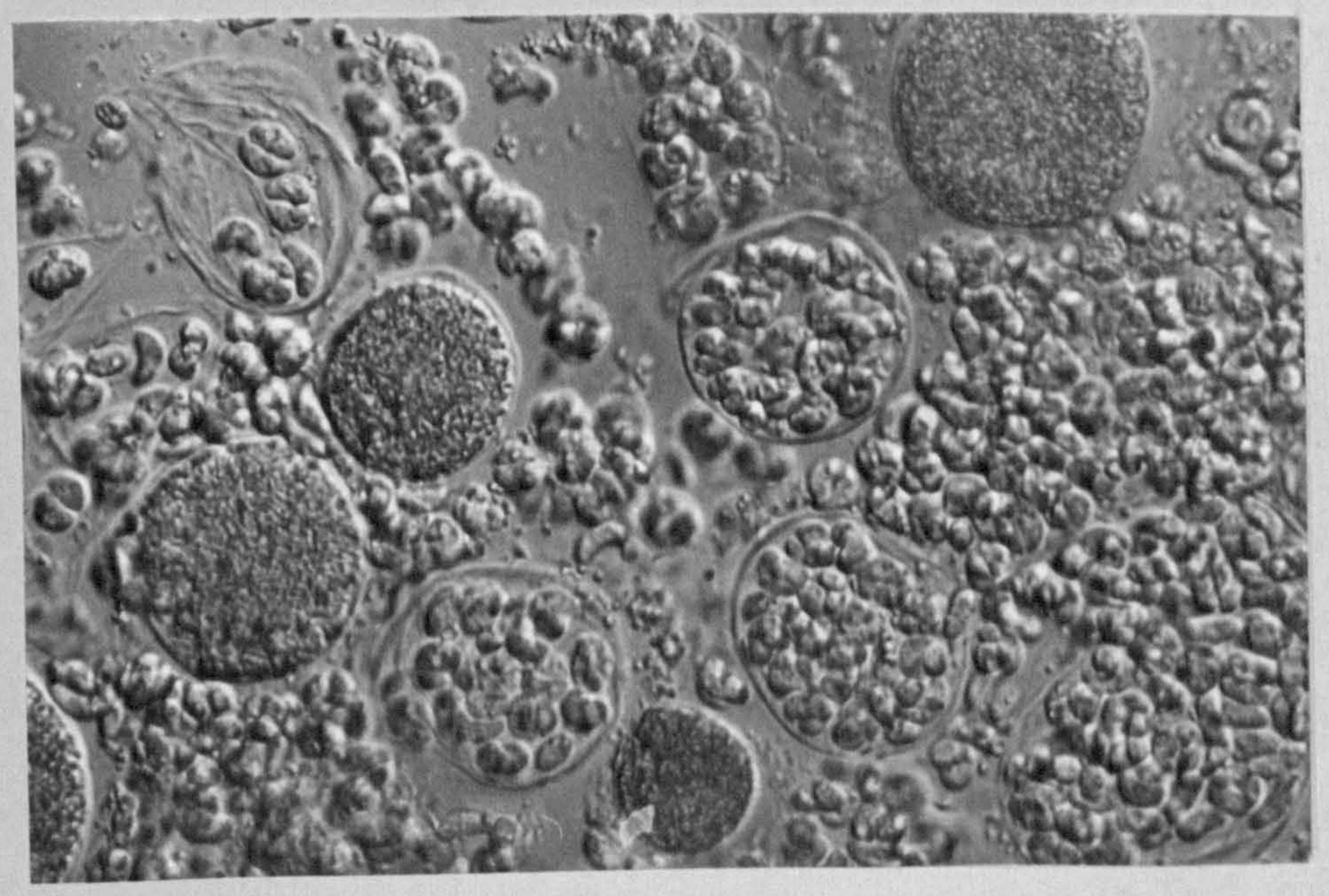

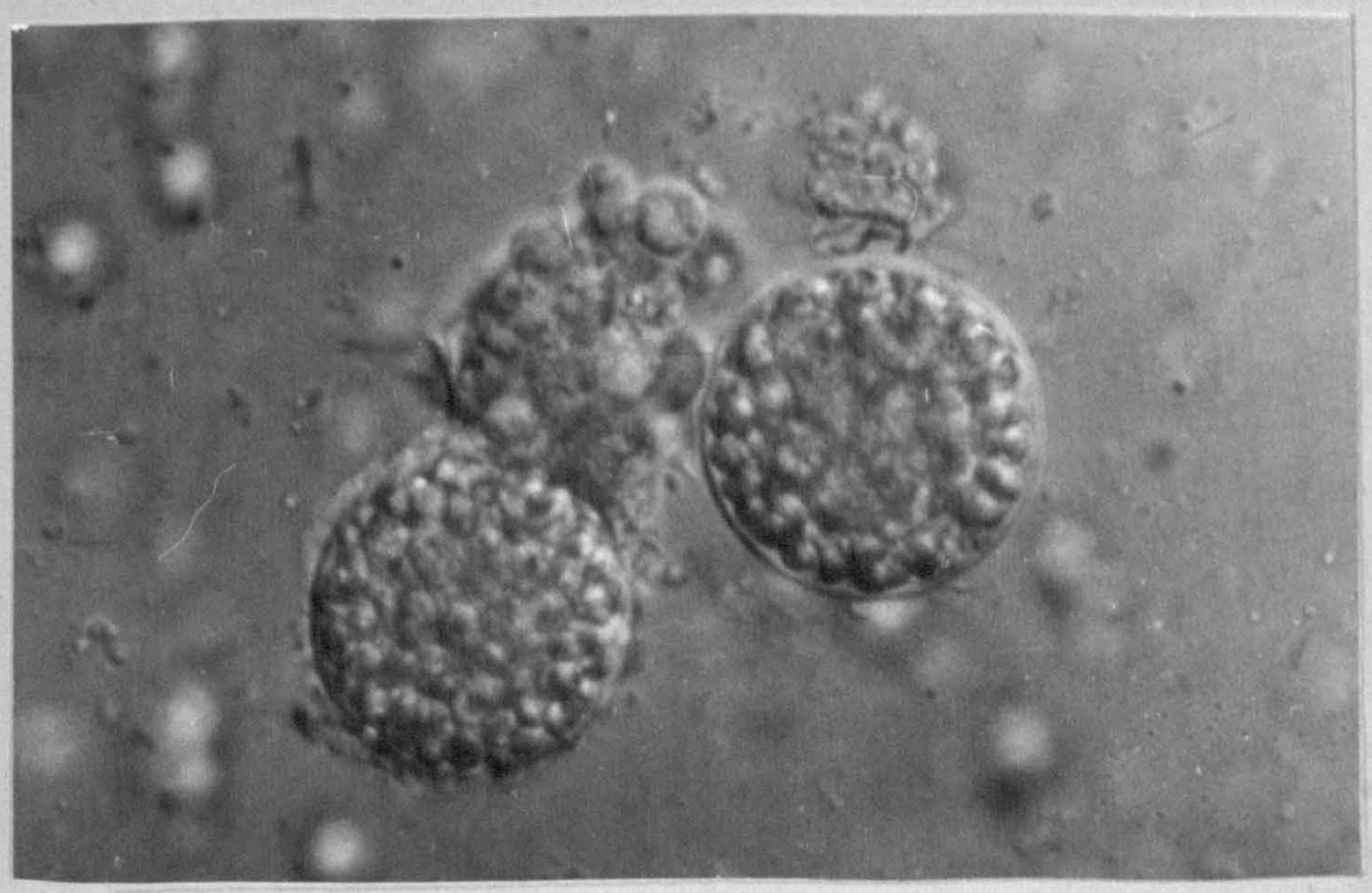

The developing coccidian oocyst

Plate 13.

Squash preparation of living oocysts of the coccidian Merocystis tellinovum. The normal position of the sporozoites is at right angles to each other.

Plate 14.

Early stage of oocyst development. A granular amoebocyte of Tellina can be seen attached to the oocyst wall. Sporocyst capsules have developed within the oocyst.

Plate 15

Sporocysts at various stages of cleavage to form daughter sporozoites. A large granular amoebocyte (arrowed) of 8 um diameter appears to contain ingested sporozoites.

All Nomarski interference phase contrast light micrographs X 1,000 oil immersion objective.

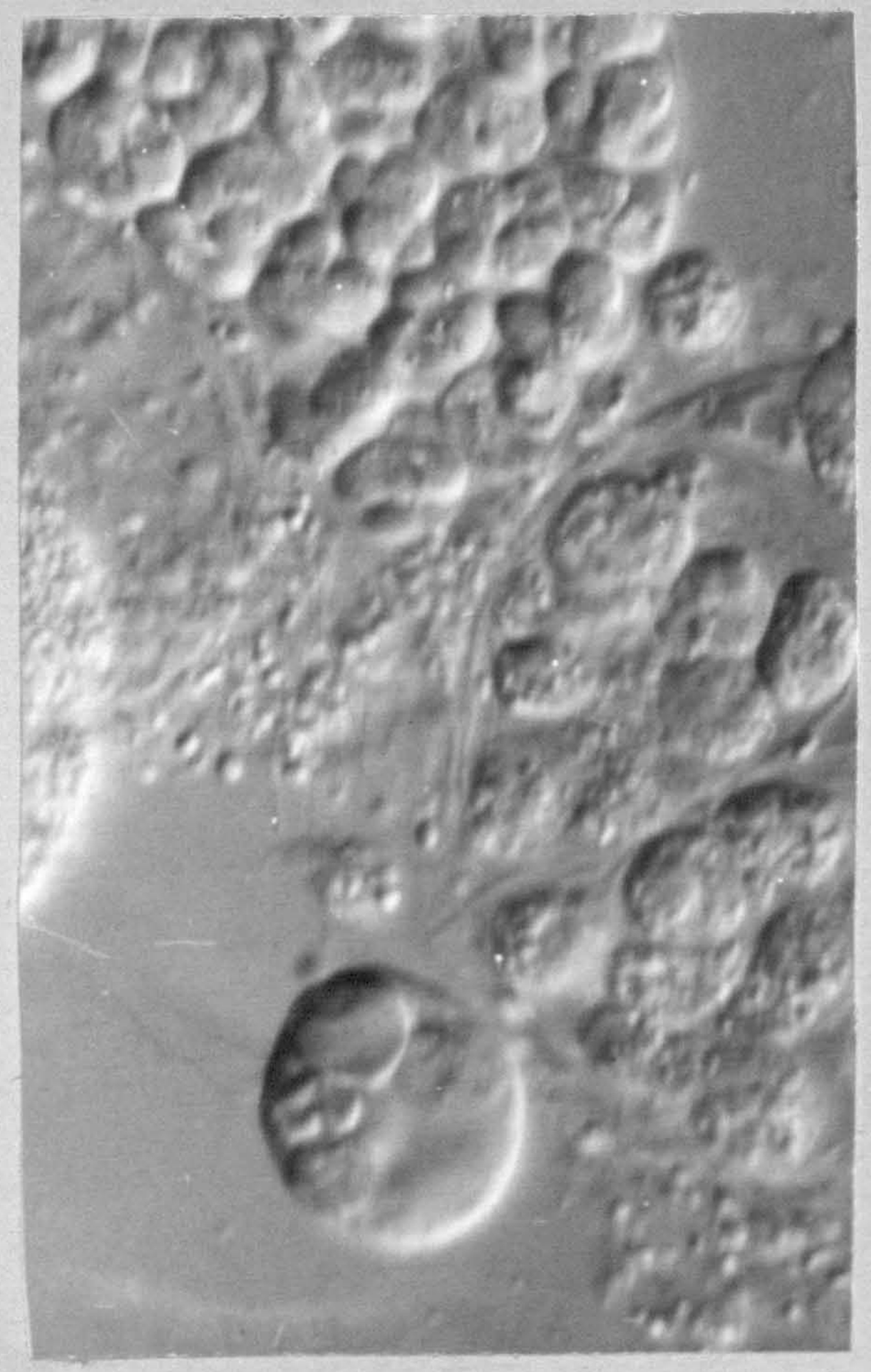

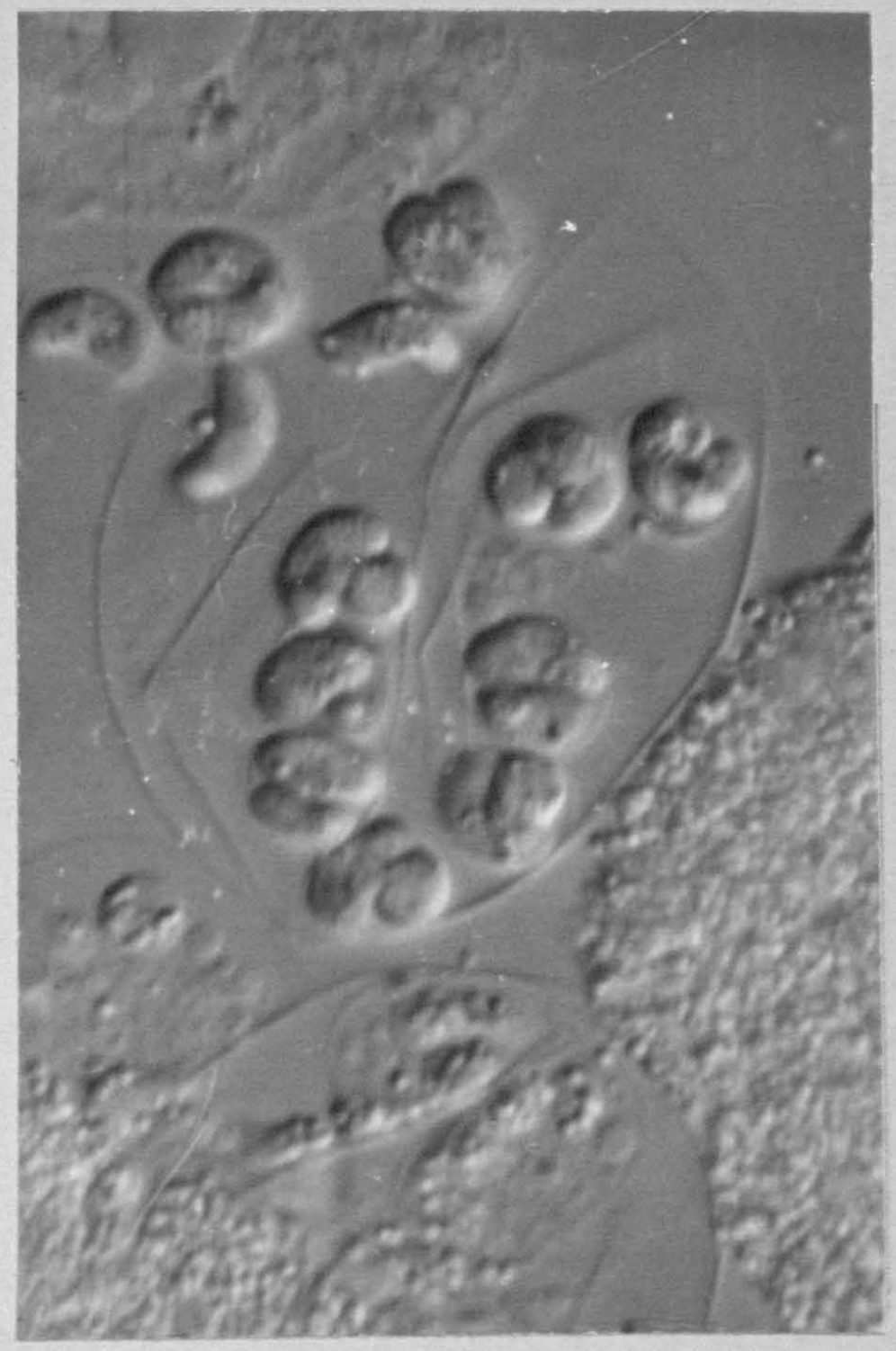

The developing coccidian oocyst

Plates 16, 17 and 18

This series of oil immersion Nomarski Interference Phase Contrast Light micrographs at a magnification of X 1,000 show various stages of sporozoite formation. Note the gradual condensation of the sporoplasm. Each sporocyst then divides to give rise to two daughter sporozoites contained within a thin capsule. The liberated sporozoites, 4 to 4.5 um in length, undergo slow flexing movements.

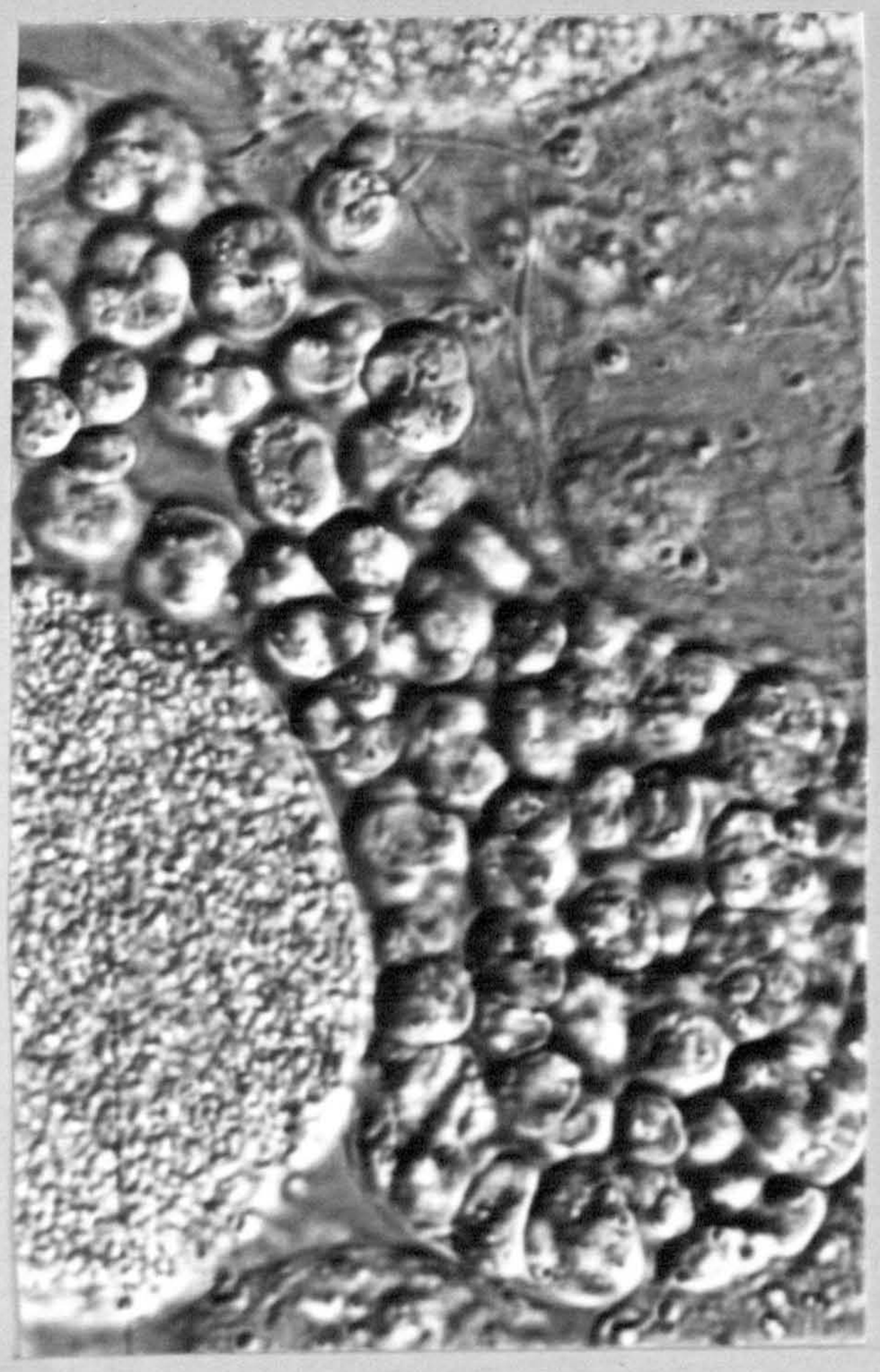

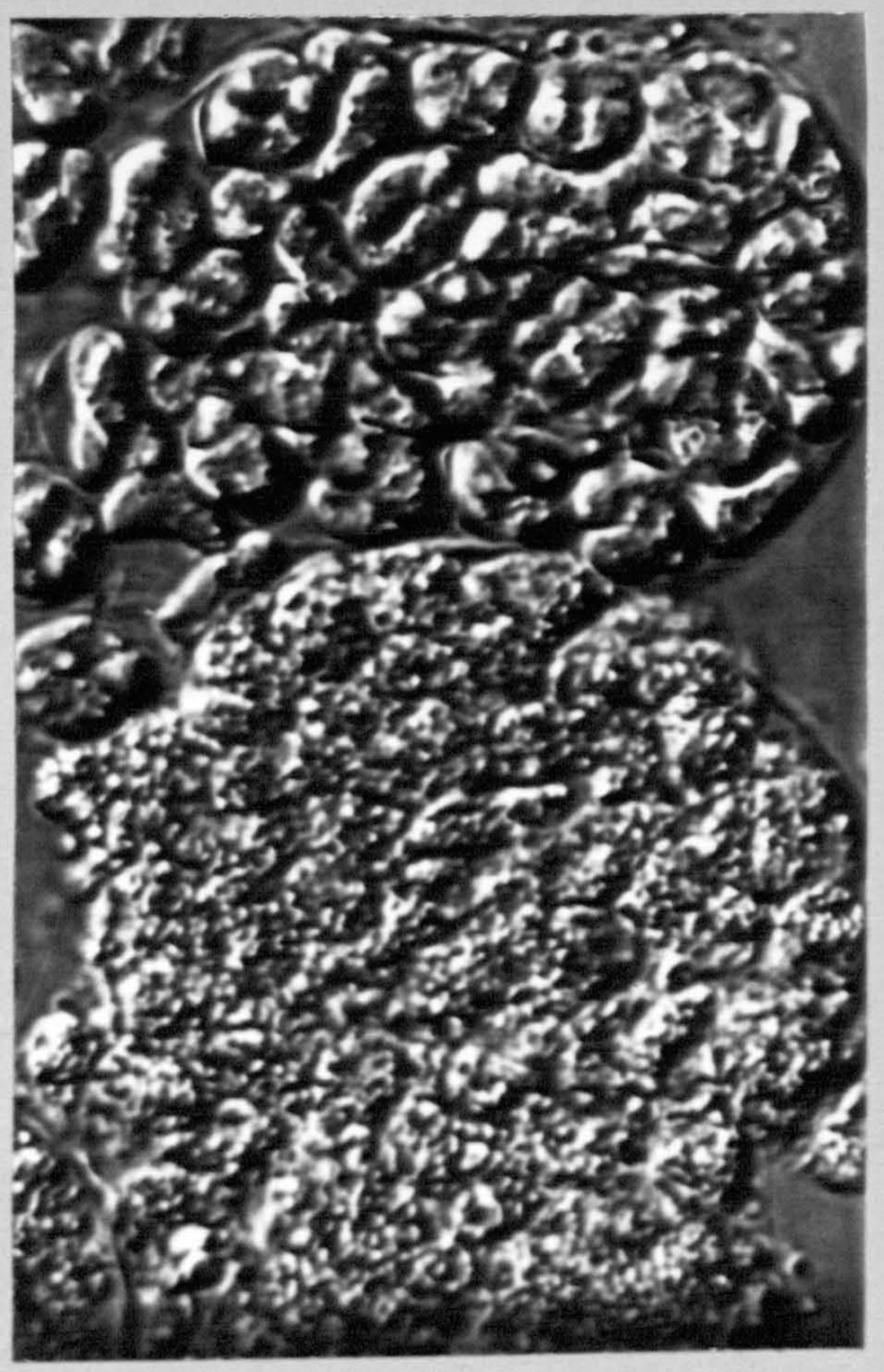

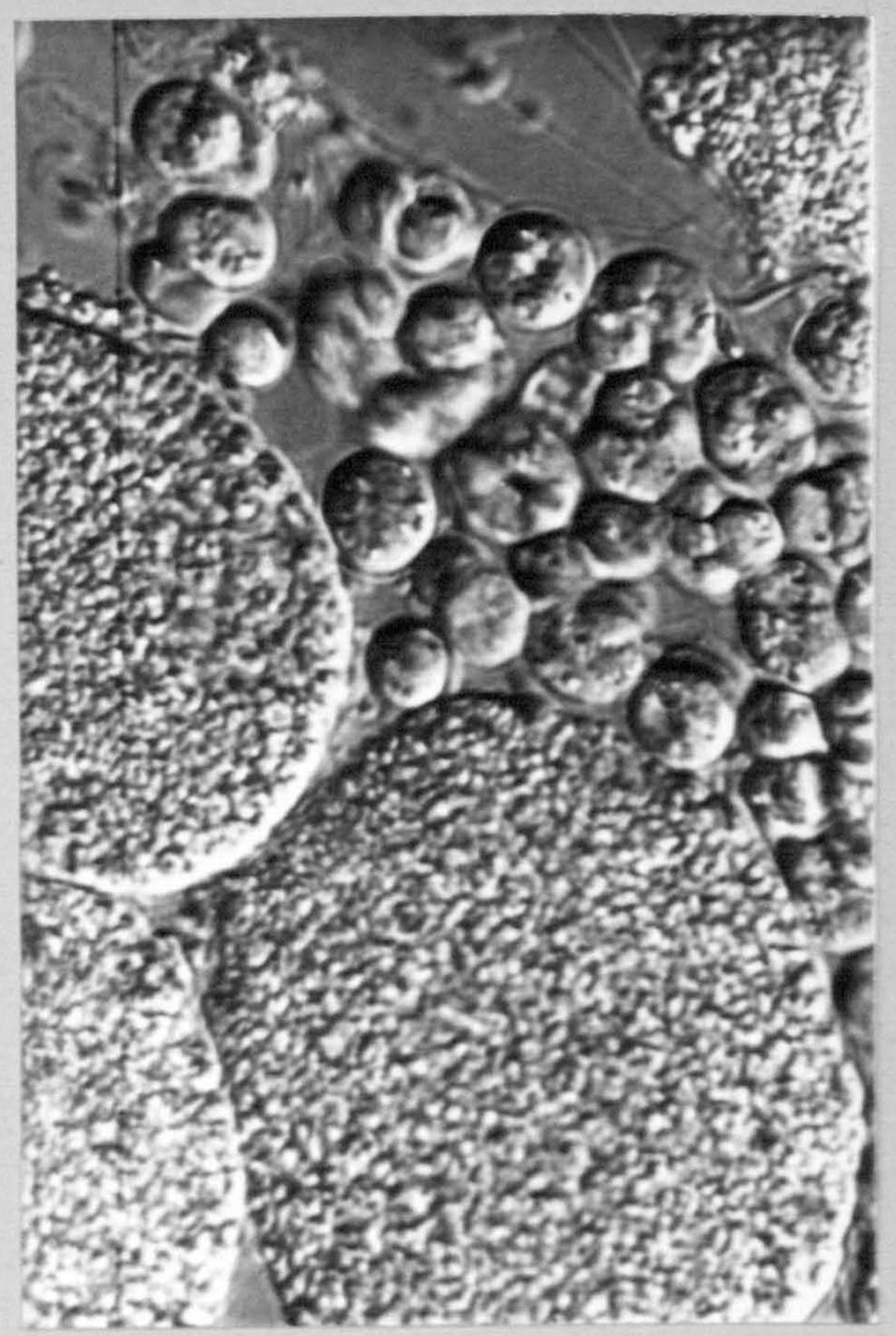

The mature coccidian oocyst

Plate 19.

Squash preparation of coccidian oocysts showing released sporozoites.

Phase contrast X 400

Bar = 10 µm

Plate 20.

A mature oocyst of Merocystis tellinovum. This oocyst is 30 µm in diameter and contains approximately 64 sporocysts. The oocyst wall appears to be double layered. Each sporocyst contains two sporozoites each 4.5 µm in length. The pointed apical end contains the apical complex and the blunt end of these comma-shaped sporozoites contains a refringent globule more clearly visible in the above micrograph. This is believed to be lipo-protein acting as a food store. the centrally located nucleus is surrounded by refringent granules.

Magn. x 2,000

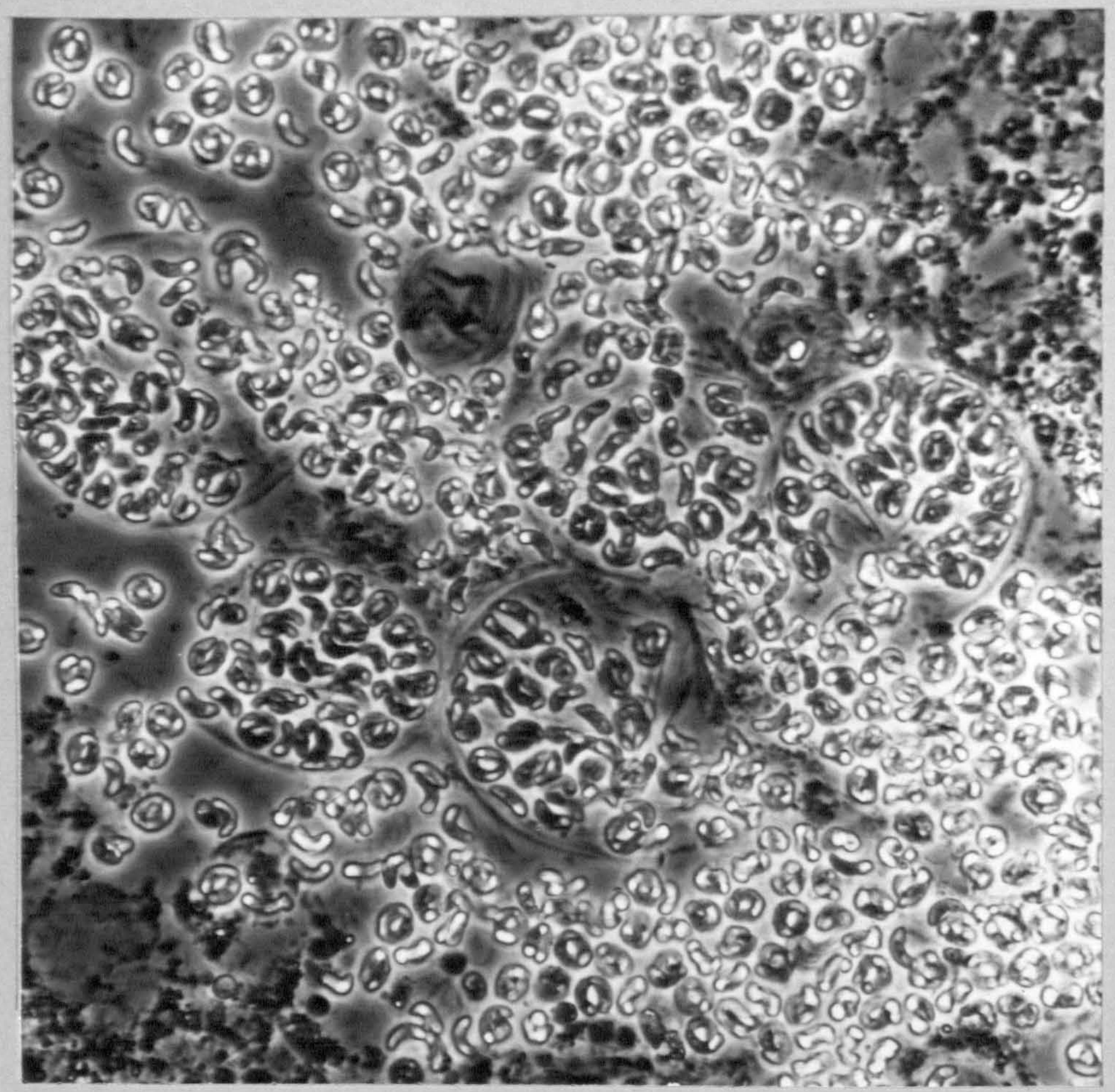

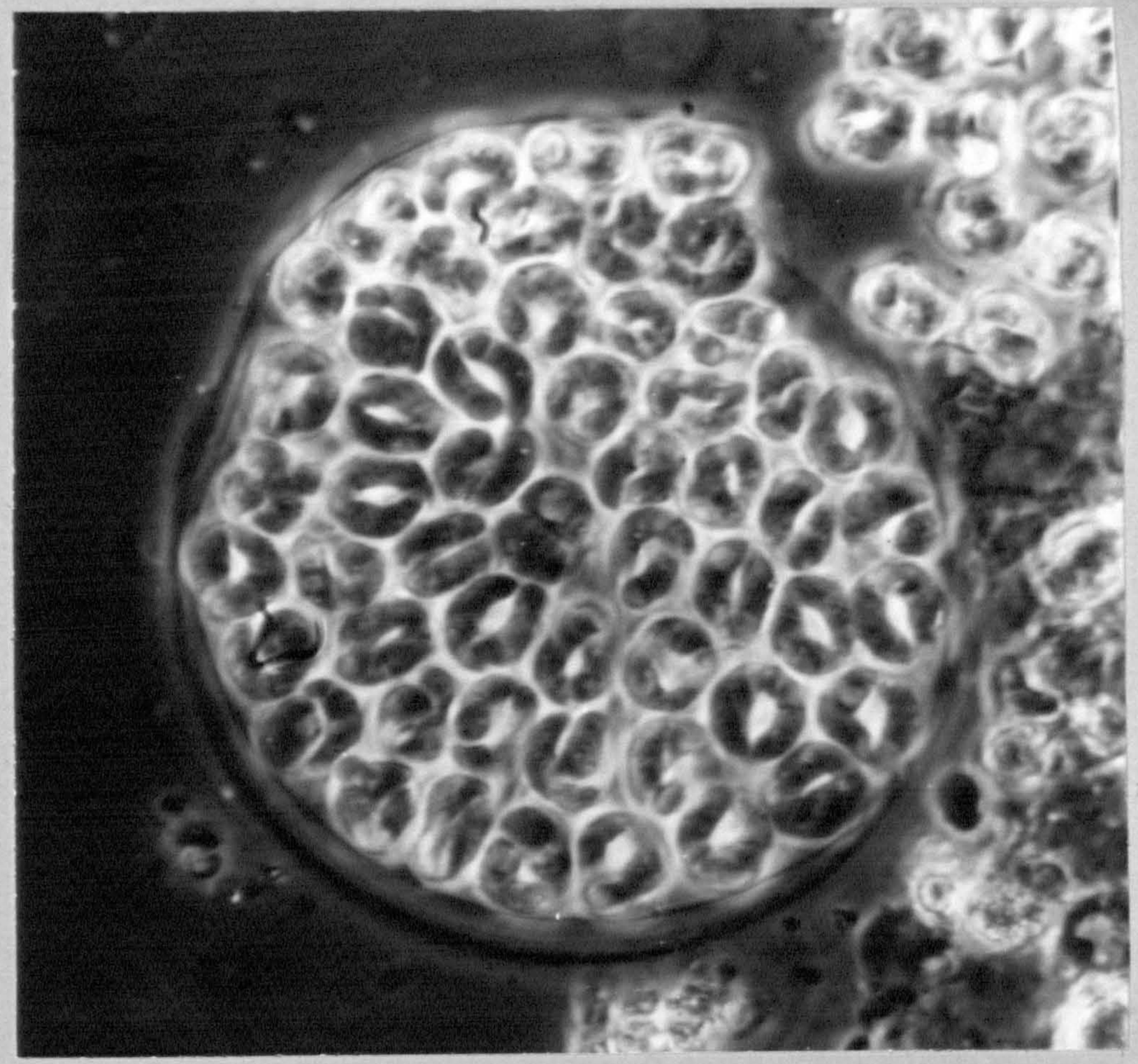

Host-Parasite relations

Plates 21 and 22.

These low-power light micrographs (x 60) (X 100) are taken from paraffin embedded sections H and E stained of the perivisceral gonadal tubules of Tellina. Very few oocytes of Tellina can be seen. The numerous spheres are oocysts of Merocystis tellinovum at various stages of development. Massive leucocytic infiltrations of the tubules can be seen at lower left in the upper micrograph. The lower micrograph is a similarly massively infected Tellina. Dark-field illumination (x 100) shows the refractile nature of the contents of a proportion of the oocysts


G
LT
G
G
LT

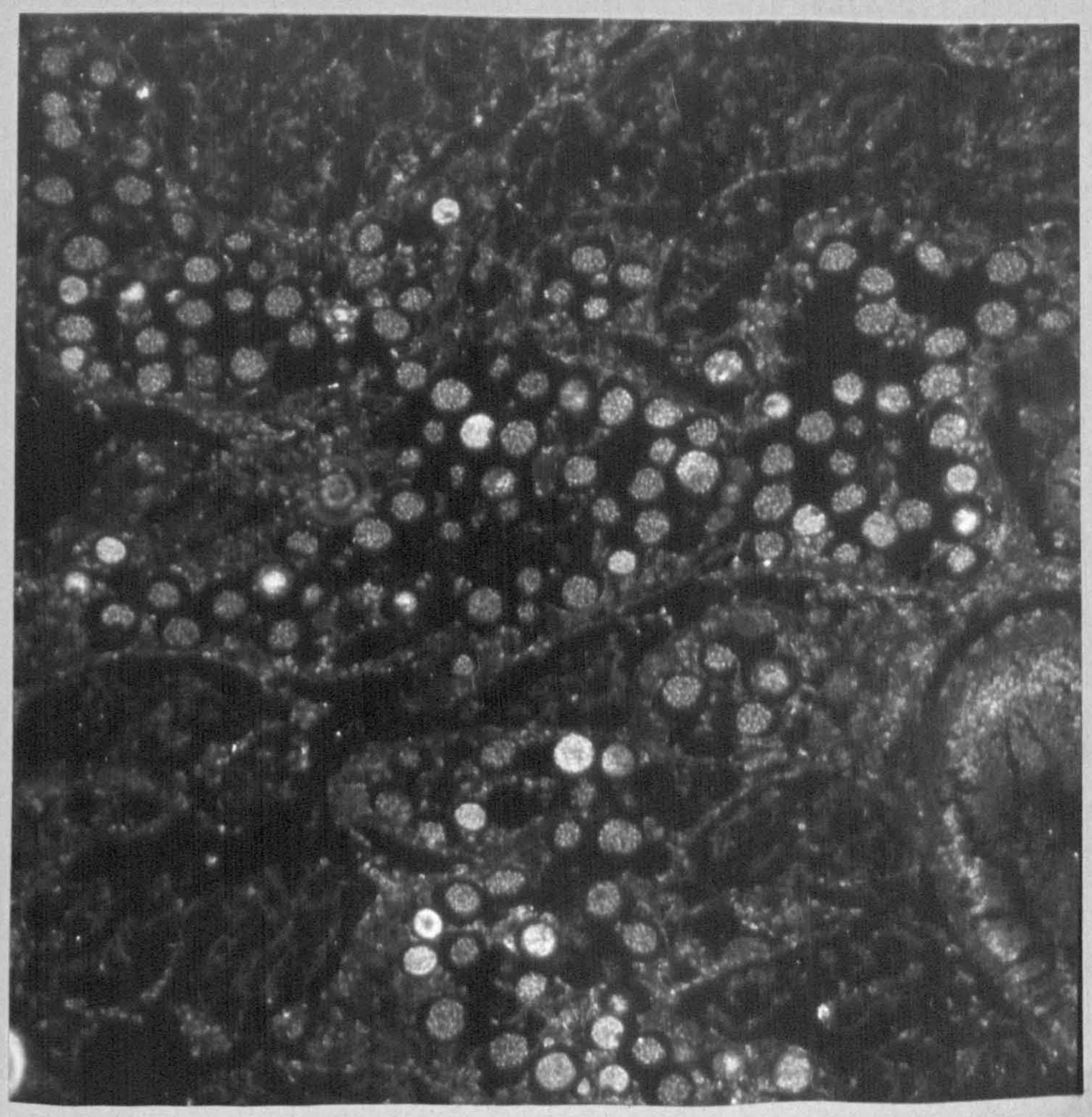

Plate 23

Low-power (X 100) light micrograph of a paraffin embedded section of the ovarian tubules of Tellina. The area within the lines is shown below. (Pl. 24.) The primary germ cells contain a mixture of sexual and asexual stages of the parasite Merocystis tellinovum. A large number of fully developed oocytes of Tellina 100 - 120 um in diameter can be seen. Some of these are attached to the tubule walls by a stalk. Others have rounded-off and are free in the lumina of the tubules.

Plate 24

Detail (X 400) of the above, showing meronts and micro- and macrogamonts. These are contained within the walls of primary germ cells. A merozoite is believed to have just entered into division in the cell arrowed. The cell on the right is believed to be a microgamont with microgametes budding off at the periphery.

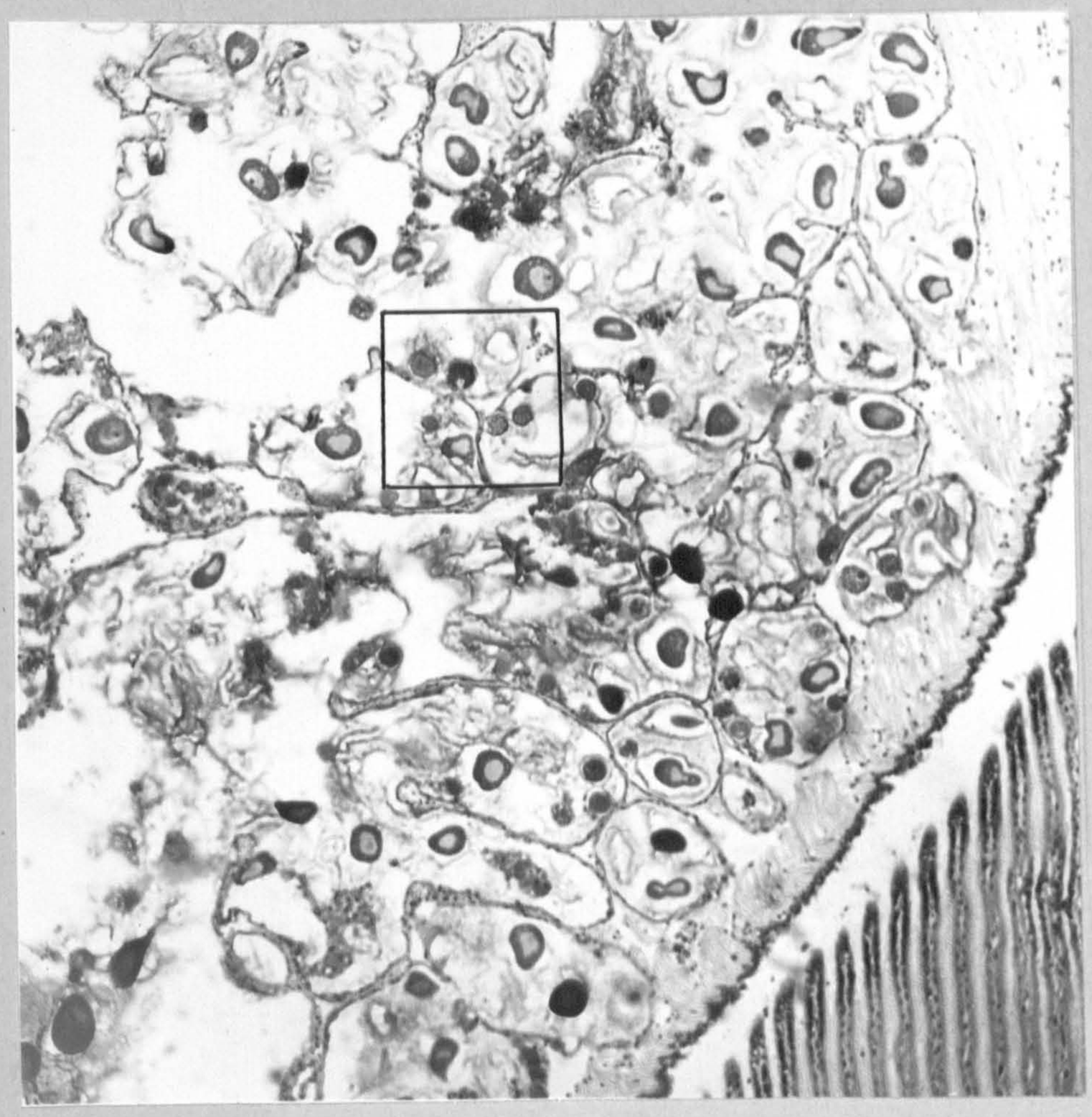

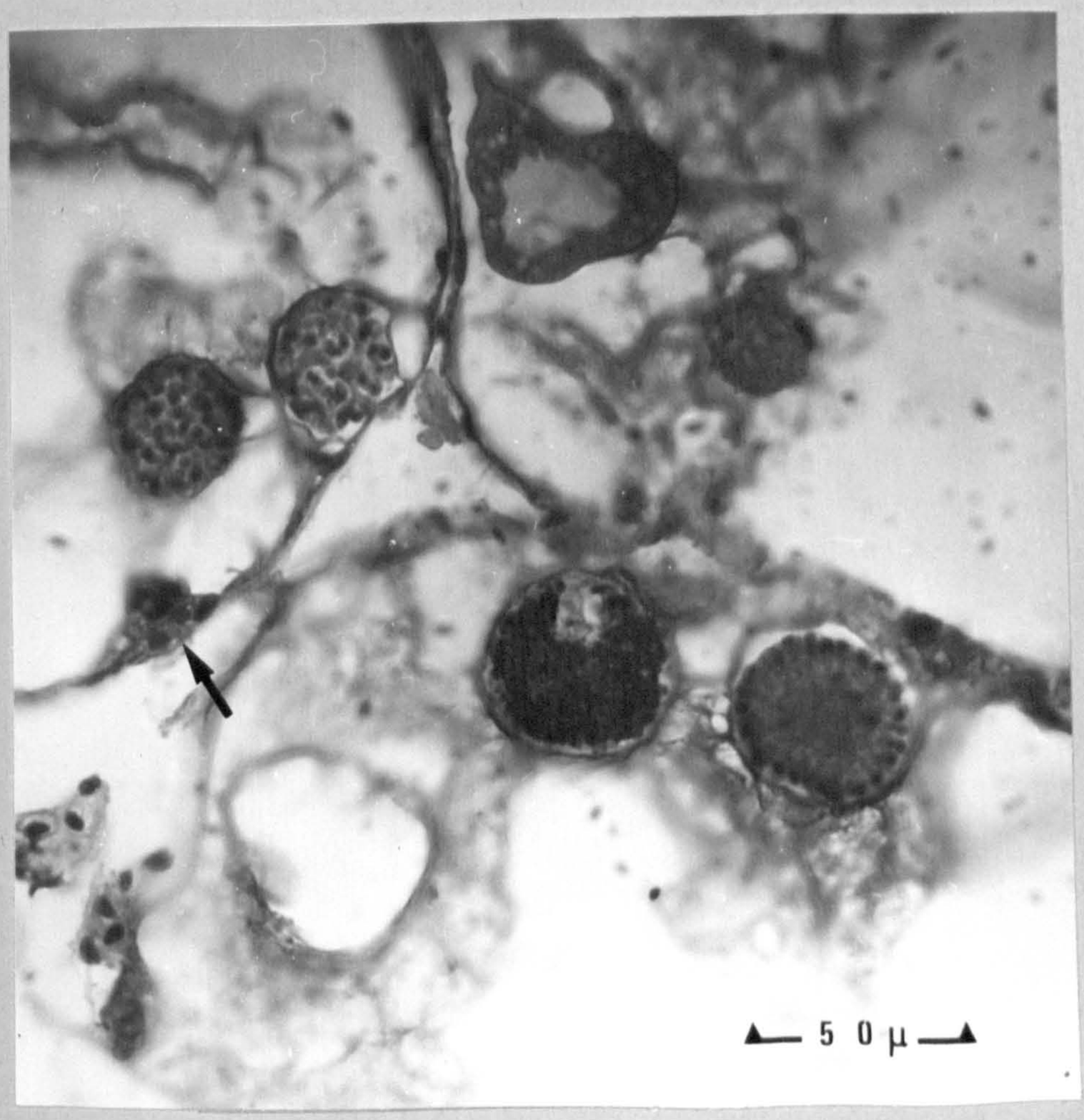
5 0 µ

Stages in the life cycle of the coccidian

Plate 25

A branch of the gonadal follicle of Tellina containing the following stages of the life cycle of the coccidium

(1) Macrogamonts

(2) Microgamonts

(3) Developing gamonts within the hosts primary germ cells

(4) Sporonts, early post fertilization

(5) Sporonts, late post fertilization

(6) Mature oocysts free in the lumen

(7) Host oocyte

(8) Ciliated protozoan

Magn. x 250

Plate 26

This phase contrast light micrograph shows a developing oocyst at centre fixed before the sporocysts have cleaved to form paired sporozoites.
(detail of plate 25)

Magn. x 400

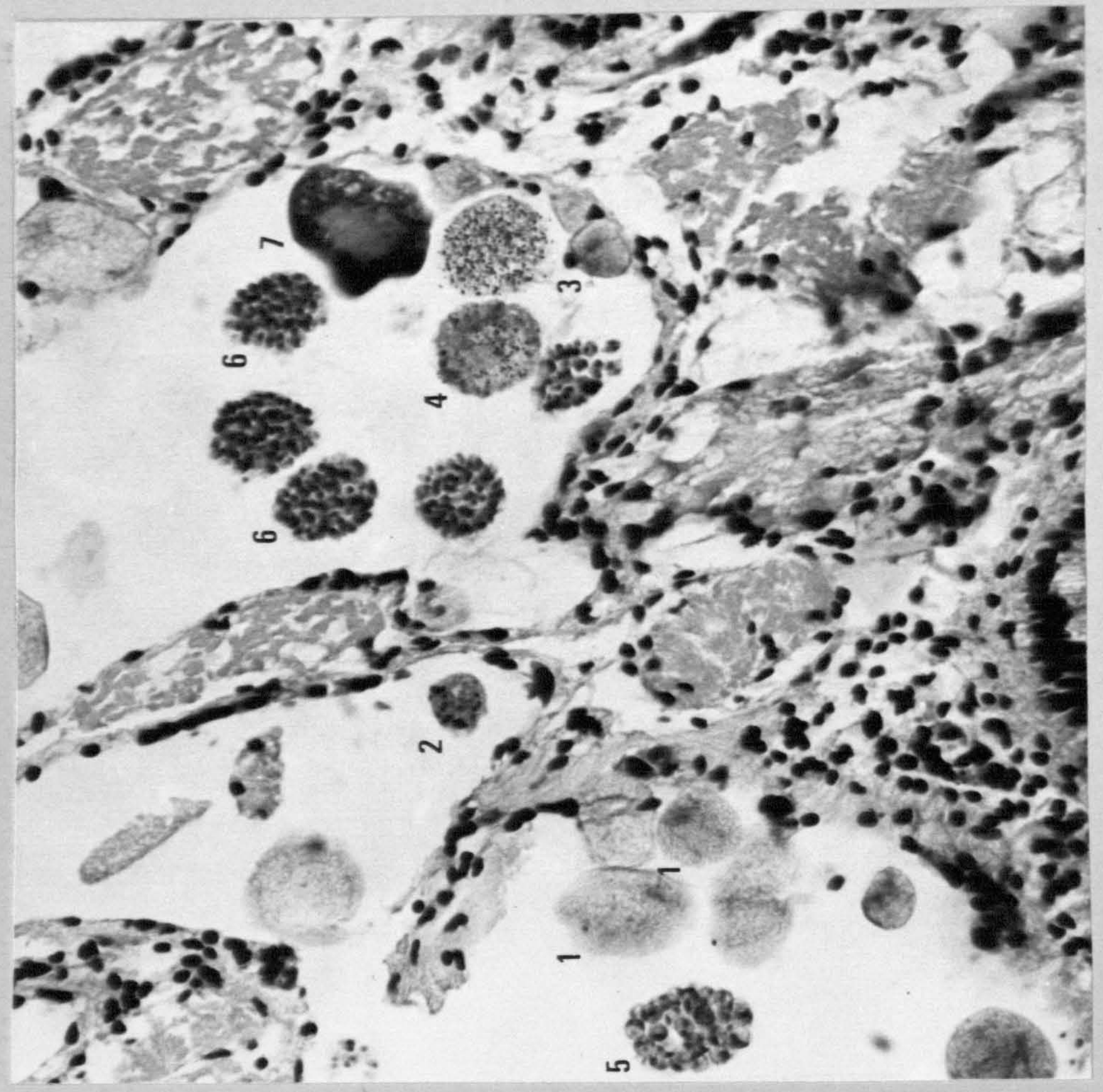
7
6
6
4
3
2
1
1
5

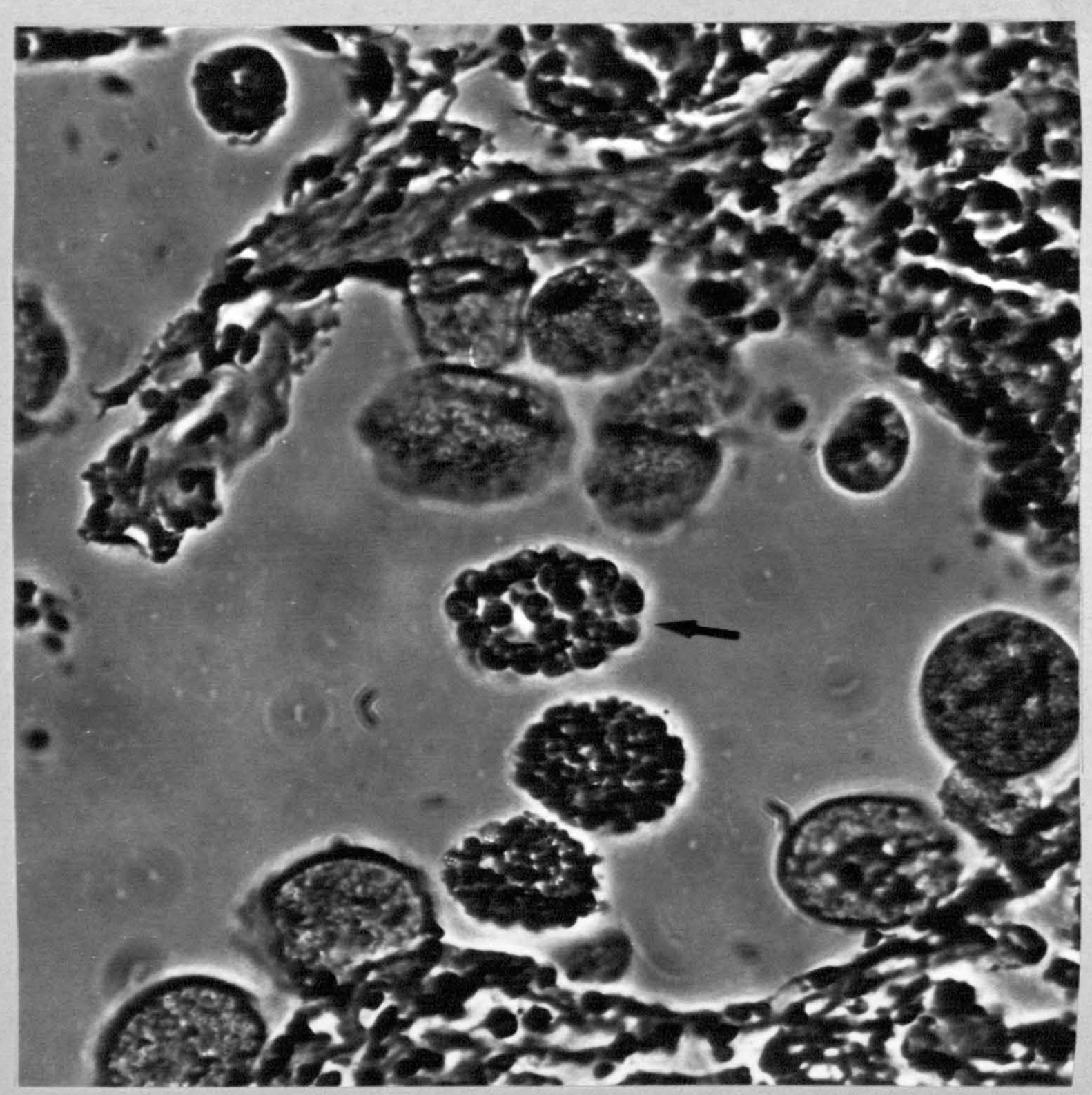

Stages in the life cycle of

the coccidian, M. tellinovum.

Plates 27 and 28

The following stages of the life cycle of M. tellinovum are illustrated in these two plates

(1) Macrogamonts

(2) Microgamonts

(3) Developing gamonts within the hosts primary germ cells

(4) Sporonts, early post fertilization

(5) Sporonts, late post fertilization.

(6) Mature oocysts free in the lumen

(7) Host oocyte attached to the basal lamina of the gonadal follicle

(8) Host leucocytes

(9) Host multinucleate amoebocytes

(10) Host muscle fibres

Plate 28 shows various units of the coccidian at various stages in the life cycle floating free in the lumen of the gonadal follicle. The parasite appears to disrupt the host cell by mechanical pressure allowing the lumina to fill with oocysts at various stages of development. Note the delicate capsule surrounding the oocyst at centre.

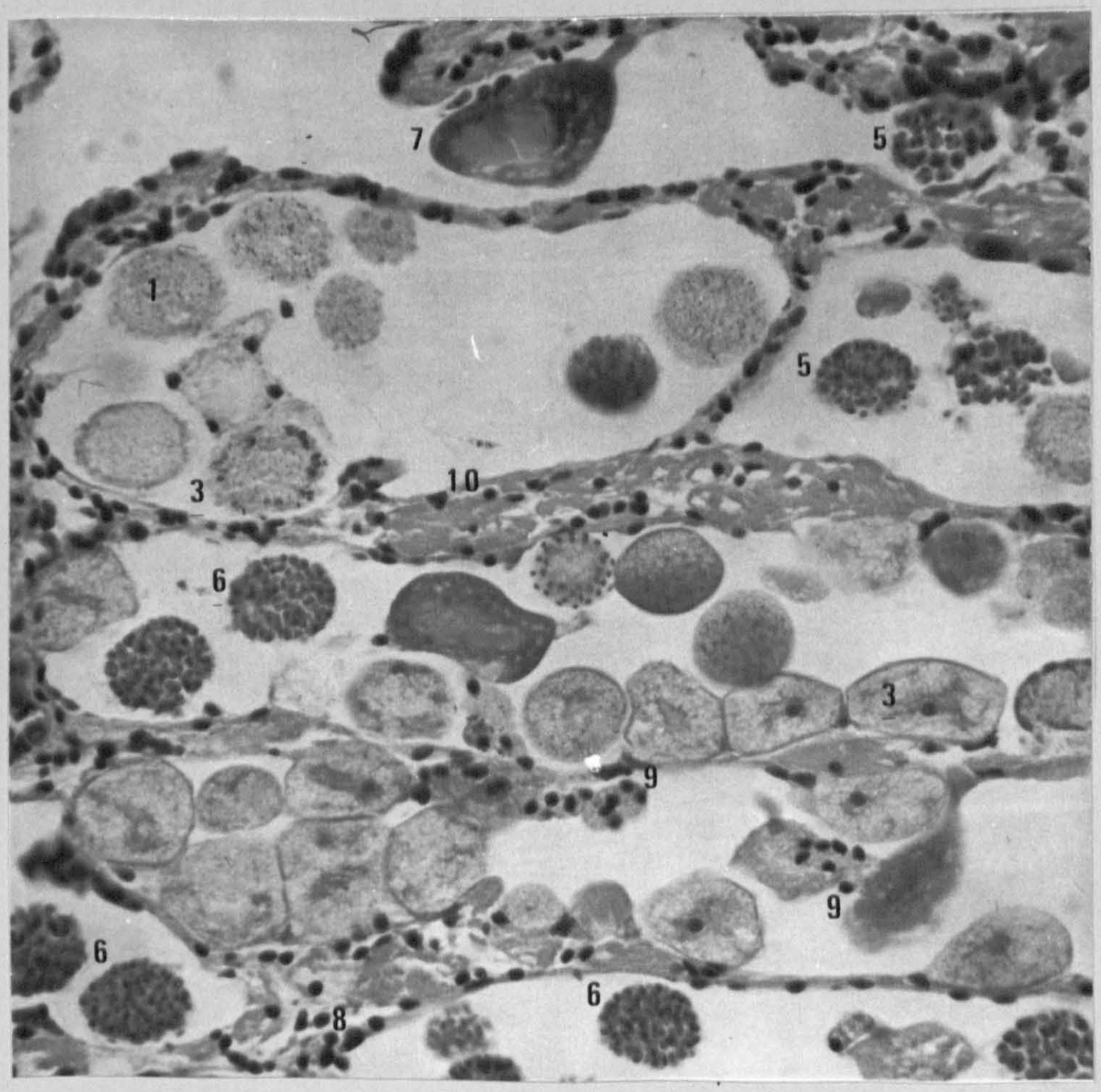
7
5
1
5
3
10
6
3
9
9
6
6
8

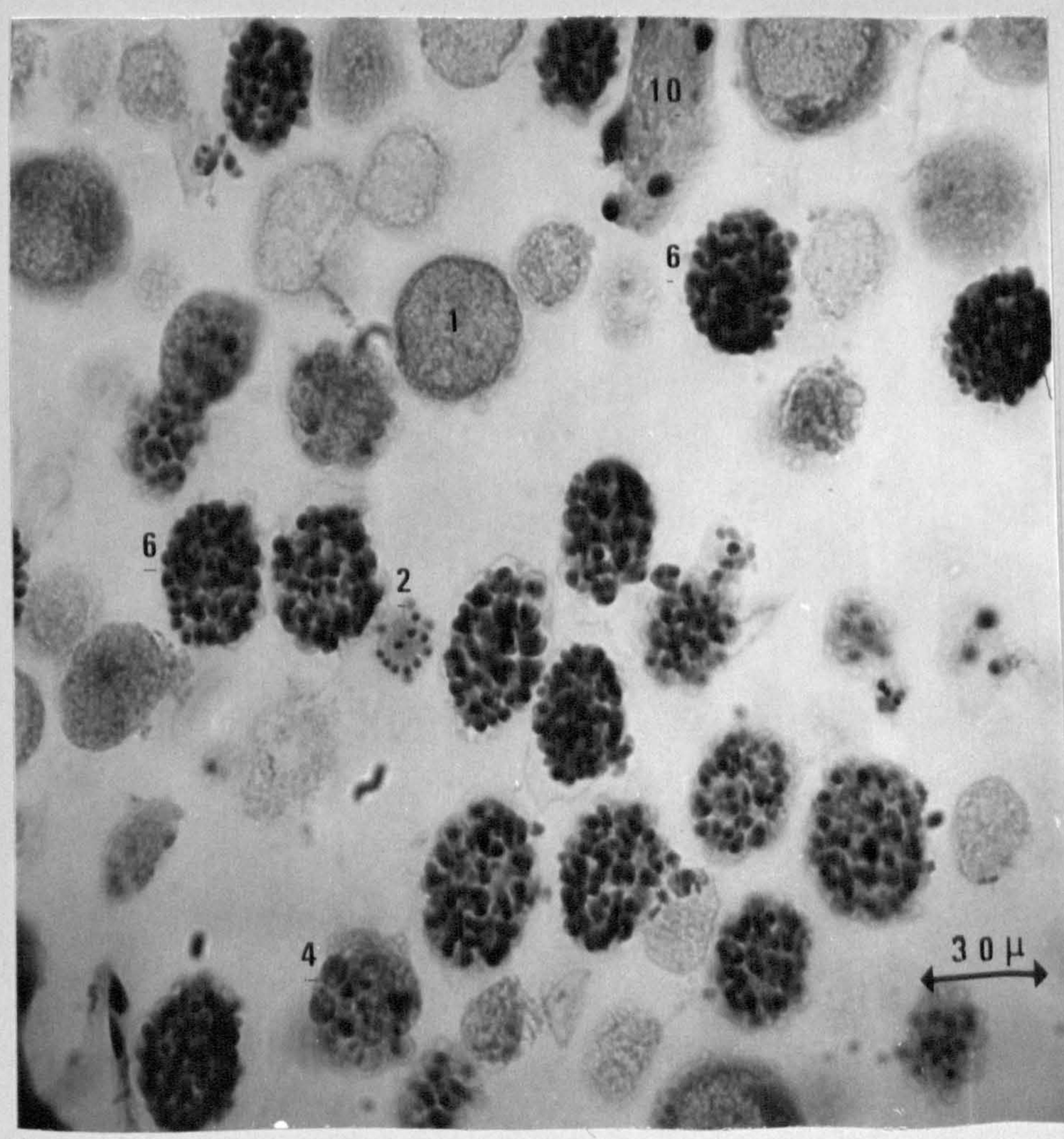
10
6
1
6
2
4
30 µ

Schizogony and gametogony in

Merocystis tellinovum.

Plates 29 and 30

Phase contrast light micrograph (x400) of the asexual phases in the development of the coccidian following penetration of the primary germ cells of the ovary by trophozoites, (see also Pl. 59) The progressive stages of division are represented by the three arrowed cells.

A mature oocyte of Tellina occupies the centre of the picture. The mucopolysaccharide envelope is best seen under phase contrast. This capsule provides nourishment and protection to the maturing egg.

Plate 30

Phase contrast light micrograph (x400) of the gonadal follicles of the ovary containing gametogonous stages of the coccidian. This figure is a detail of plate 27.

Both plates magn. x 400

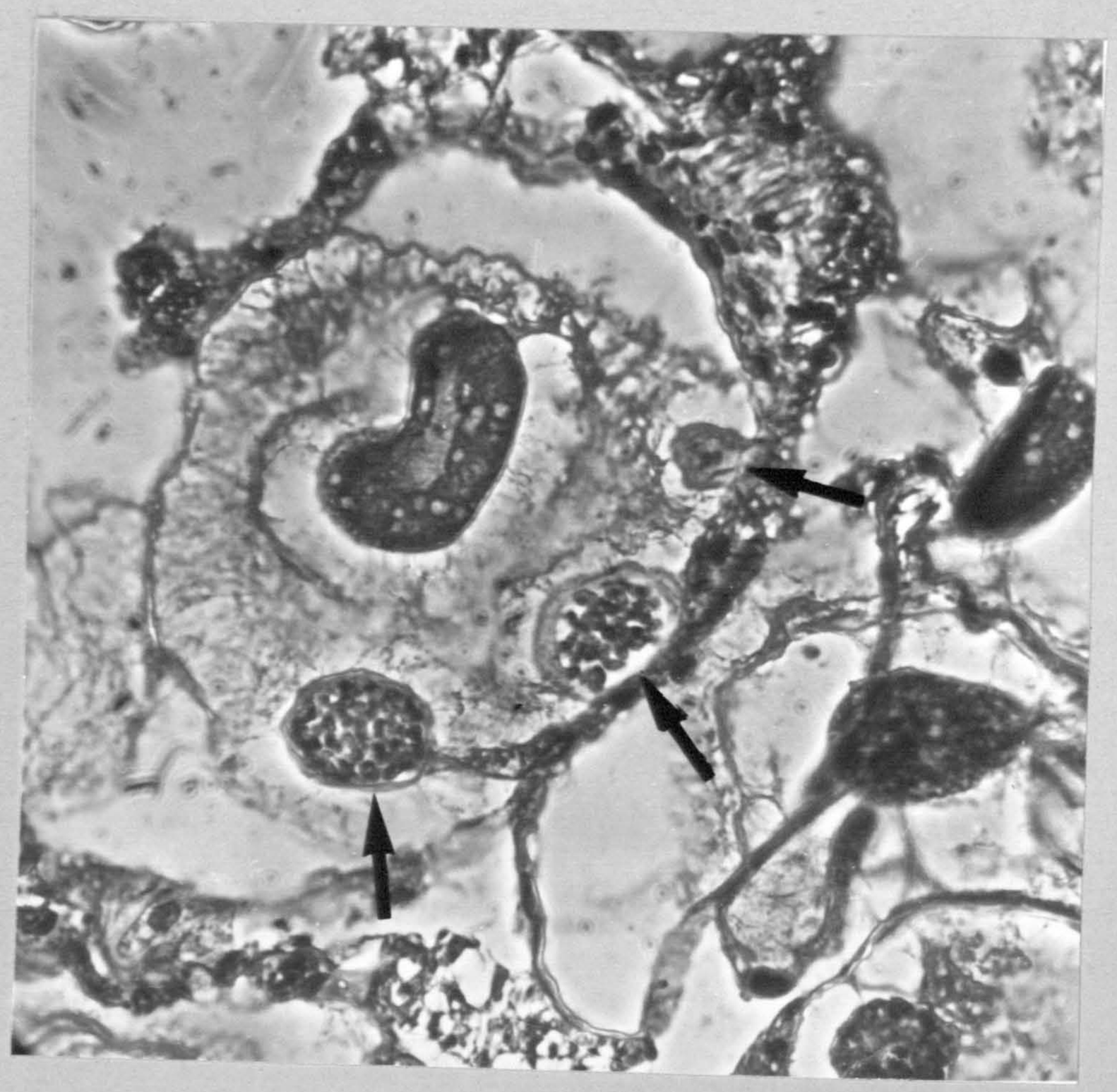

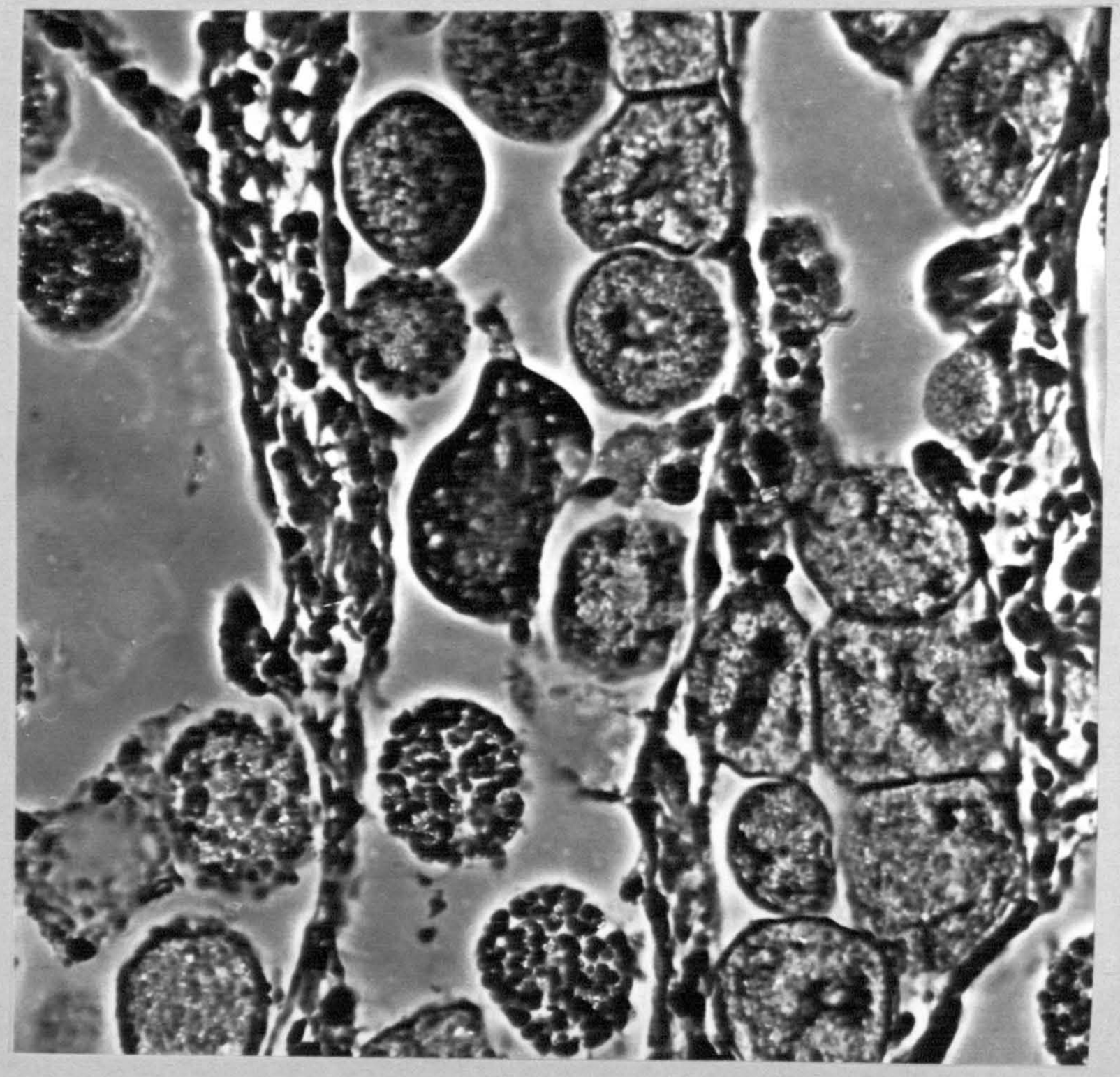

Defense Reactions of the Host

Plates 31 and 32

These light micrographs (X 400) of the lumen of an ovarian tubule shows massive leucocytic invasion enmeshing the coccidia in various stages of development. A parasitophagous vacuole has developed around the encapsulated parasites.

Both plates magn. x 255

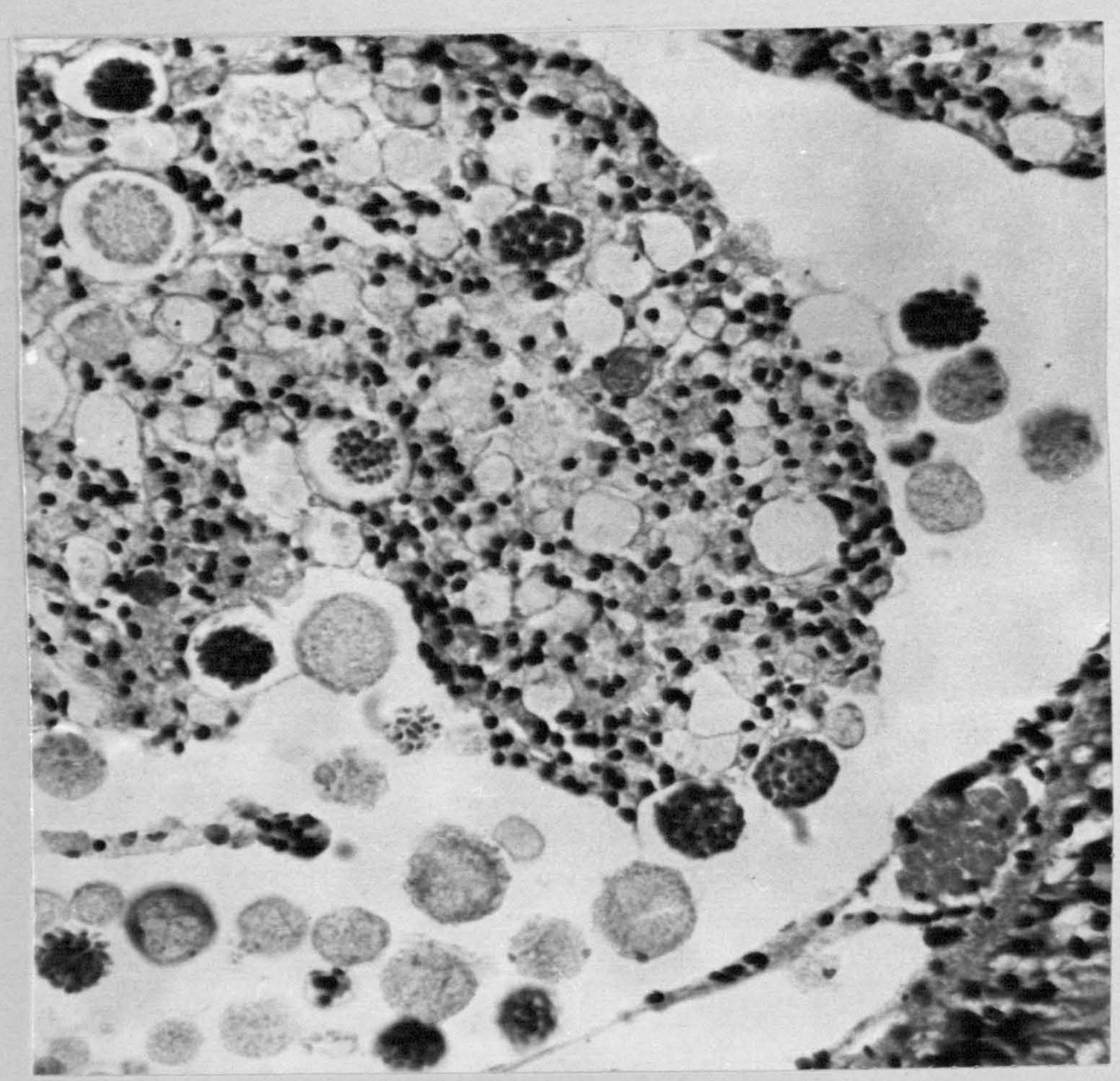

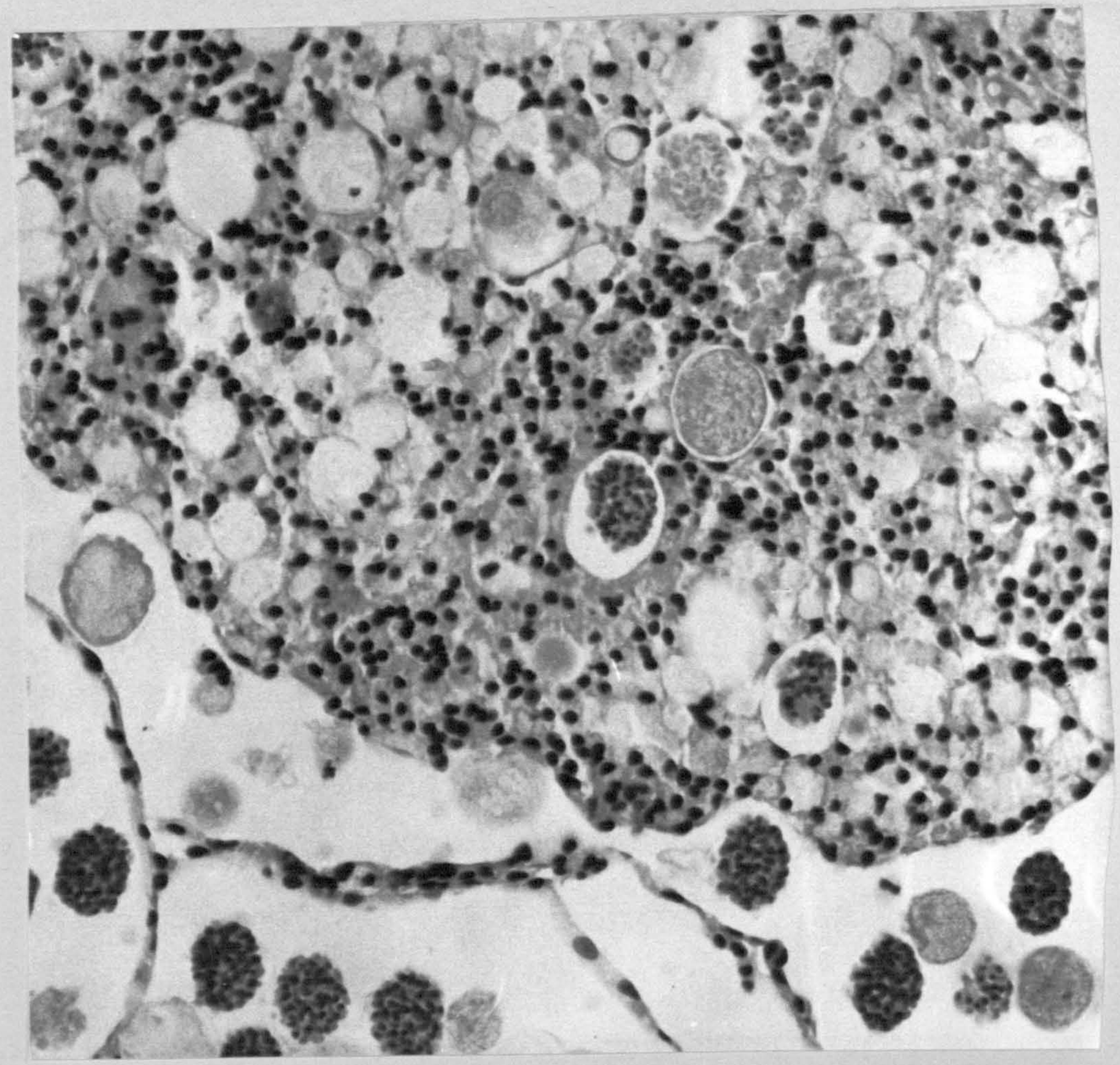

The Developing Oocyst

Plate 33

Low power (X 1,000) electron micrograph of encapsulated coccidia at various stages of development and senescence. Numerous mono- and multinucleate amoebocytes surround the coccidia. The parasite at the centre is believed to be a fertilized macrogamont in the process of becoming a mature oocyst as at left. Amoebocytes containing necrotic remnants of coccidia can be seen in phagocytic vacuoles. An empty parasitophagous vacuole is depicted at top right.

Plate 34

Fertilised macrogamete (Zygote) within a fibrocytic capsule. Necrotic amoebocytes are contained within the capsules. The flagellar profiles are from holotrichous ciliates that are frequently encountered in the lumen and haemocoele of the host. Electron micrograph X 1,500.

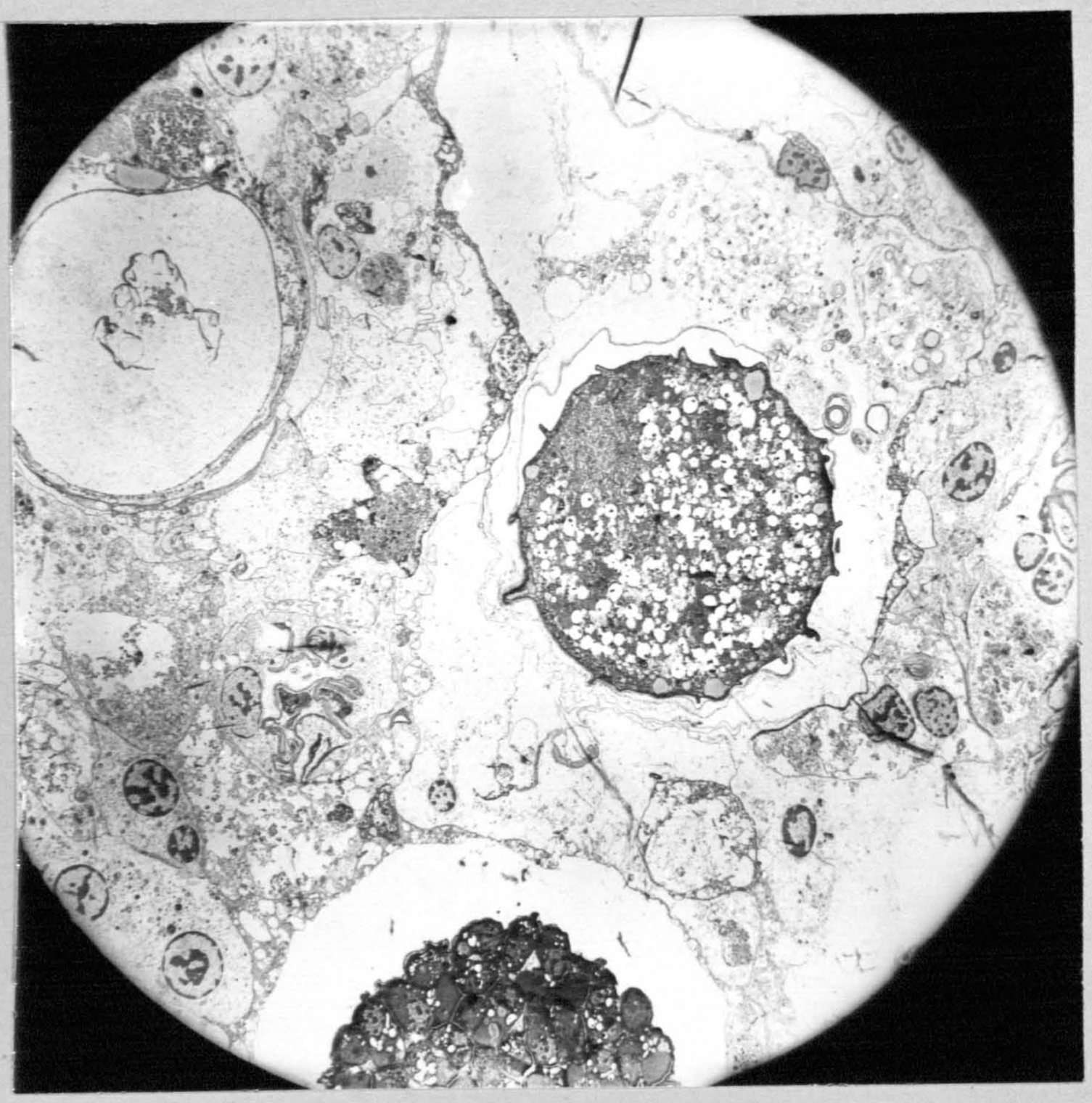

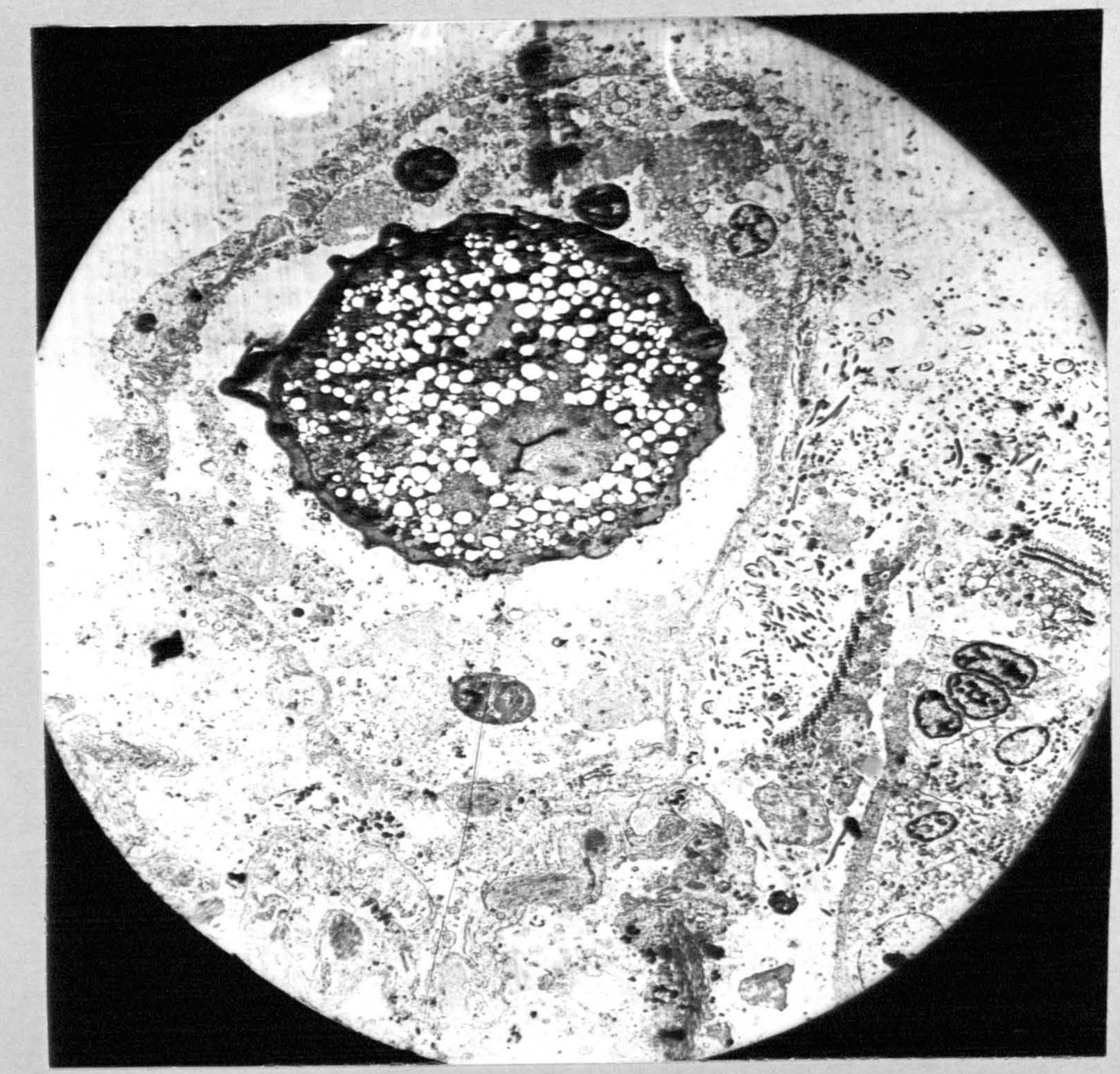

The development of the coccidian oocyst

Plate 35

A developing oocyst (X1,500) with sporocysts at the precleavage stage corresponding with light micrographs plates 16, 17 and 18.

Plate 36

A mature coccidian oocyst. The sporocysts have cleaved to give two daughter sporozoites which are comma shaped and lie at right angles to each other. Note the crenulate nature of the oocyst wall.

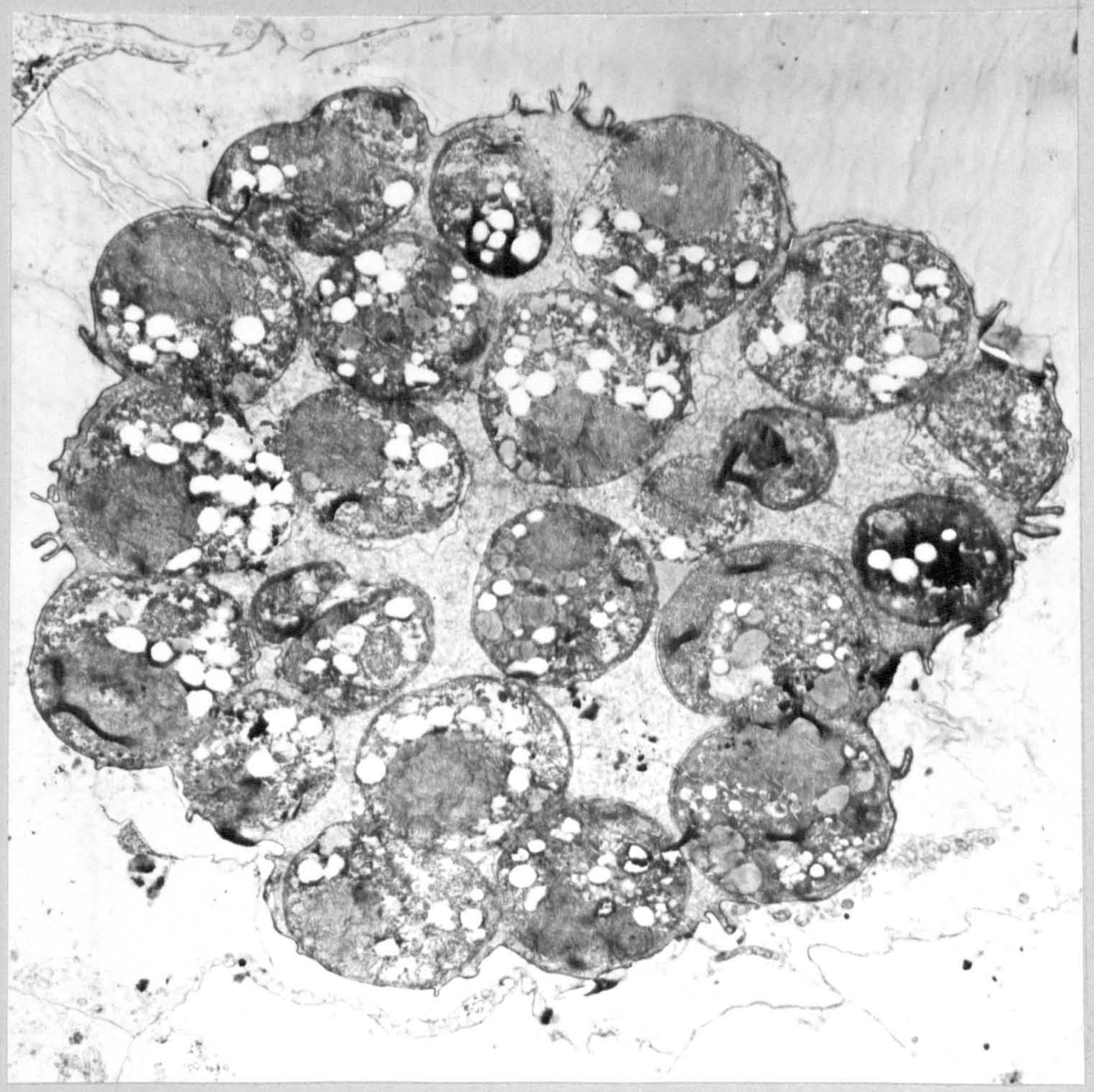

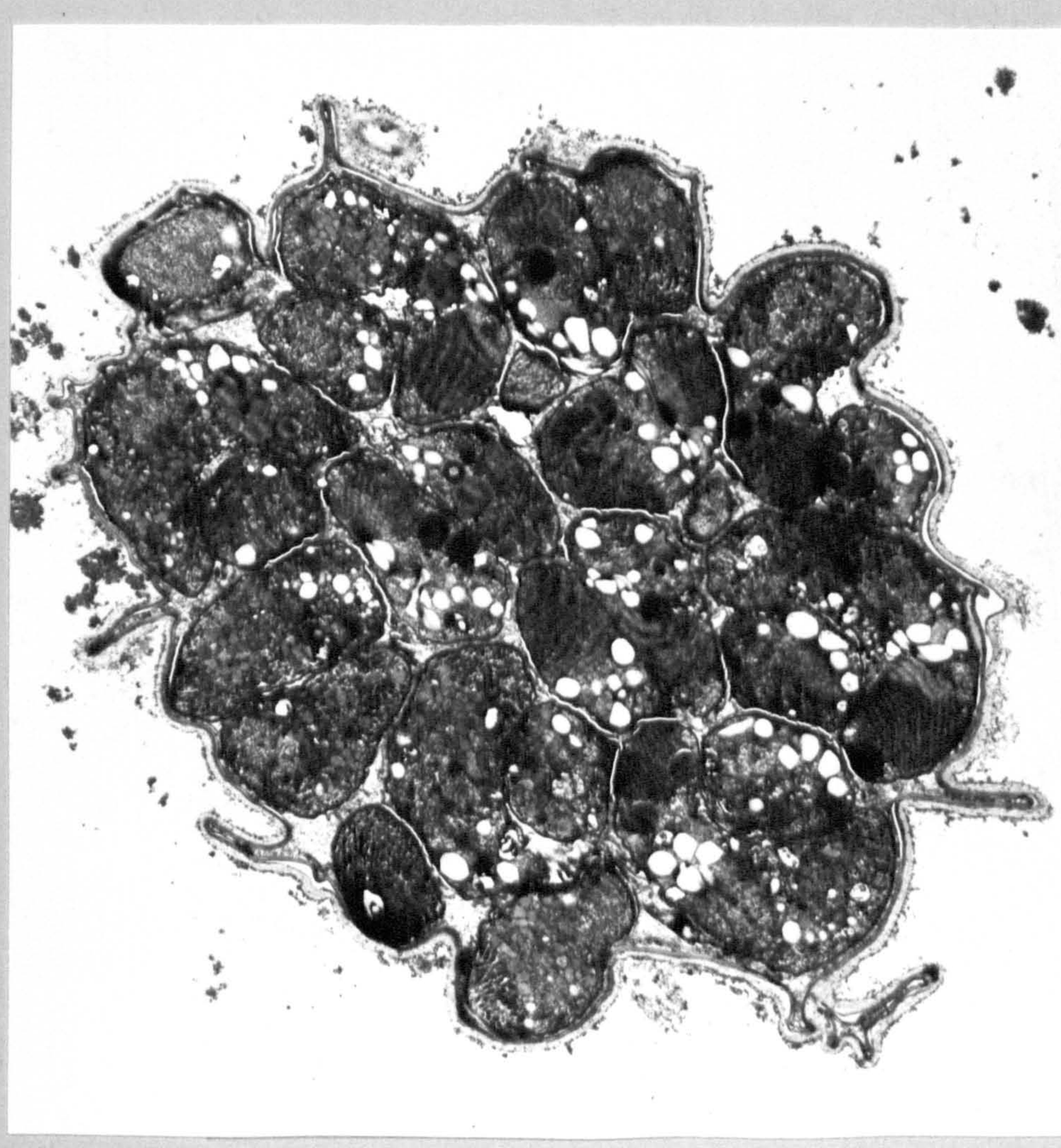

The fine structure of the developing oocyst of the coccidian

Plate 37

Sporocysts containing paired sporozoites lying at right angles to each other. See also text figure 8. Note the presence of micronemes, numerous rhoptries, nuclei with condensed chromatin and the numbers of electron dense and electon lucent vesicles containing a variety of food storage materials.

Magn x 1,500

Plate 38

Detail from the oocyst above.

The sporoplasm has shrunk away from the resistant oocyst wall. Rhoptries in cross section have electron lucent centres (arrowed)

Magn x 6,000

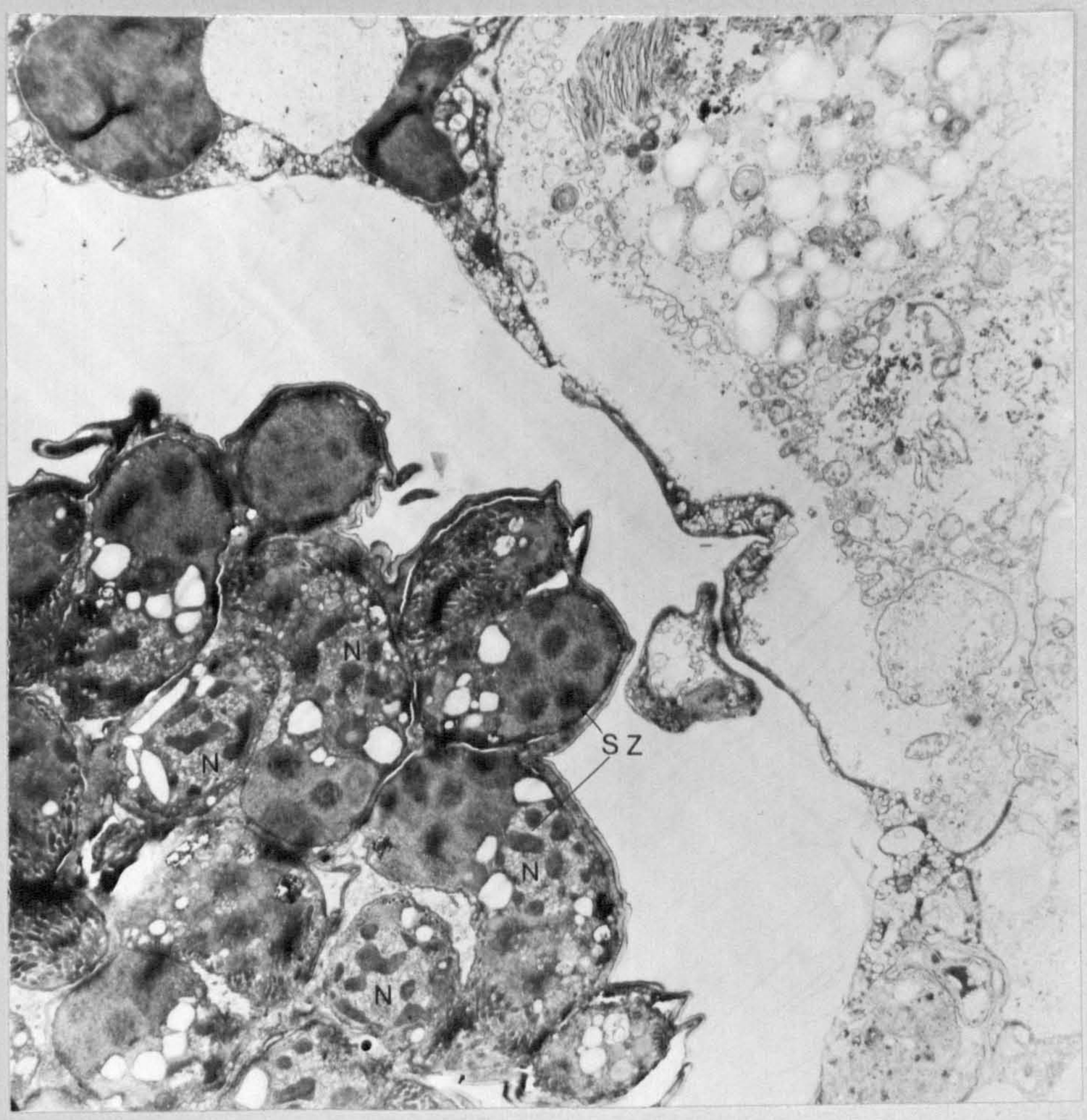
N
N
SZ
N
N

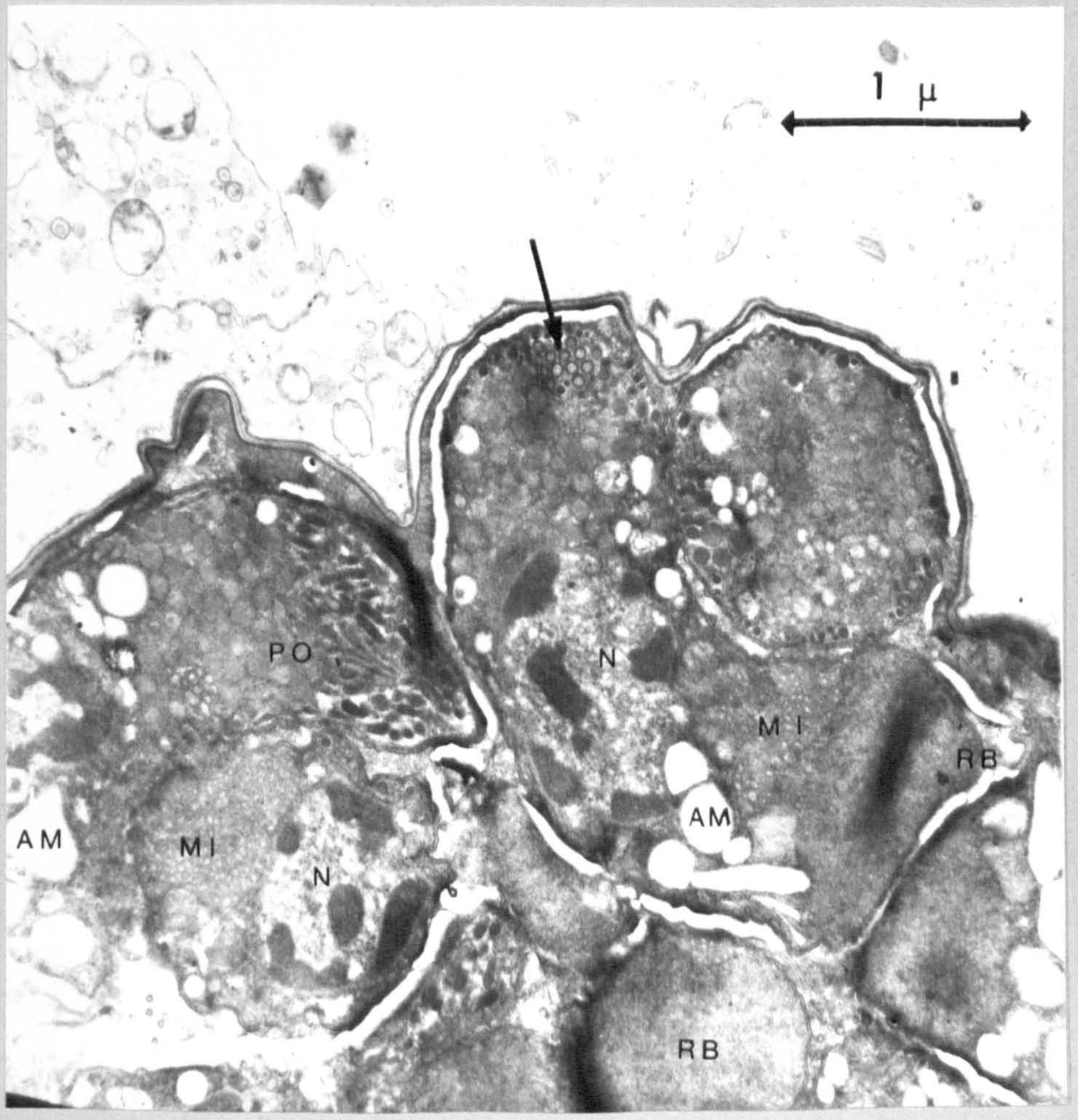
1 μ
PO
N
MI
RB
AM
AM
MI
N
RB

The fine structure of the developing oocyst

Plate 39

Detail from plate 36. The paired, comma shaped, sporozoites have three main components. (1) the nucleus and associated mitochondrion (2) The apical complex of micronemes and rhoptries and (3) the posterior lipo-protein food storage material and associated electron dense and electron lucent vesicles presumably containing lipid and amylopectin.

Magn. x 10,000

Plate 40

Detail of the above. Note the presence of subpellicular micro-tubules (arrowed) and the trilaminate nature of the sporozoite wall.

Magn x 15,000

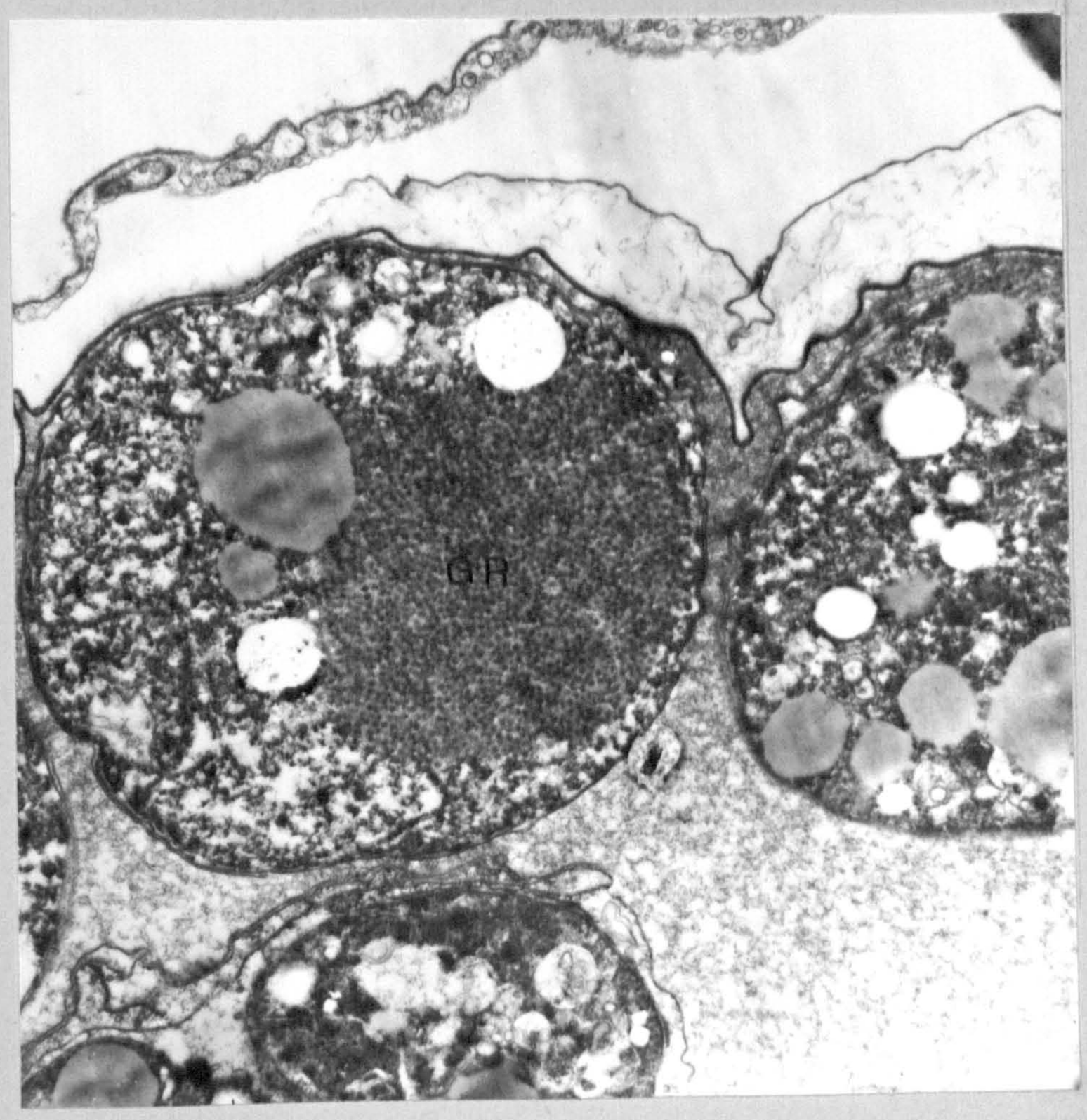
GH

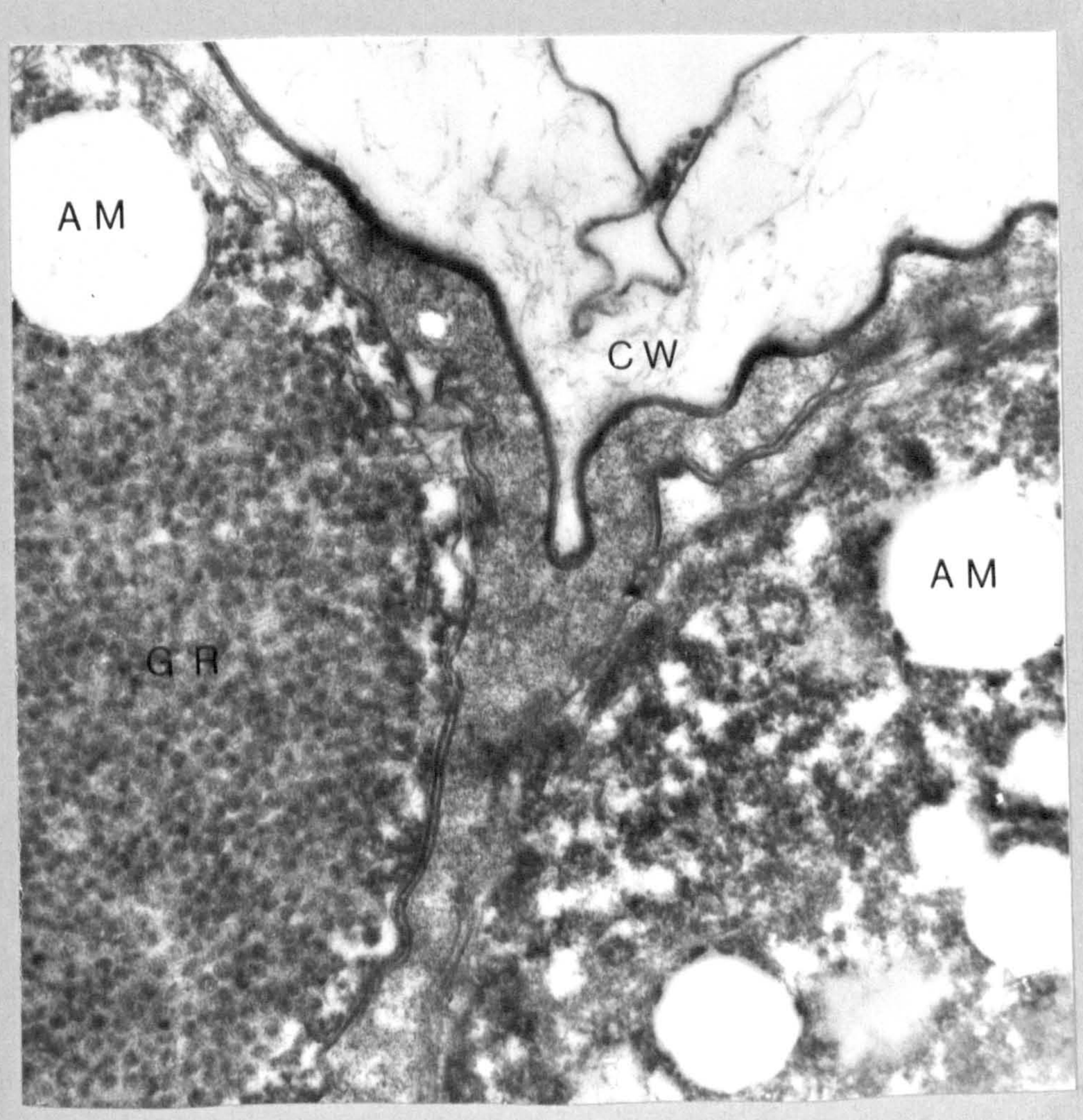
AM
CW
AM
GR

The fine structure of the developing oocyst

Plate 41

Electron micrograph (X 10,000), the mature oocyst, detail of sporozoites from the preceding EM. Note medium electron dense food storage vacuoles, and electron lucent vacuoles believed to contain amylopectin.

Plate 42

Maturing oocyst. The lipo-protein granules have not fully condensed into the crystalline arrays that are a feature of the mature sporozoites. The dense osmiophilic vacuoles probably contain lipid material.

Magn. x 15,000

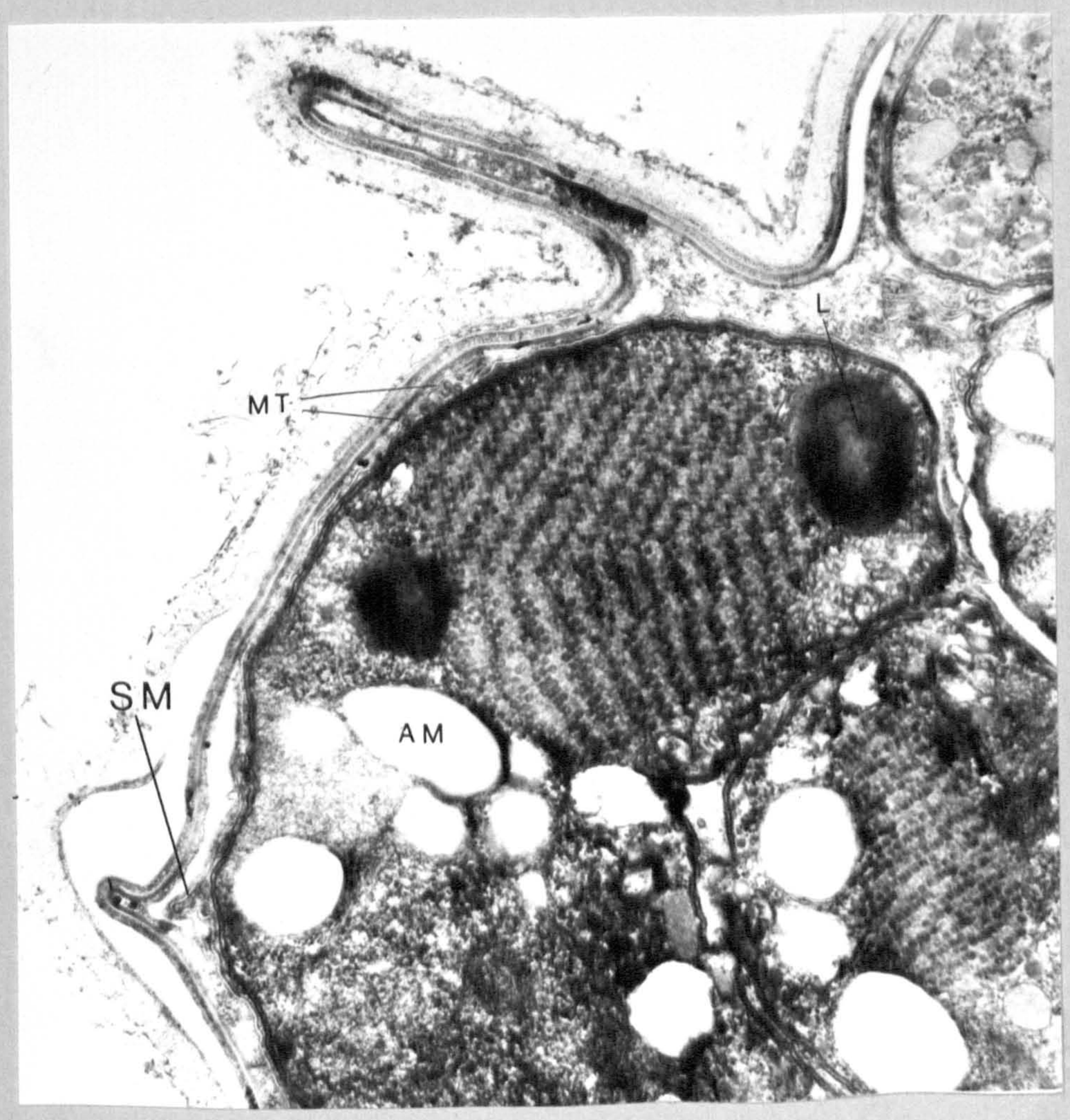
L
MT
SM
AM

The fine structure of the sporozoite

Plates 43 and 44

Details of the apical complex (x20,000) showing micronemes, rhoptries and the multistratose nature of the pellicle. The tripartite nature of the sporozoite wall is clearly seen in plate 43.

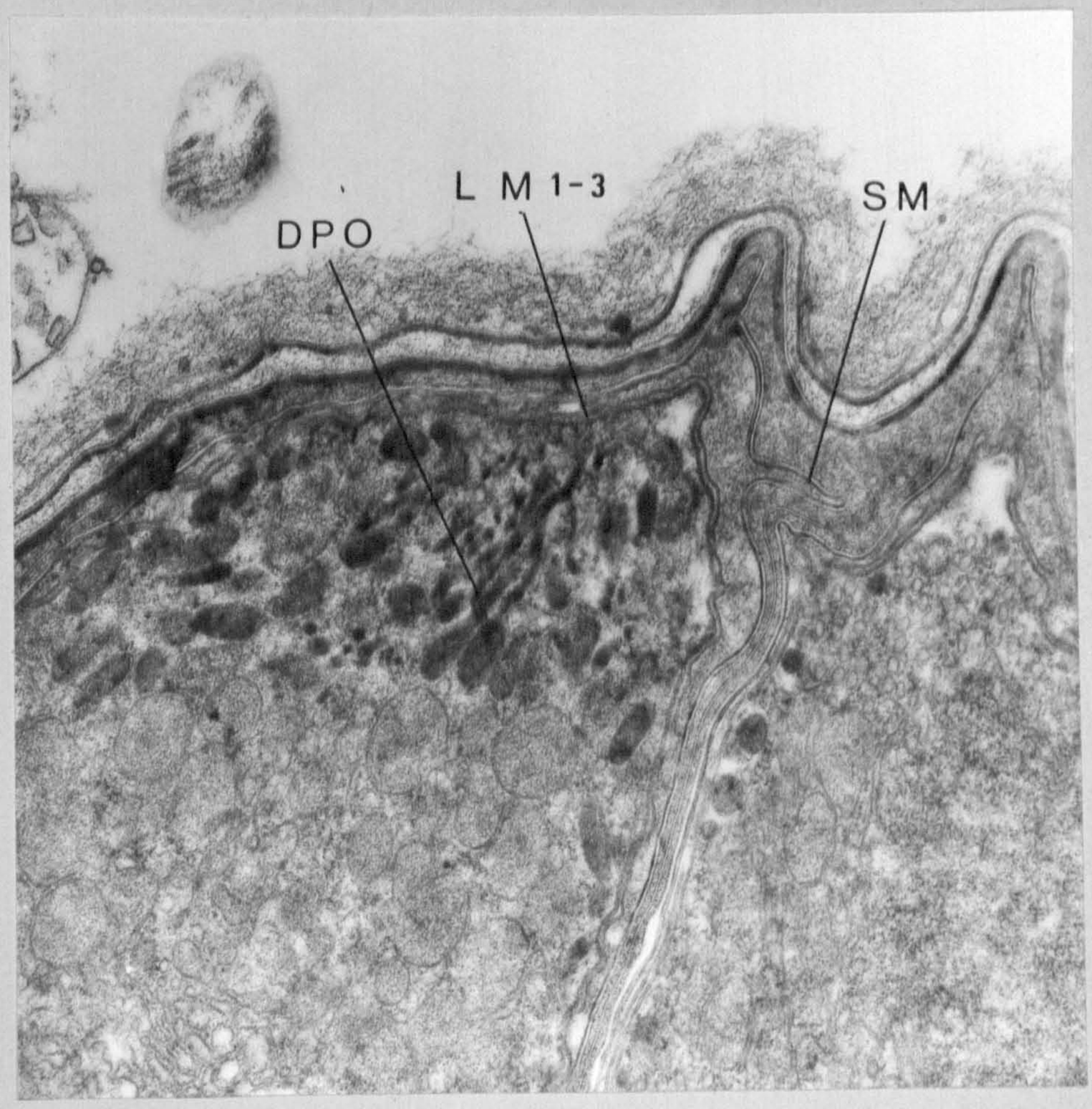
DPO
L M 1-3
SM

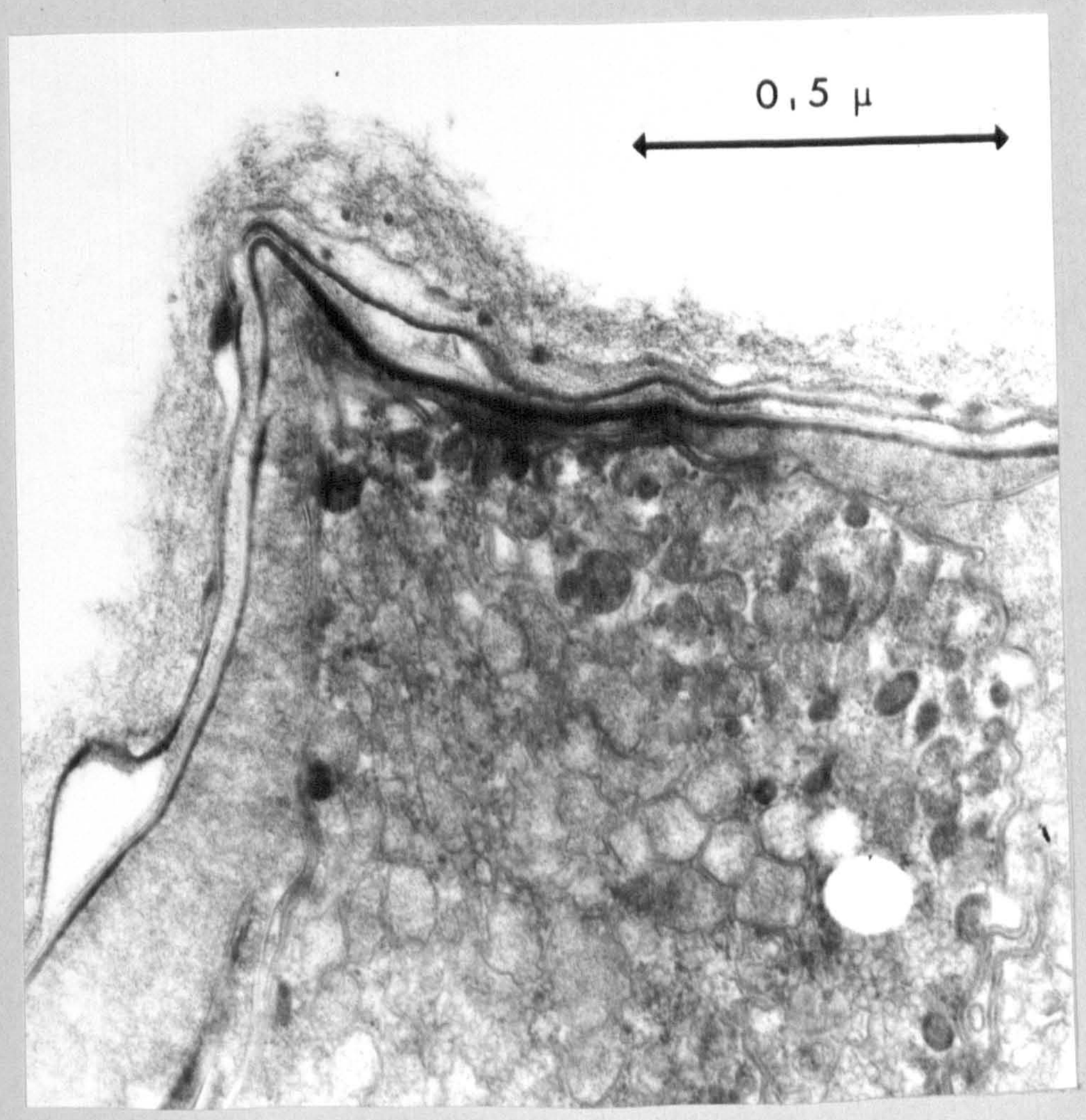
0,5 µ

The fine structure of the oocyst wall

Plates 45 and 46

Micropore-like structures of the oocyst wall with branching tubular processes are believed to be connected with thickening of the oocyst wall and are thought to be secretory rather than absorptive in function.

These structures appear to be unique to this coccidian. Unlike micropores they are only found in the oocyst wall. Magnification (a) X 25,000, and (b) 40,000.

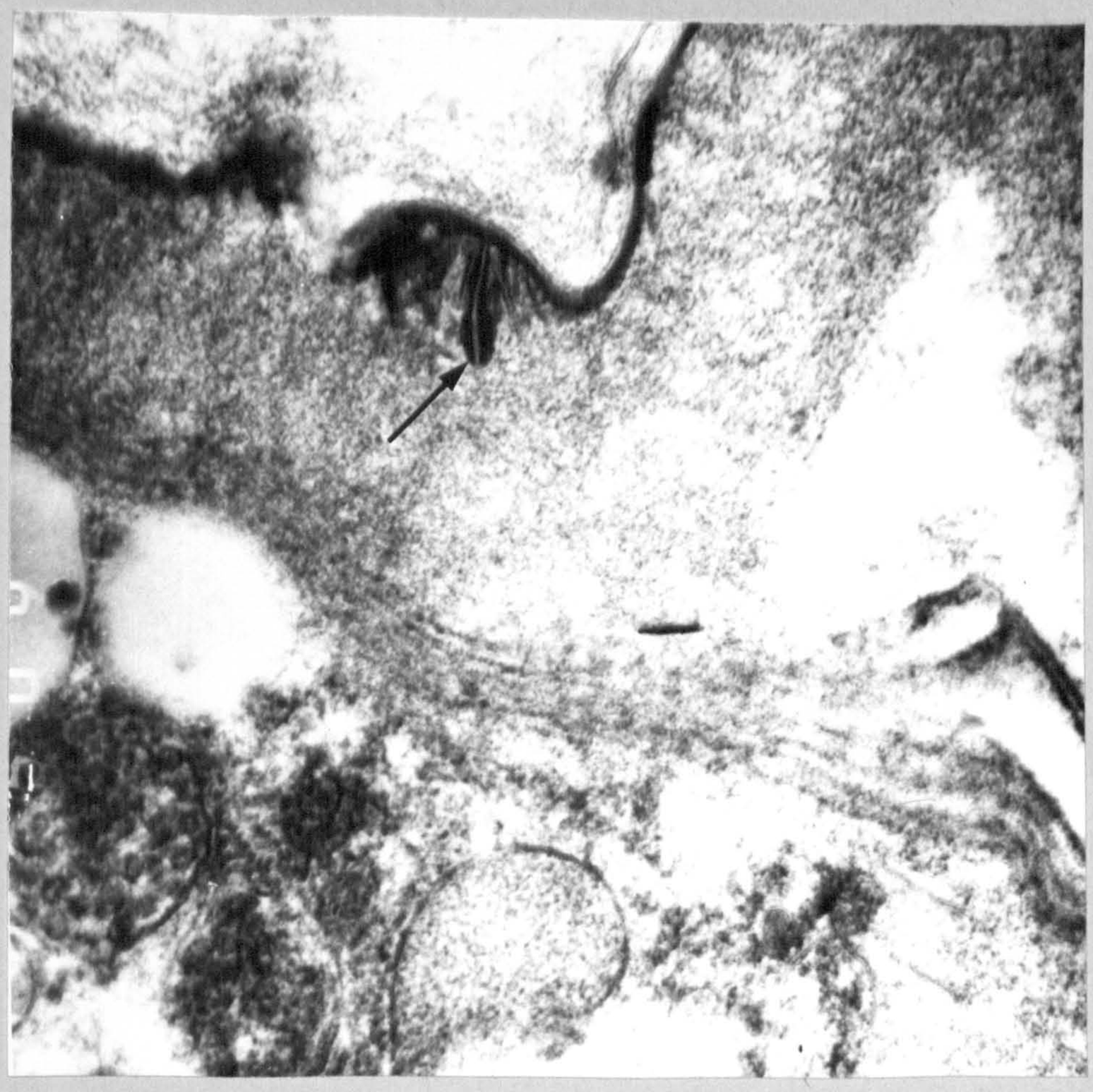

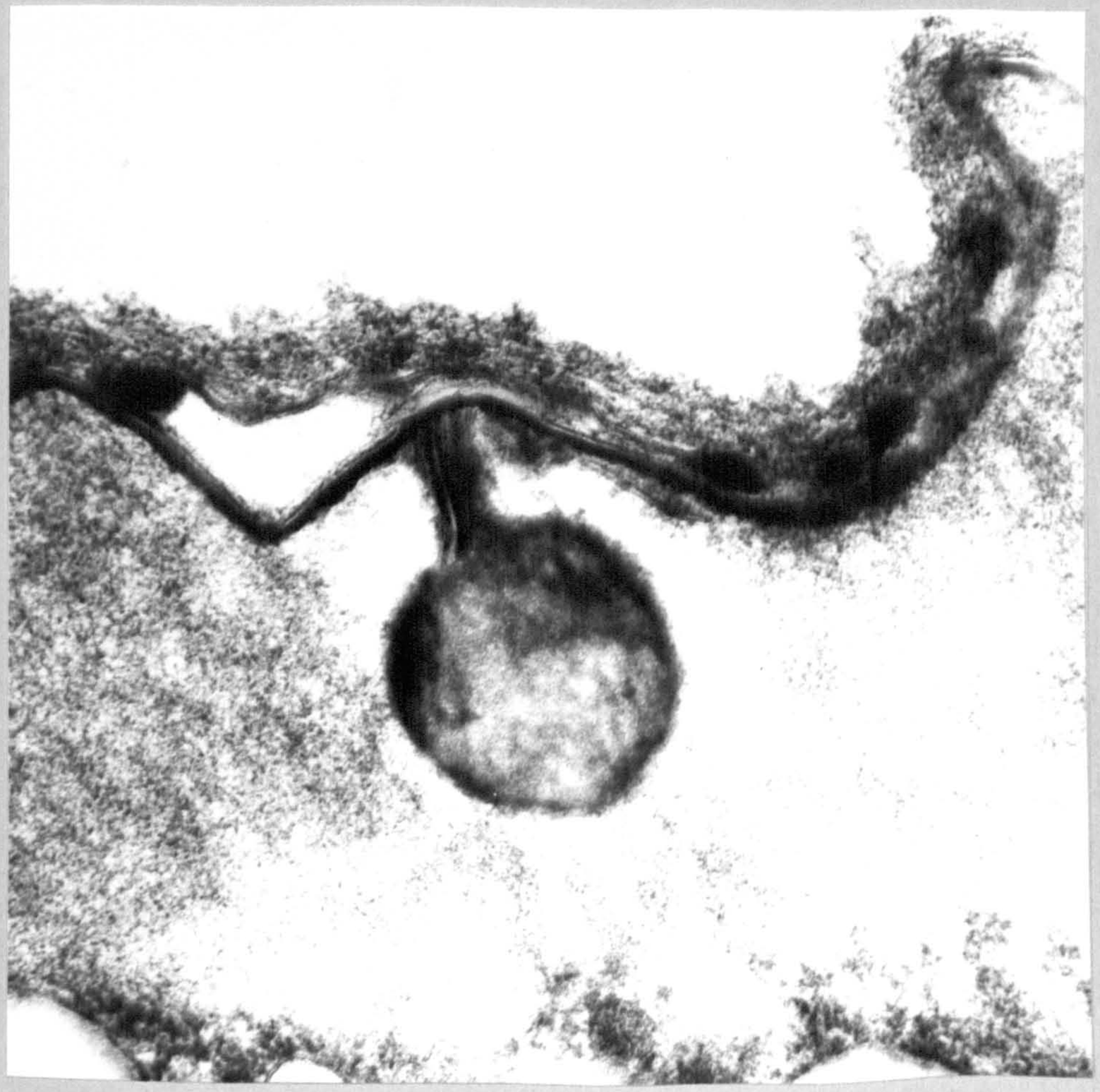

The fine structure of the sporozoite

Plate 47

Ultrastructural features of mature sporozoites. Tubular elements in cross section (magnification X 25,000).

Plate 48

Ultrastructural features of mature sporozoites. Rhoptries are bounded by a unit membrane and have a diameter of 100 nm. There is evidence of a central rod of the diameter of a microtubule.in the centre of the rhoptries.

Note the subpellicular microtubules (arrowed). Magnification of 40,000. Uranyl actetate/potassium permanganate staining.

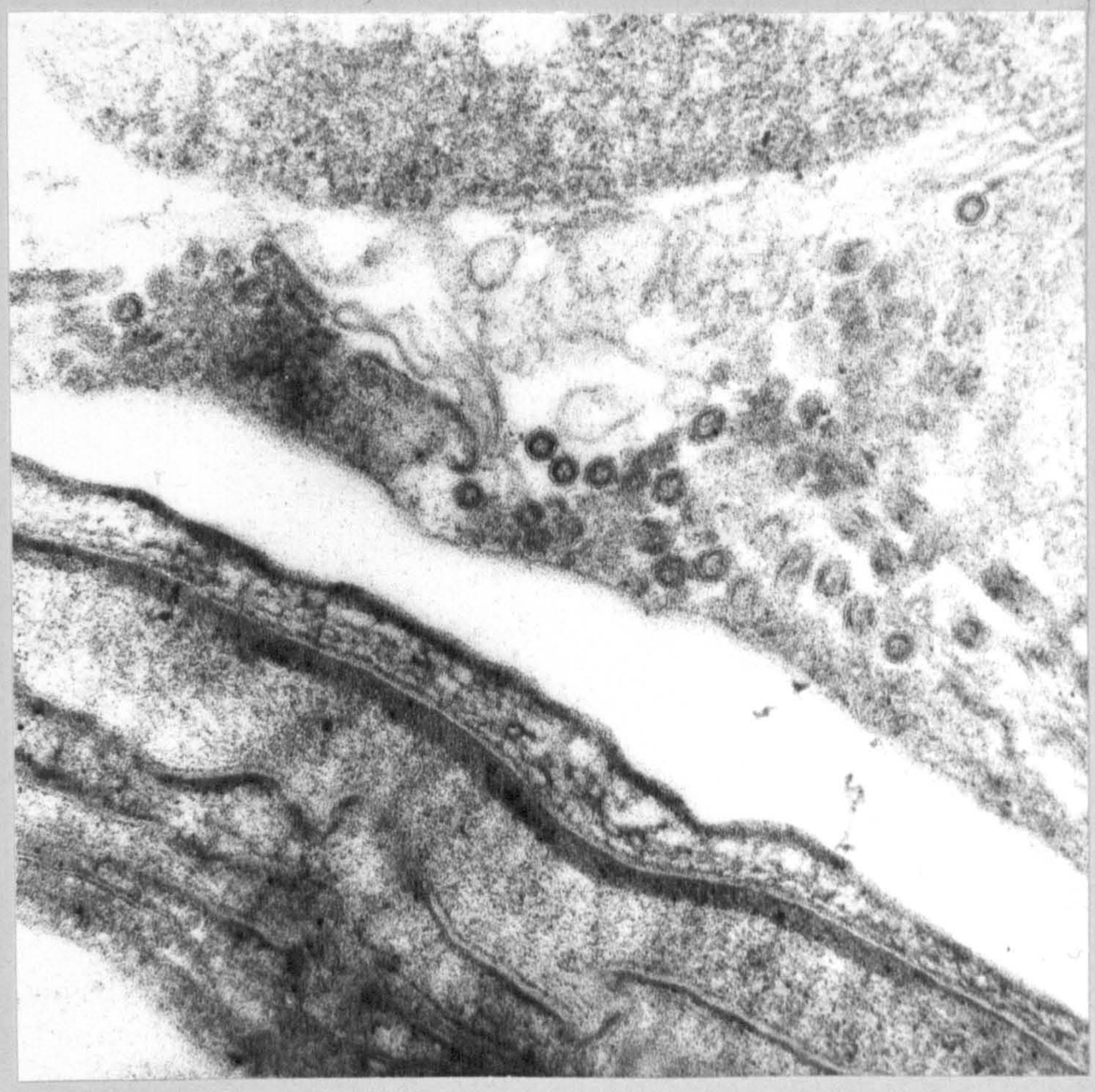

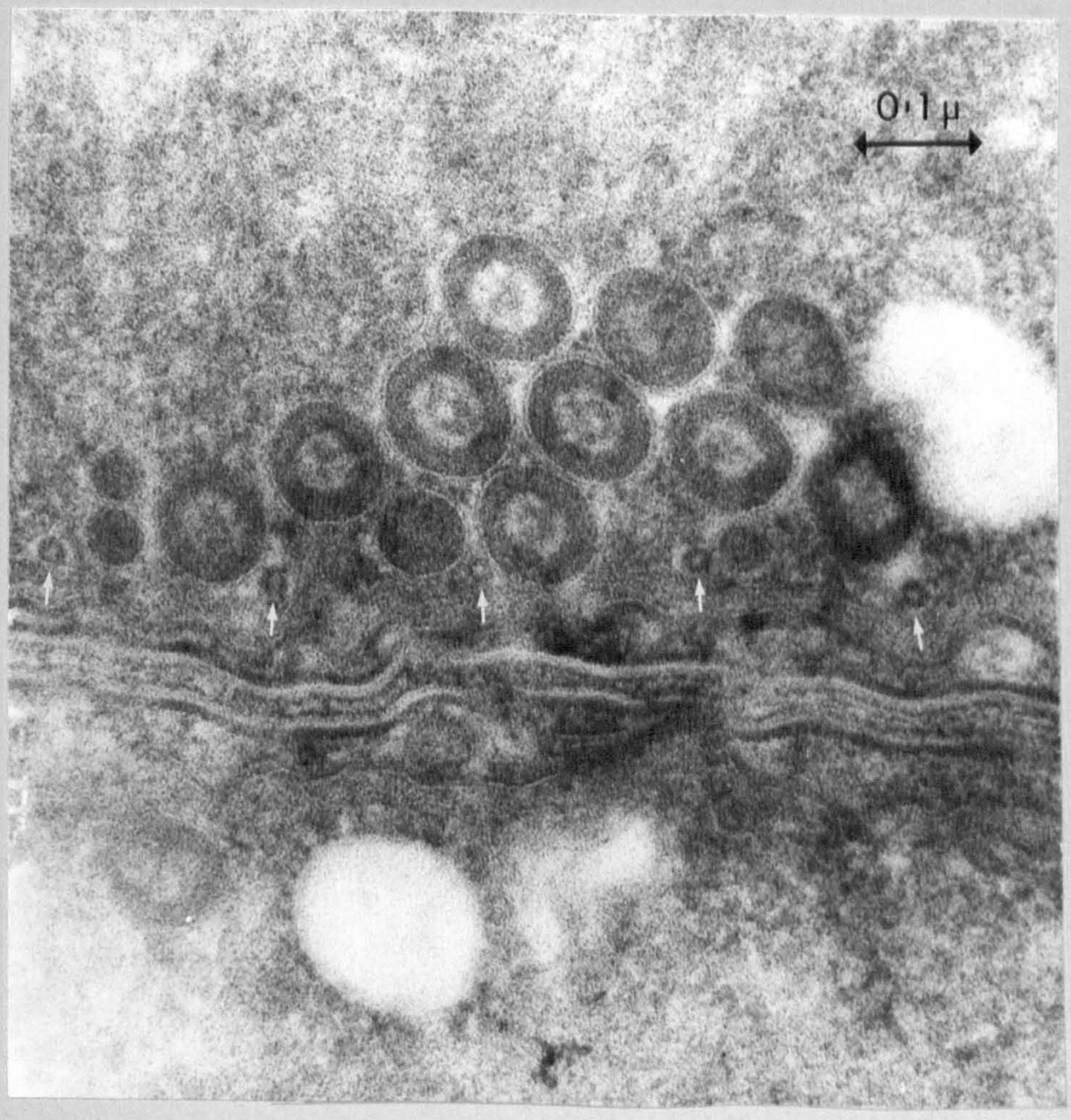
0,1 µ

Microgametogenesis of the coccidian

Plates 49 and 50

The early development of microgametes from the microgamont. Condensation of the nucleoplasm at the periphery of the microgamont cytoplasm. Numerous mitochondrial profiles having characteristic tubular christae surround the nuclei. Elevations of the surface occur above each nucleus. In this elevation are located the basal bodies from which the flagella of the microgametes later develop. The central cytoplasm is highly vesiculate and glycogen granules are much in evidence. Electron micrographs (X 15,000)

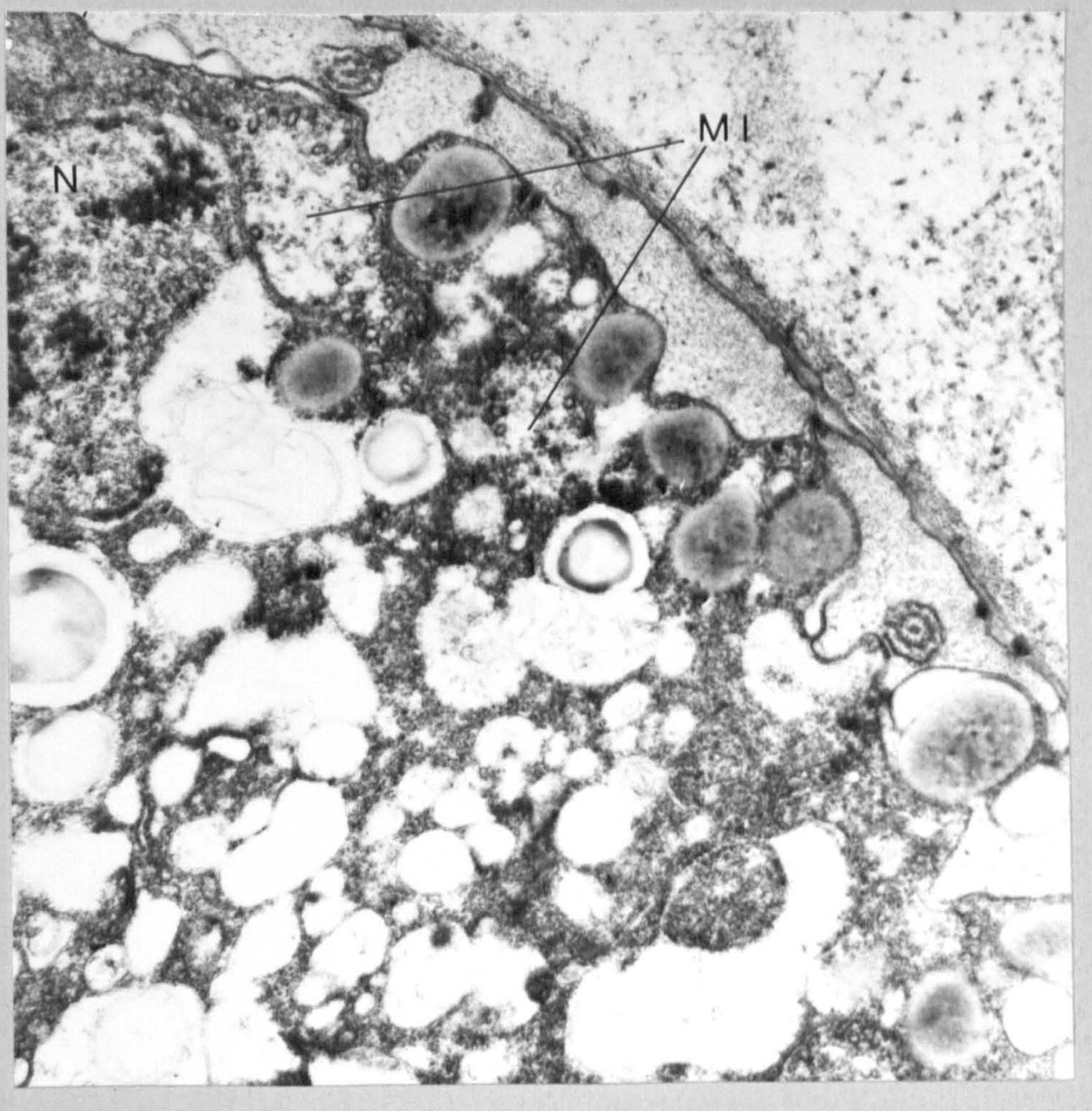
N
M I


0·4 μ
M I
B
N

Microgametogenesis of the coccidian

Plates 51 and 52

Electron micrographs of the differentiation phases of microgameto-genesis. The nucleus is contained within a cylindrical outgrowth of the peripheral zone of the cytoplasm of the microgmmont. The immature ovoidal microgamete ultimately becomes separated from the microgamont. A meshwork of microtu-ules in longitudinal section surrounds the basal body of the flagellum in the upper micrograph. In both, micro-tubules underlying the bounding membrane of the microgamete can be seen. Two basal bodies can be seen in the vicinity of the nucleus in the lower micrograph. Free axonemal progiles of flagella lie sub-pellicularly.

It seems likely that breakdown of the double layercd wall must take place to allow the microgametes to escape. See also text fig. 7. and plates 53 and 54.

Magn x 15,000

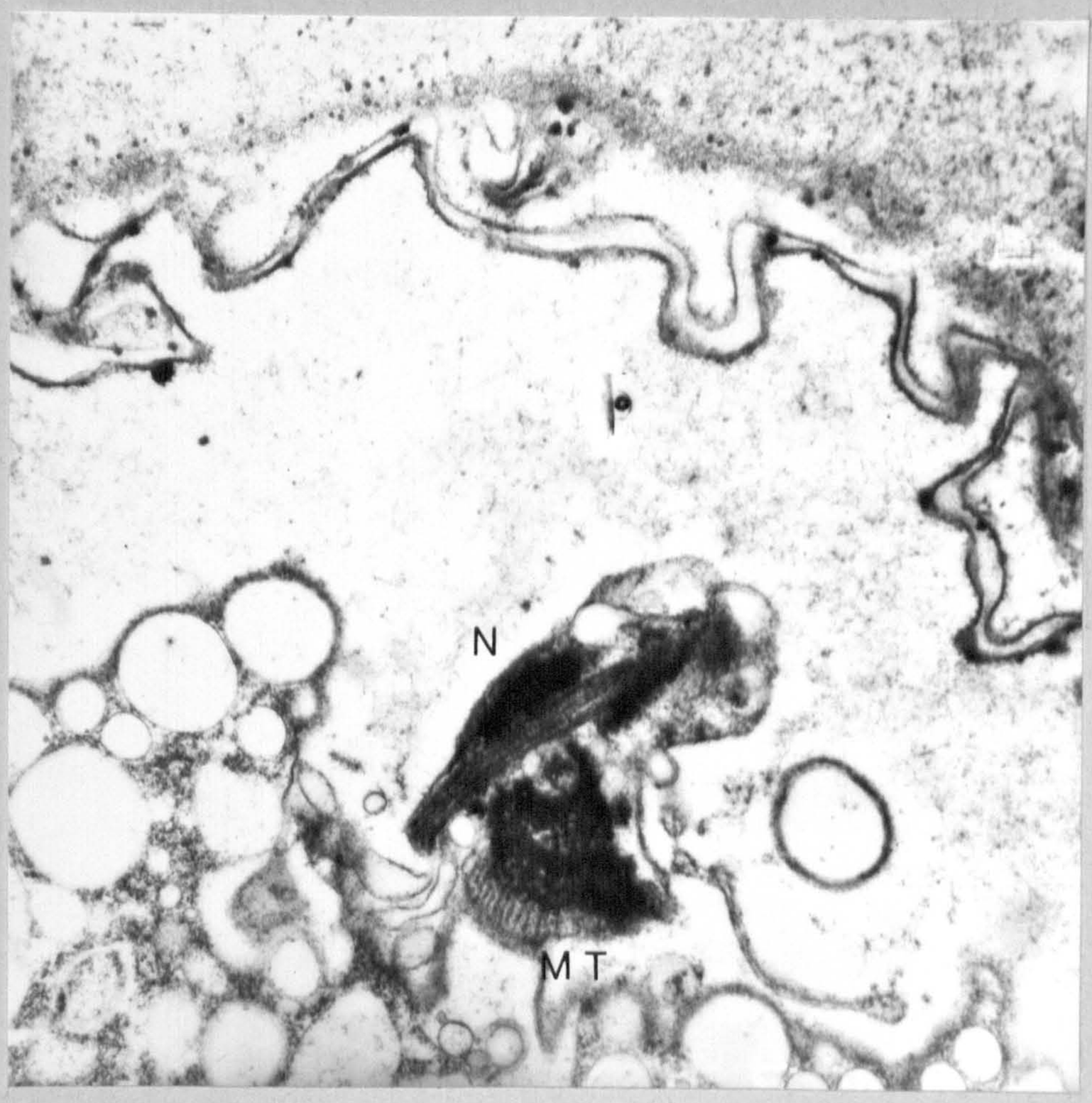
N
MT

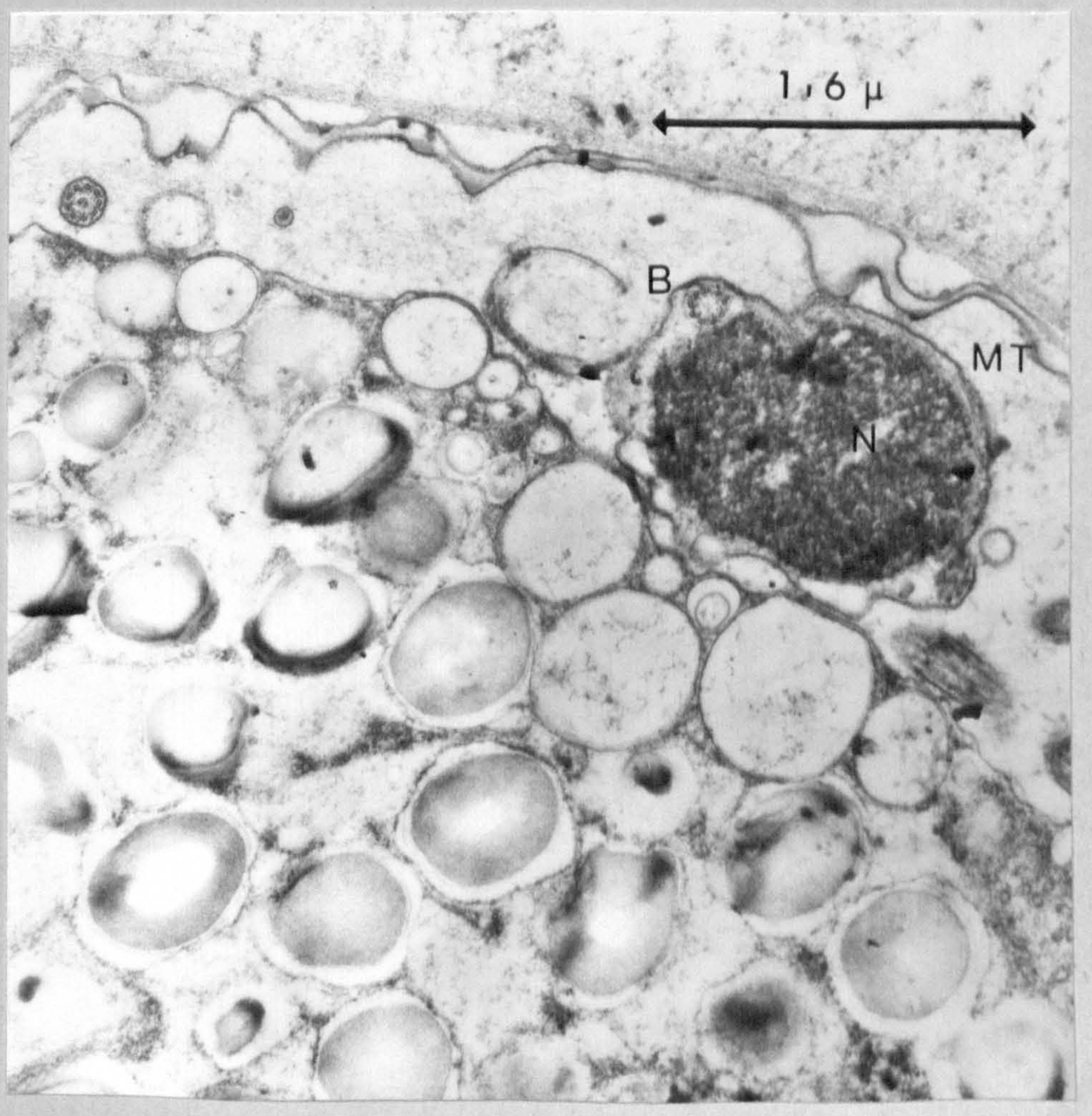
1,6 µ
B
MT
N

The macrogamont at fertilization and the fine structure of microgametes

Plate 53

A mature macrogamont post fertilization. Profiles of microgametes surround the macrogamont. In other species of coccidia it has been observed that a canal-like outgrowth of the nucleus approaches the surface and the microgamete penetrates only at this place. This appears to be the pattern in M. tellinovum.
Magn. x 8,000

Plate 54

As in the upper micrograph, numerous vesicles thought to be wall forming bodies lie immediately adjacent to the wall. Poly-saccharide granules are observed in close association with lipid inclusions and glycogen containing granules are scattered throughout the cytoplasm. The contents of these vesicles has been inferred from the appearance of similar stages in the genus Eimeria. Profiles of the spheroidal biflagellate microgametes show the band of 12 microtubules seen in TS in the upper and LS in the lower. The spheroidal mitochondrion lies within a cup-shaped nucleus containing condensed chromatin. (Magn. x 15,000)

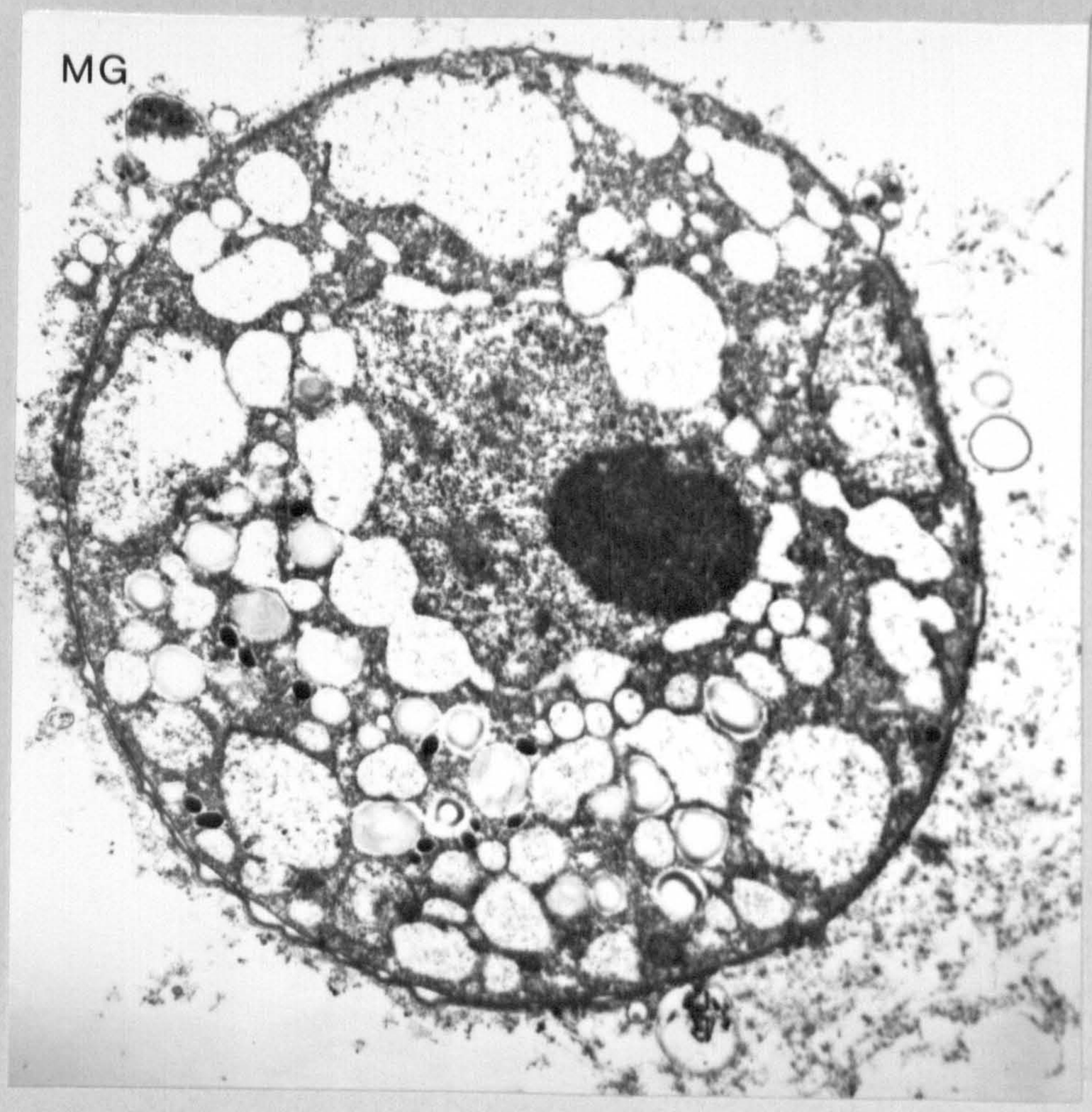
MG

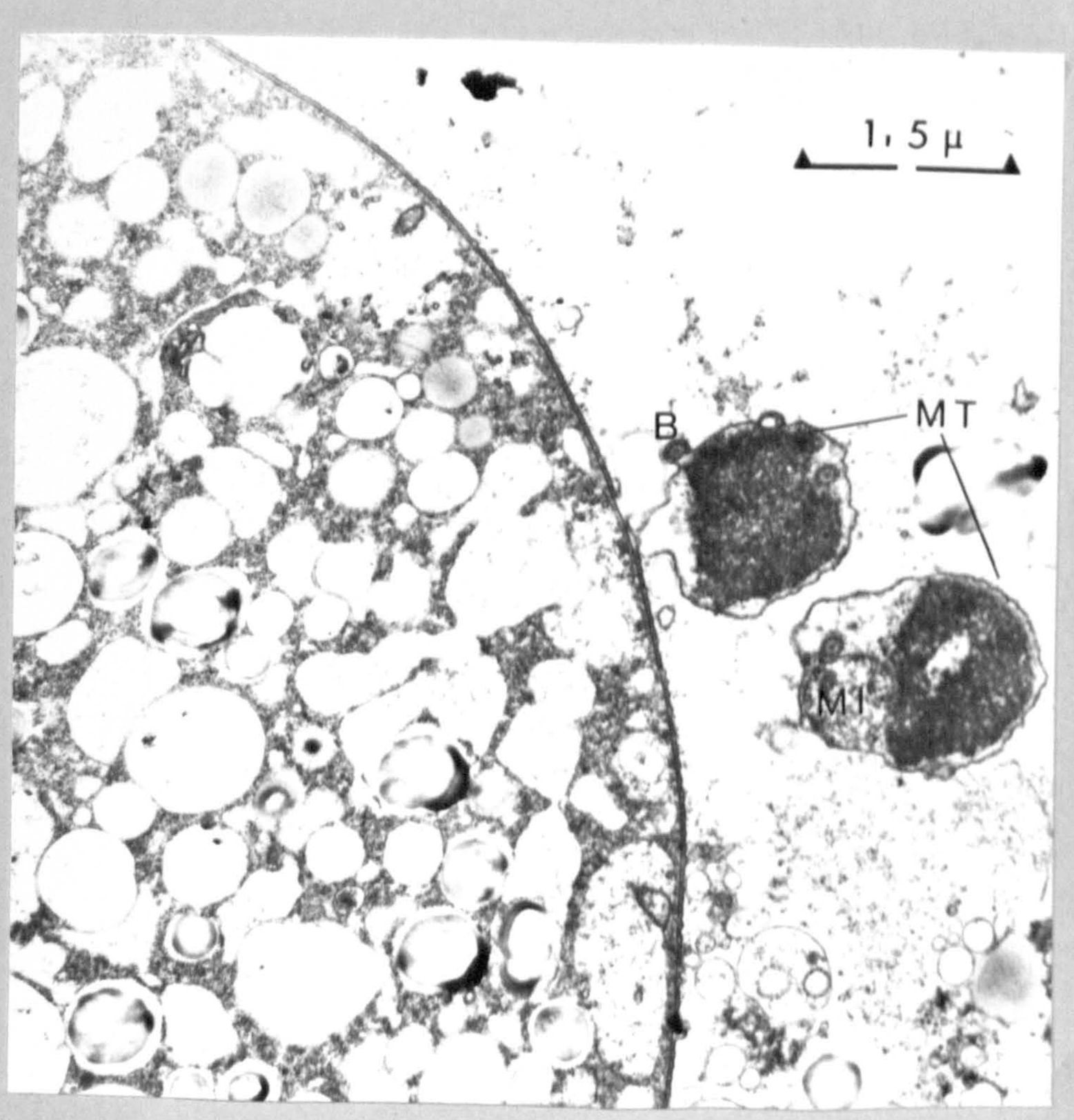
1,5 µ
B
MT
M1

Plate 55

The vestigial sporoplasm (X 8,000) of the microgamont following release of microgametes. The double layered envelope in this instance is surrounded by a mucilaginous layer. A maturing microgamont with microgametes forming is visible at lower right.

Plate 56

Naked sporoplasm (X 8,000) believed to be from a microgamont is shown at centre right. This e.m. is serial with the above.

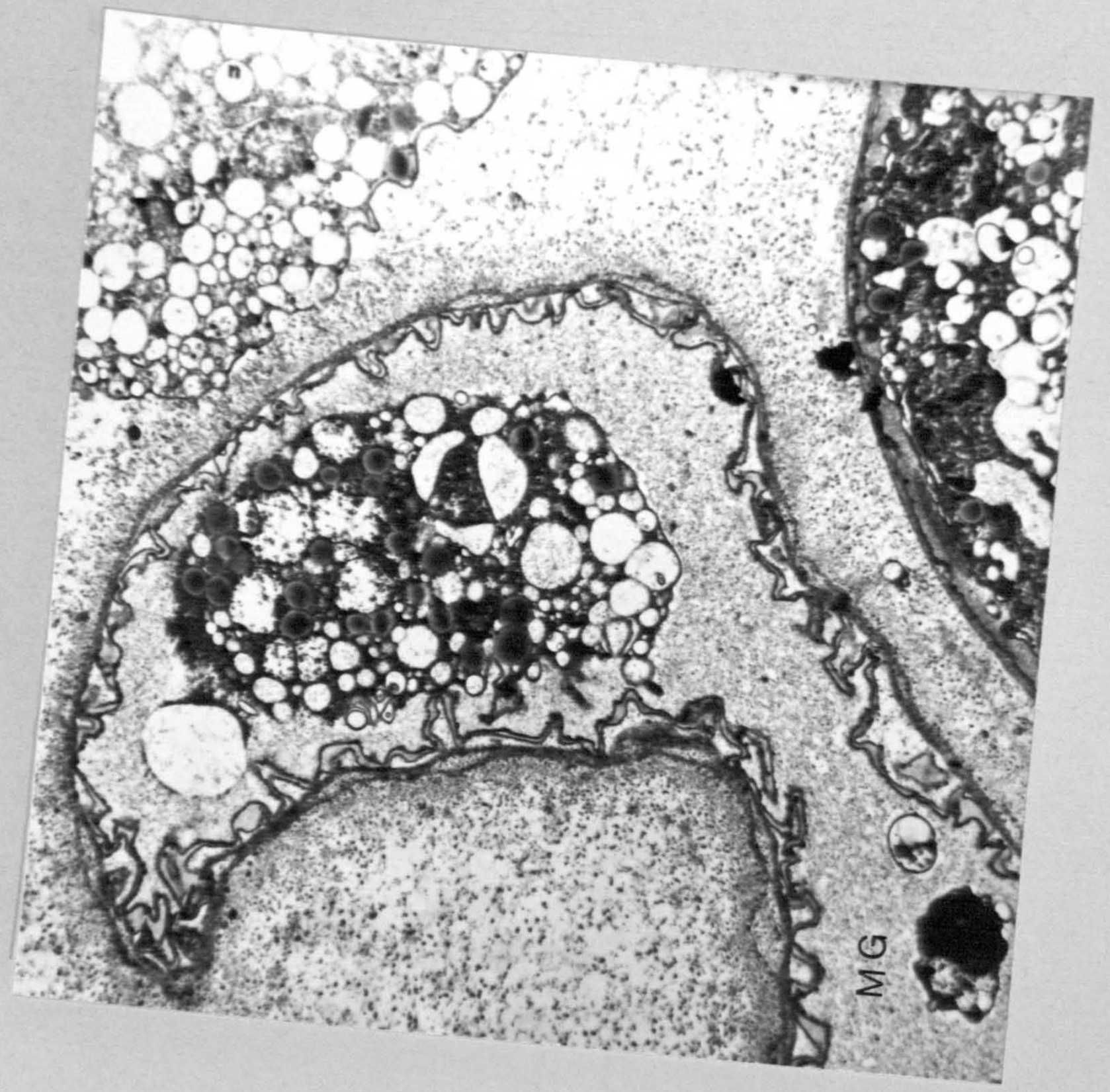
M.G

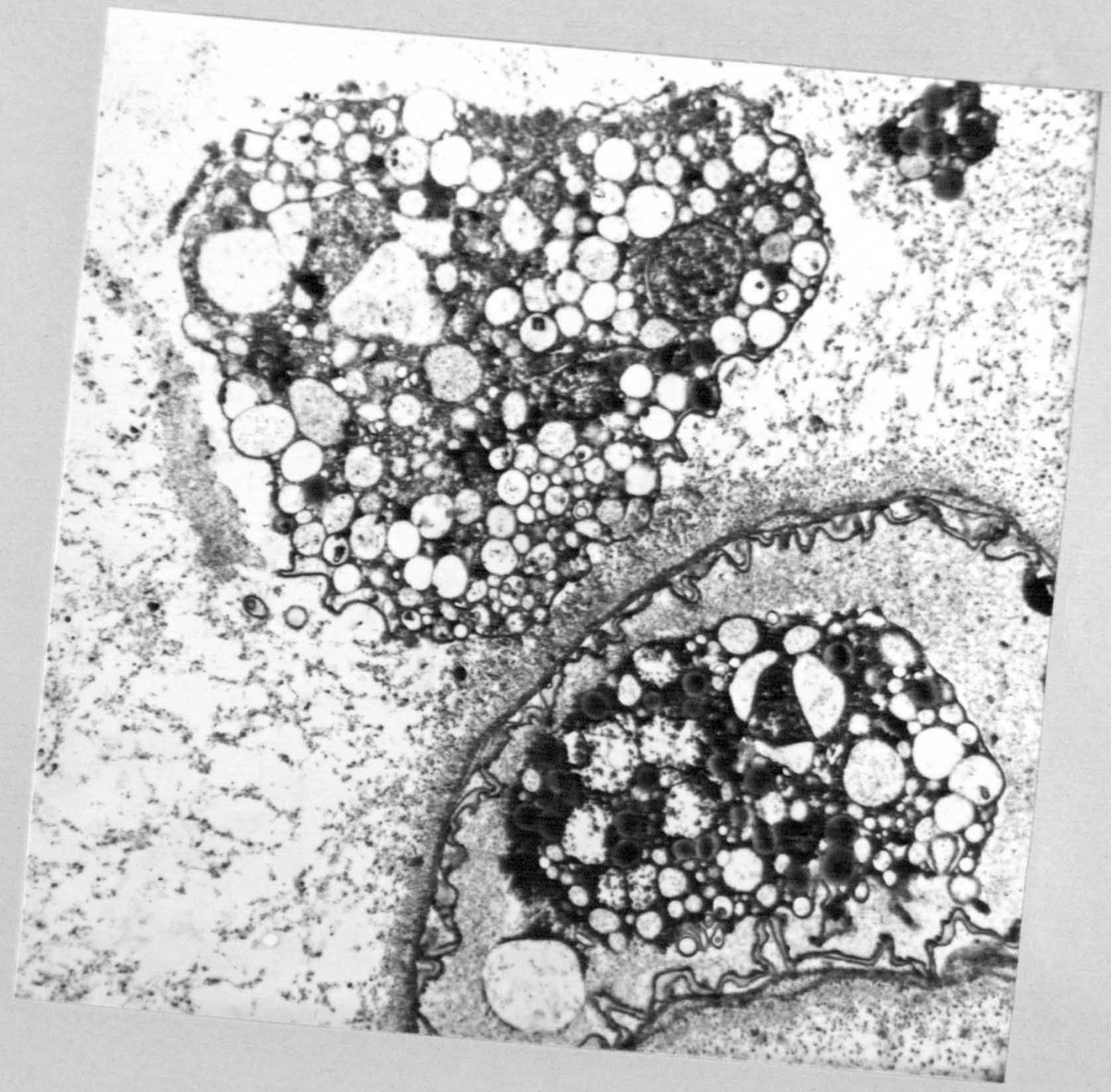

The Infectious Units of M. Tellinovum

Plate 57

A sporozoite (trophozoite) in the intralobular haemocoele of the digestive diverticuli post release from a sporocyst. The parasite appears to be enveloped in the cytoplasm of a host amoebocyte. Alternatively the surrounding cytoplasm might be the cellular debris from a ruptured cell.

Plate 58

Electron micrograph (X 5,000) of the above sporozoite showing details of the cytoplasm and the nuncleus. Profiles of three mitochondria can be seen. The apical complex of micronemes, rhoptries and microtubules are in evidence but no micropore can be seen. The characteristic double layered pellicle (see plates 43, 44 59 and 6o) can be seen.

SZ

RC

n

Infectious units of the coccidian

Plate 59

This low-power (x1,500) electron micrograph of a primary germ cell of the ovary embedded in a mucilaginous matrix shows that it has been penetrated by a merozoite (trophozoite) of the coccidian. The fissure at the posterior end of the parasite suggests that first division is about to take place.

Plate 60

This electron micrograph (x 15,000) of the merozoite shows the rhoptries and micronemes of the apical complex and a band of subpellicular microtubules. Note the close association between the parasite and the host's cytoplasm.

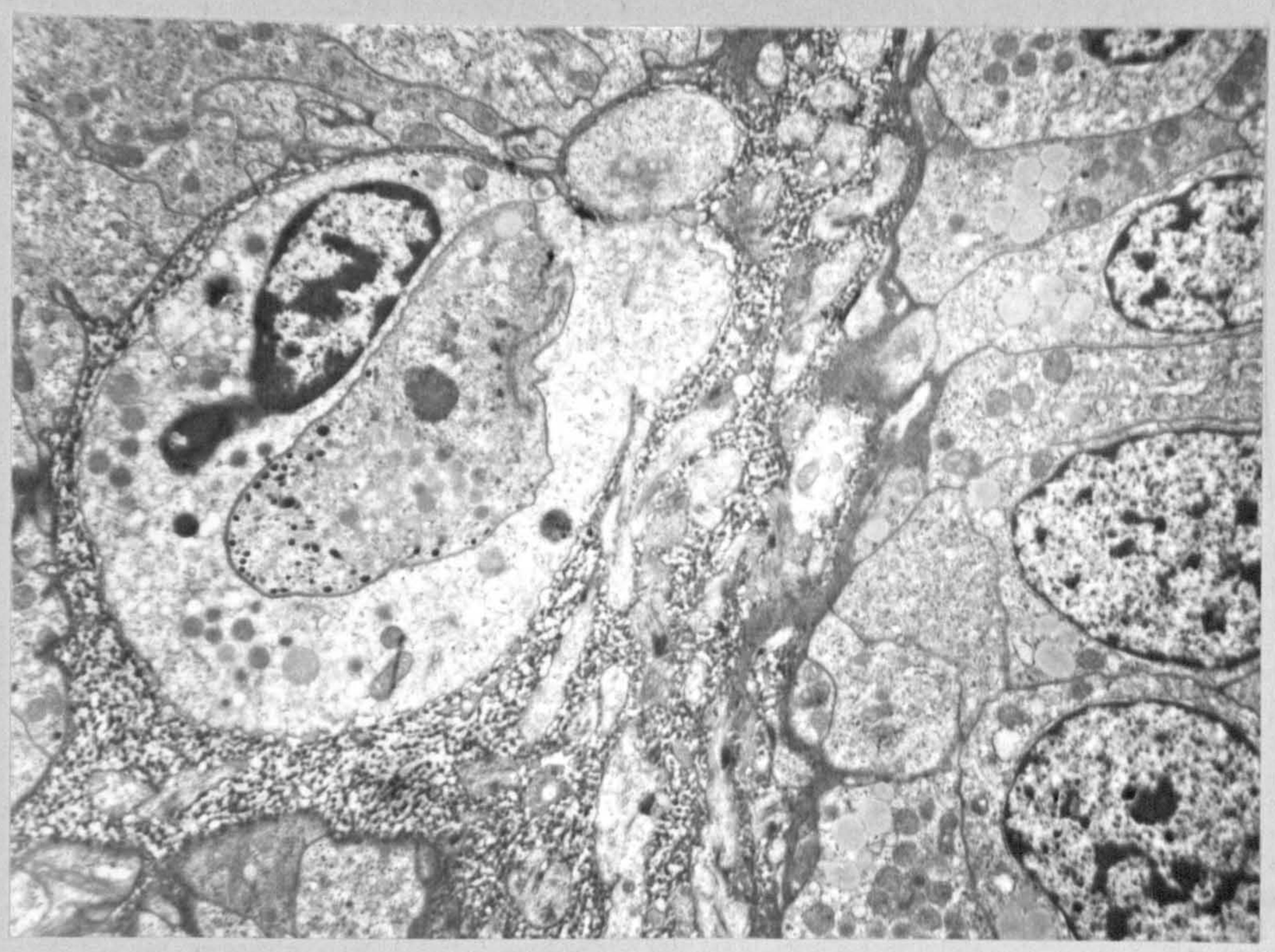

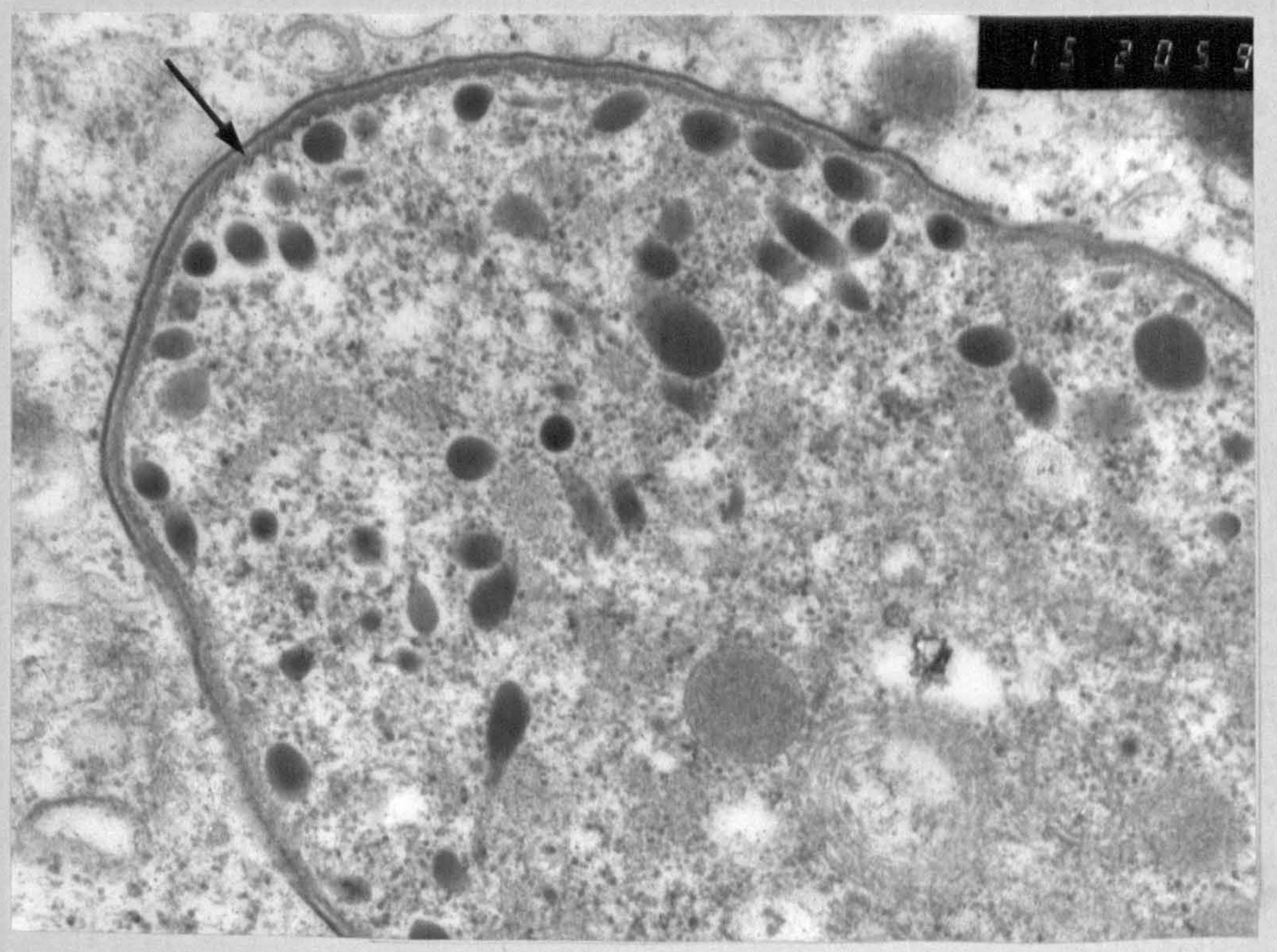
15 20 53

Scanning electron micrographs of the coccidian oocyst

Plates 61, 62 and 63

This series of scanning electron micrographs show the architecture of the oocyst wall and bear out the evidence from transmission electron micrographs that the walls of the oocyst are crenulate at maturity.

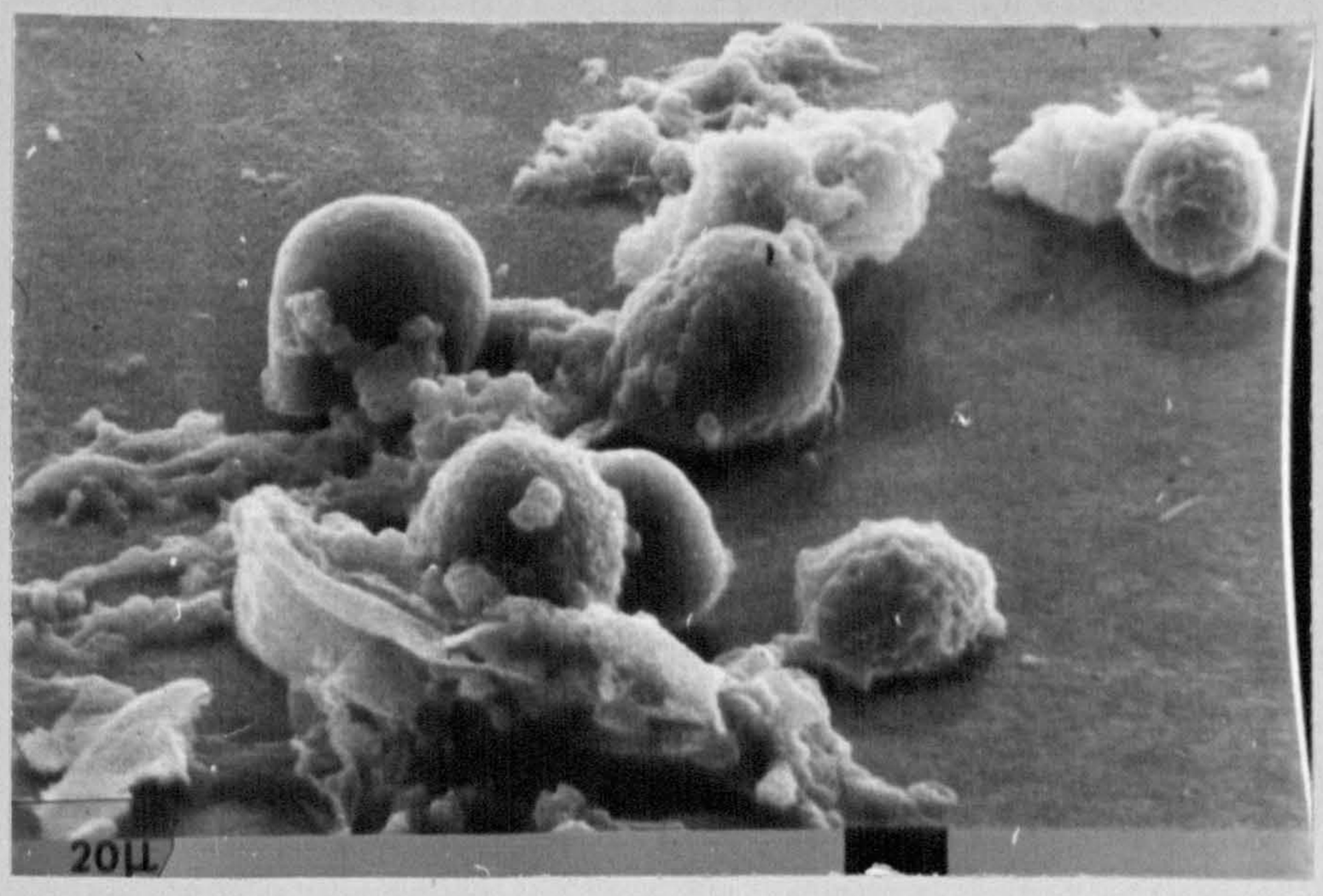
20μ

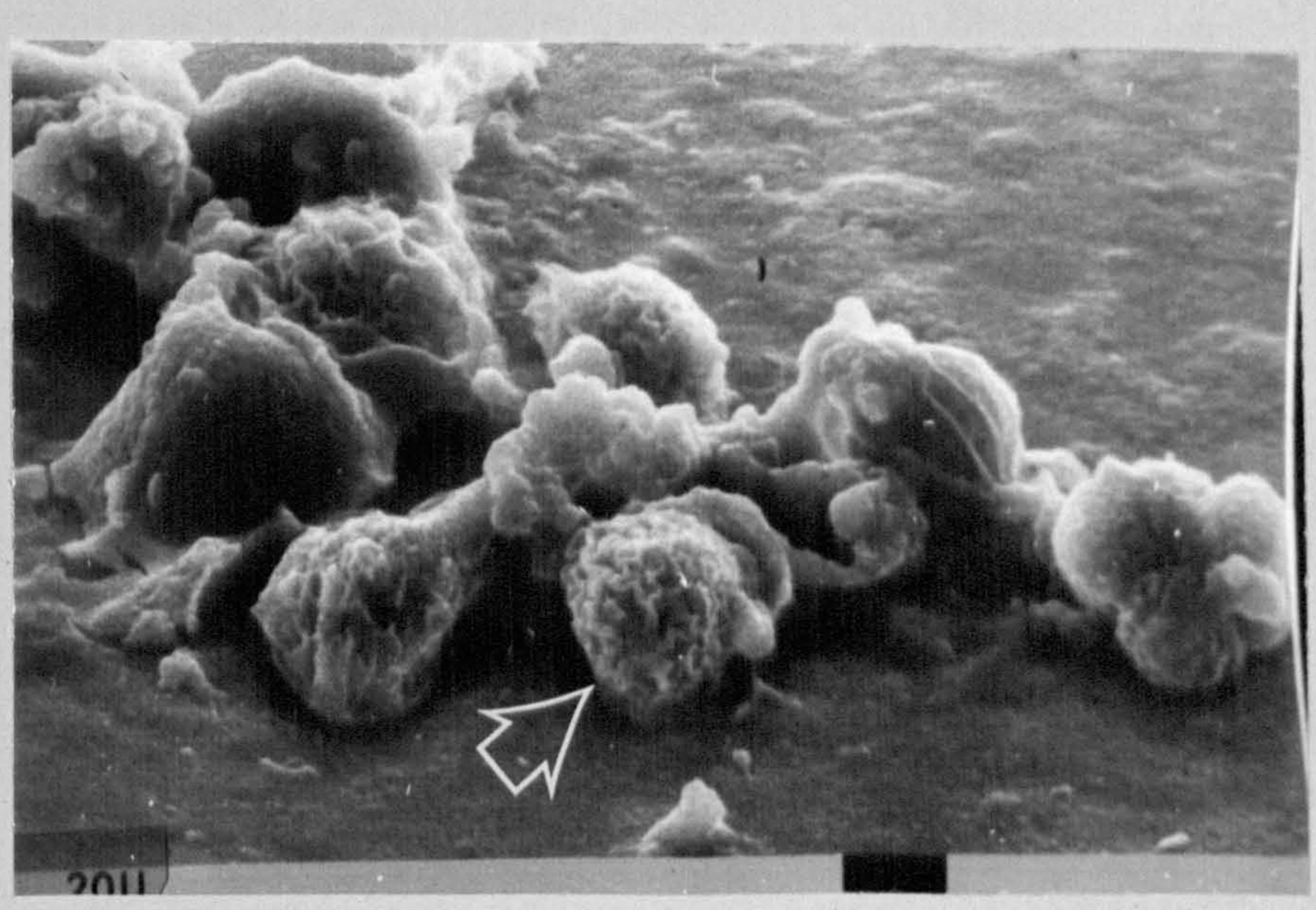
20μ

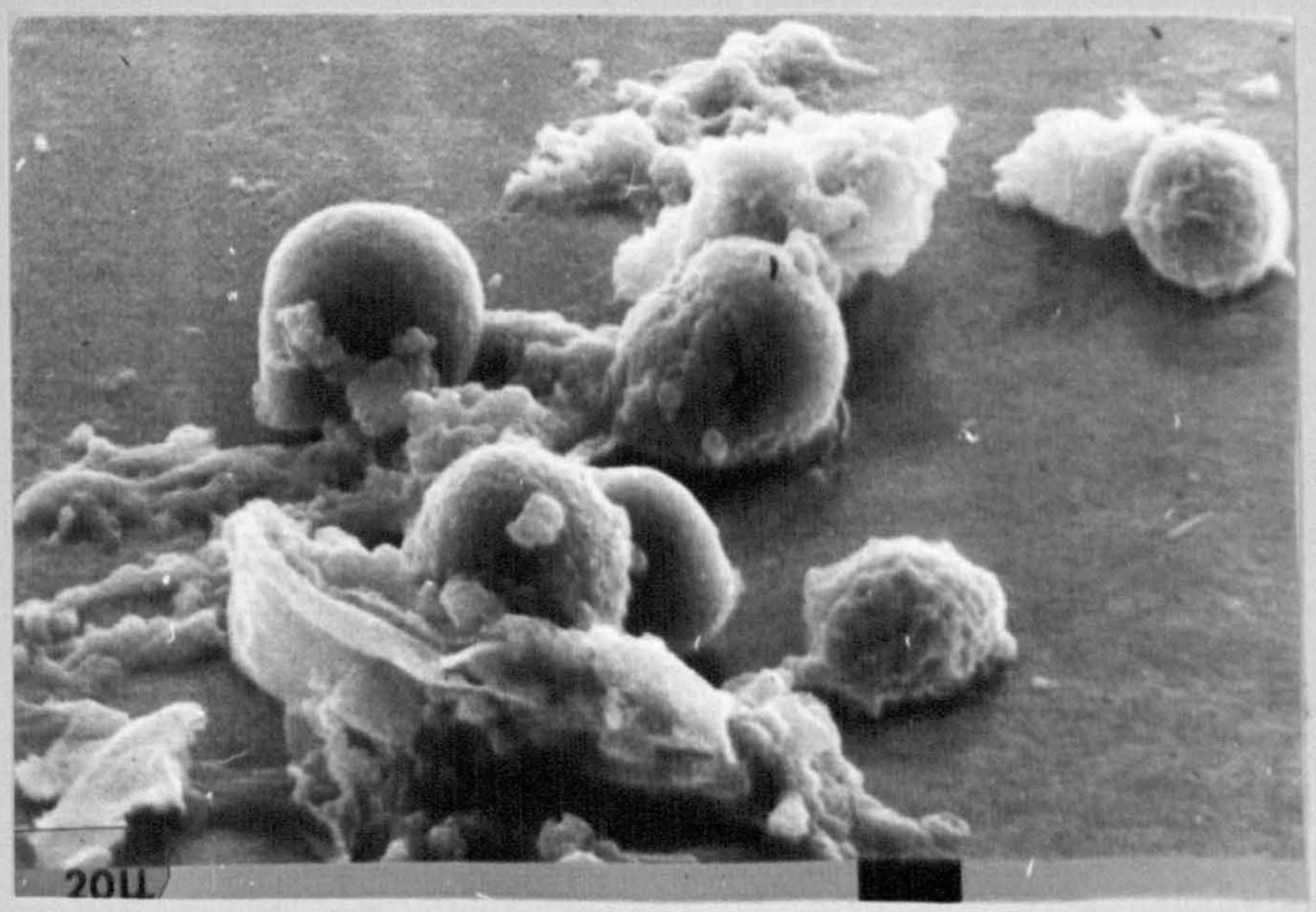
20μ

Degeneration of the coccidian

Plates 64 and 65

Fibrocytic encapsulation and phagocytosis of the coccidia by host amoebocytes and the formation of fibroblast-like cells have been observed by light microscopy. (see plates 31 and 32). These electron micrographs confirm the light microscope observations and show the necrotic remnants of various stages in the life cycle of the coccidian which seem to consist mainly of amylopectin and glycogen granules.

upper plate - 1,500

lower plate - 2,000

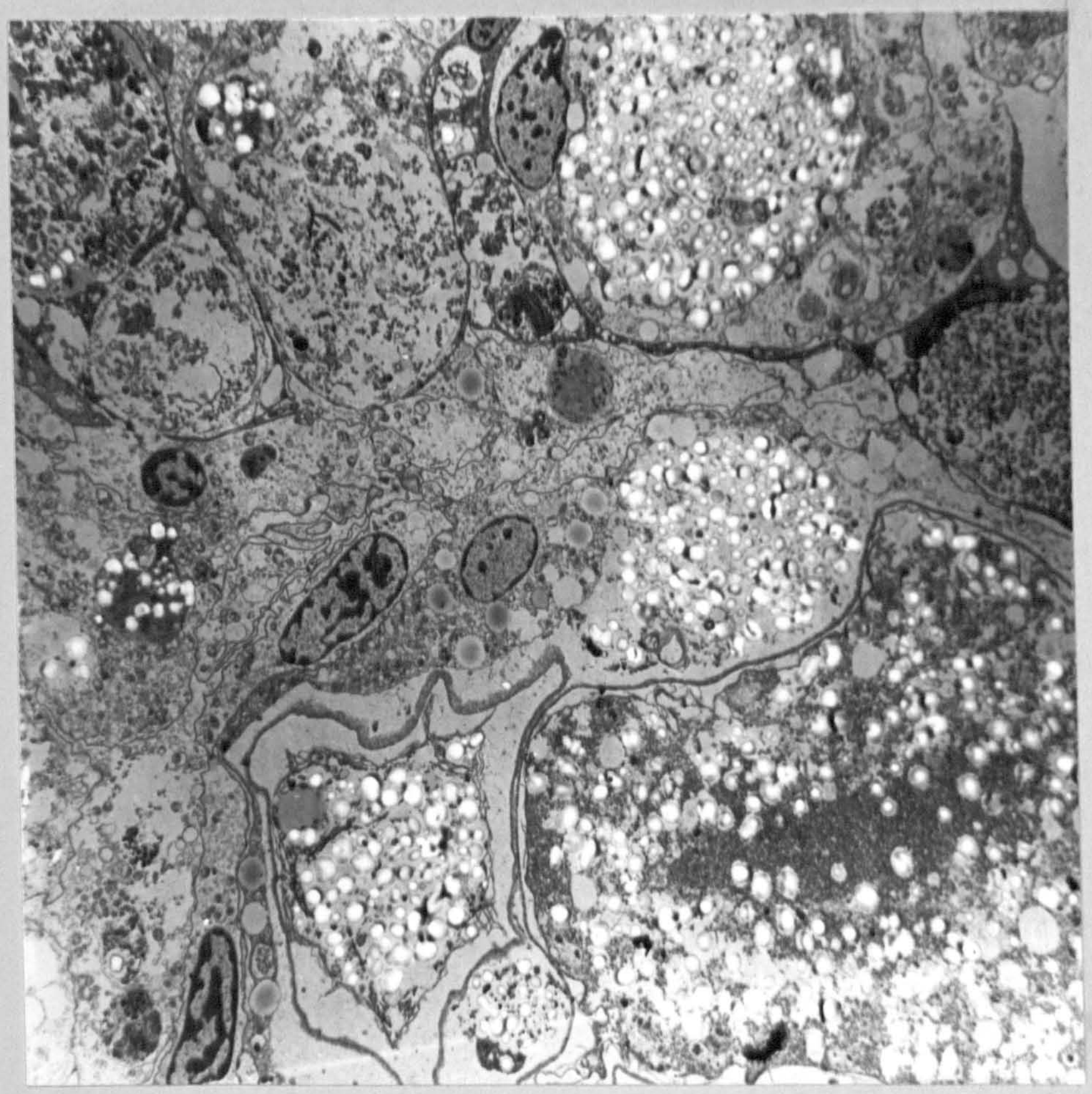

Defence mechanisms of the host, Tellina

Plate 66

A collection of mononuclear amoebocytes adhering to the basement membrane of a lobe of the digestive gland acini. These cells are phagocytic and migrate freely through epithelial tissues to sites of irritation and invasion by parasites. This form of leucoyytosis was commonly observed (see plates 21, 22, 31 and 32). Endothelial cells containing secretory cells line this sinus. (magn. x 2,000)

Plate 67

A multinucleate (granular) amoebocyte. These phagocytic cells are common in tissues containing parasites and are thought to initiate encapsulation.

(Magn. x 4,000)

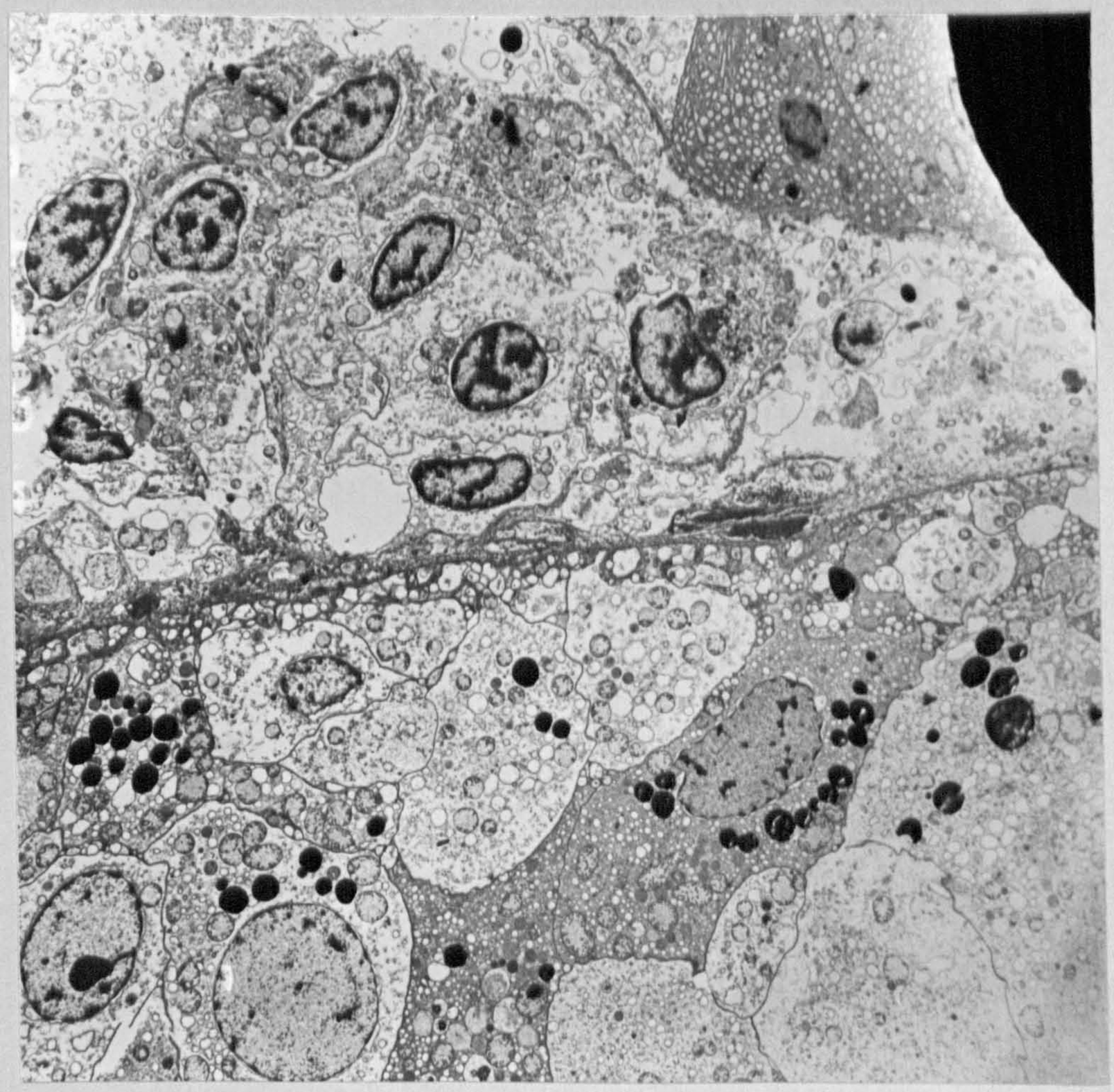

Hyaloklossia sp. A coccidian of the kidney of Tellina.

Plate 68

The kidney of Tellina showing the numerous oocysts and sporozoites of a coccidian parasite thought to be of the genus Hyaloklossia - perhaps H. pelseneerii.

(Magn x 200)

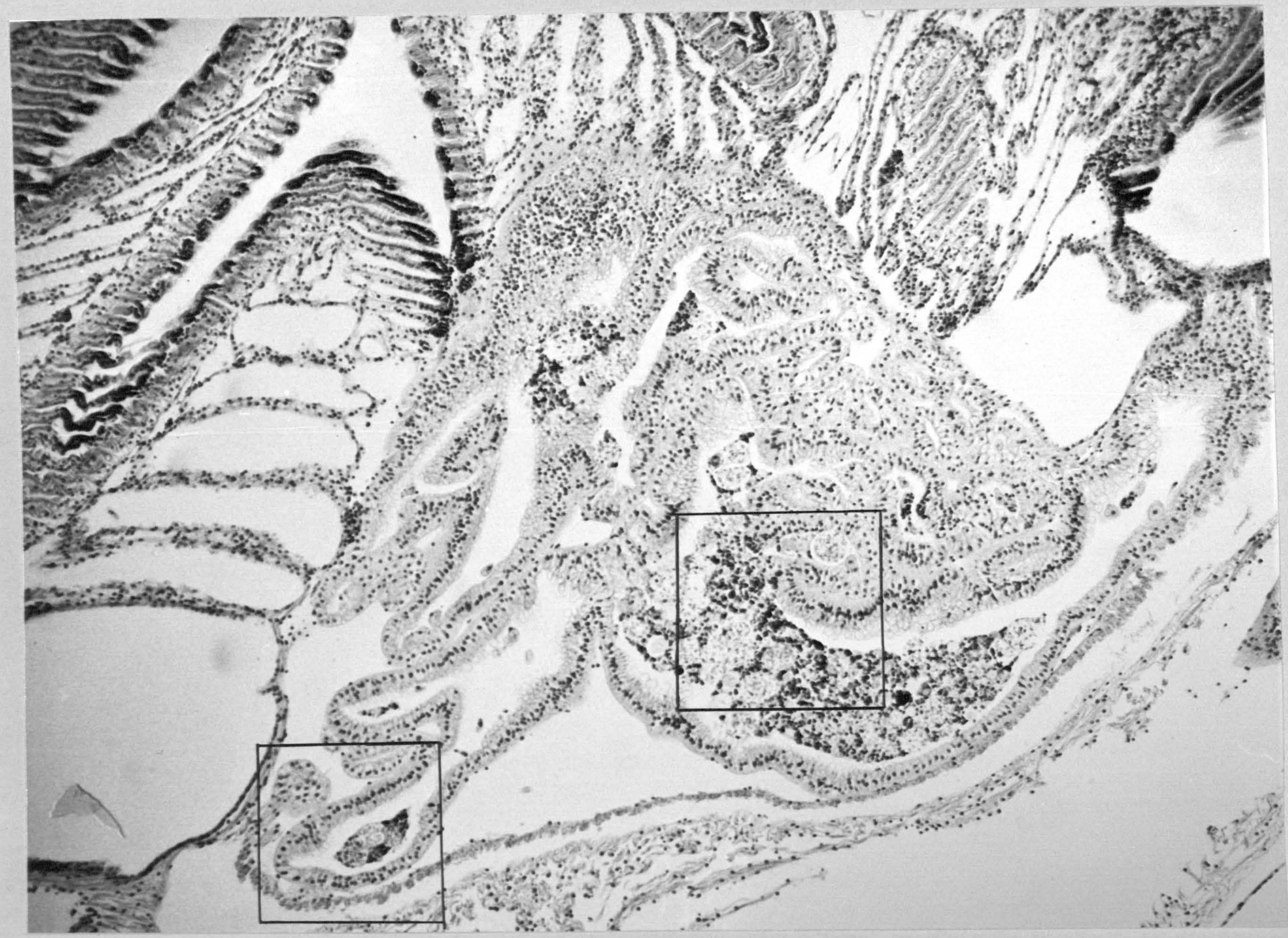

Hyaloklossia sp. a coccidian parasite of the kidney of *Tellina*.

Plate 69

Detail from plate 68. Note the elongated paired sporozoites and the massive leucocytic inflitration of the kidney lumen,

Plate 70

Sporocysts with elongate paired sporozoites enmeshed by granular and agranular amoebocytes.

(Both plates, magn. x 800)

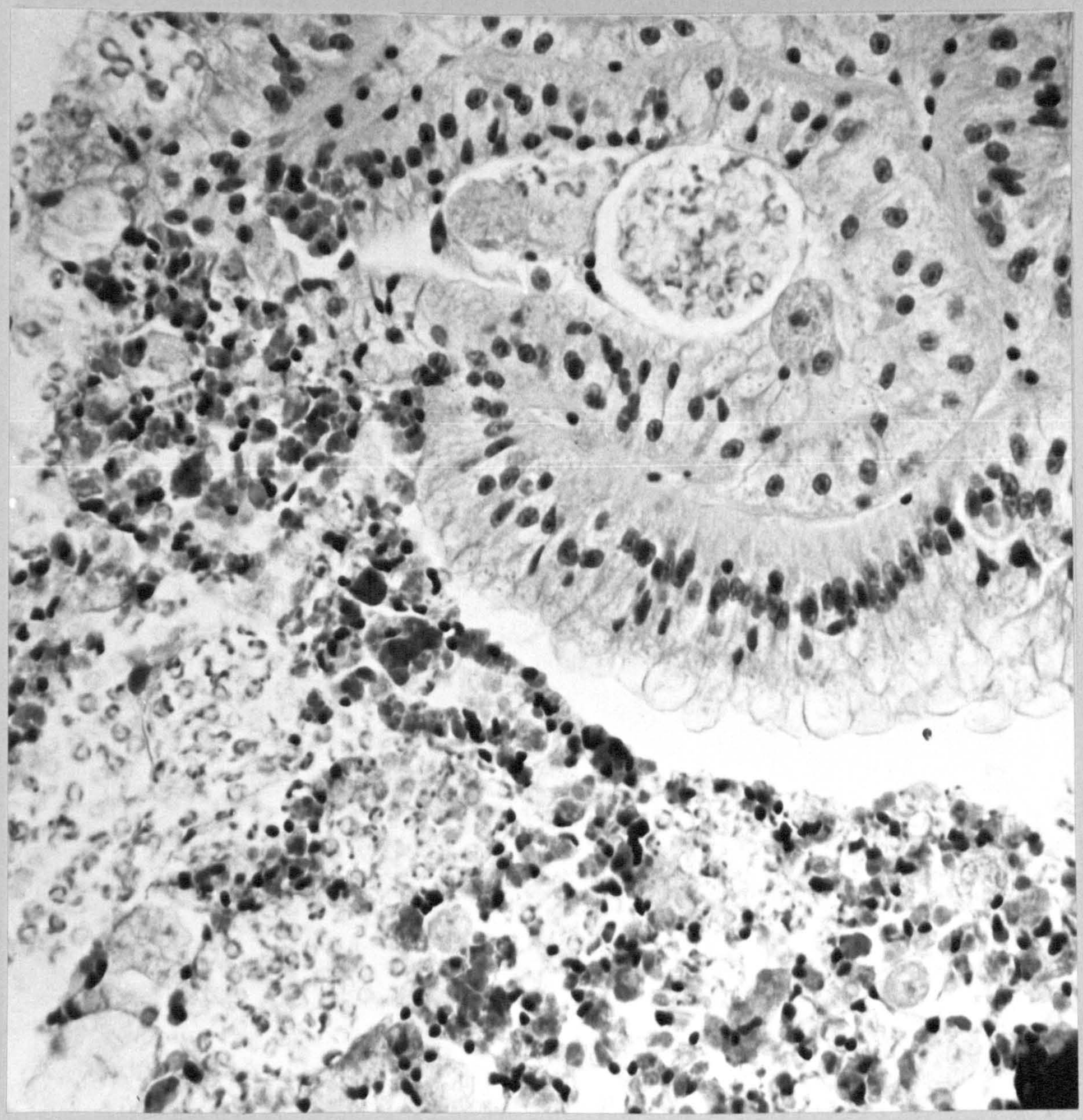

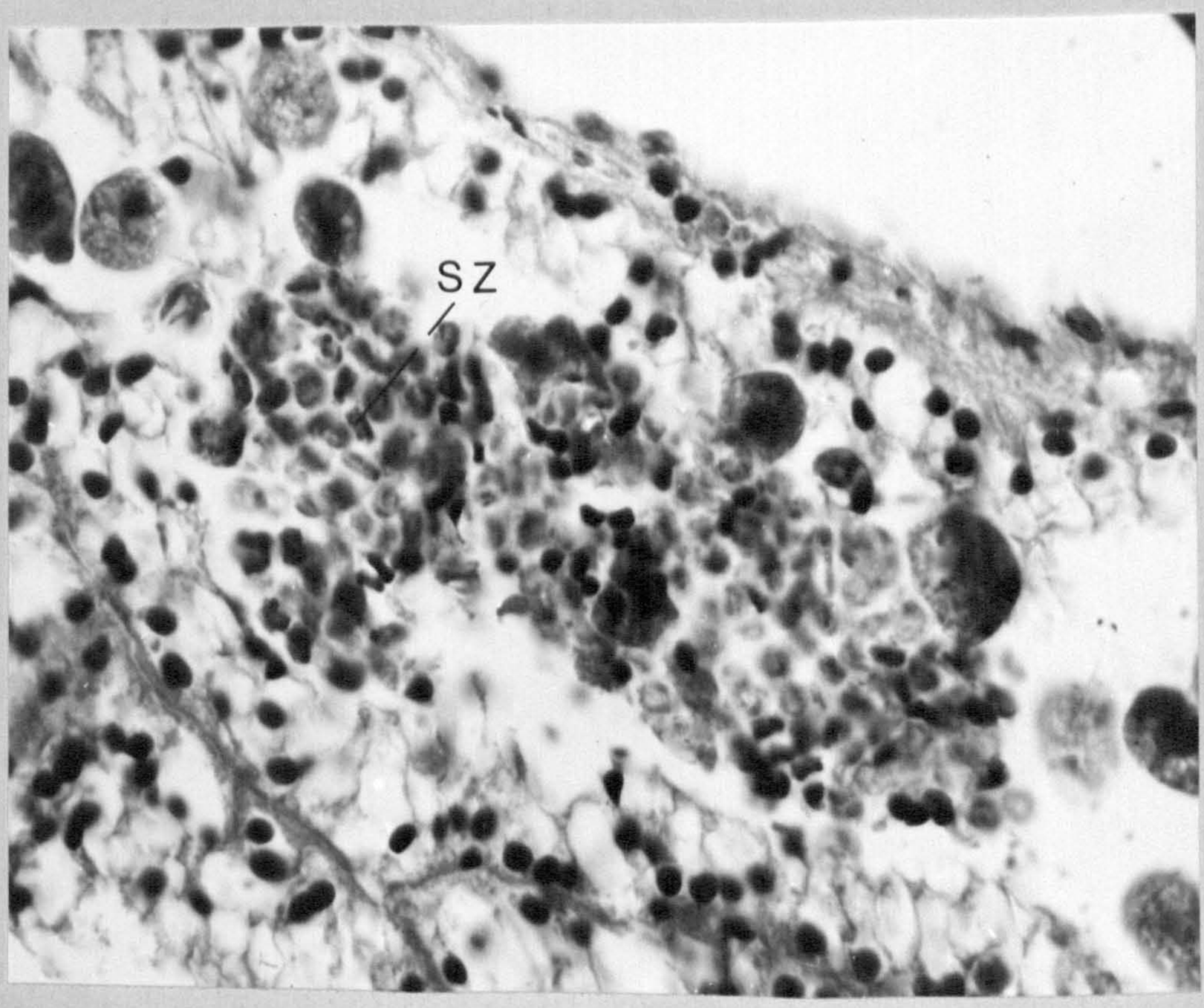
SZ

Hyaloklossia sp. A coccidian of the kidney of *Tellina*

Plate 71 a and b

Details of the preceeding light micrographs

Magnification of x 800

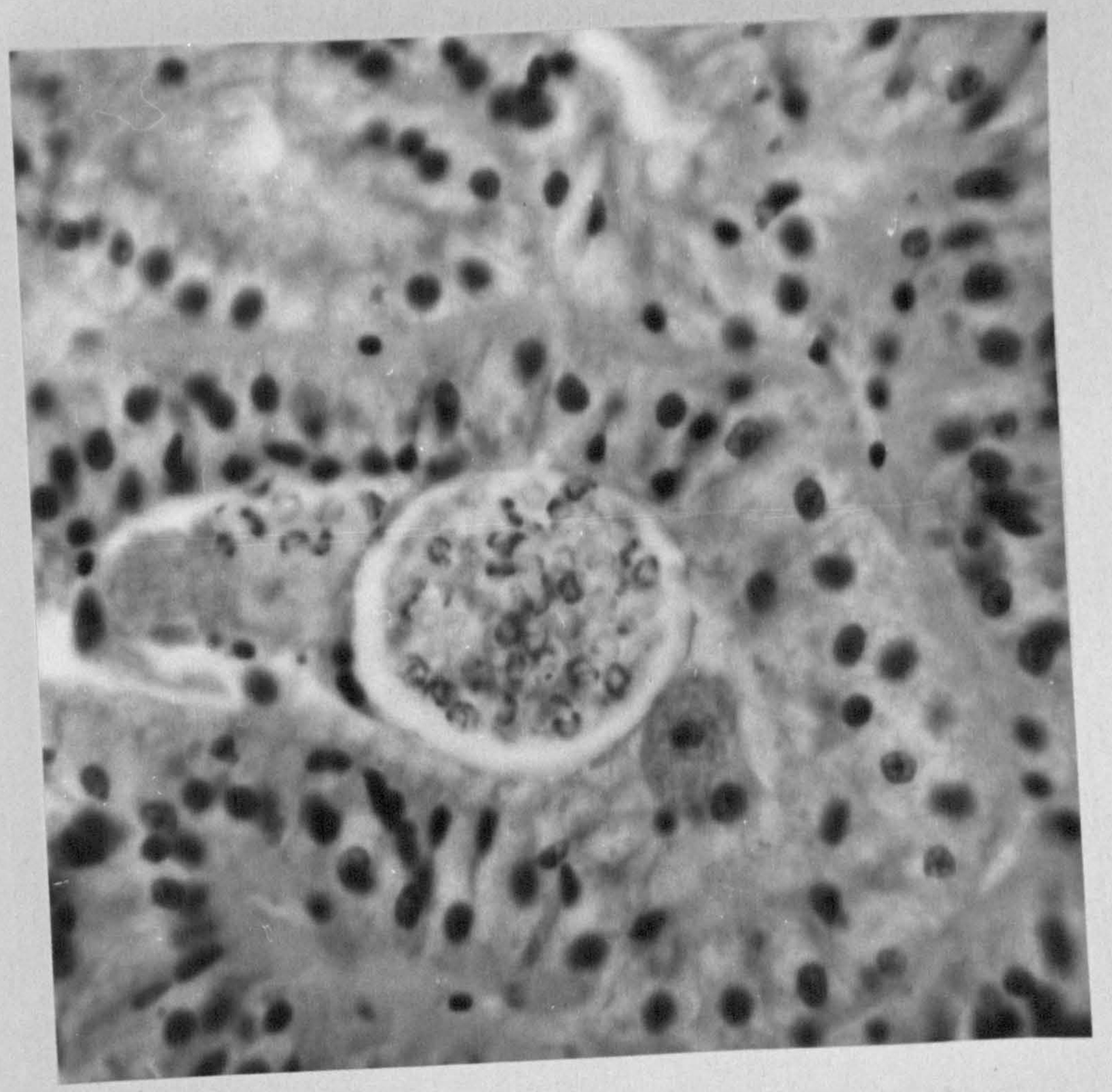

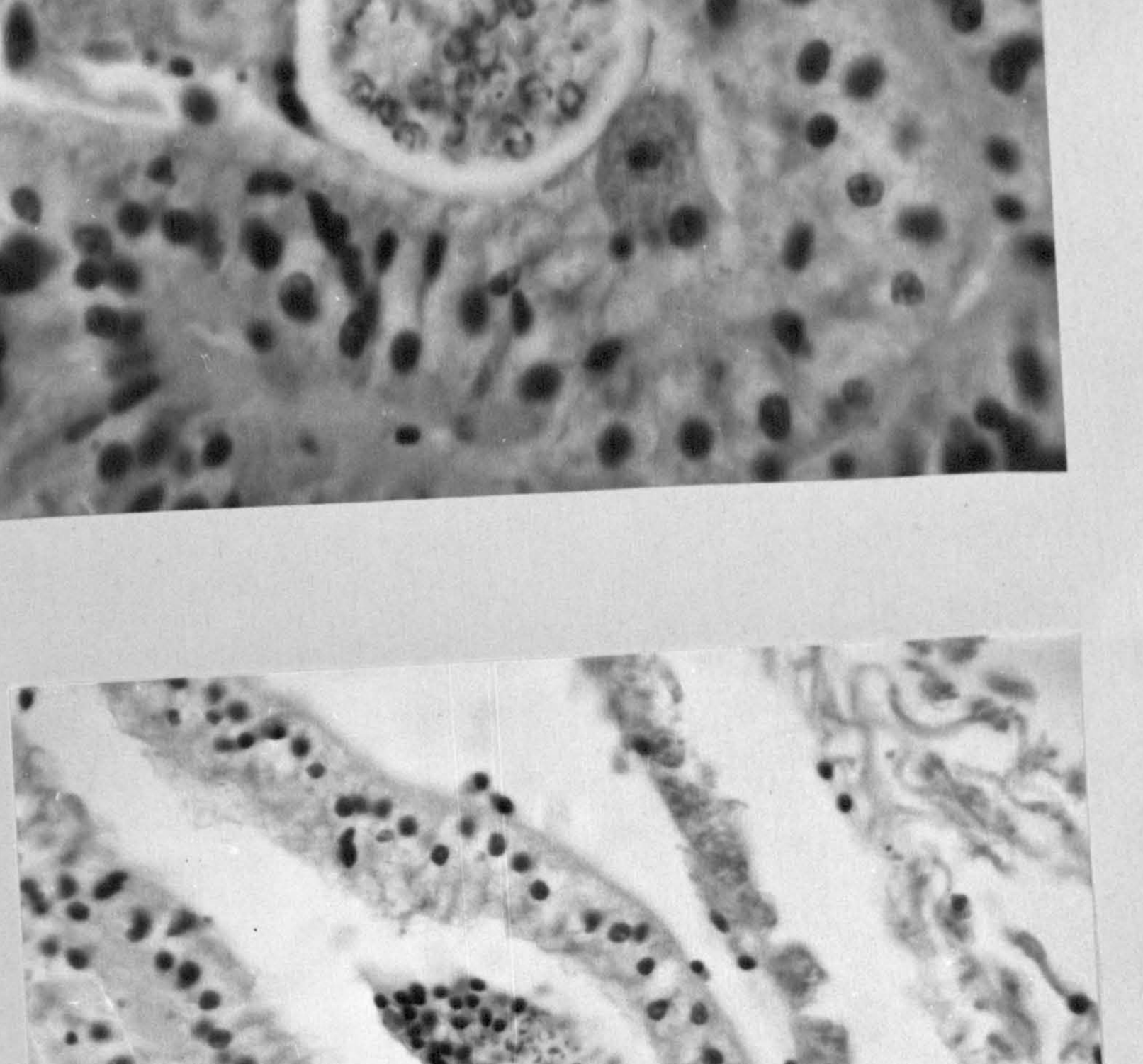

SECTION THREE

The normal digestive gland.

The absorptive cells

Plate 72

Digestive gland acini showing the nature of the absorptive cells in contradistinction to the secretory cells in plates 74-77.
The sinus at centre is lined with endothelial cells and contains numerous cells of the haemolymph. A dead cell is prominent at centre right. X 1500

Plate 73

The effects of the MLO on the host cells

The margin of a dead cell showing the necrotic remnants of the cytoplasm and the nucleus. X 6000

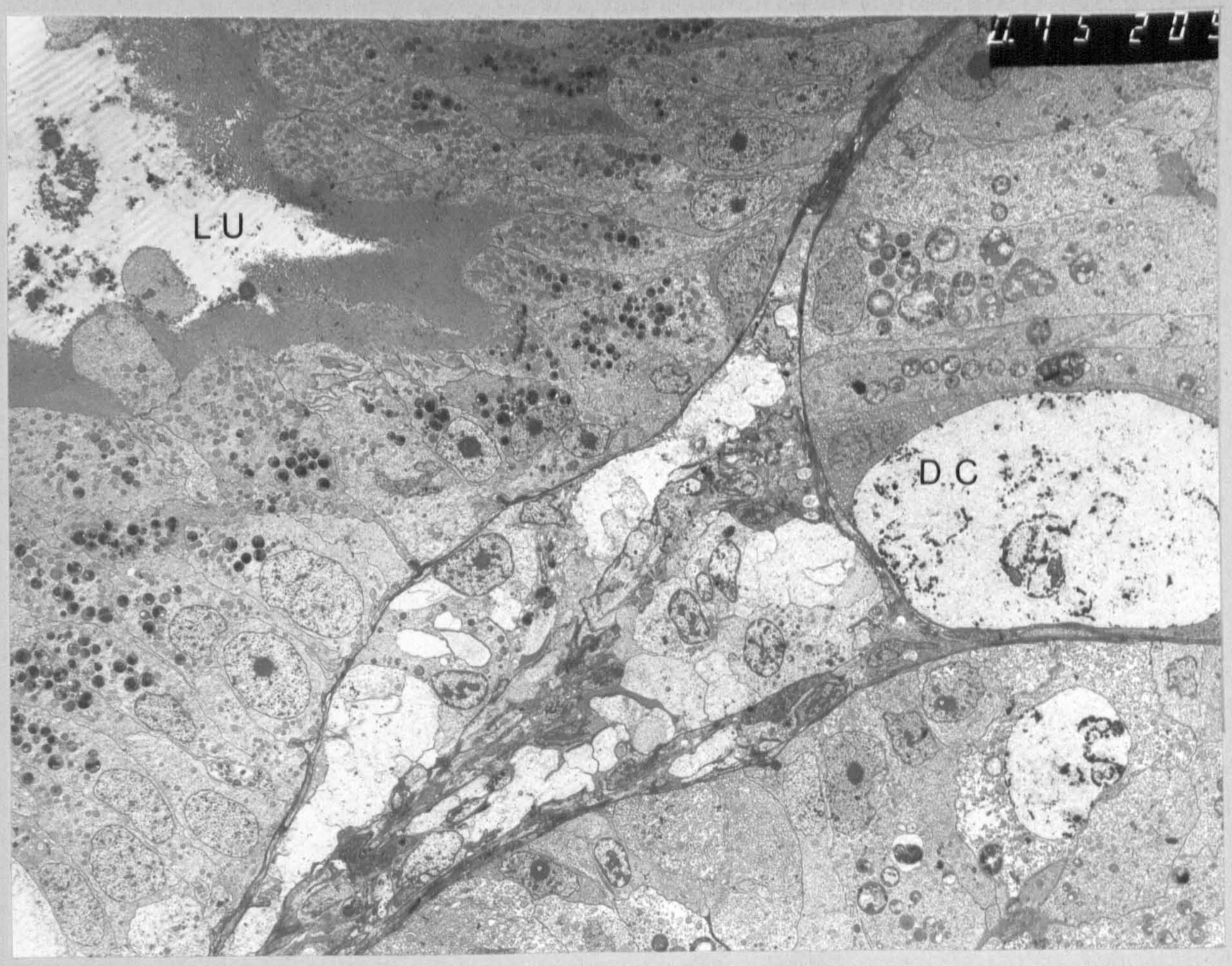
LU
DC

DC
N
N

The fine structure of the absorptive cell

Plates 74 and 75

Electron micrographs (X 10,000) of typical digestive cells of the digestive gland. These cells are details from the preceding electron micrographs. Heterolysosomes (HL) and residual bodies (RB) abound although heterophagosomes and pinosomes are notably absent suggesting that the cell is at an excretory phase in its metabolism.

The distal end of the central cell contains very numerous mitochondria. Degenerate mitochondria are believed to be budded-off with 'blebs' of electron pale cytoplasm and microvilli. These 'secretory spherules' have been described as containing enzymes which are released for the processes of extracellular digestion in the stomach. No evidence to support this hypothesis is provided by these electron micrographs as no lysosomal structures could be detected in these secretory or fragmentation spherules. It is believed their function is purely excretory.

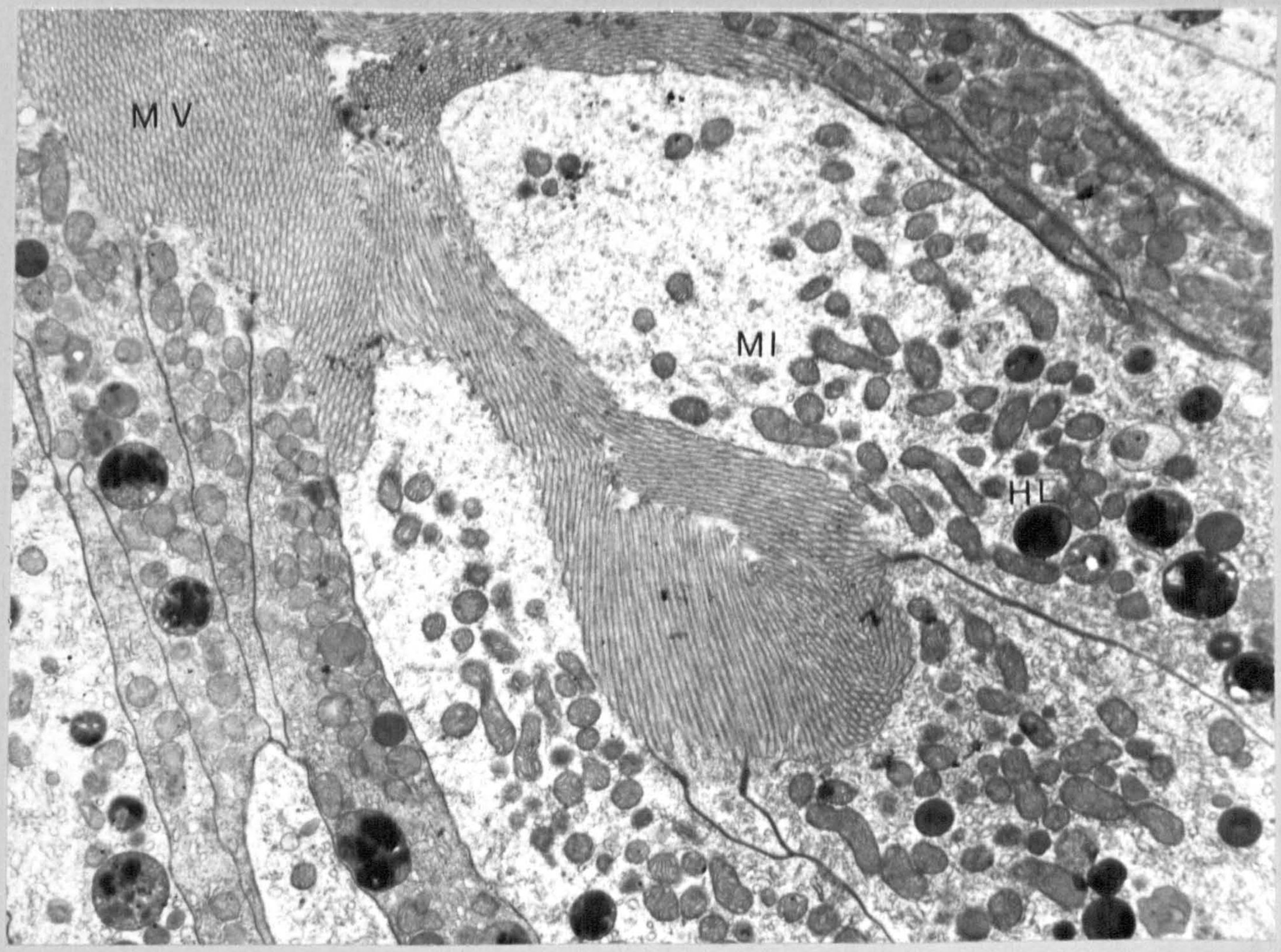
MV
MI
HL

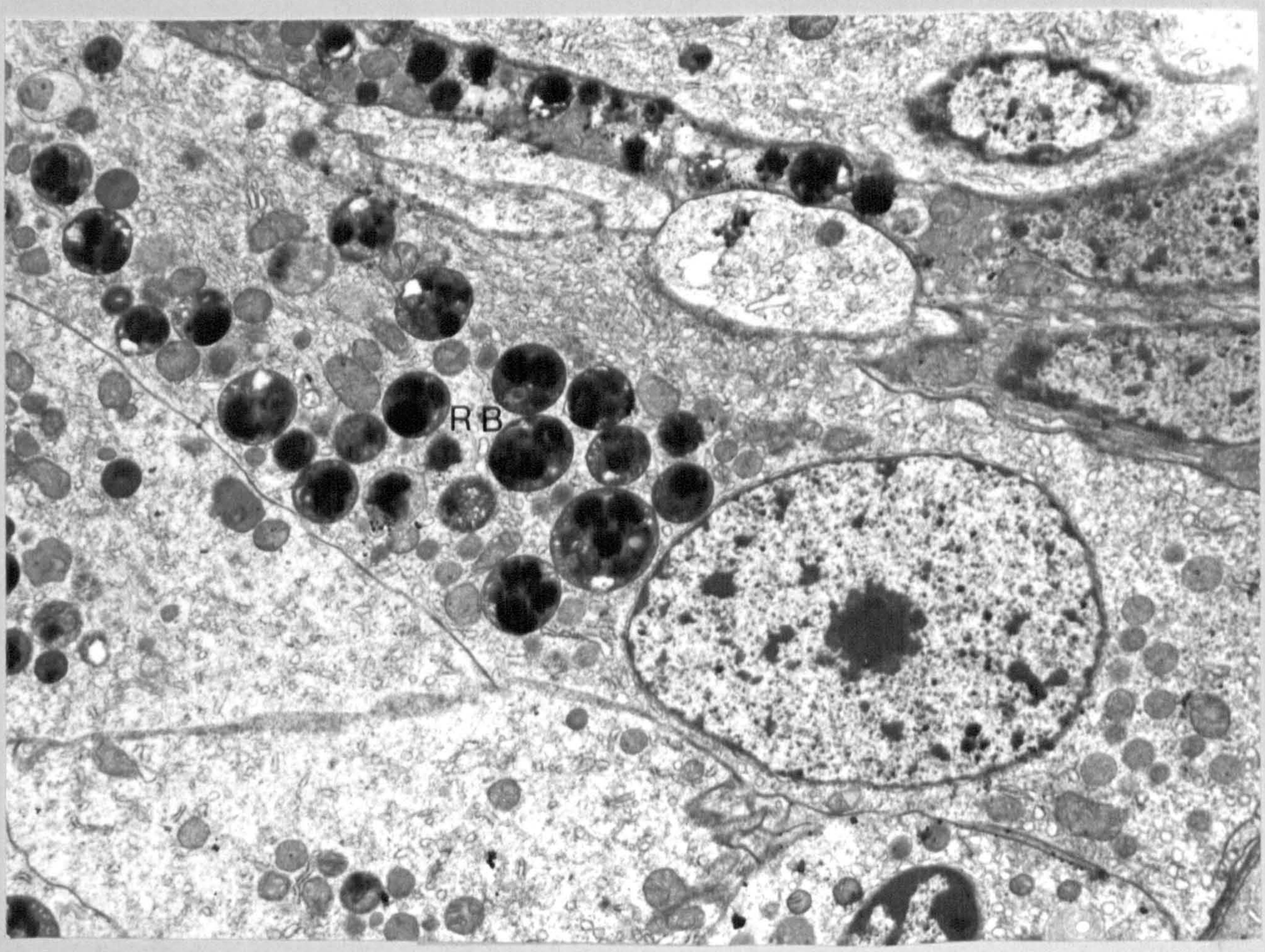
RB

Ultrastructural appearance of the normal digestive gland. Secretory cells

Plate 76 and 77

Young, pyramidal secretory or basophil cells immediately post-division. These cells are actively synthesizing the new cell boundary between them as indicated by the presence of Golgi bodies, numerous ribosomes, vesicles and mitochondria.

Dividing secretory cells were frequently encountered in the digestive gland suggesting that there is a high 'turn-over' in these metabolically active cells

Detail of the zone of division of dividing secretory cells.

(Both plates, magn. x 8,000)

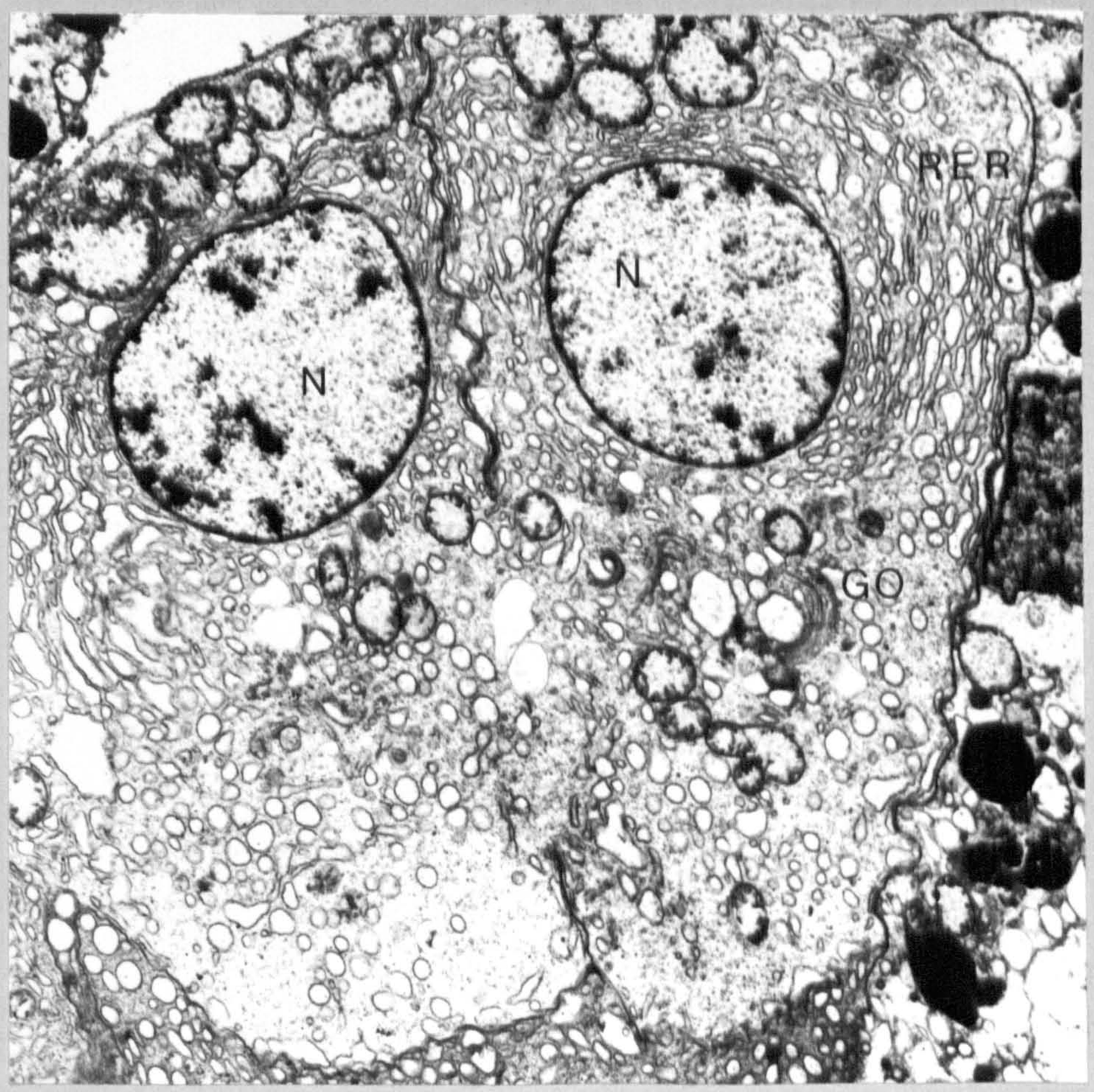
N
N
RER
GO

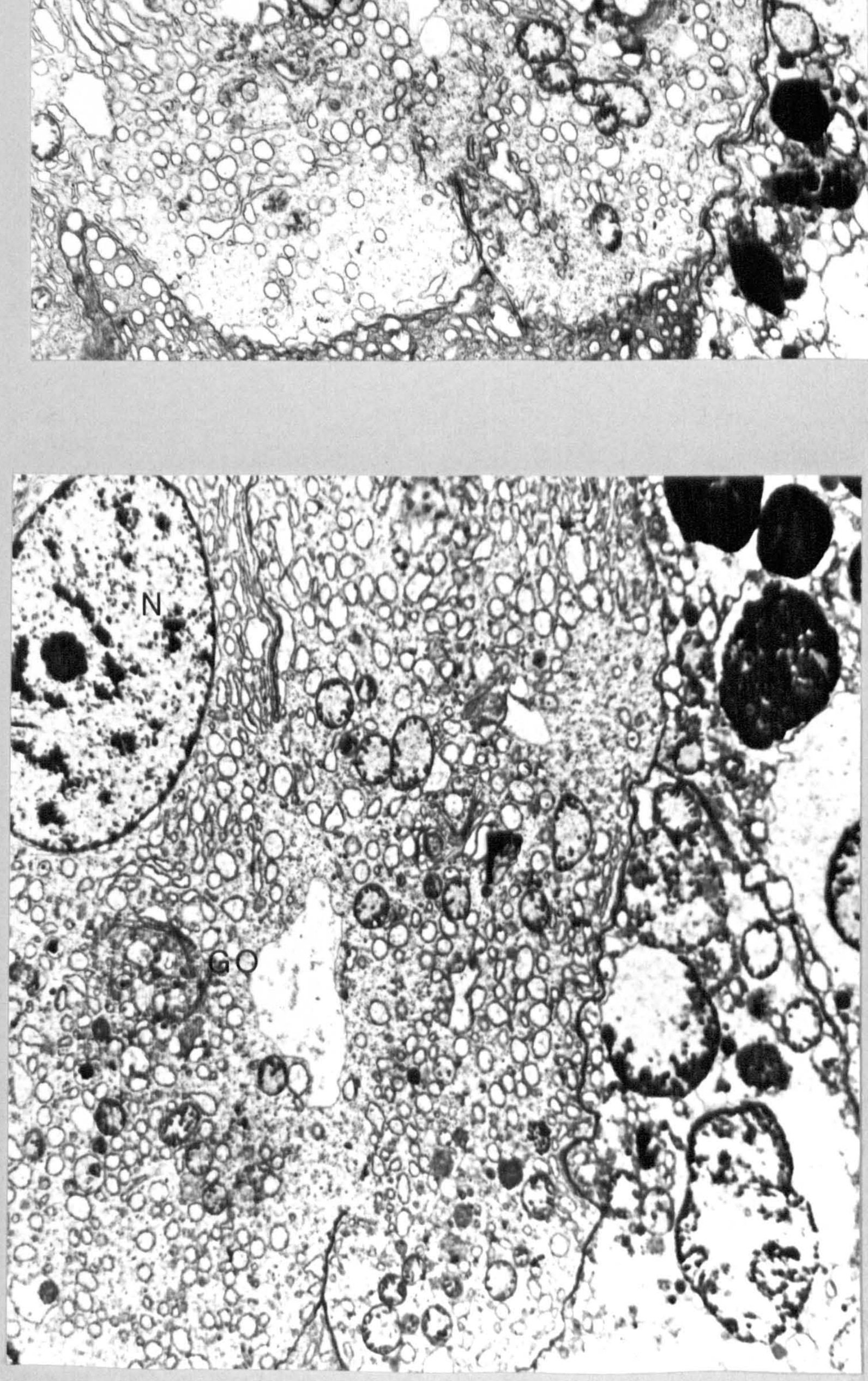
N
GO

Plate 78

Section of the lobe of a digestive acinus. A secretory cell pair having the characteristic pyramidal shape, well developed granular endoplasmic reticulum, well defined cup shaped Golgi zone and numerous secretory vesicles derived from the Golgi body. The boundary between the digestive and secretory cells is well defined. Magnification X 2,500

Plate 79

The endoplasmic system of the secretory cell. Numerous profiles of Golgi bodies are believed to be "packaging" the products of the endoplasmic reticulum. The distended peripheral regions of the Golgi saccules bud off secretory vesicles which coalesce to form primary lysosomes (arrowed).

Detail of micrograph above. Magnification X 10,000

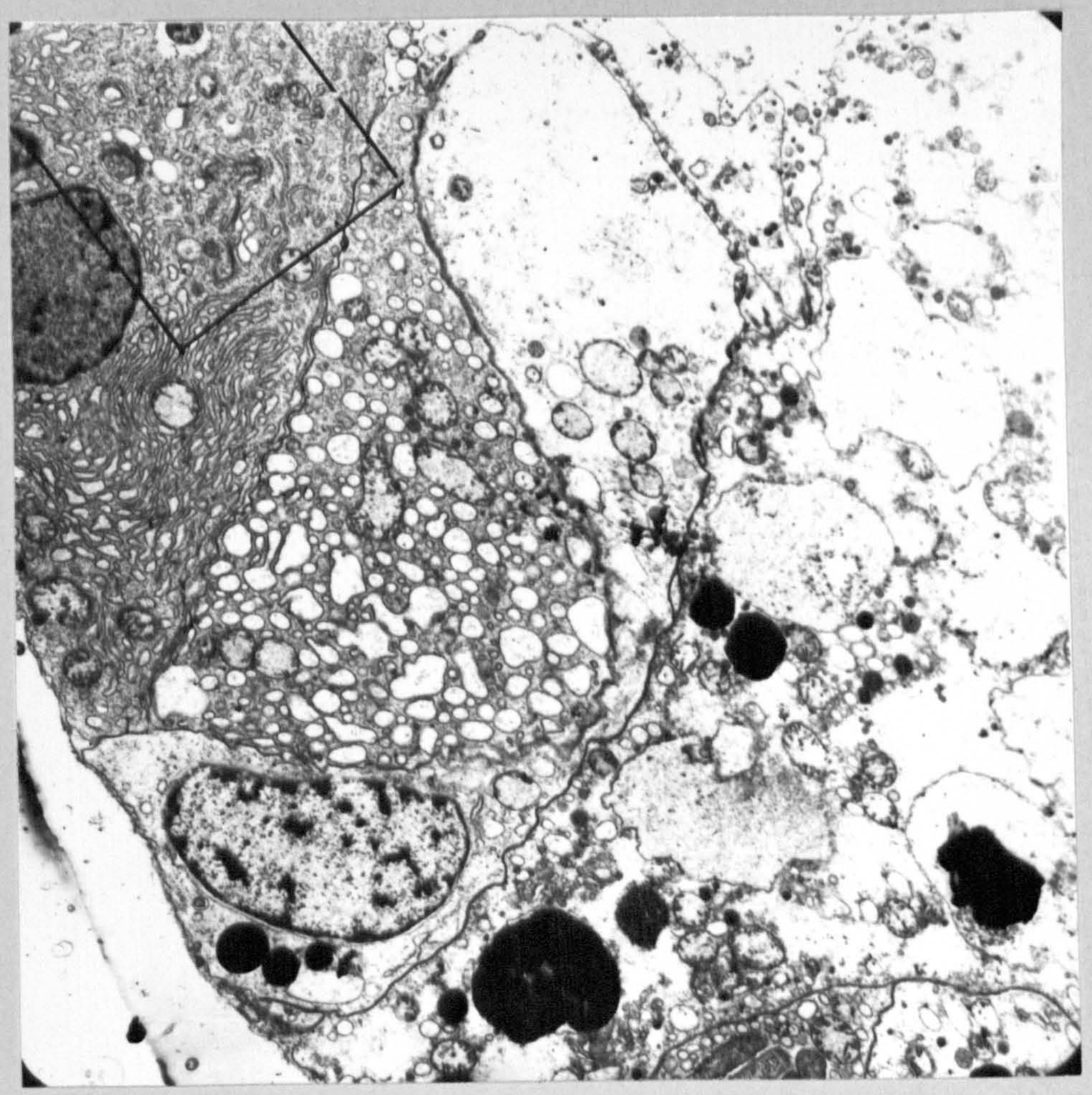

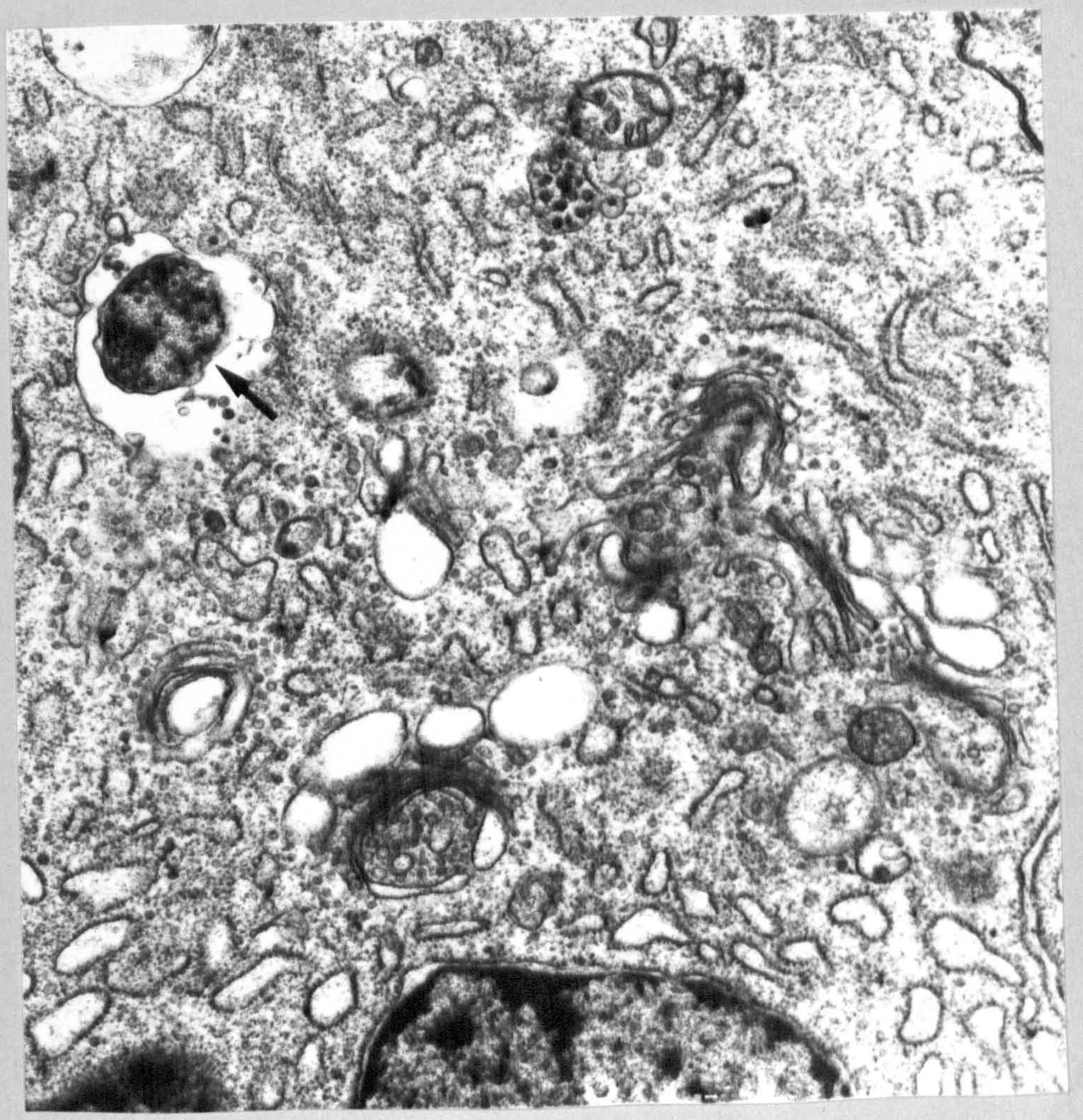

Plate 80

Electron micrograph (X 6,000) of the margins of absorptive cells at a secretory phase in their metabolic activity. Cellular debris with numerous profiles of degenerate mitochondria can be seen between the lobes of the absorptive cells. The dense microvillous brush border of the absorptive cells seems to fill the lumen of the tubules of the digestive gland.

Plate 81

Detail of the above electron micrograph (X 12,000). The electron-dense osmiophilic nature of excreted material interdigitating between the lobes of the absorptive cells is thought to be lipid in nature mixed with cellular debris.. See also Figures 101, 128 Note the presence of residual bodies embedded in this matrix. Very numerous profiles of microvilli characterize the absorptive cells.

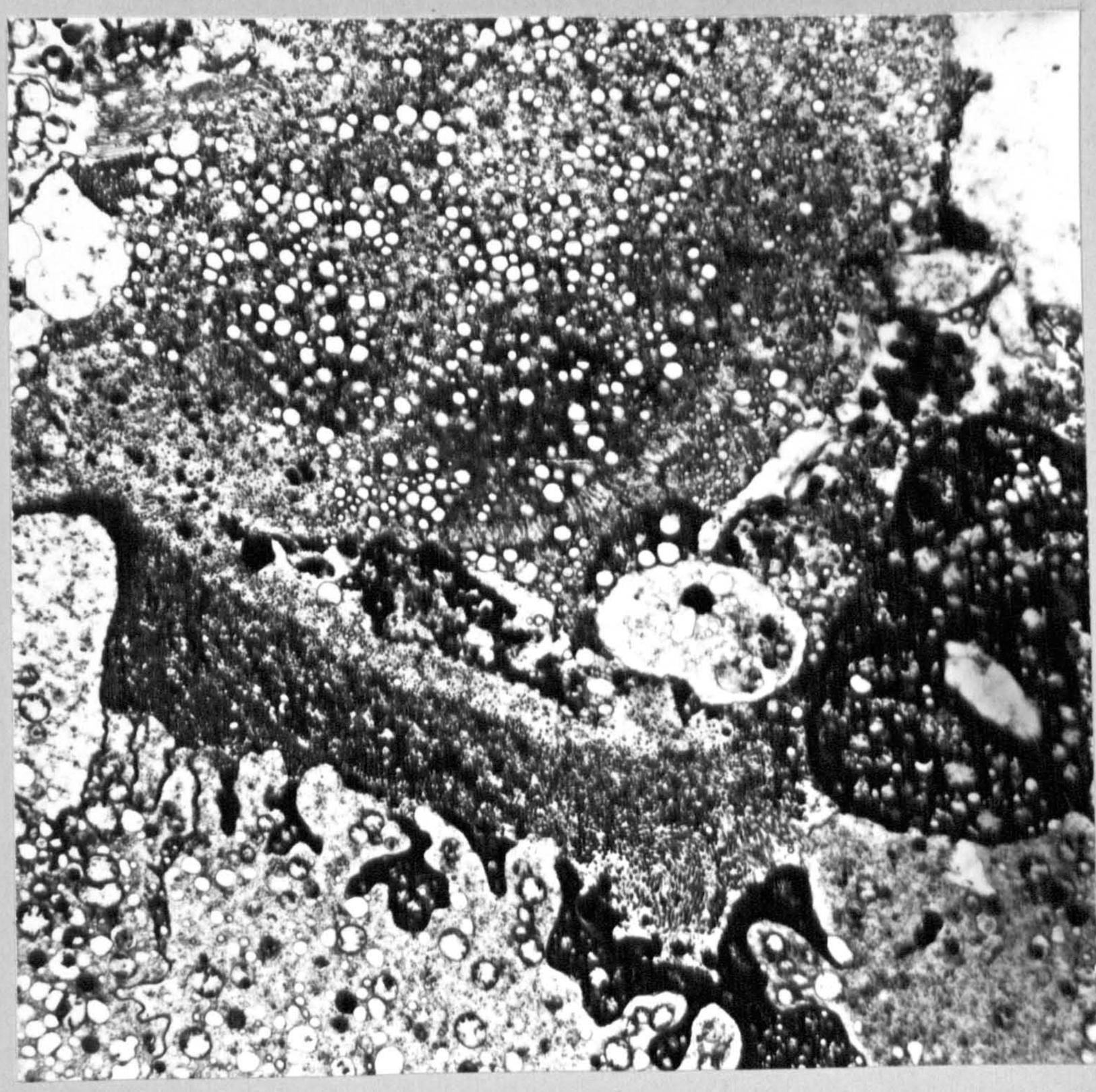

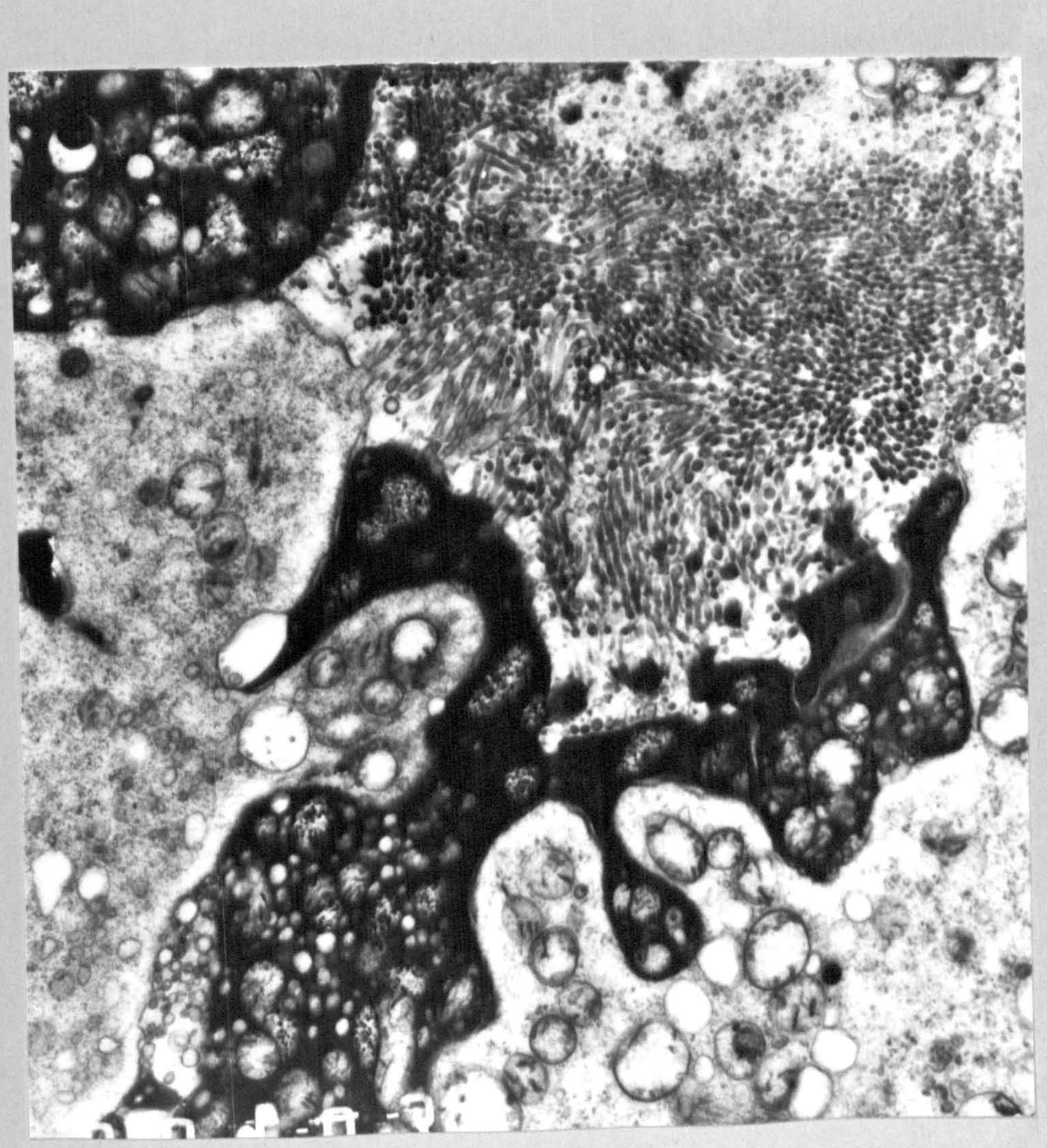

Digestive tubules heavily infected with MLO

Plate 82

Low power light micrograph (X 100) of the digestive tubules of Tellina. Note the numerous lacunae formed by the disruption of basophil cells that have been infected with MLO. The tubules in the lower left of the photograph are believed to have been stripped of their epithelial lining by the autolytic action of the disrupted secretory (basophil) cells thus leaving the bare basement membranes.

Plate 83

Detail from the centre of the above Figure. The crypts of basophil cells contain very numerous cytoplasmic inclusions representing various stages of development of MLO within cells. Magnification X 250.

Paraffin embedded sections, formalin fixed, stained with Heidenhains Haematoxylin and Eosin.

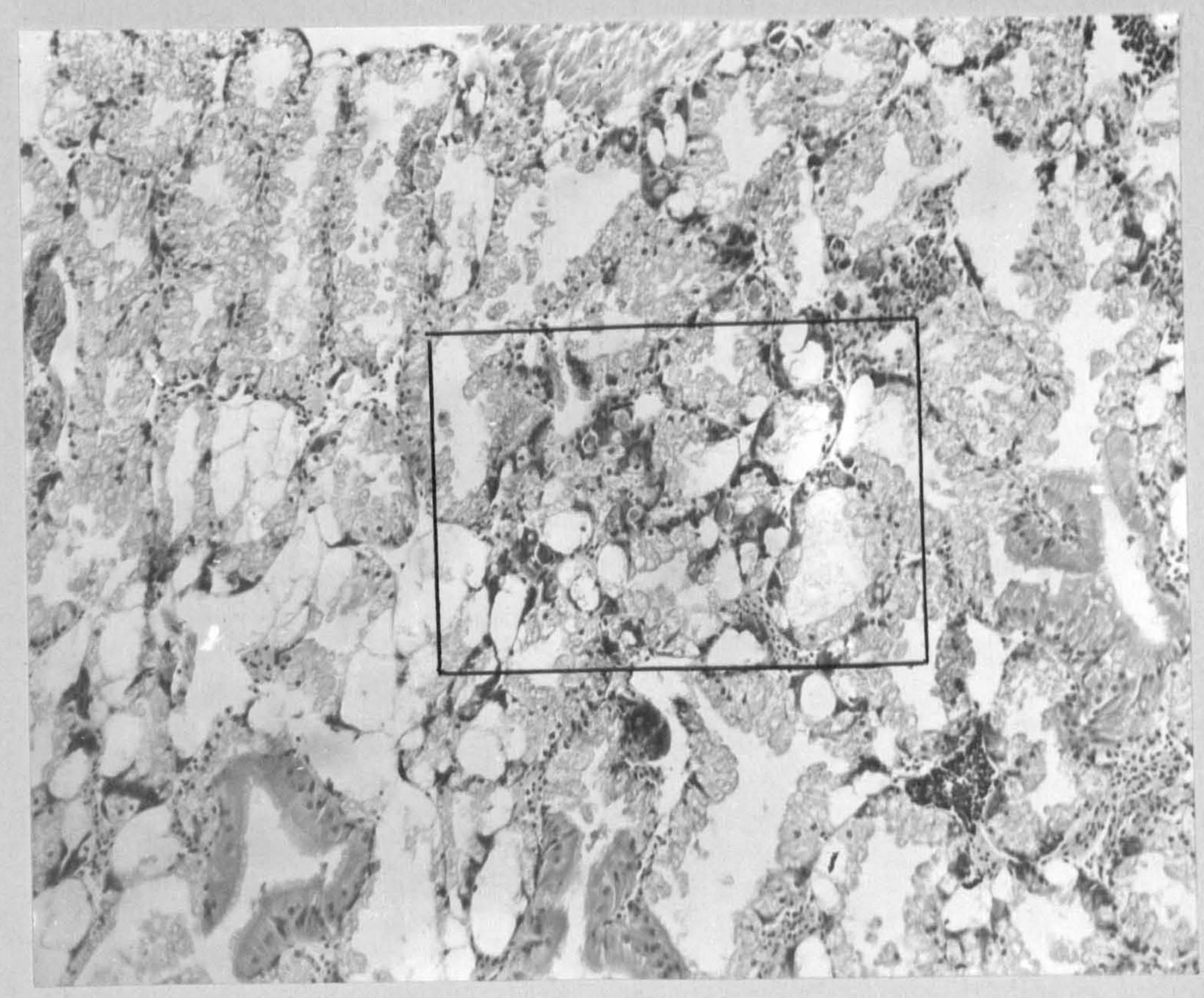

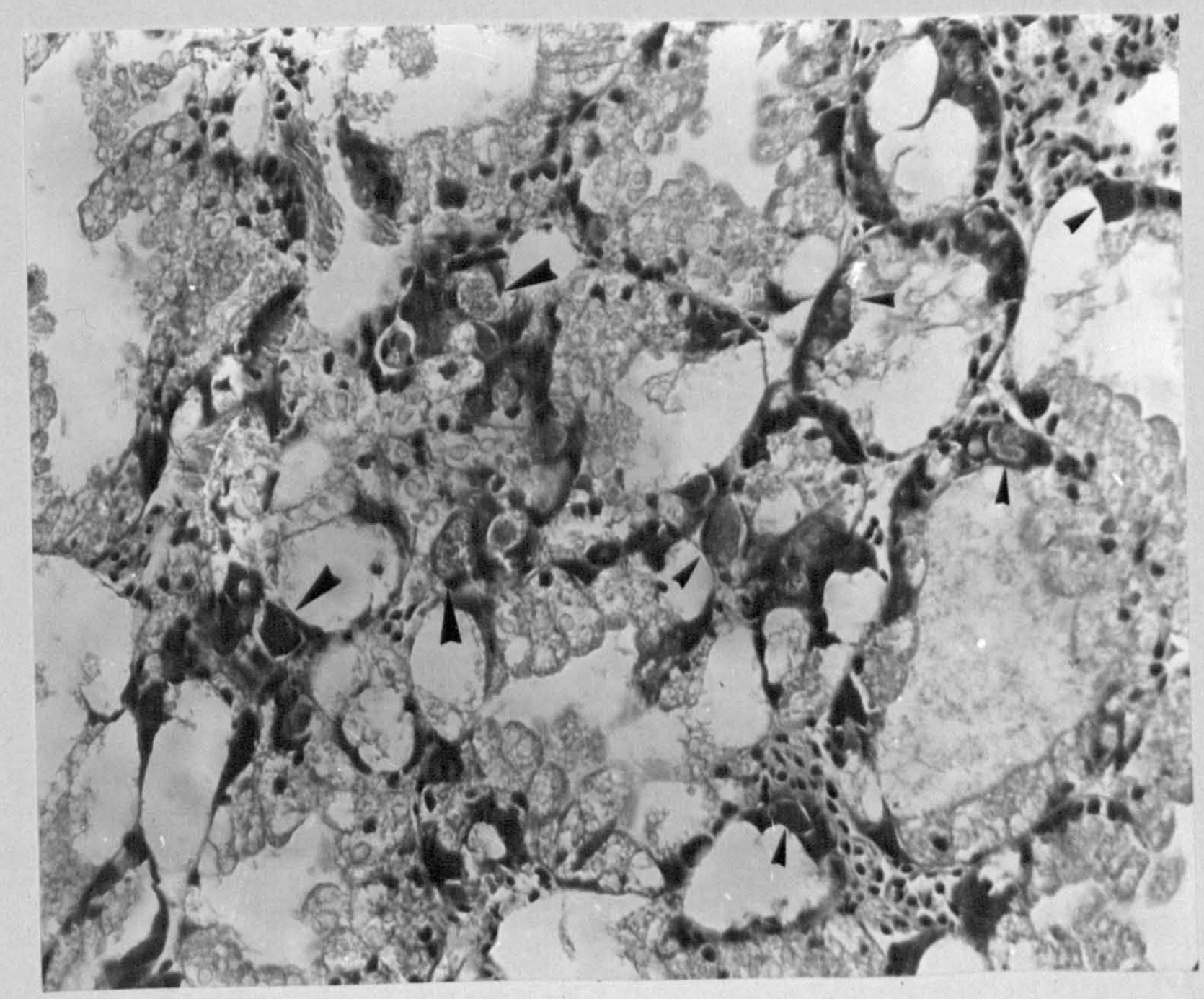

Digestive tubules heavily infected with MLO

Plate 84

This low-power light micrograph (x 63) shows the labial palps (1), sub-oesophogeal ganglion (2), stomach (3) and branching digestive gland tubules of Tellina. Ctenidial filaments (4) and a branch of the gonadal follicles packed with coccidia and leucocytes (5) can also be seen, (Magn. x 60)

Plate 85

Detail (x 100) of the above. This plate should be compared with plates 86 and 87 overleaf. The very large number of cells infected with MLO will then be apparent. Parts of the gland are at different stages of absorption and breakdown. These are marked A and B respectively.

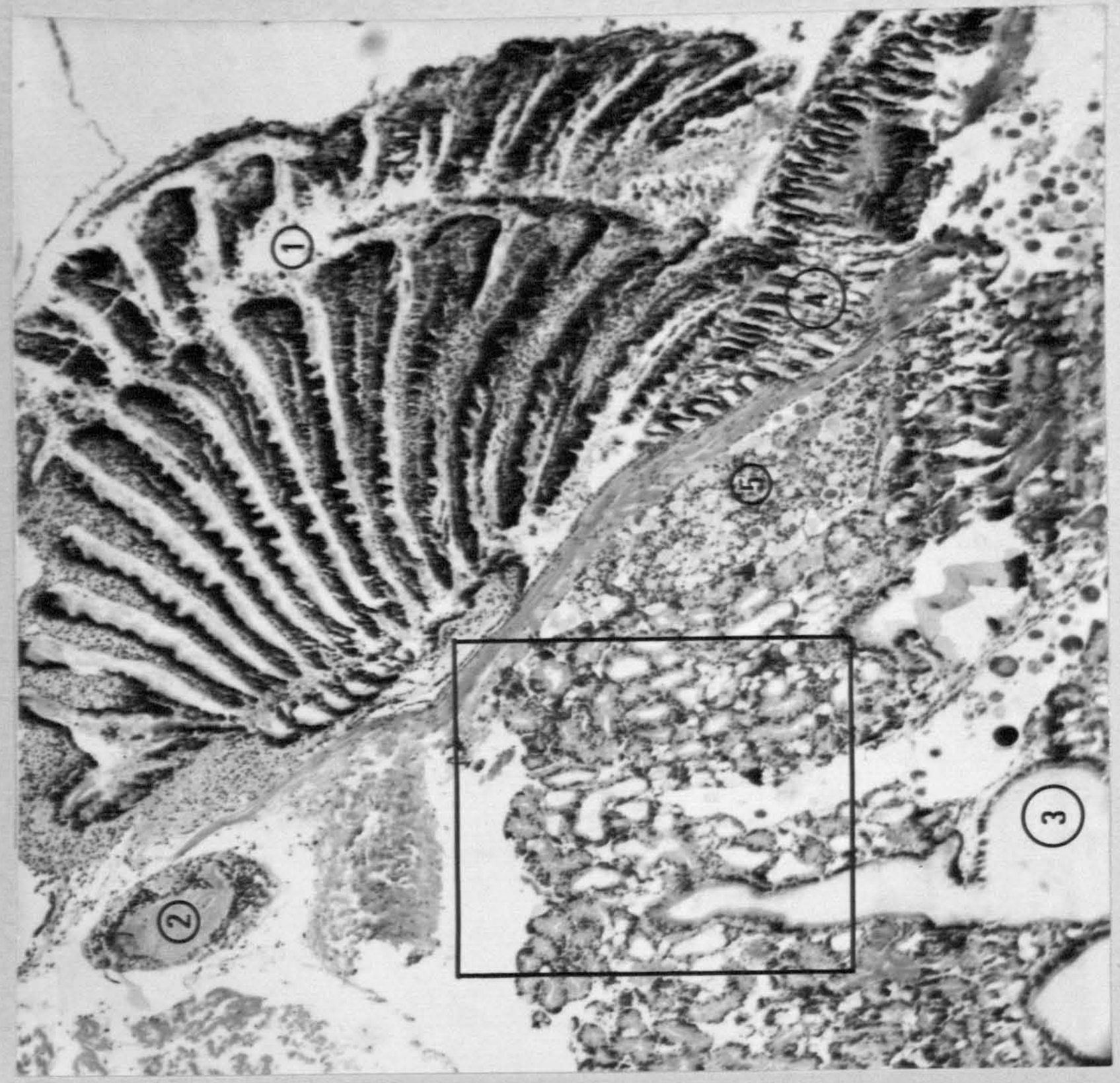
①
②
③
④
⑤

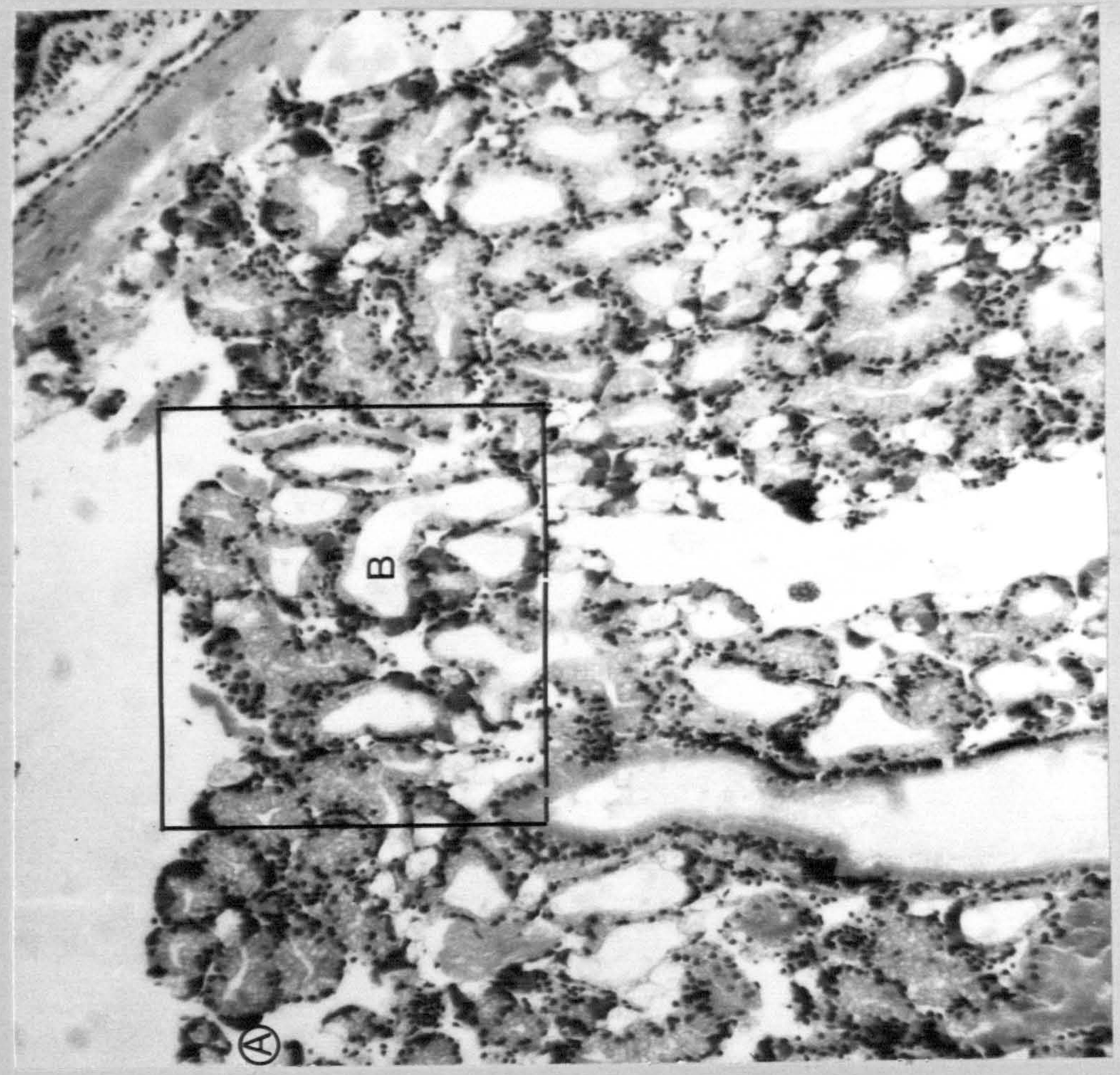
B
Ⓐ

Digestive tubules heavily infected with MLO

Plates 86 and 87

Thes plates (x 250) are serial sections of the same area of digestive gland tubules. This shows the spherical nature of the MLO inclusions. The absorptive cells appear healthy and unaffected These can be seen at the stages of absorption and breakdown.

A low-power magnification of this gland is shown in plates 84 and 85.

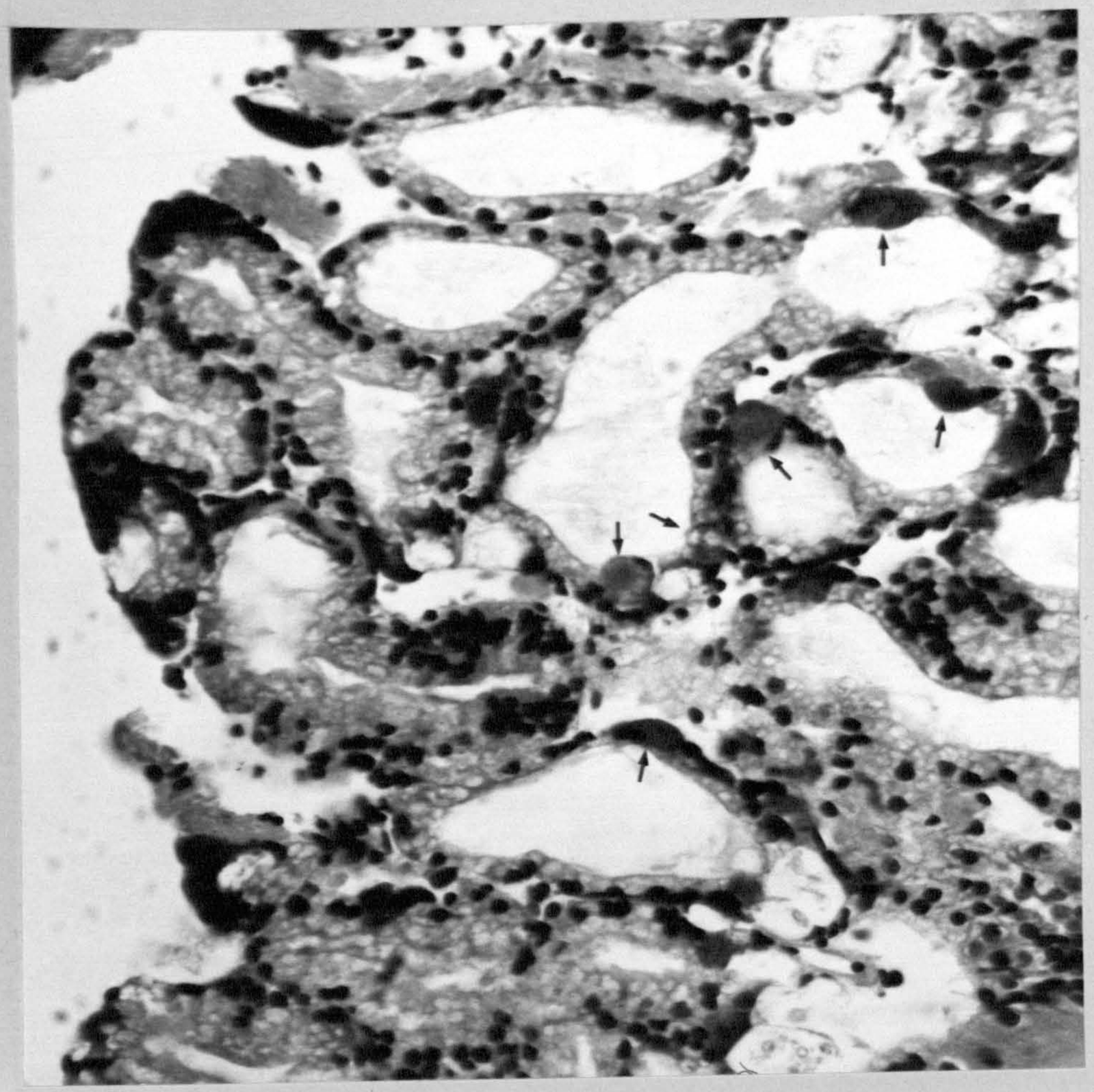

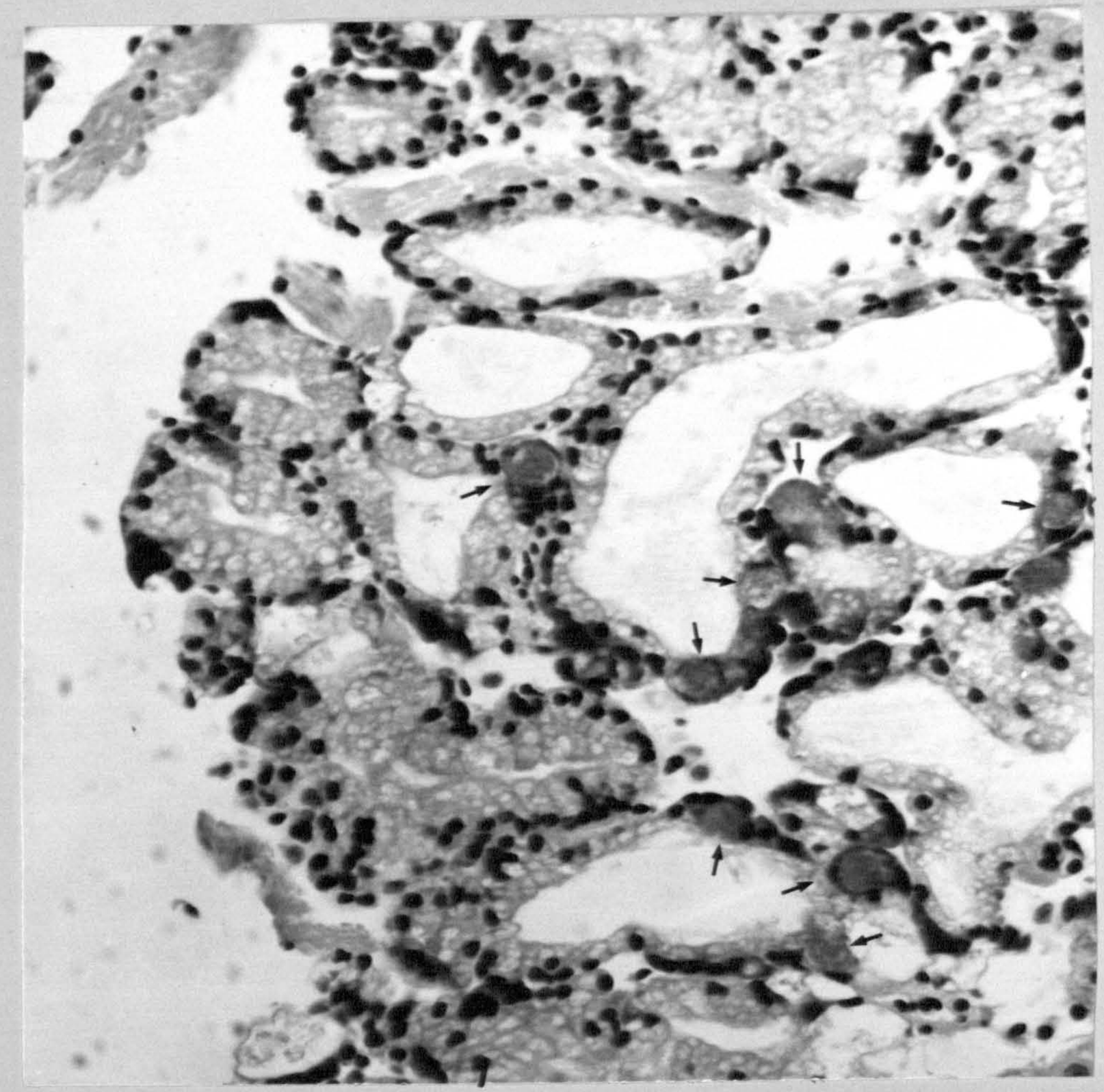

The effect of MLO on the appearance of the digestive tubules

Plate 88

Low power light micrograph of the digestive diverticuli of Tellina (X 100).

In contrast with the preceding light micrographs the absorptive epithelial cells of the digestive tubules are low and cuboidal typical of the appearance of 'starved' individuals. The densely basiphilic MLO inclusion bodies are spherical in outline. The lacunae are believed to be the remains of lysed baso-phil cells following infection by MLO.

Plate 89

Detail of the above plate. Note the presence of leukocytes surrounding a ciliated portion of the tubule at centre. Magnification X 250. The granular appearance of inclusion bodies can be observed at this magnification.

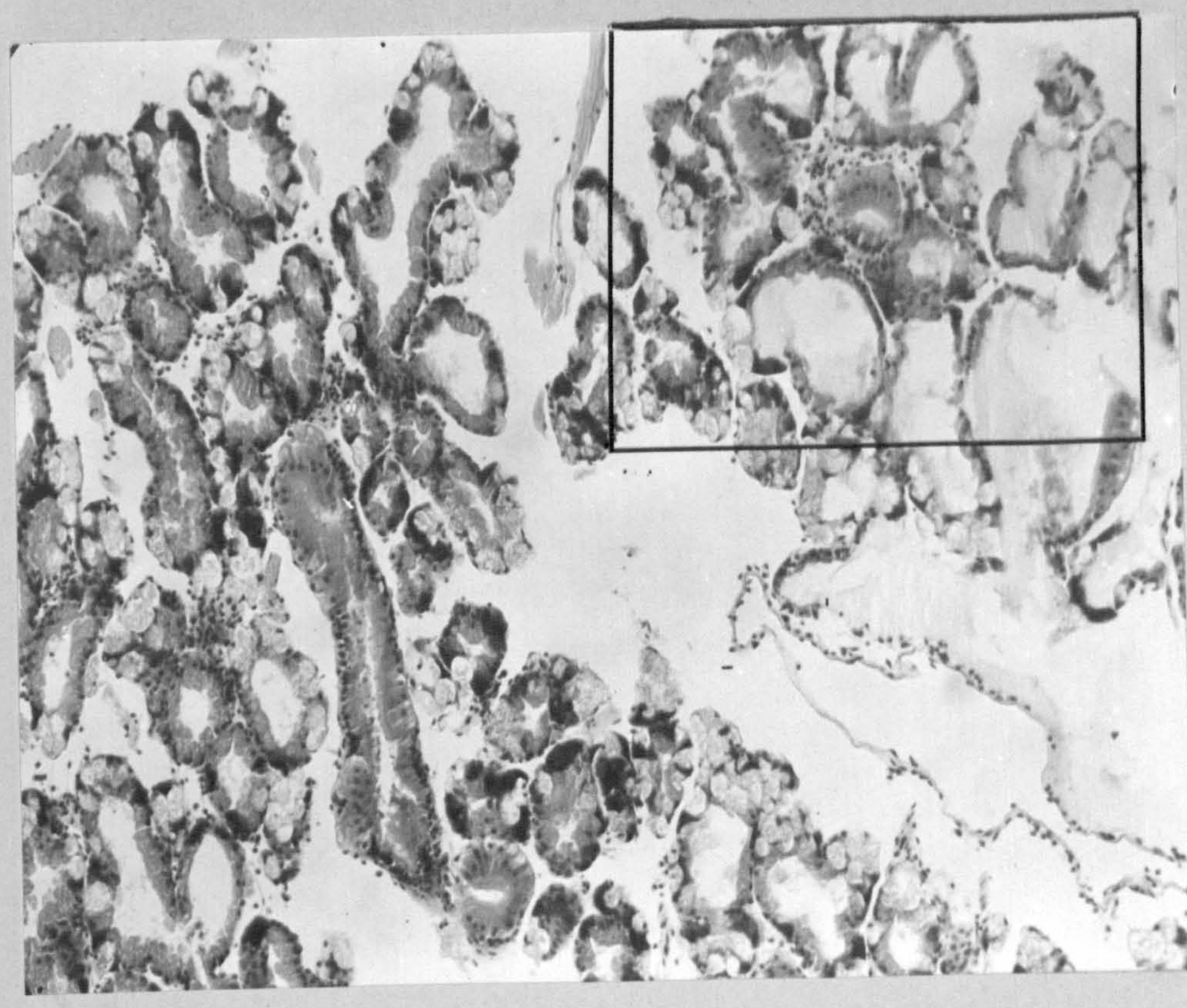

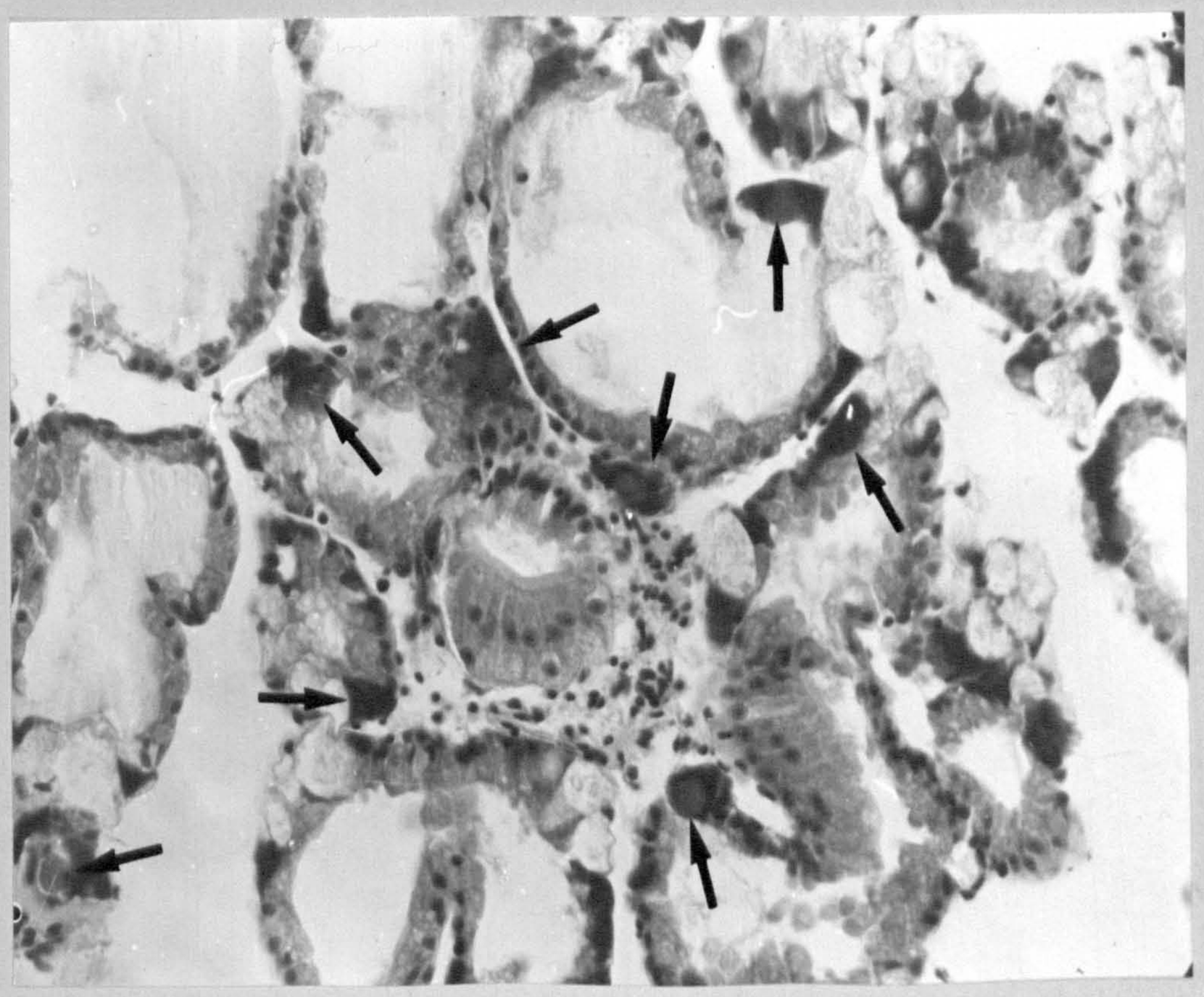

Digestive gland tubules of Tellina at an advanced stage of infection with MLO

Plate 90

The secretory (basophil) cells show various stages of invasion by MLO. The breakdown of the cytoplasm of these cells is believed to release lysosomes which produce autolysis in the neighbouring tissues.

The muscle fibres (m.f.) that are a feature of these micrographs are commonly seen ramifying throughout the gland. They may have the function of helping in the expulsion of waste material from the gland by periodic contractions.

Areas of melanization are a feature of the lower light micrograph. Melanic centres are often seen in older individuals thought to have harboured MLO infections for some time.

Plate 91

Light micrographs X 800 of H and E stained sections.

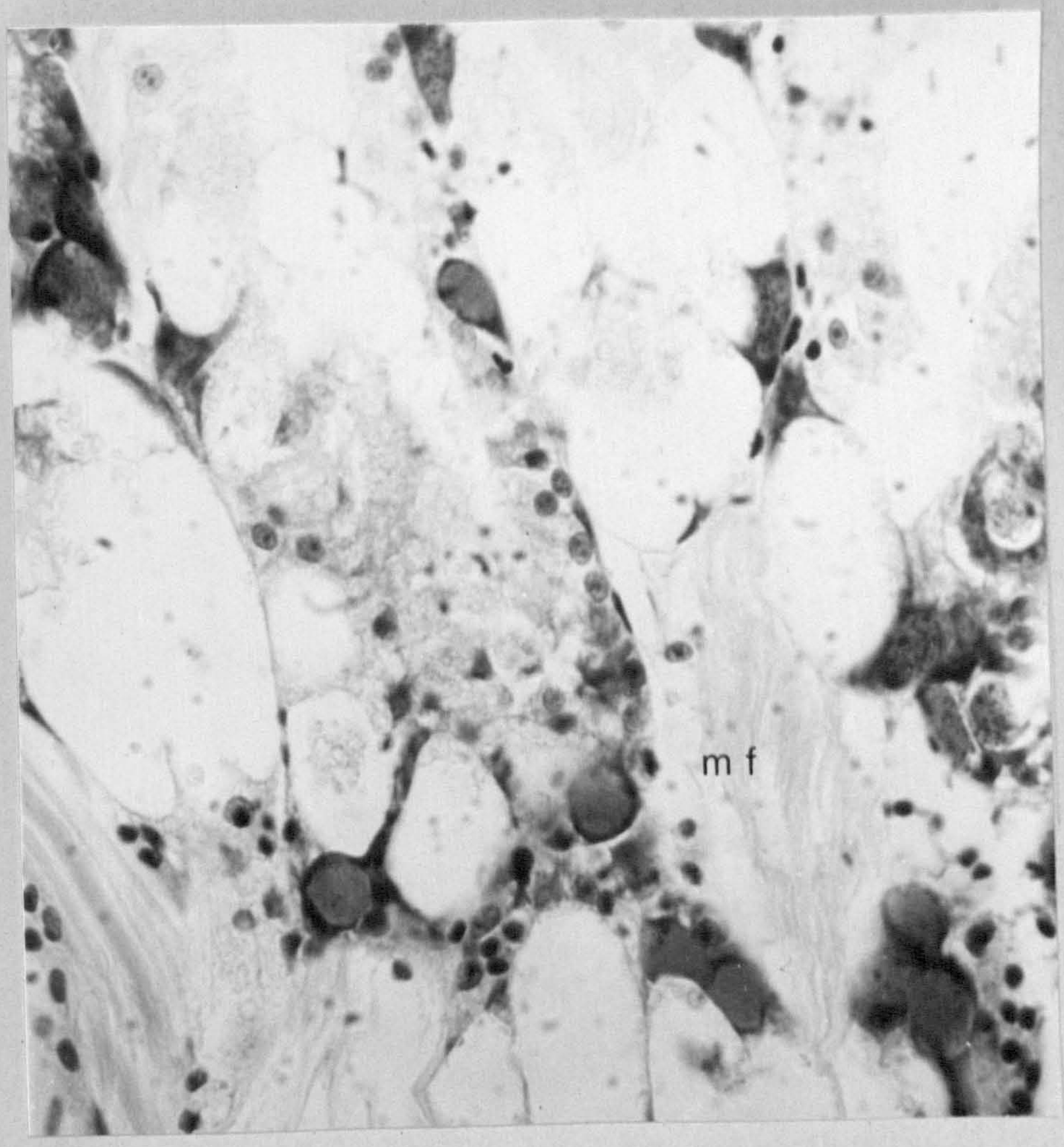
m f

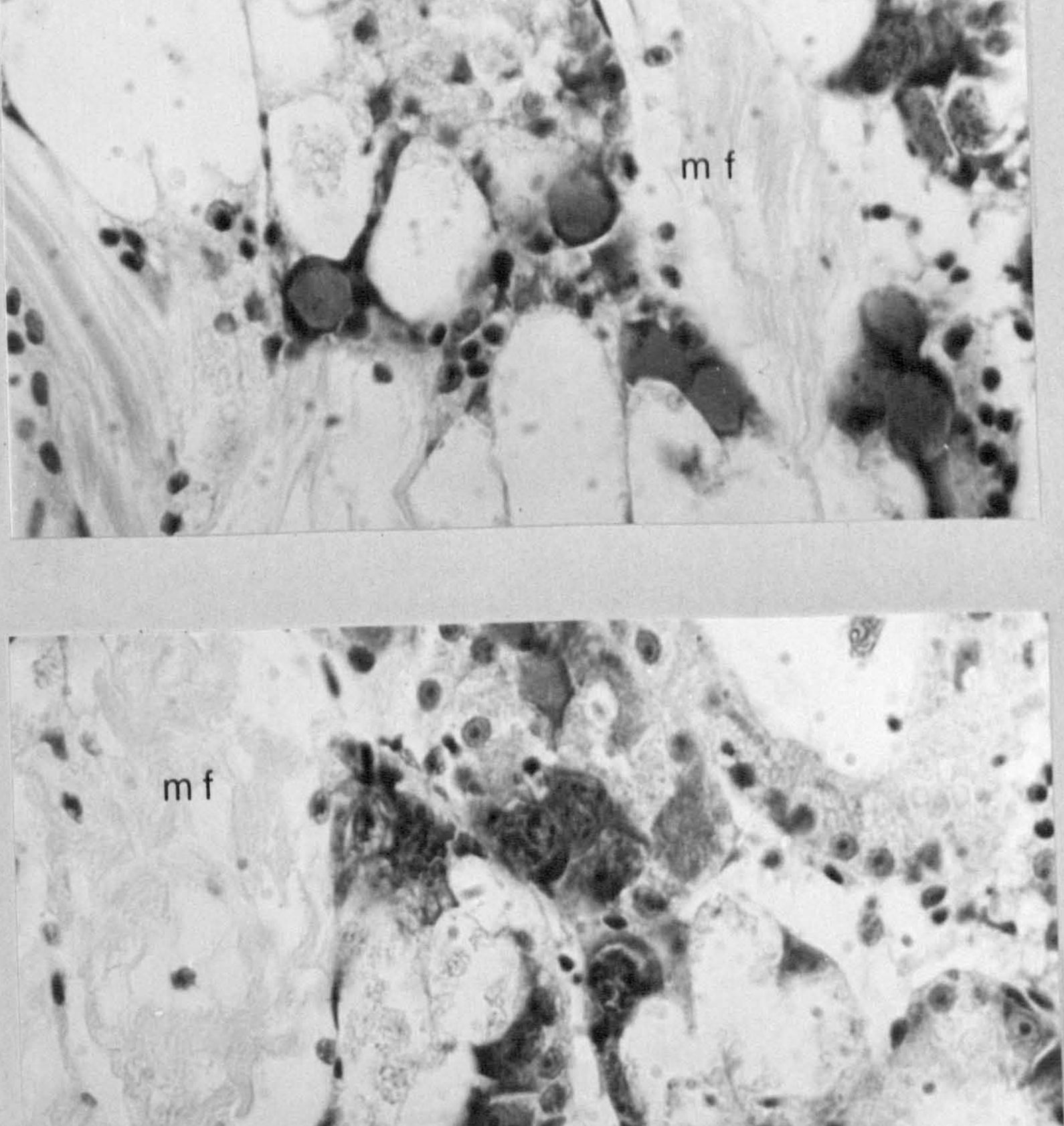
m f
m f

Histochemical staining of MLO inclusions

Plate 92

Phloxine tatrazine staining of 8 um cryostat sections. Inclùsion bodies are avidly phloxinophilic. (Mag X 400).

Plate 93

Haematoxylin and eosin staining of 8 um cryostat sections. The inclusions are eosinophilic. Note the "owls eye" appearance of the nuclei. (Magn. x 400).

Plate 94

Cryostat section 10 um thick of the same individual used for acridine orange staining as shown in plates 95-100. The spherical nature of the inclusions is apparent in these thicker sections. (Magn. x 400)

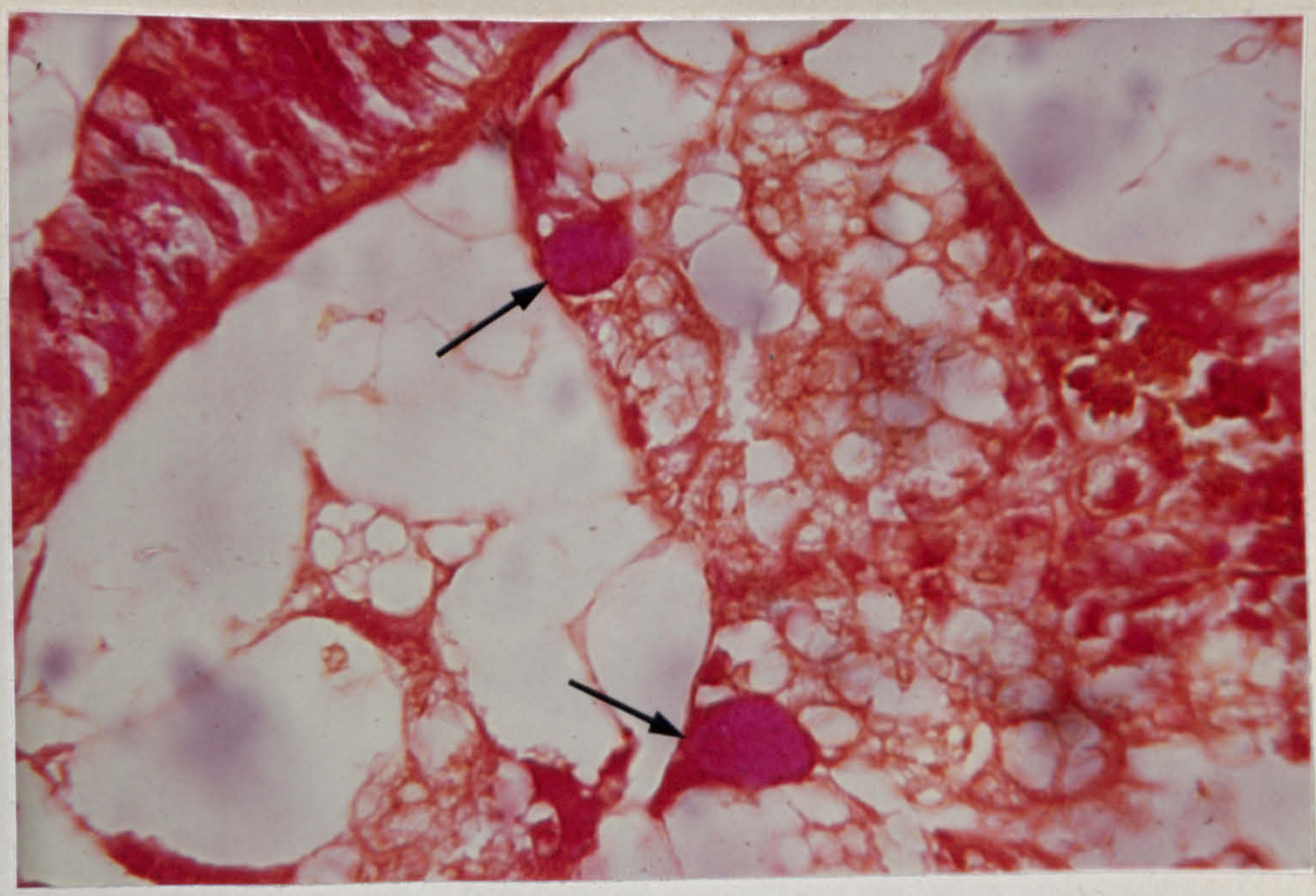

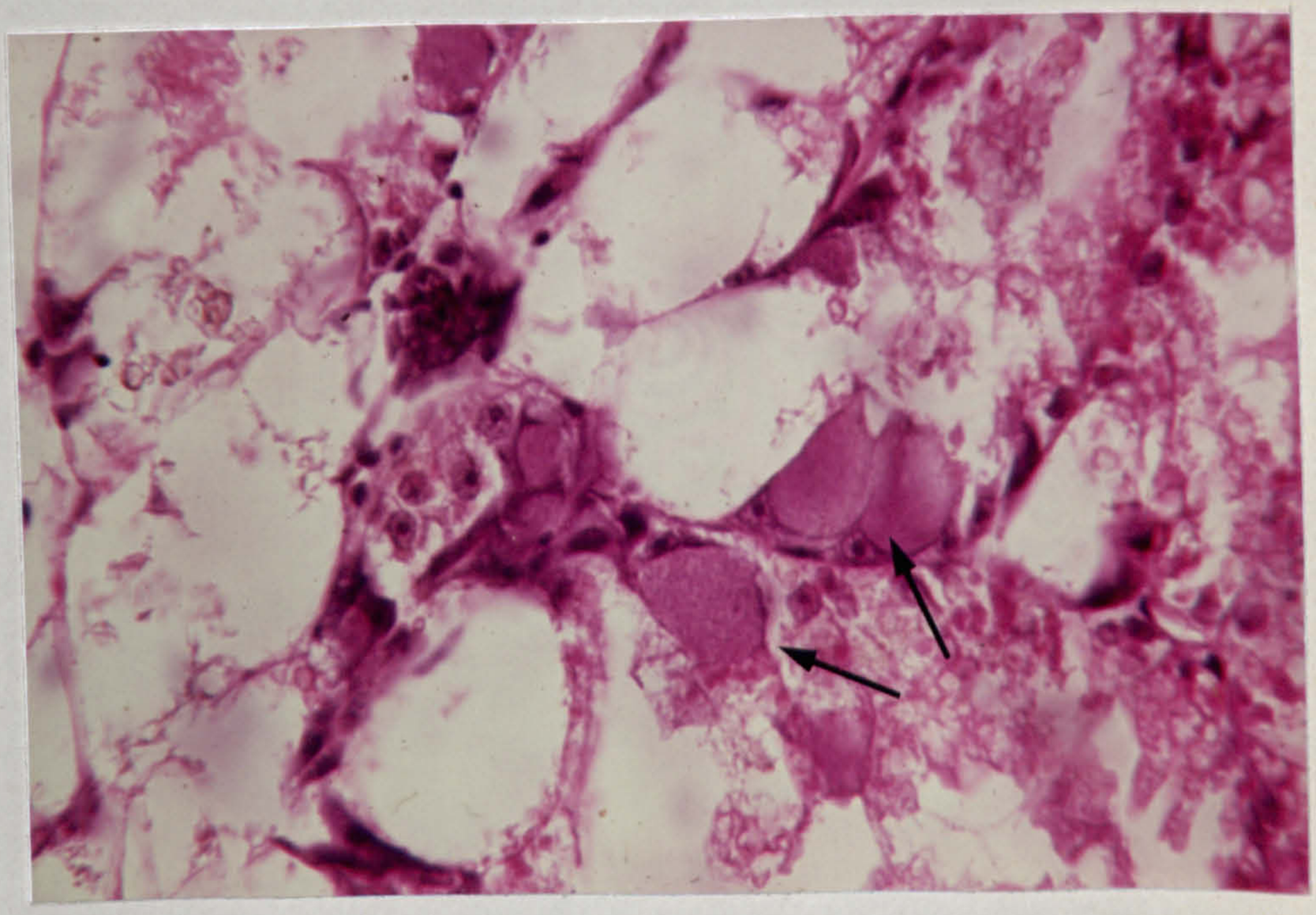

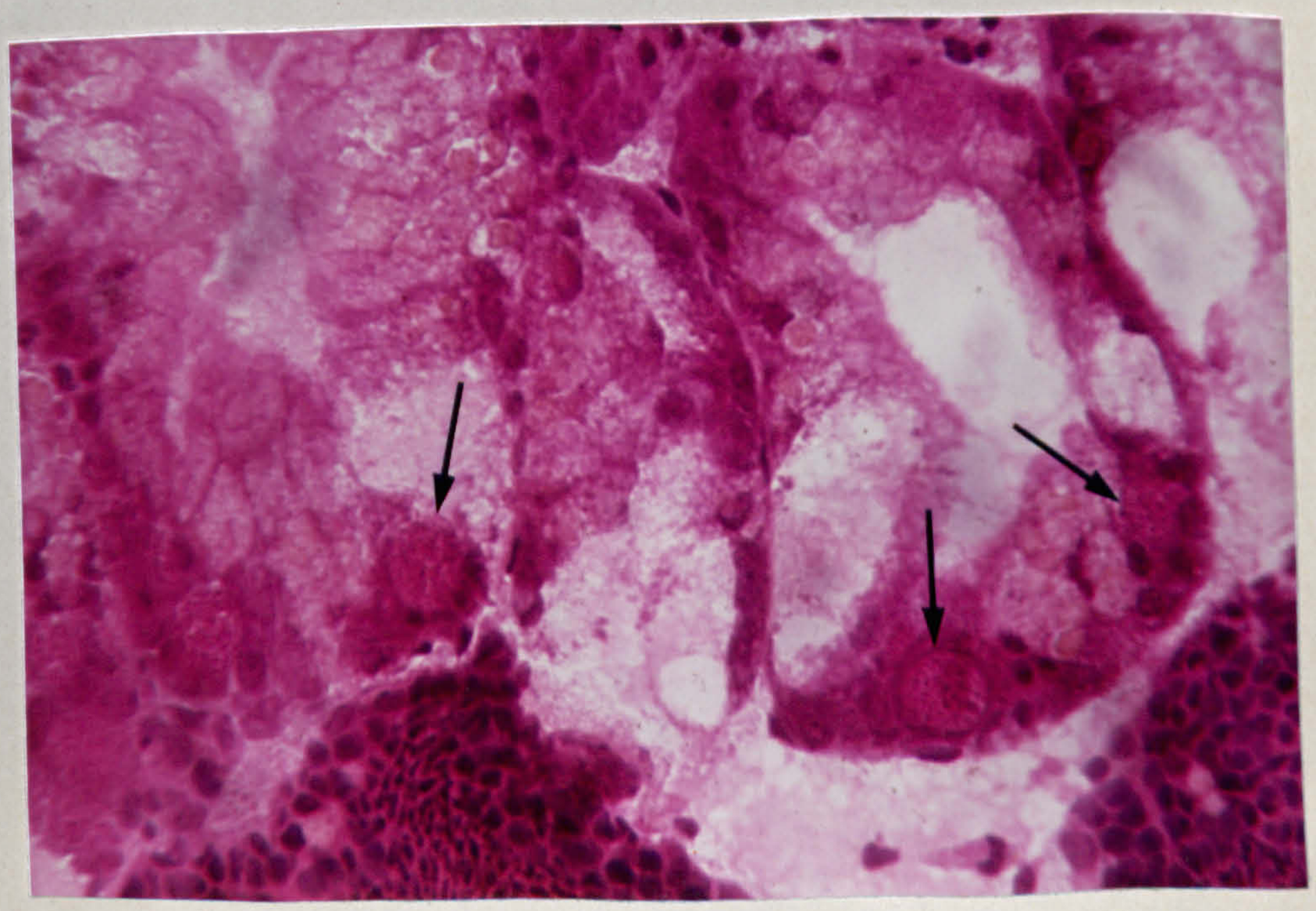

Fluorescent staining methods using acridine orange to show up concentrations of RNA and DNA in the digestive gland

Plate 95

Low power light micrograph of a cryostat section of digestive gland. MLO inclusions are believed to show as bright dots of yellow-gold fluorescence. Magnification of X 100.

Plate 96

Micrograph (X 250) of gut wall and digestive diverticuli. A prominent yellow inclusion body can be seen at centre bottom.

Plate 97

Micrograph (X 400) of MLO inclusion body in the cytoplasm of a secretory wall.

This stain shows DNA - Yellow, RNA - Green

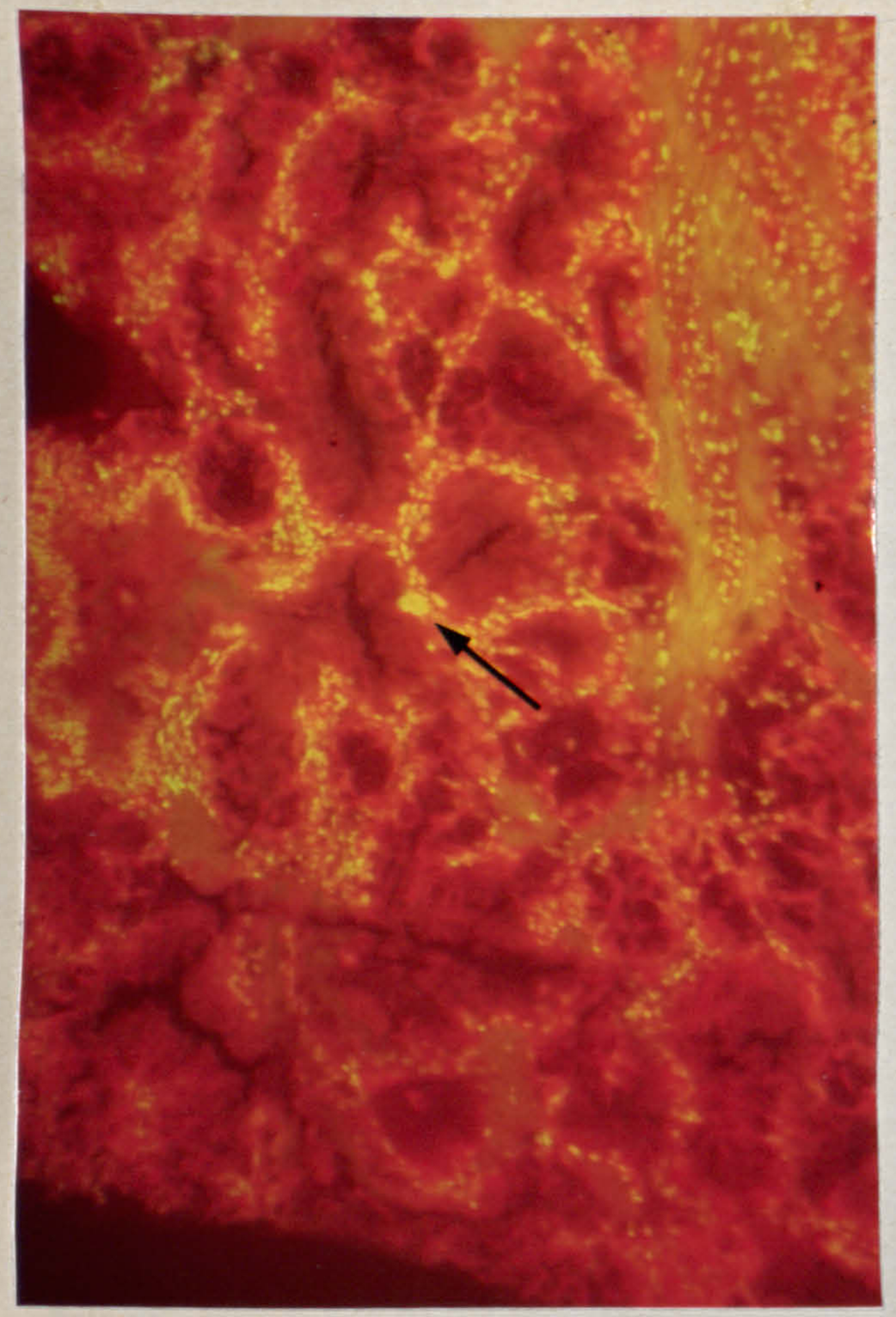

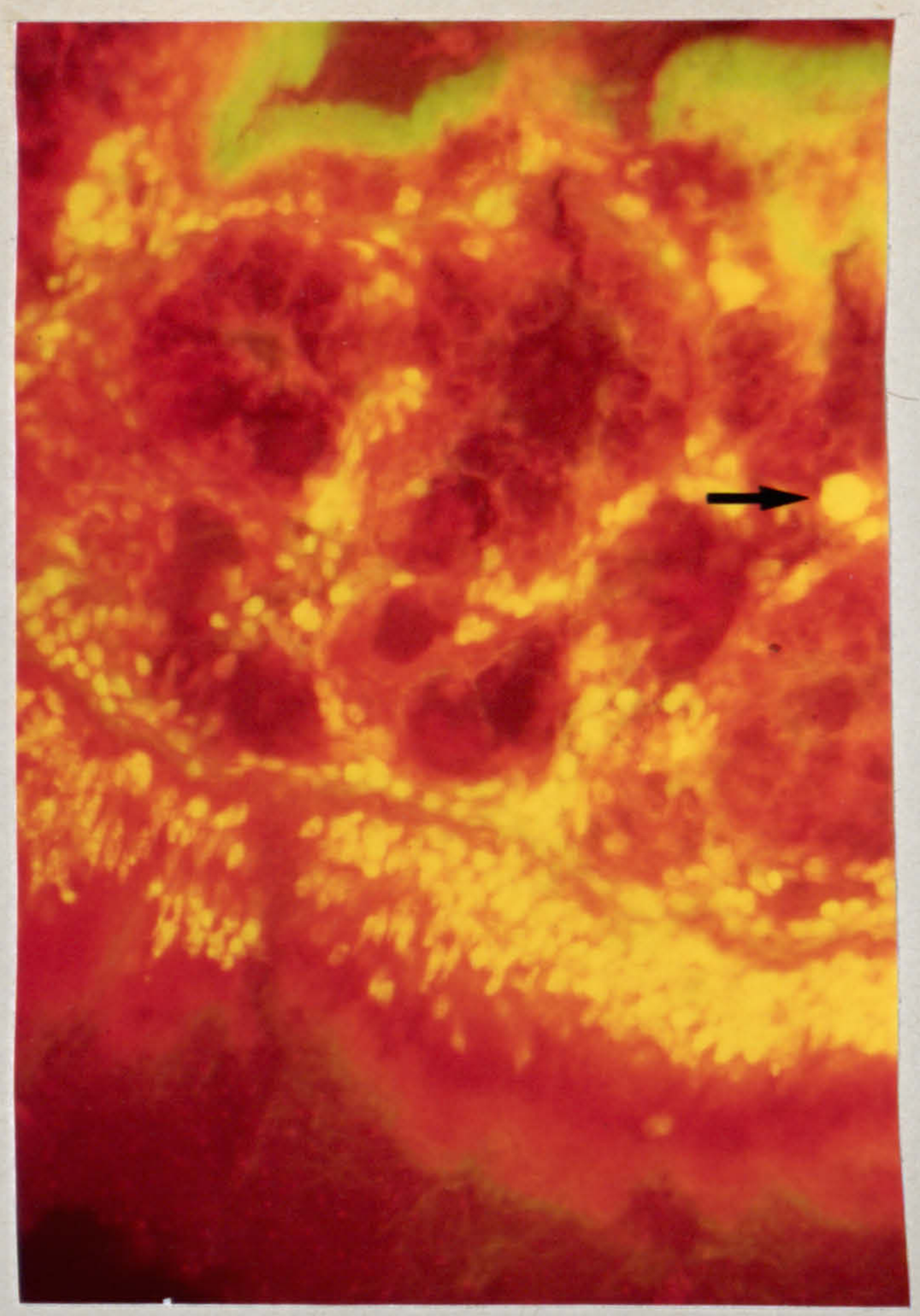

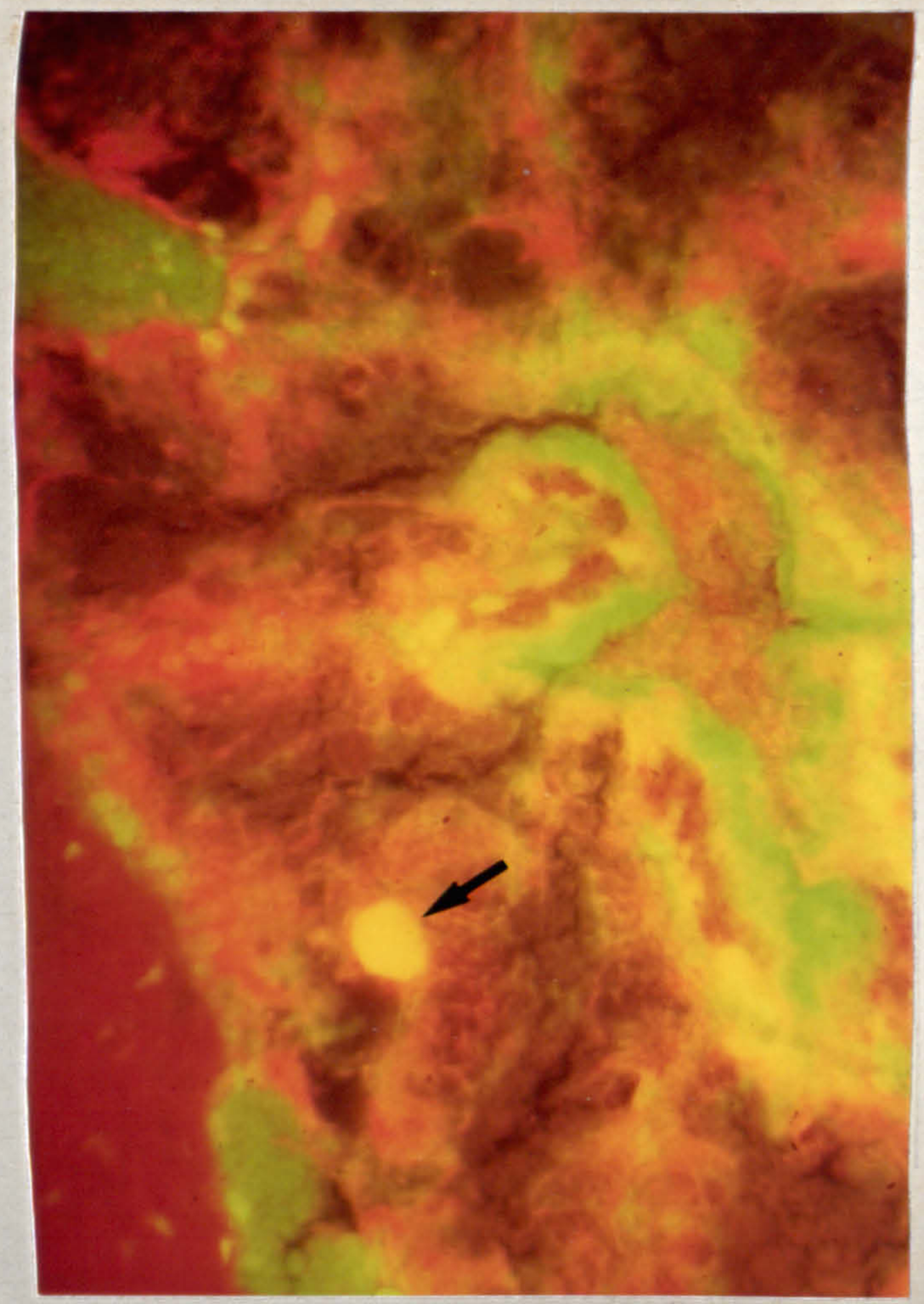

Acridine orange fluorescent staining of digestive diverticuli frozen sections

Plate 98

Muscle fibres show green; MLO inclusions orange/yellow; cytoplasm is red and nuclei yellow green. Magnification of X 250.

Plate 99

As above. Gut wall can be seen at left. Magnification of X 400.

Plate 100

As above. MLO inclusions stain orange-yellow. Magnification of X 400.

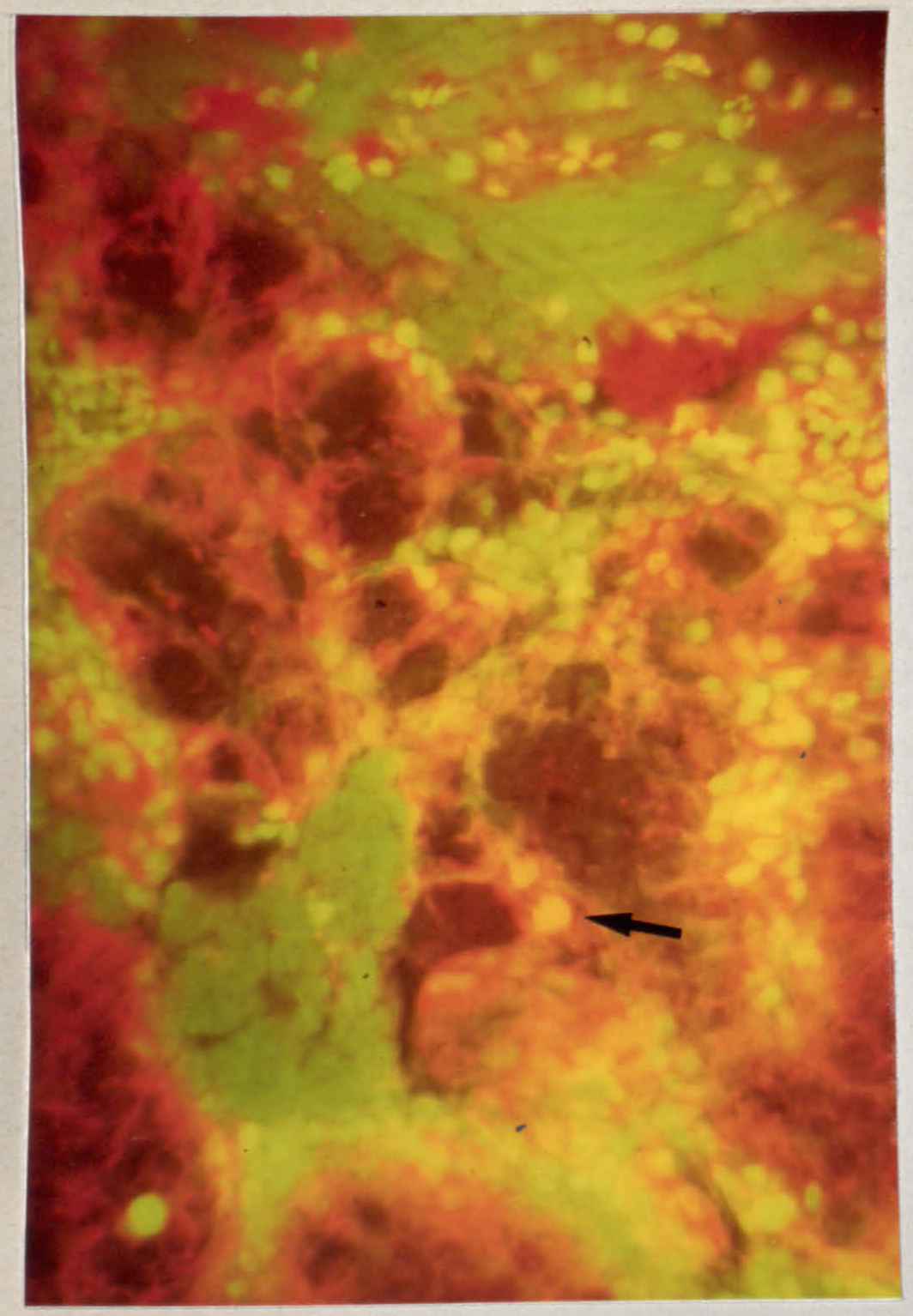

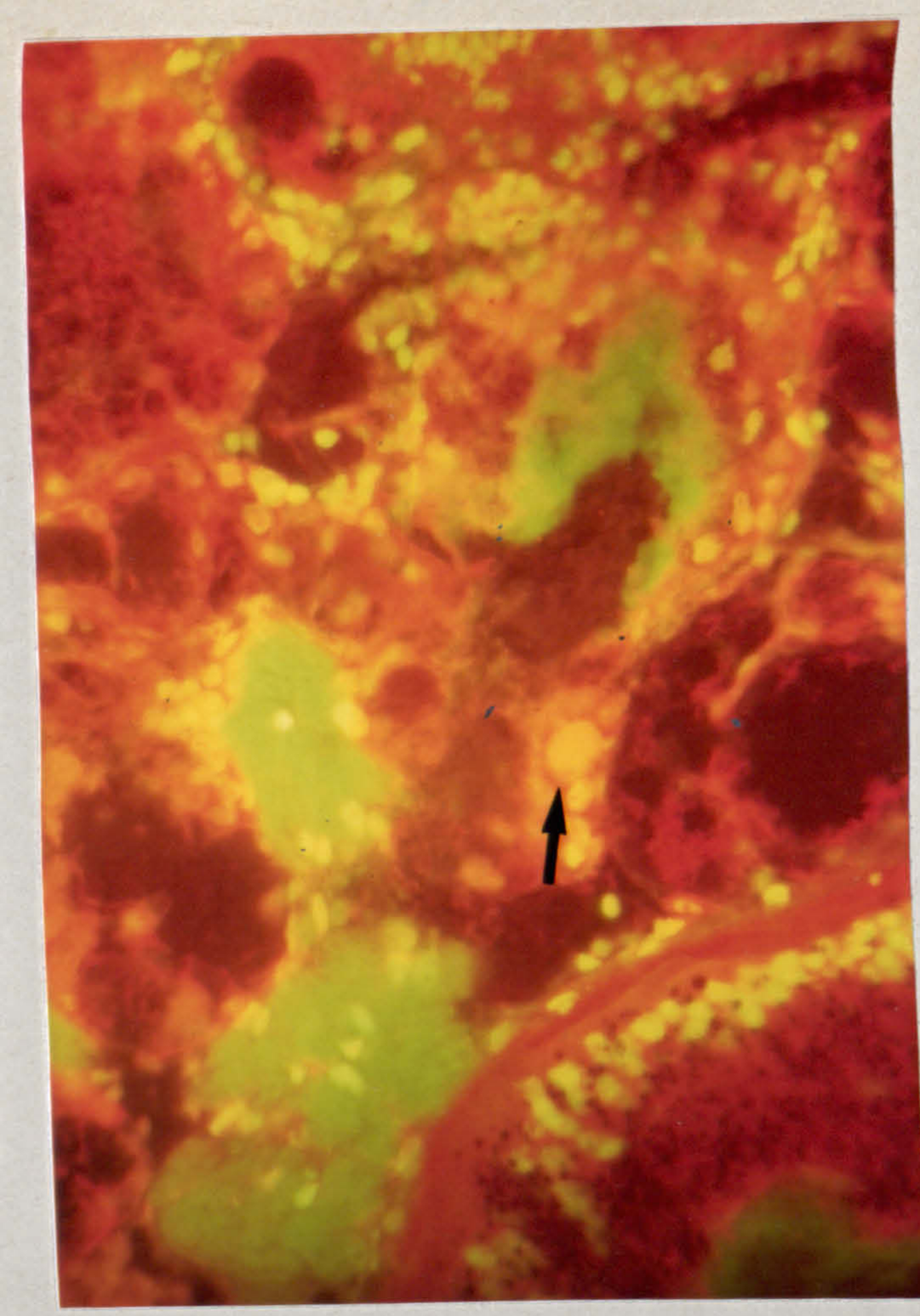

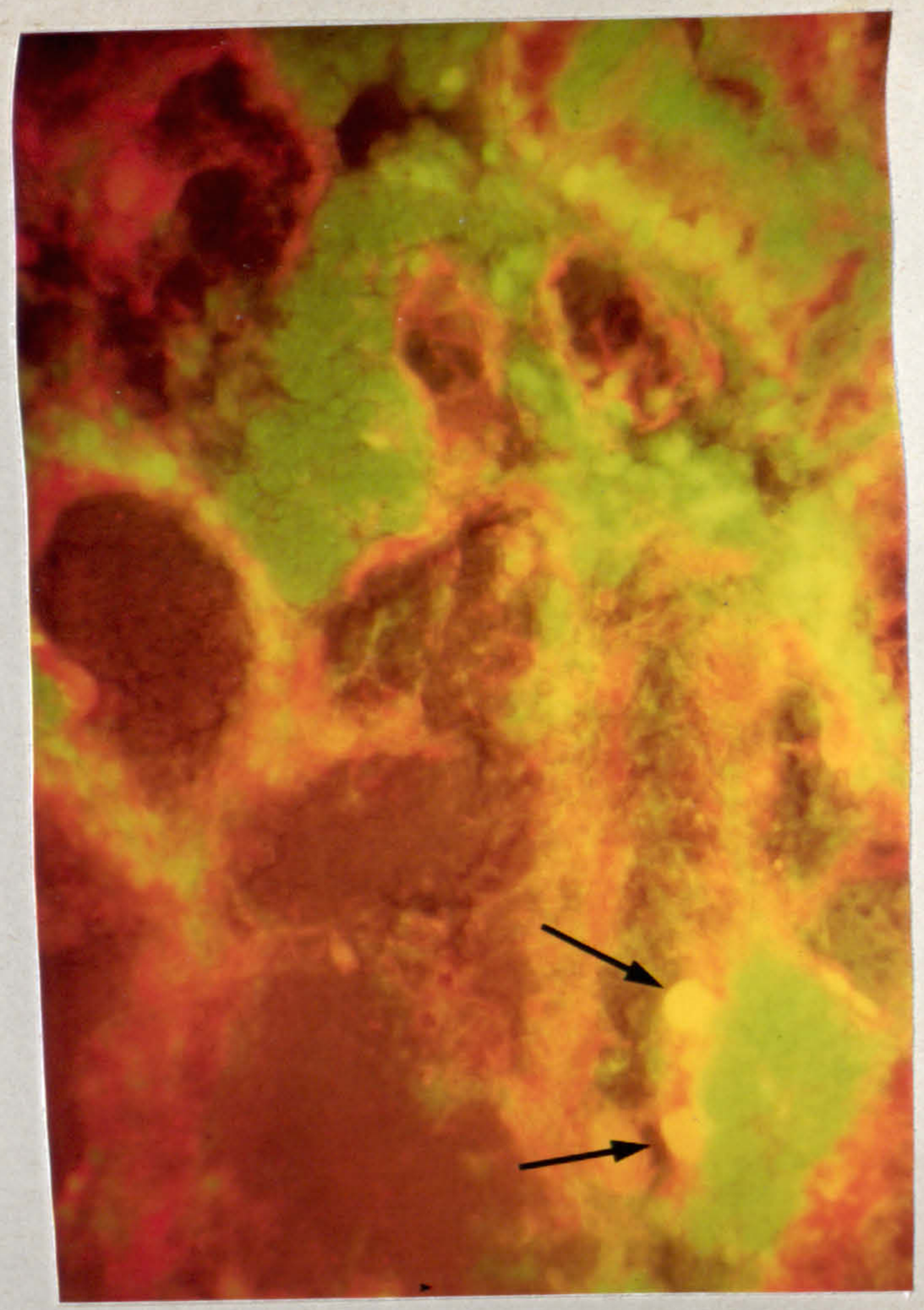

The vacuolation of the digestive gland resulting from the presence of the mycoplasma-like organism.

Plate 101

Low power phase contrast light micrograph of araldite embedded digestive gland fixed in 2.5% glutaraldehyde and 1% osmium tetroxide. Numerous dead cells can be seen within the tubules (x100)

Plate 102

Magnification (x400) of the portion outlined above. A progression from small spherical inclusions within the cytoplasm above the nucleus through to hypertrophied cells with the nucleus and cytoplasmic contents of the host cell flattened against the basal lamina of the tubules and finally lysis of the cell appears to exist. The stages are marked by the cells labelled 1, 2, 3 and 4.

Plate 103

This phase contrast light micrograph was observed with the oil immersion lens. The pleomorphic nature of the MLO within this cell can be seen. (Magn. x 1,200)

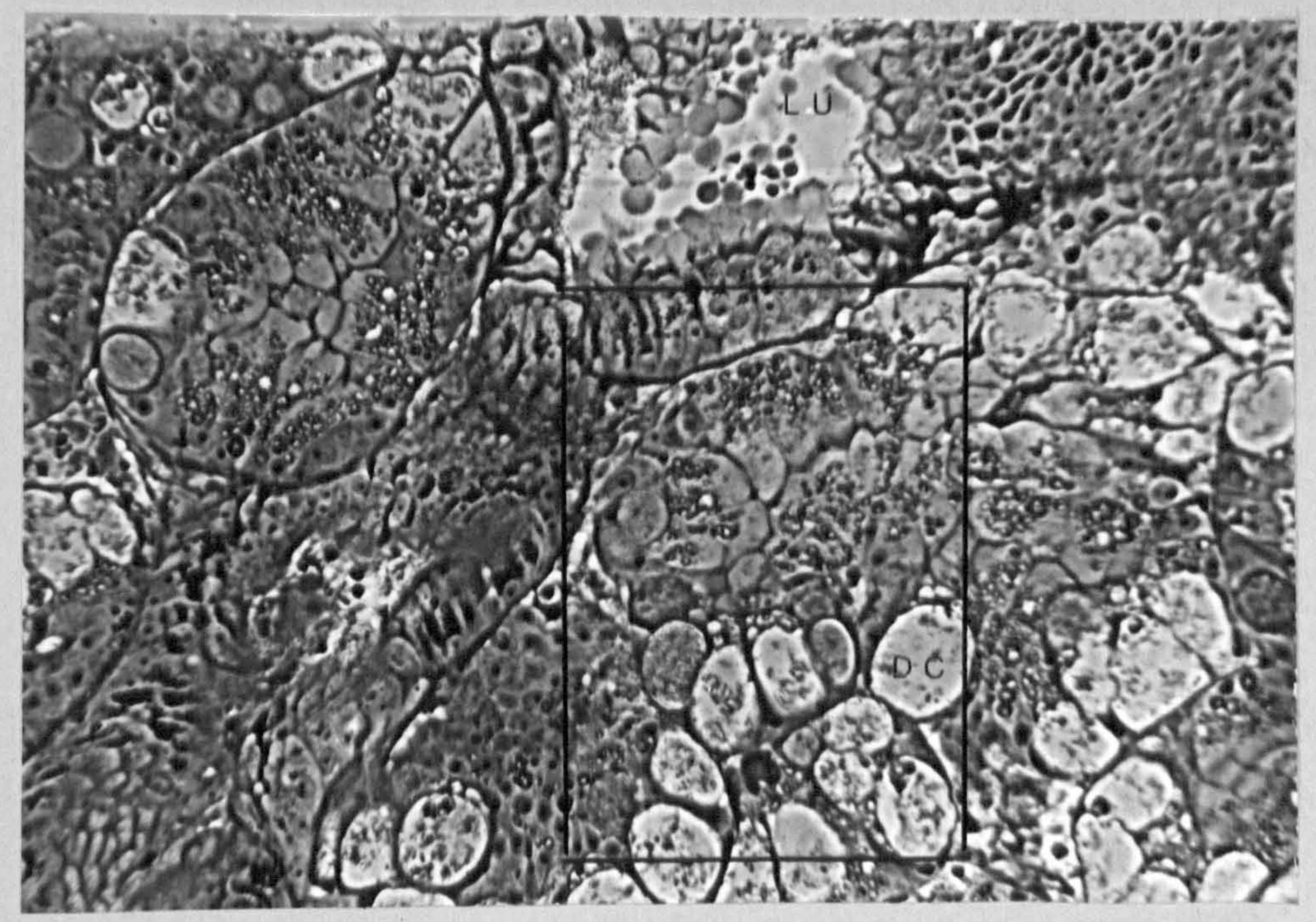
LU
DC

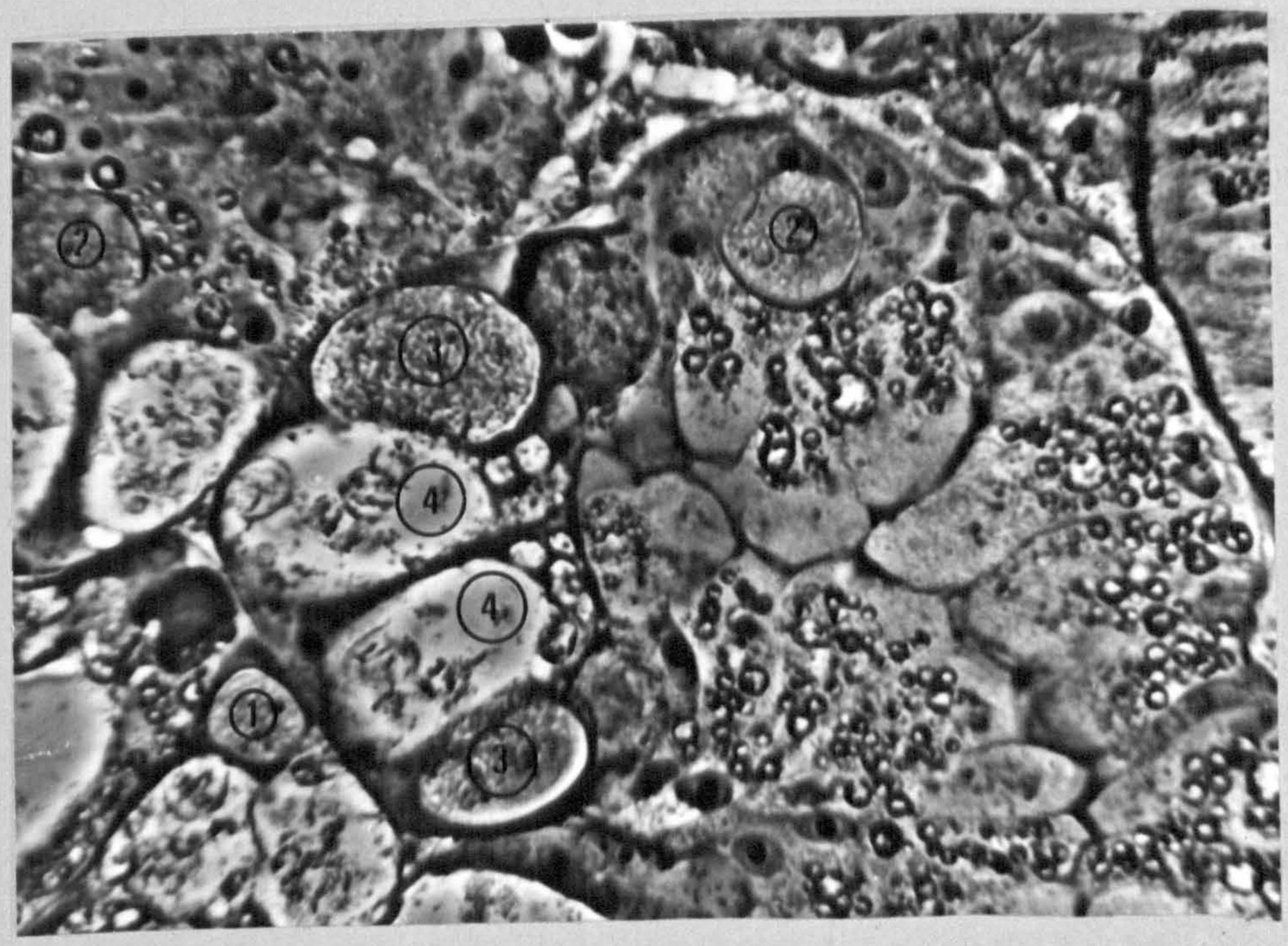
2
3
4
4'
4"
1
3

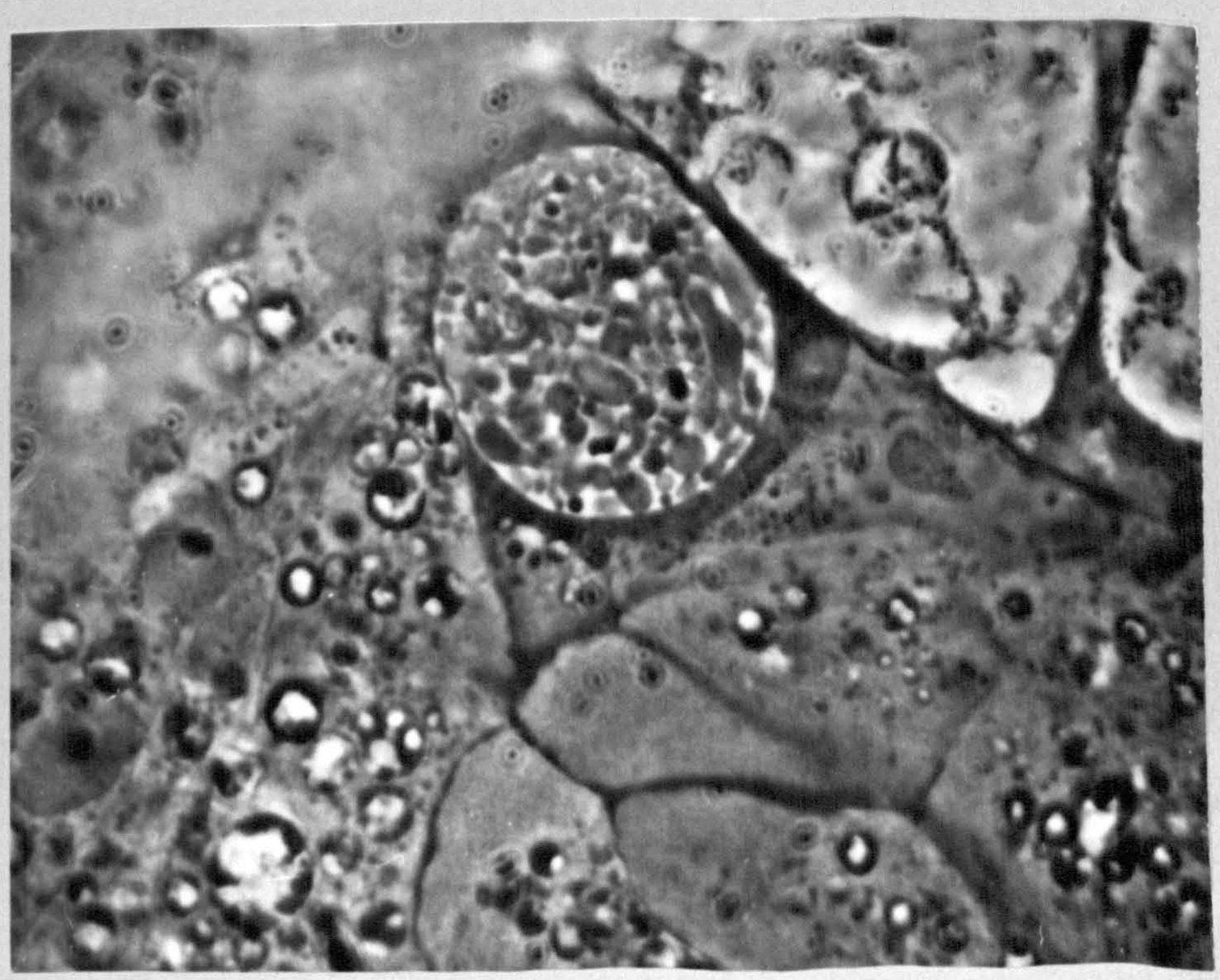

On the nature of the inclusions of the secretory cells of the digestive gland.

plate 104

This low power electron micrograph (x750) makes the link with the light micrographs (plates 101, 103 and 103) preceeding this. Note the presence of 3 spherical inclusions containing numerous coccoid organisms ranging between .1 to .8 um in diameter. The electron dense cell also contains these organisms. The profiles of 3 dead cells can also be seen

Plate 105

Dctail of the inclusion cell at top right in plate 104. A few scattered viral particles can be seen in the mycoplasma organisms contained within the membrane bound inclusion. (x 8,000)

Plate 106

Detail of the electron dense cell at centre right of plate 104. Note the presence of numerous paracrystalline arrays of virus particles within the MLO's. (10,000)

Plate 107 (x 3,000)

Detail of the two spherical cells at left in104. The MLO's in the lower cell do not contain virus.

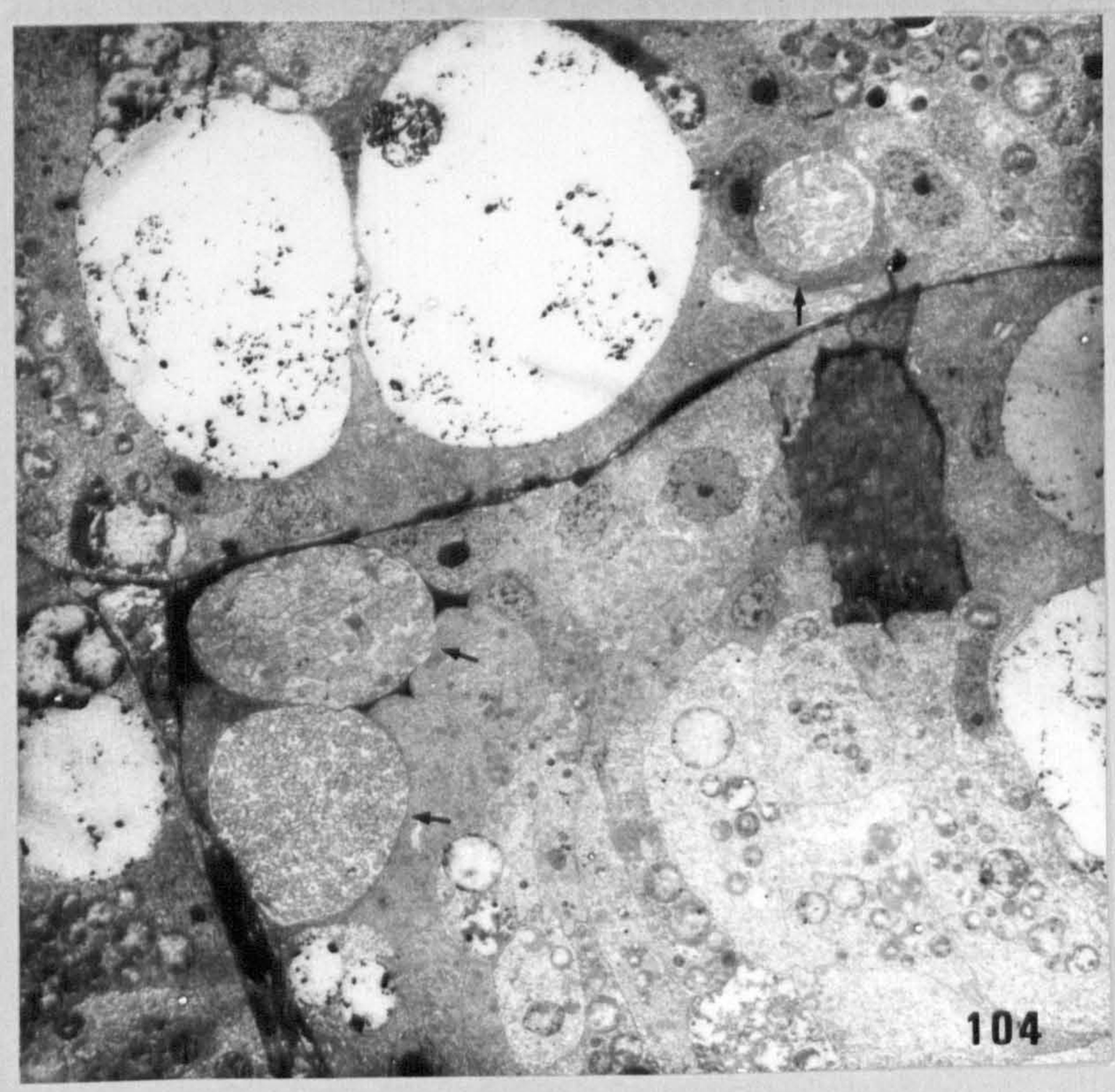

104

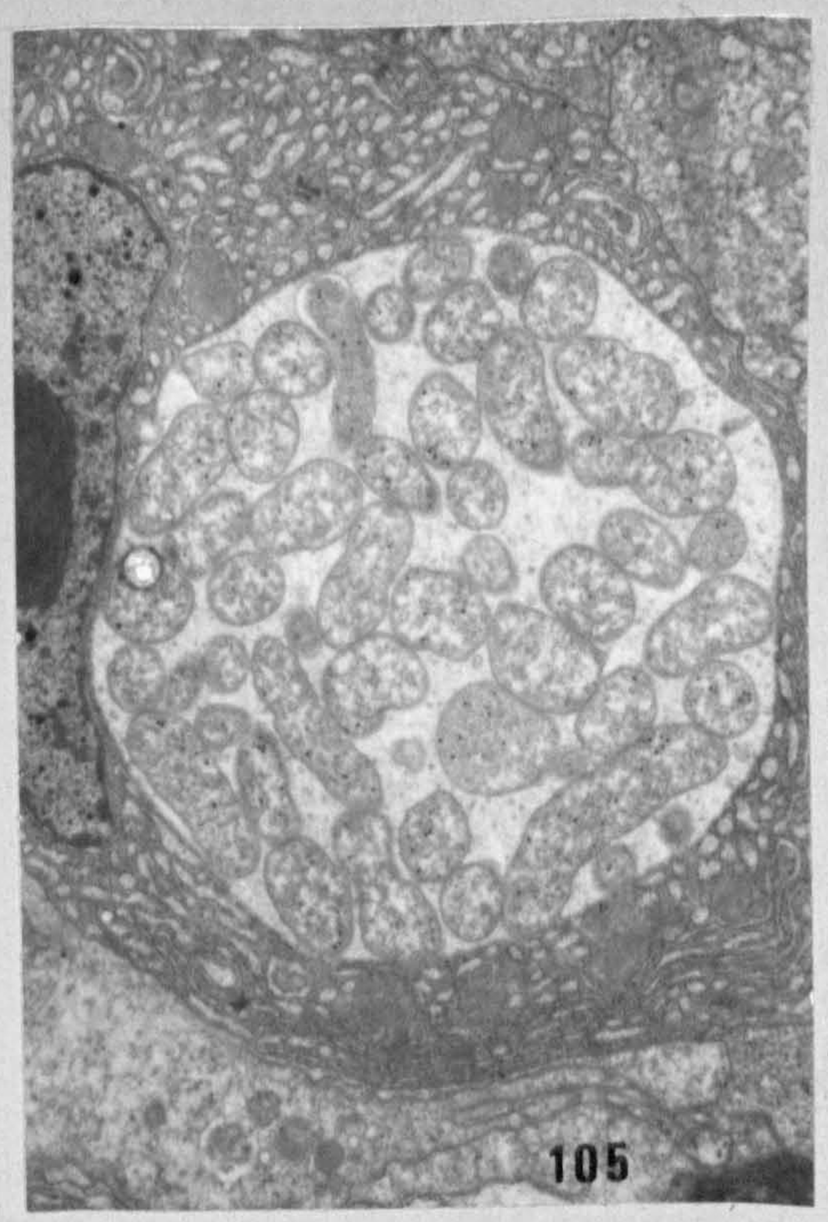

105

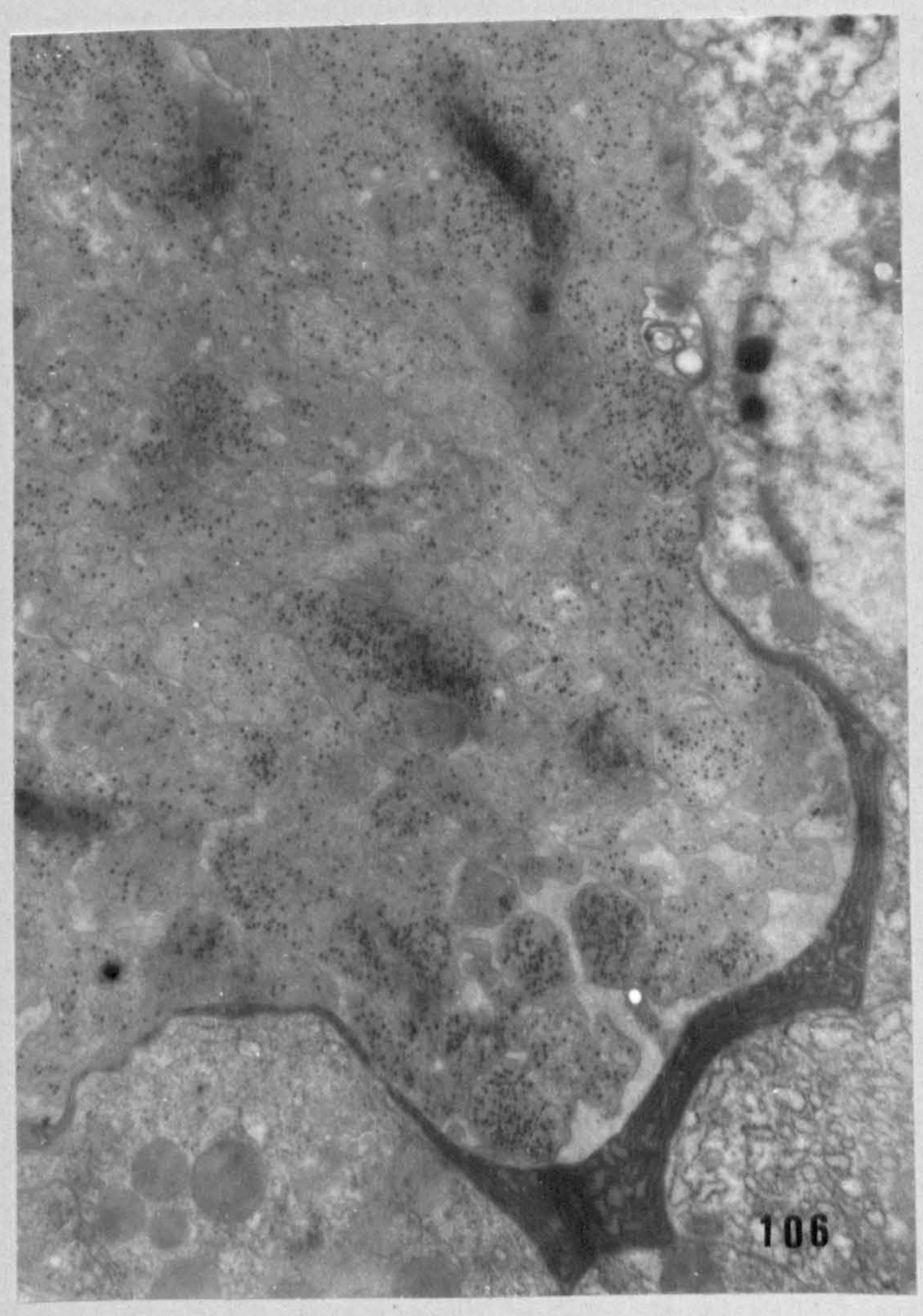

106

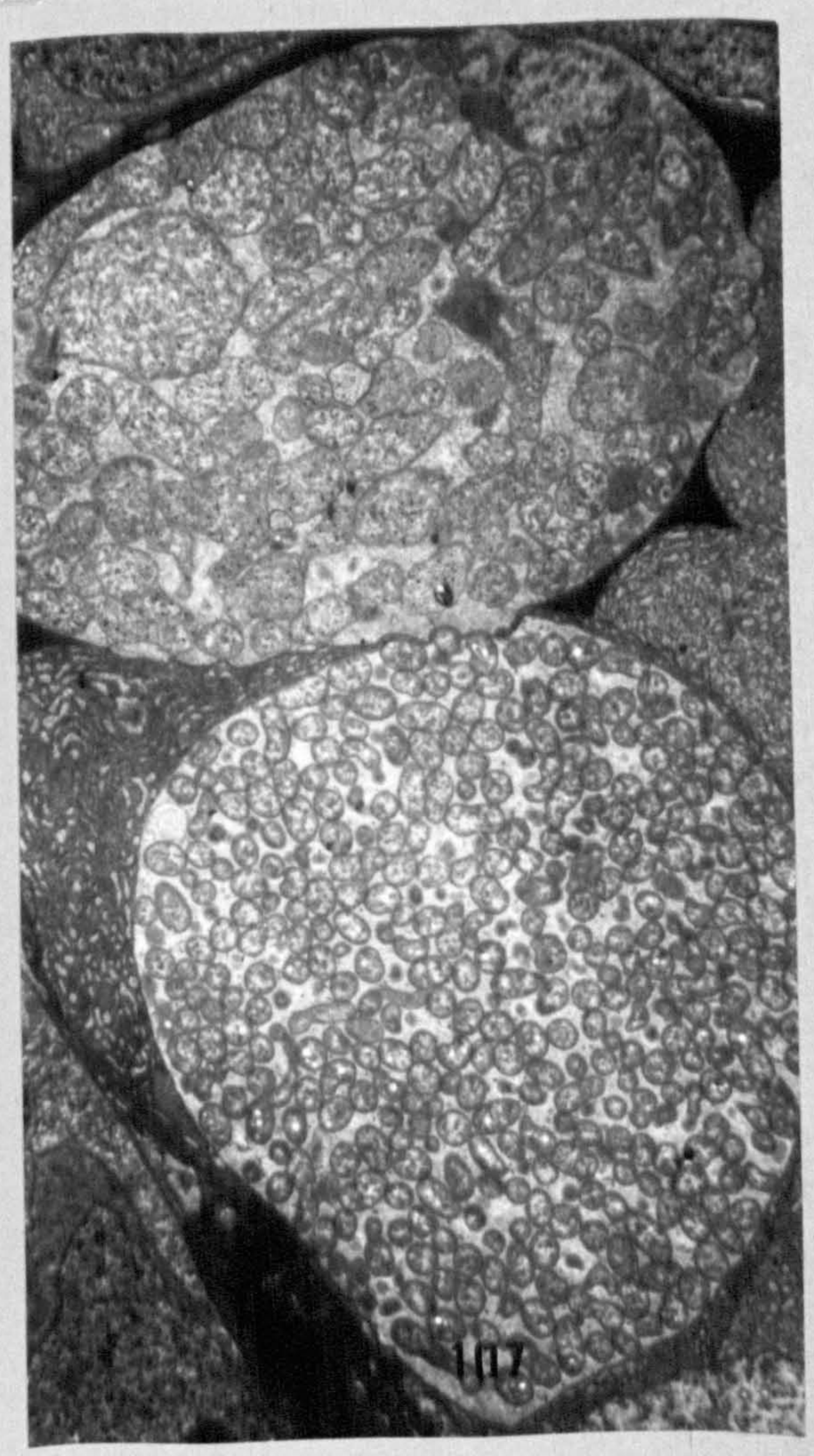

107

The fine structure and mode of replication of the MLO

Plate 108

Detail from plate 107 overleaf. There is a marked difference in appearance between those microrganisms containing phage (at left) and those free of virus particles. Phage containing cells appear 'leaky'. (magn. x 10,000)

Plate 109

Note the characteristic 'chain of beads' appearance of the MLO at left. The cells appear to reproduce by synchronous replication of the genome followed by constriction of the cytoplasm at regular intervals. New cells appear to pinch off from this chain.

(Magn. x 12,000)

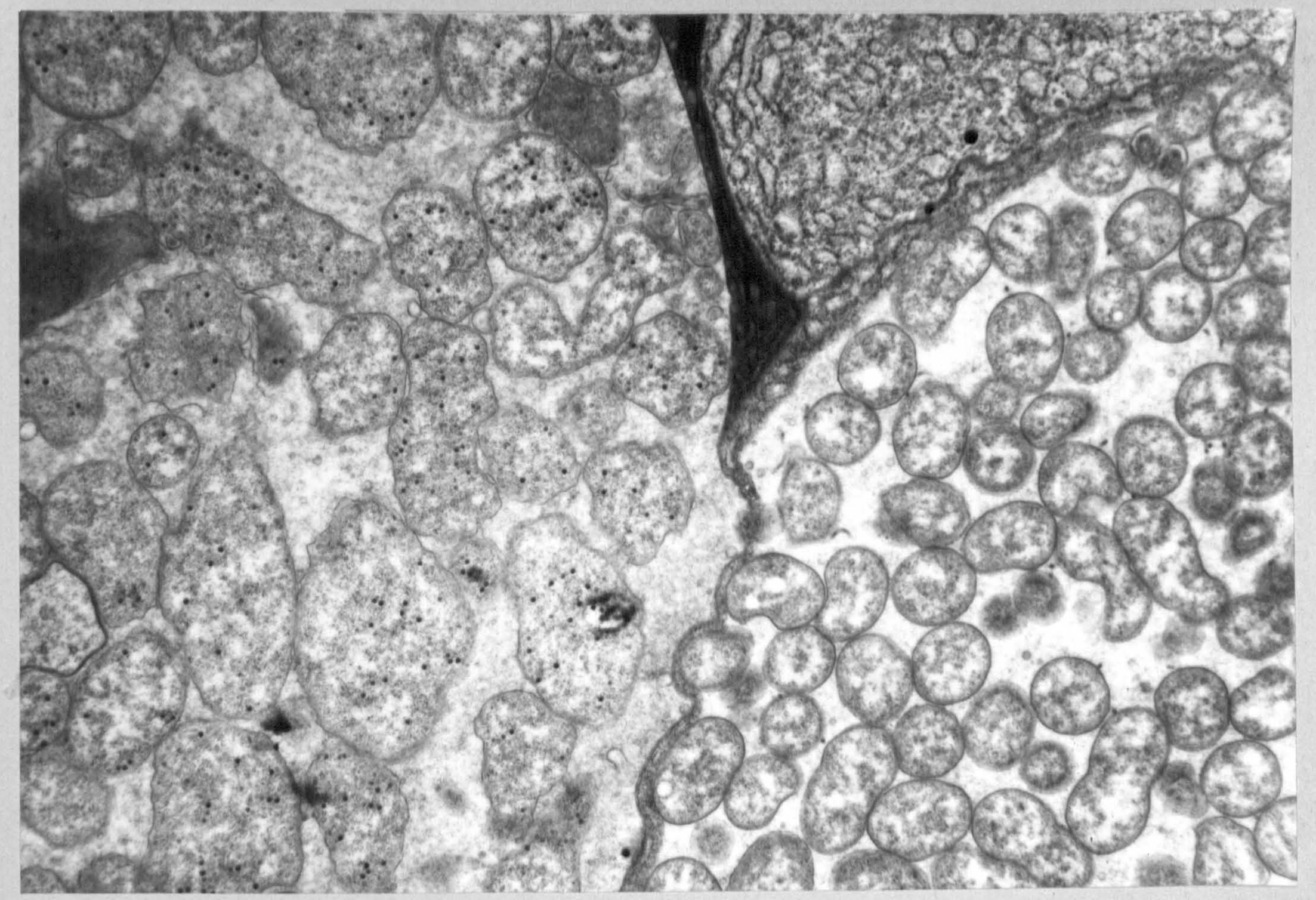

The early stages of infection of secretory cells with MLO's.

Plates 110 and 111

These low power electron micrographs illustrate the early phase of the development of an inclusion within the cytoplasm of secretory cells. The top plate is of a section of digestive gland from an individual fixed in December at Kames Bay, Millport. The lower is of an individual Tellina fixed in April at West Sands St. Andrews. Note the well developed endoplasmic reticulum in both cells. The membrane bound vacuole enclosing the MLO is most clearly seen in the upper micrograph. The MLO's in the lower plate contain virus particles whereas those illustrated above do not.

Upper plate x 5,000

Lower plate x 8,000

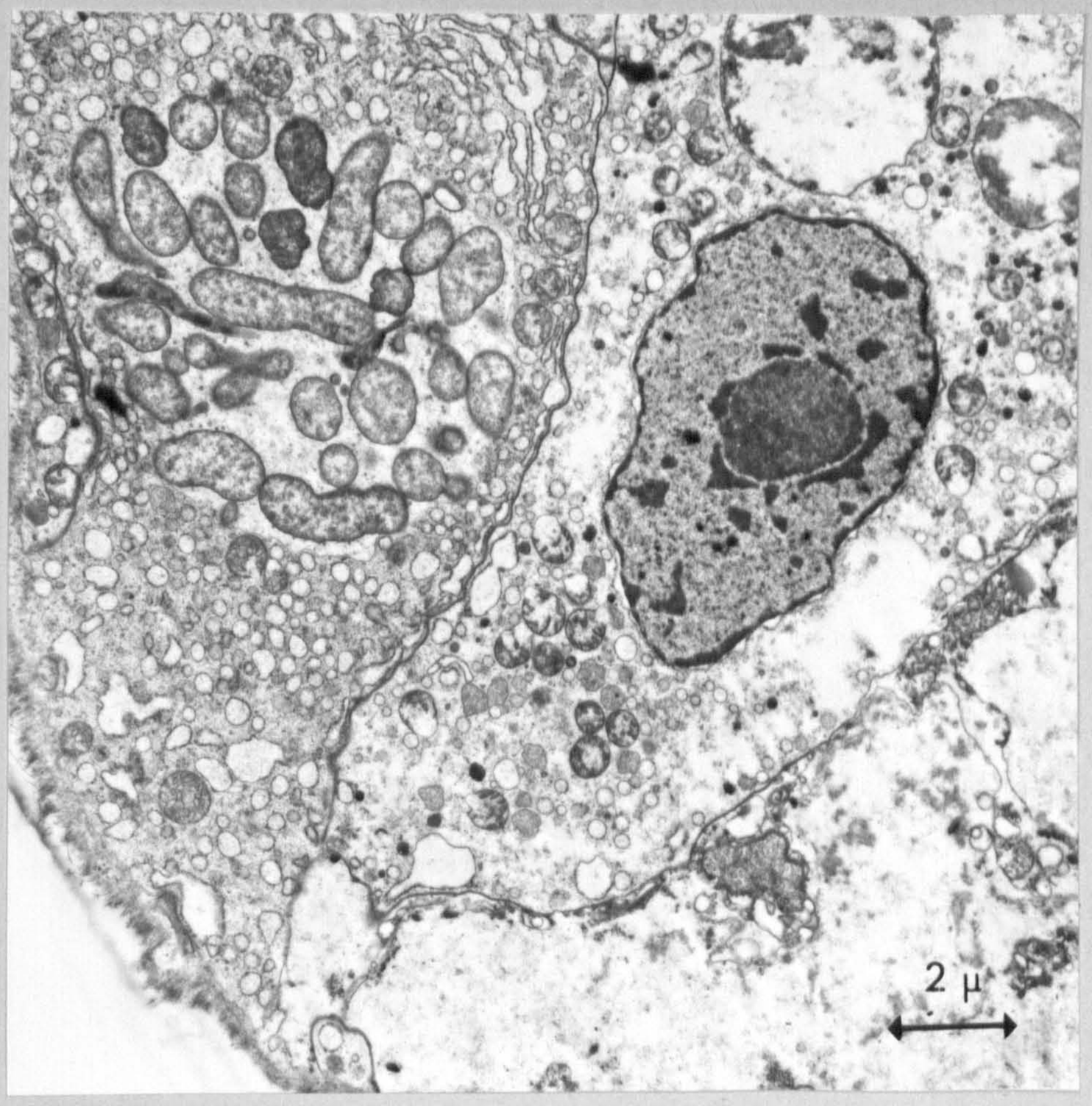
2 µ

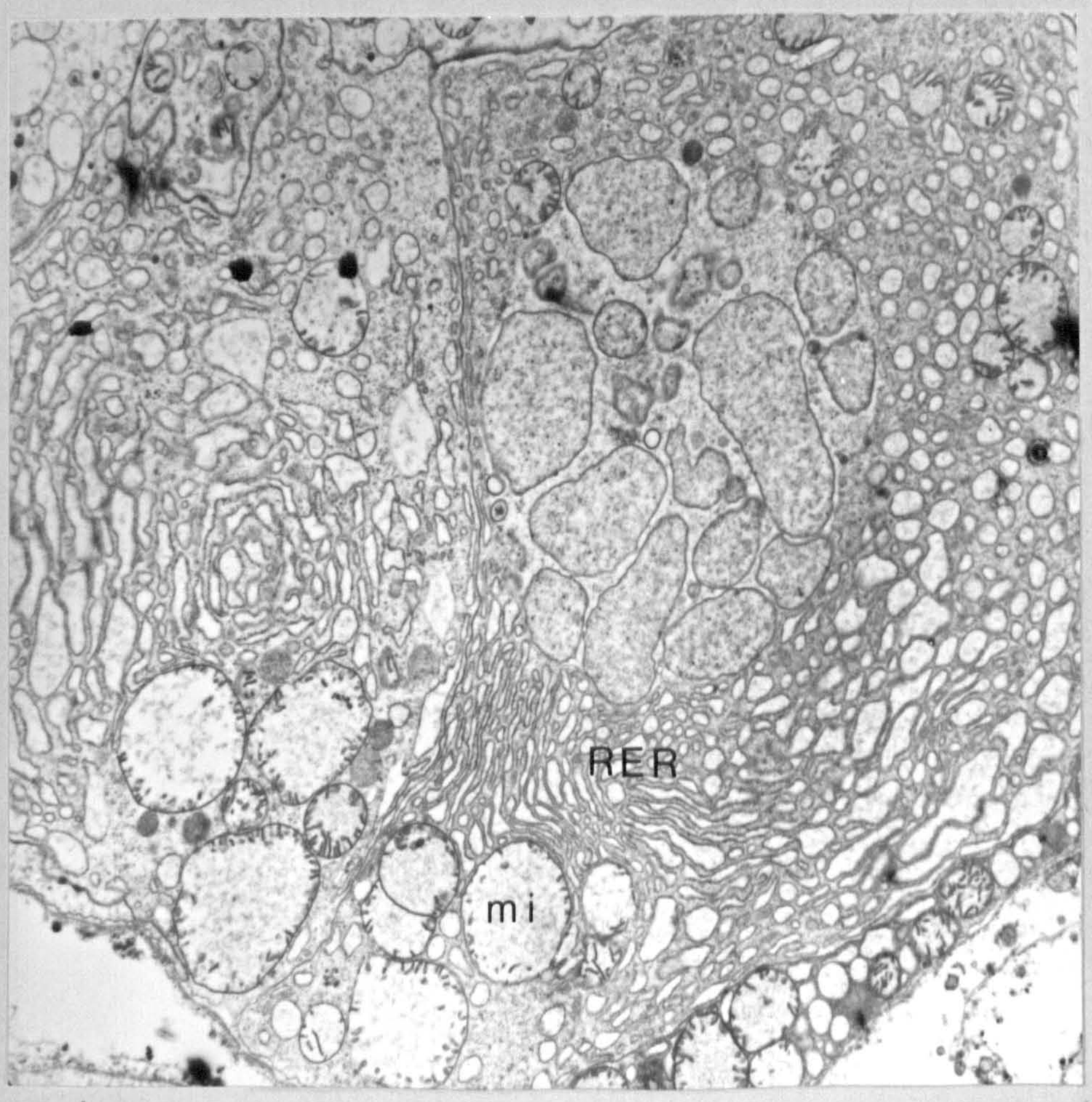
RER
mi

Early and final stages of MLO invasion of secretory cells in the digestive gland

Plate 112

Low power electron micrograph (X 1,500) of a dead cell (*) believed to have resulted from the lysis of an infected cell of the type seen in the left of this micrograph. Digestive cells containing heterolysosomes and residual bodies can be seen in the lower part.

Plate 113

Detail of the membrane bound inclusion from the above Figure containing pleomorphic MLO. Scattered phage heads can be seen in the centre of the MLO.

Note the small, protruding, compact 'blebs' with electron dense matrices. These are believed to represent elementary bodies at an early stage of formation.

The large filamentous form arrowed appears to be undergoing fragmentation.

(Magn. x 10,000)

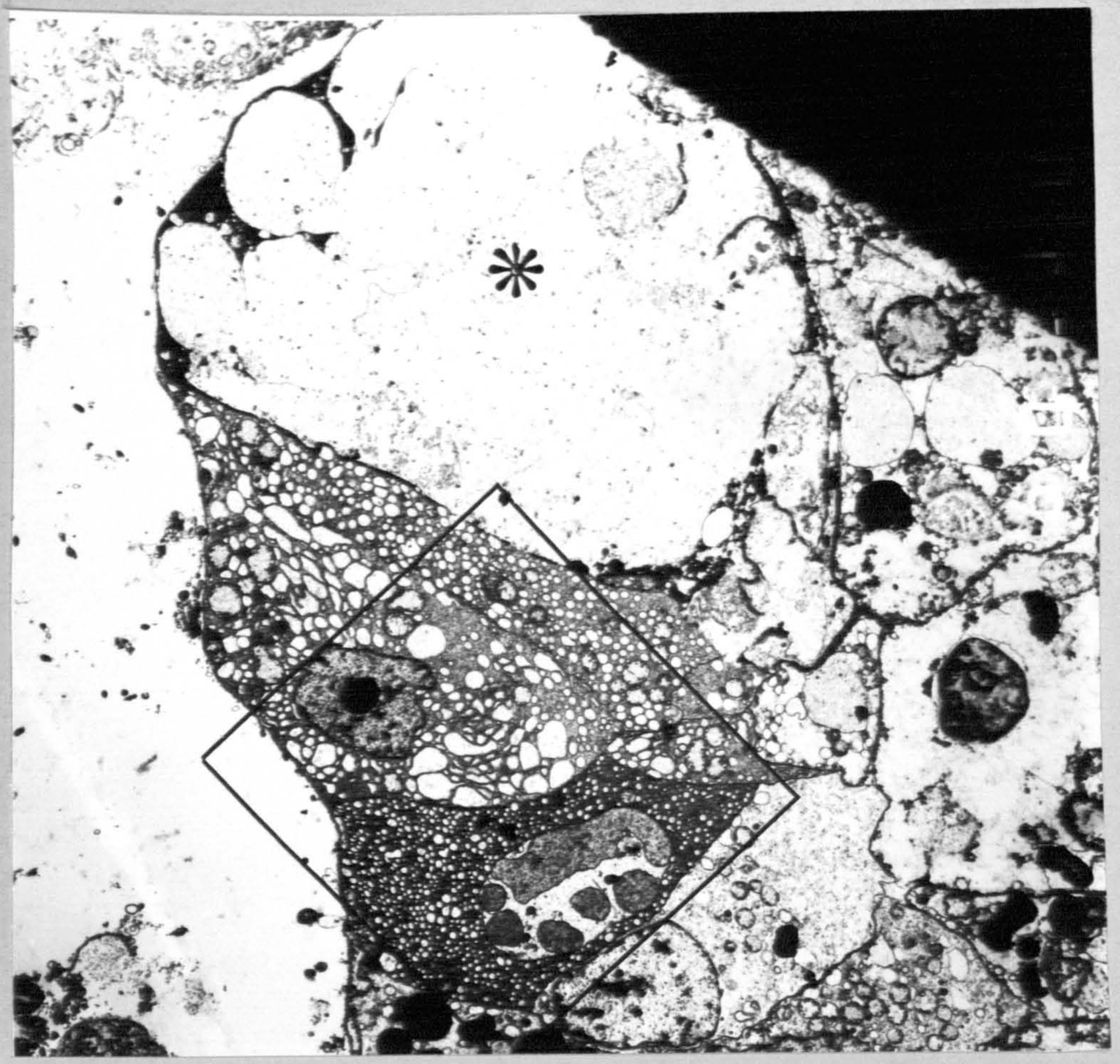

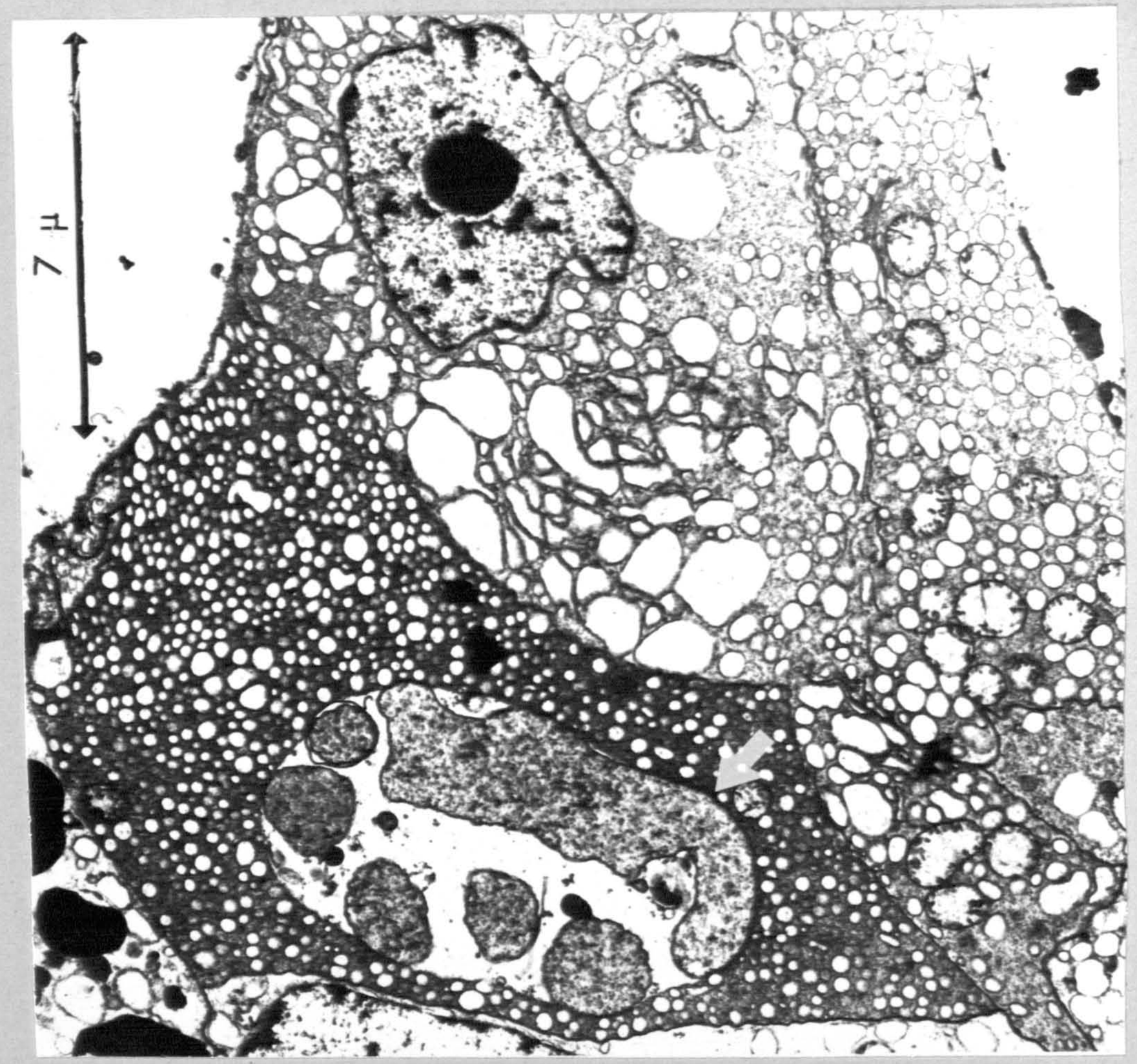
7 μ

Electron micrographs of the early stages of MLO invasion of secretory cells

Plate 114.

A low power electron micrograph (X 4,000) of a lobe of the digestive acini. The basophil cell at top centre has a karyorhectic nucleus and has a central cytoplasmic inclusion of mycoplasma-like organisms containing phage-virus. This cell is believed to represent an early stage of MLO infection. A digestive cell containing lysosomal bodies occupies the centre of the micrograph.

Plate 115

Detail of plate 114 above. Note the absence of a nuclear membrane, dense profiles of endoplasmic reticulum and scattered phage head particles within MLO. Two of the MLO spherules appear to have undergone lysis (arrowed) with consequent release of phage-virus.

(Magn x 20,000)

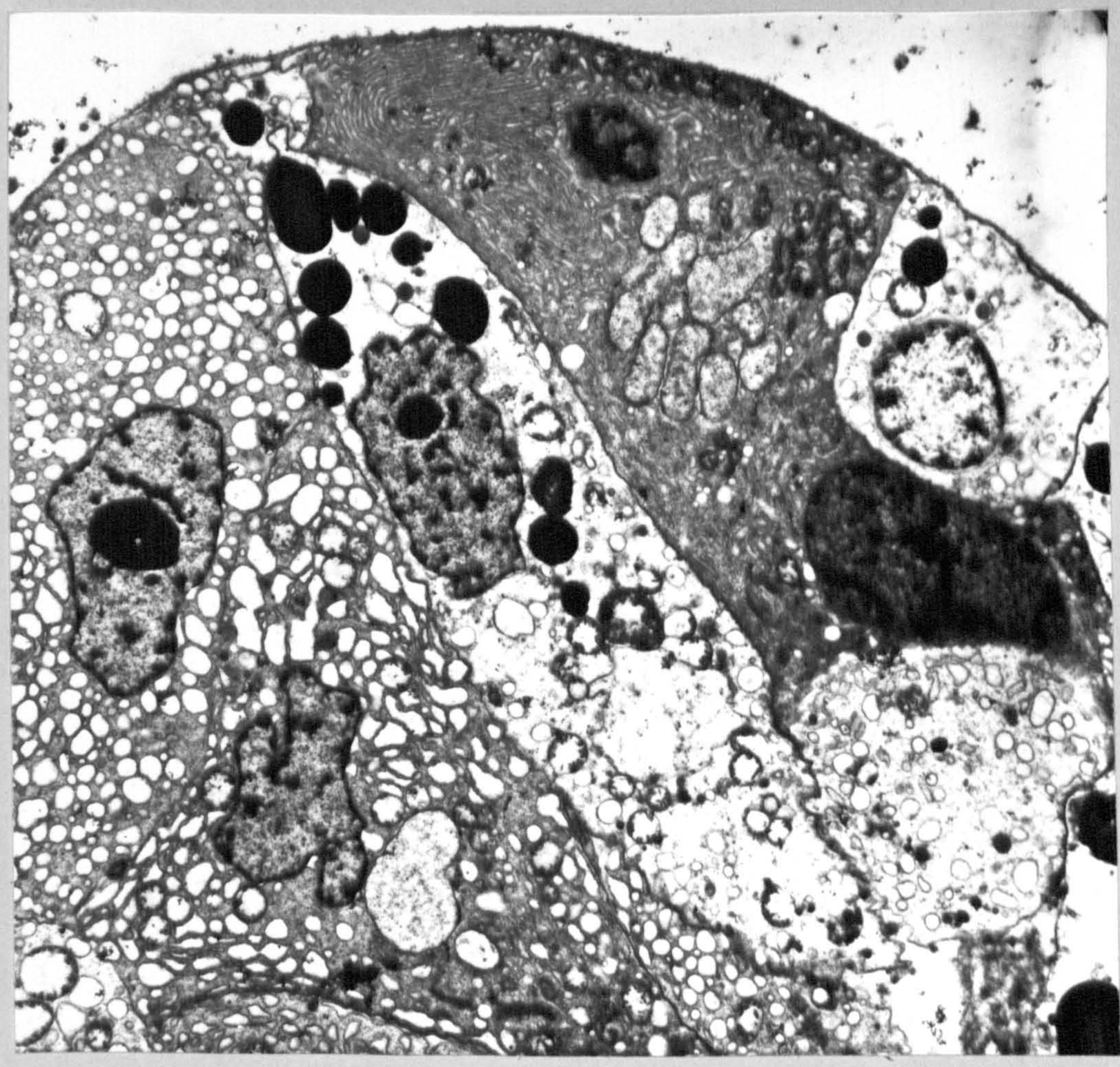

Electron micrographs of early stages of MLO invasion of secretory cells

Plate 116

Detail of Plate 114 . Note the characteristic densely granular cytoplasm with numerous whorls of rough endoplasmic reticulum of the secretory cell which surrounds the MLO spherules. Magnification X 12,000.

Plate 117

Detail of plate 116 above. The striated rod-like structures has virions in close association with it. It is believed that these rod-like structures may be involved in viral replication although just how is not understood. These structures are most often seen in close association with the membrane bounding these MLO spherules. The possibility that these striated rods might be phage tails at a stage in replication has also to be considered.

The characteristic stellate appearance of the prokaryotic nuclear region is arrowed. Elementary bodies (EB) lie between the pleomorphic spherules. Magnification X 25,000.

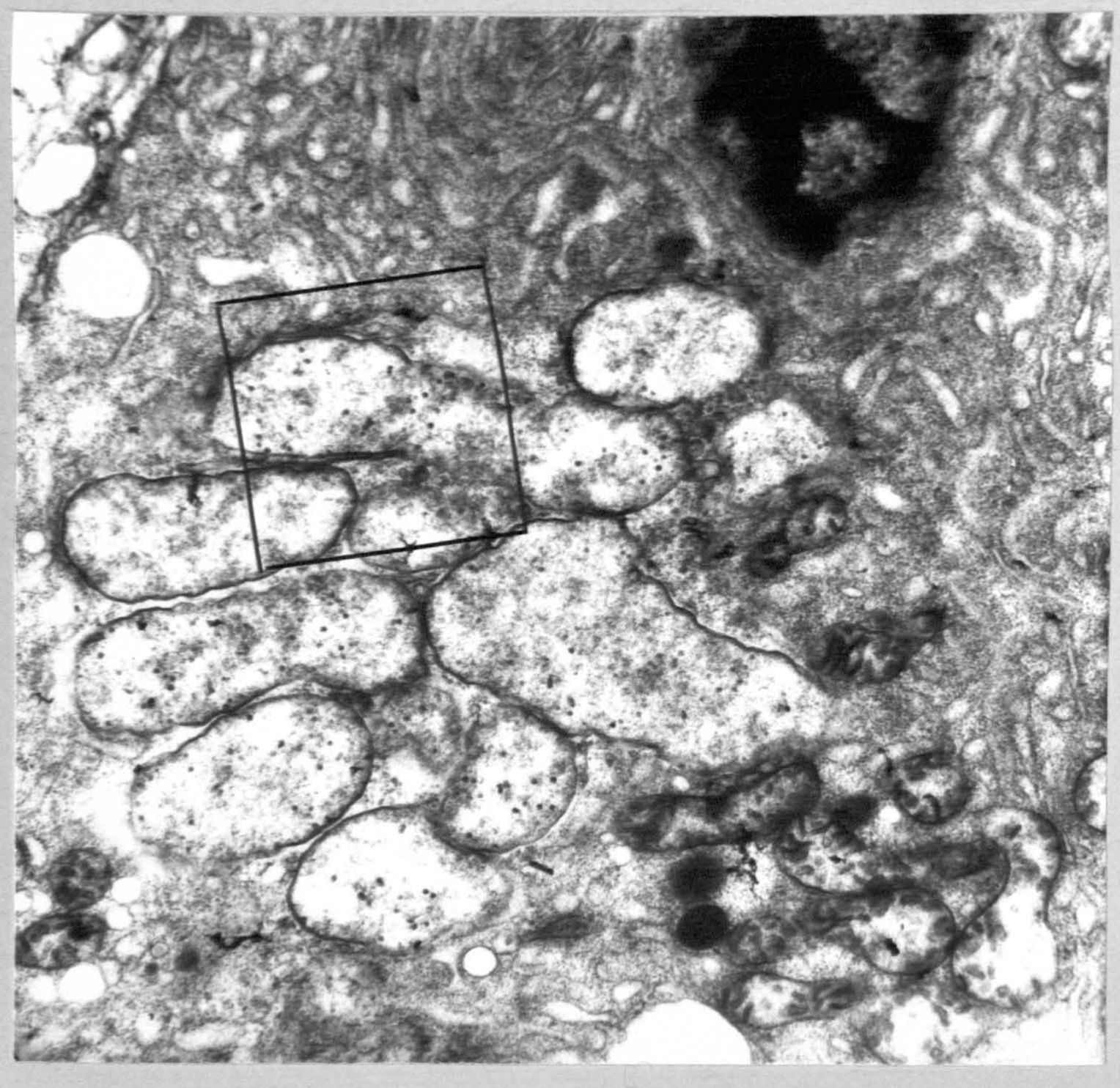

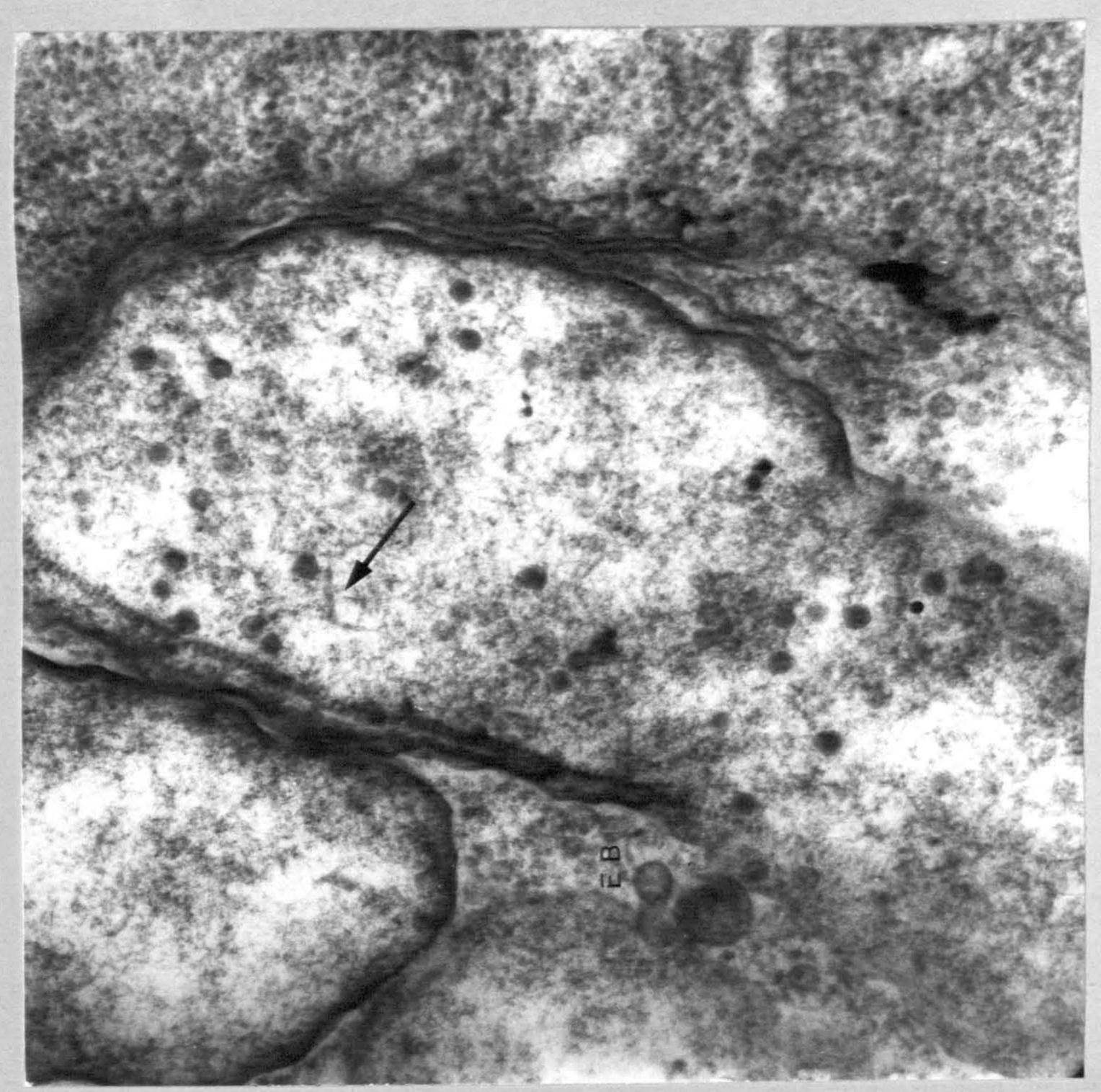
EB

The cytopathic effect of the MLO on the host cell

Plate 118

This low power electron micrograph of a secretory cell has the characteristic 'jagged' outline of a MLO containing cell where the MLO themselves are packed with virus. The nucleus is pycnotic, osmiophilic and possesses a convoluted outline with greatly dilated nuclear envelope. The diagonal line across the micrograph is caused by a tear in the formvar coating of the grid on which the sections are mounted

Plate 119

Detail from plate 118. Note the dispersed chromatin and pronounced rimming of the chromatin at the nuclear margins. It seems likely that this nucleus was at an early stage of karyorexhis. Note also the distended nuclear pores (arrowed)

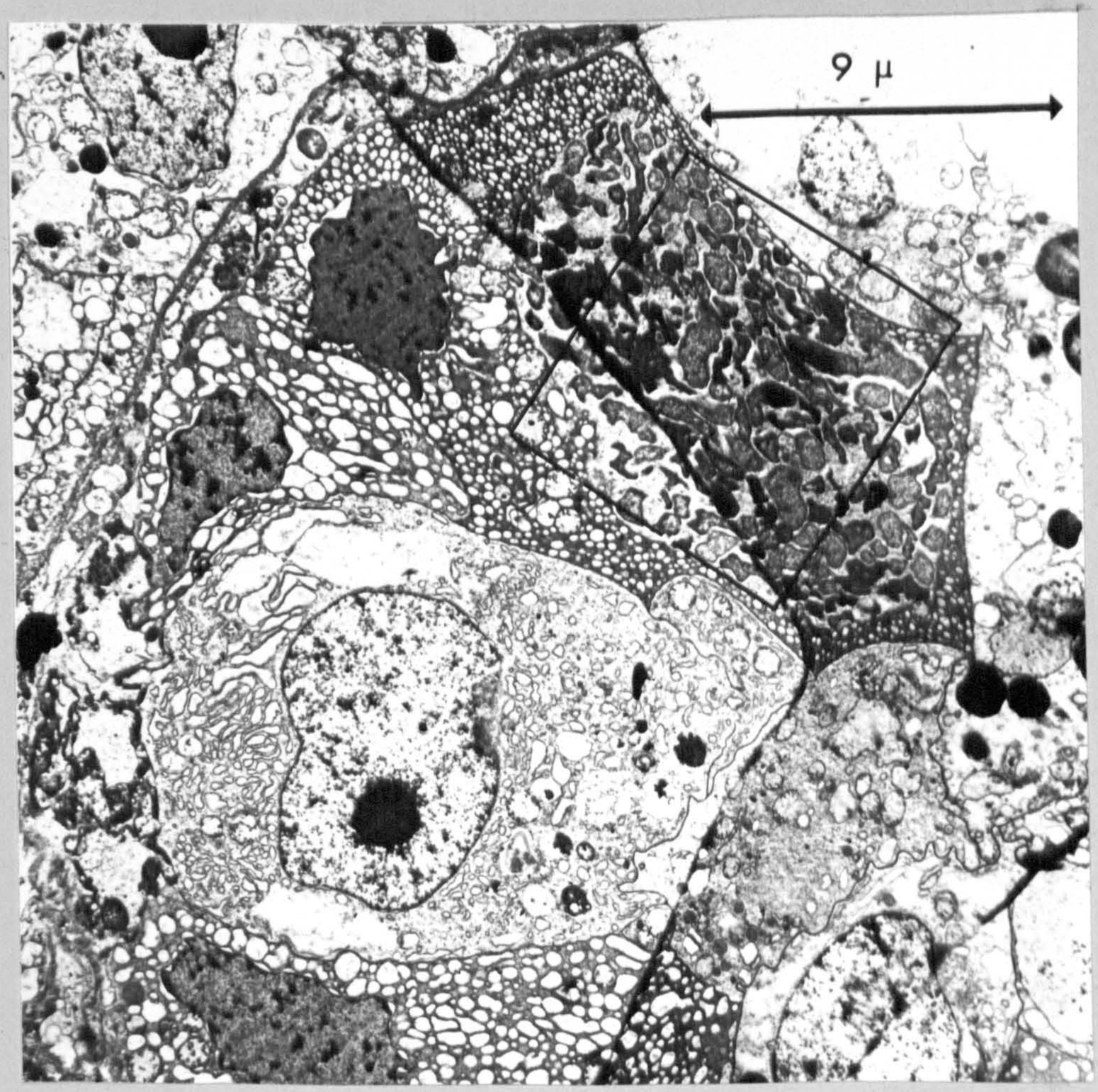
9 μ

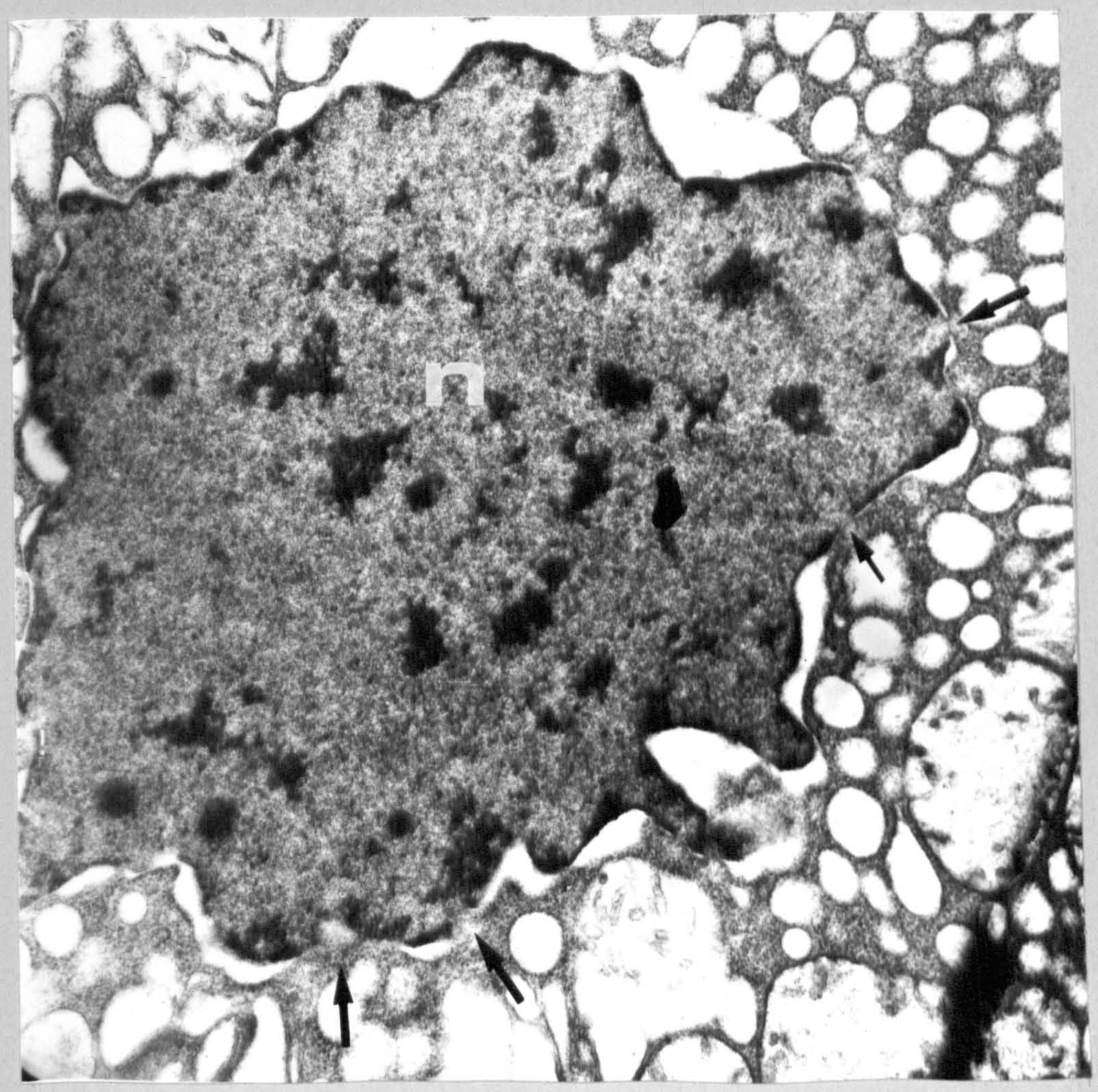
n

Ultrastructure of the phage and associated rod-like structures

plates 120 and 121

These plates are details from plate 118 Note the dense paracrystalline arrays of virus having hexagonal outlines. Striated rod-like structures can be seen in association with the viral arrays.

The upper micrograph gives evidence of the presence of a cell wall having a rippled or wavy structure. This is characteristic of the Rickettsiales. The presence of a cell wall is in doubt in those cells that do not contain virus.

Upper plate x 10,000

Lower plate x 50,000

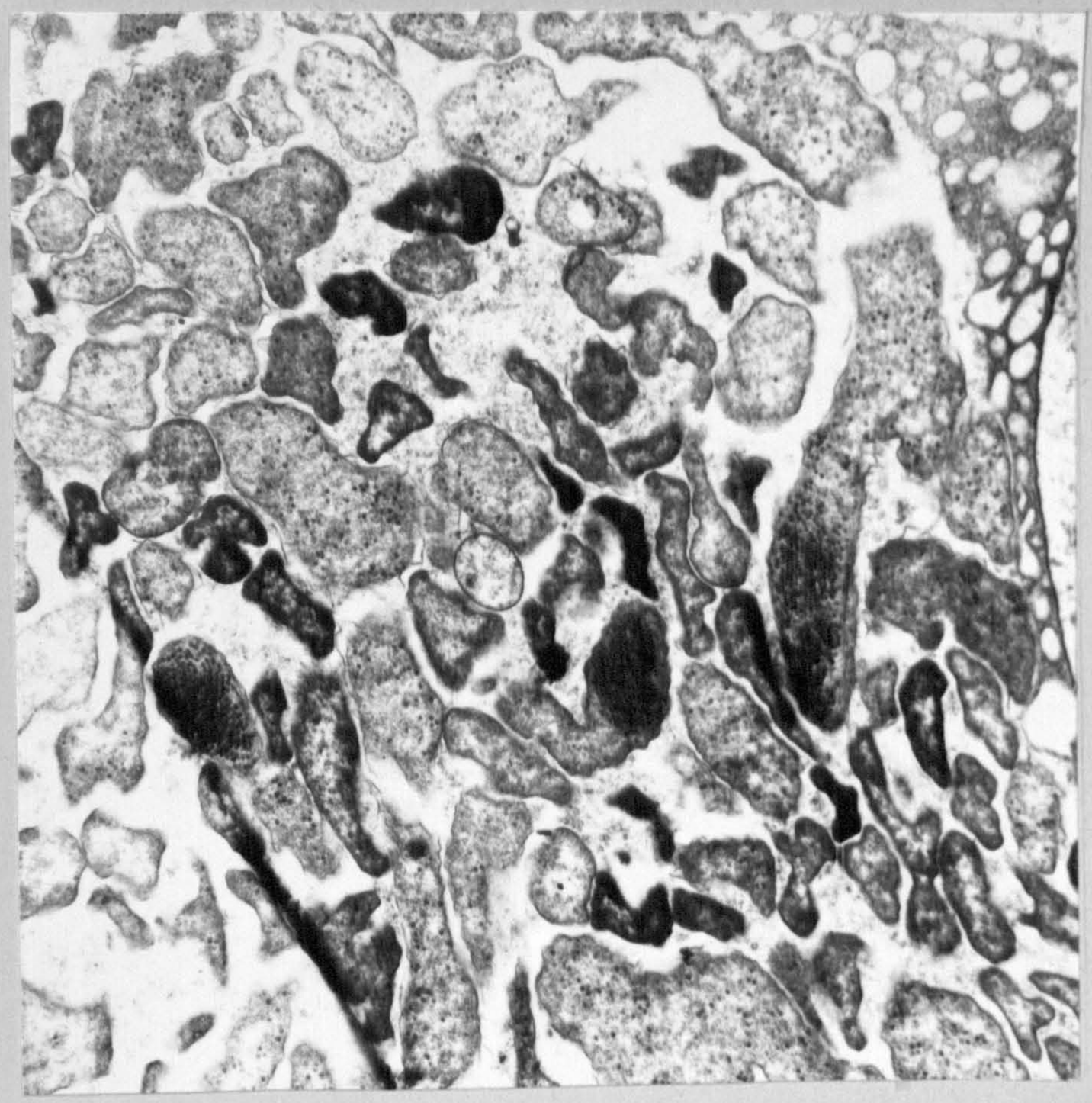

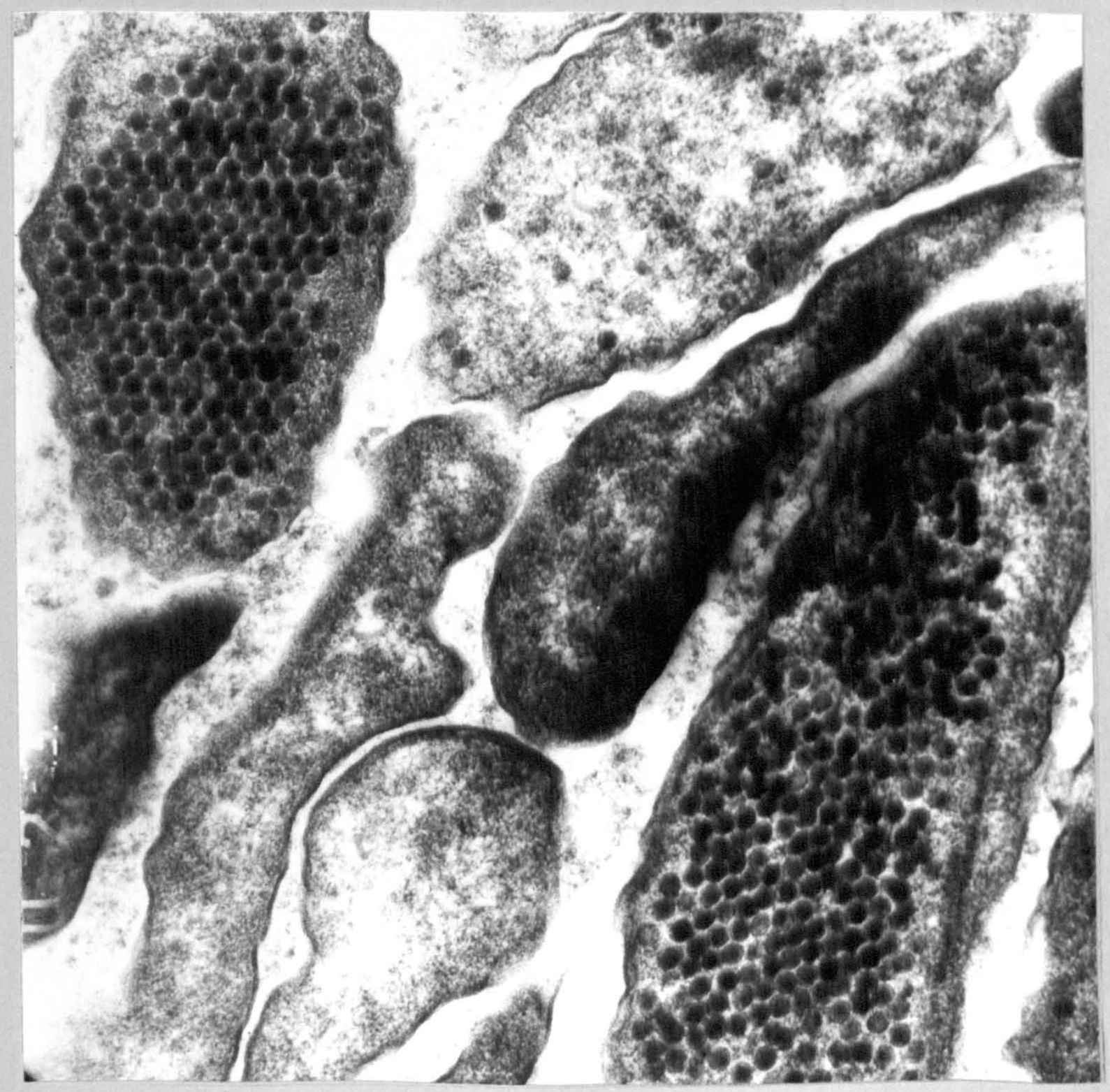

Secretory cells at a late stage of infection by MLO

Plates 122 and 123

Electron micrograph (X 12,000) of a grossly distended secretory cell filled with densely packed MLO spherules containing scattered phage-virus.

The necrotic remnants of the cytoplasm have been pushed to the margins of the cell by the growth of the invading organism.

A similar cell from a population of Tellina on the East coast of Scotland illustrating the ubiquitous nature of the MLO and the consistent morphology of the spherules.

Magnification of 15,000.

Five types of MLO differing in size and electron opacity are discernible:

1) Small compact spherules with highly opaque cytoplasmic matrices.
2) Small intermediate spherules containing a moderately opaque cytoplasm.
3) Large intermediate spherules with moderately opaque cytoplasm.
4) Intermediate spherules with low opacity cytoplasmic matrices.
5) Fully developed large spherule with low opacity cytoplasmic matrices.

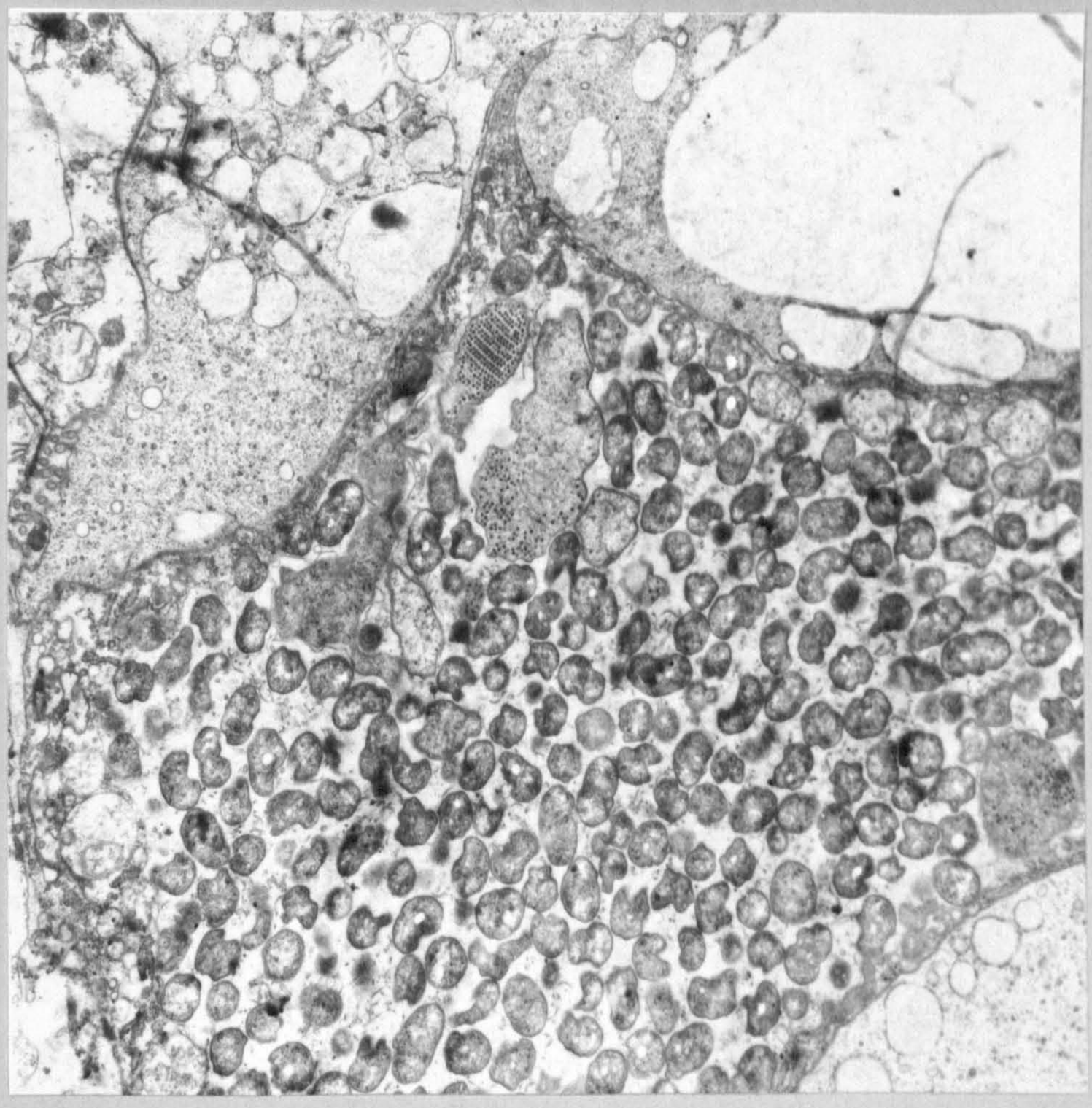

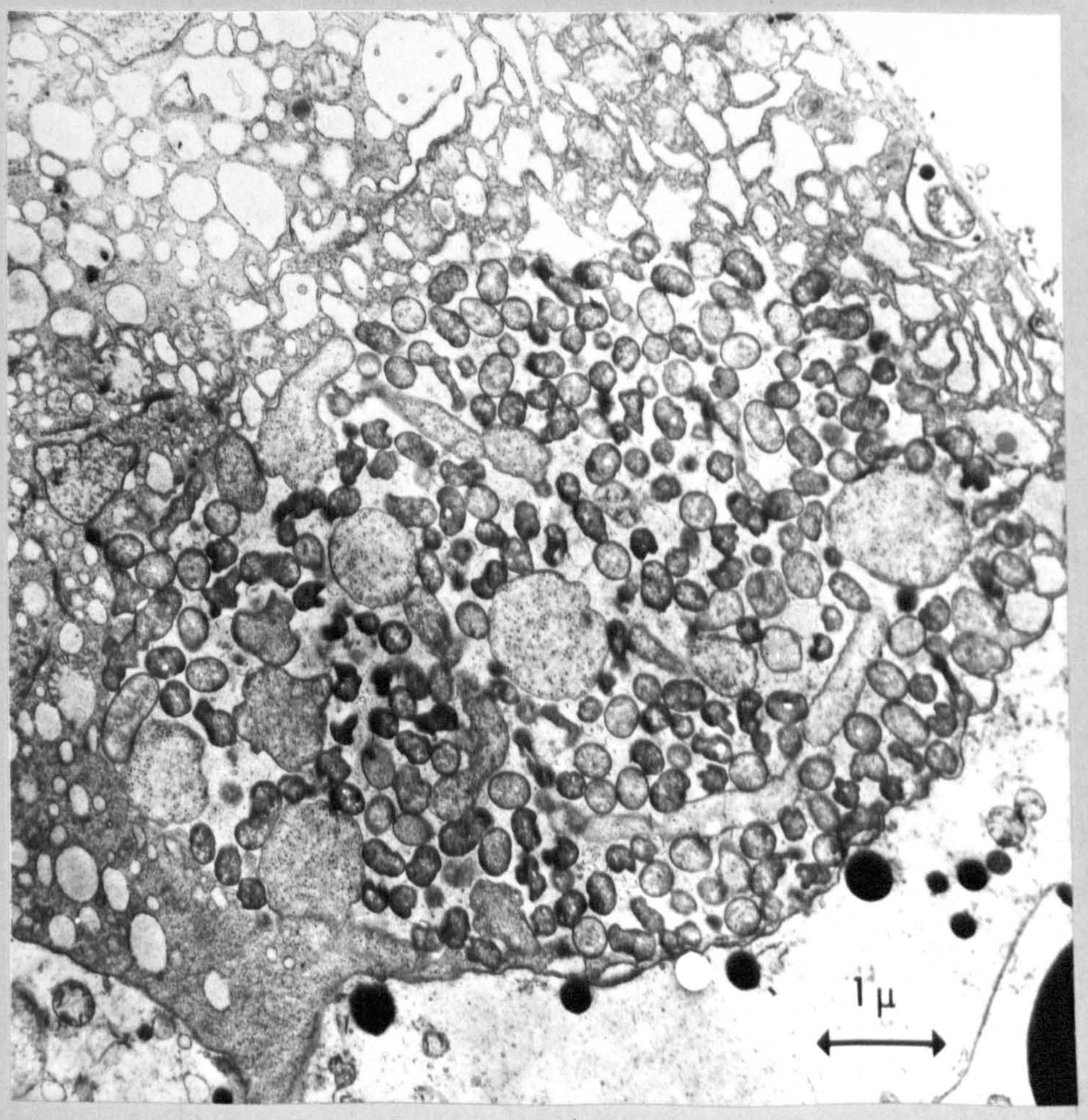
1μ

Ultrastructure of the phage and associated rod-like structures.

Plates 124 and 125

These plates are details of plate 122. The electron-dense, osmiophilic core of each virion is surrounded by a protein coat which occasionally appears to have a spherical outline. The individual capsids are delineated by the stellar processes of the core. Each virion measures 50 nm in diameter.

(Magn. x 40,000)

Virions at different stages of development can be seen and striated rods. Since these are only found in cells containing virus and then only in association with cells containing virus it seems that there is a causal relationship between the two. They may be viral components, virus modified cell products or merely a cellular reaction

(Magn. x 70,000)

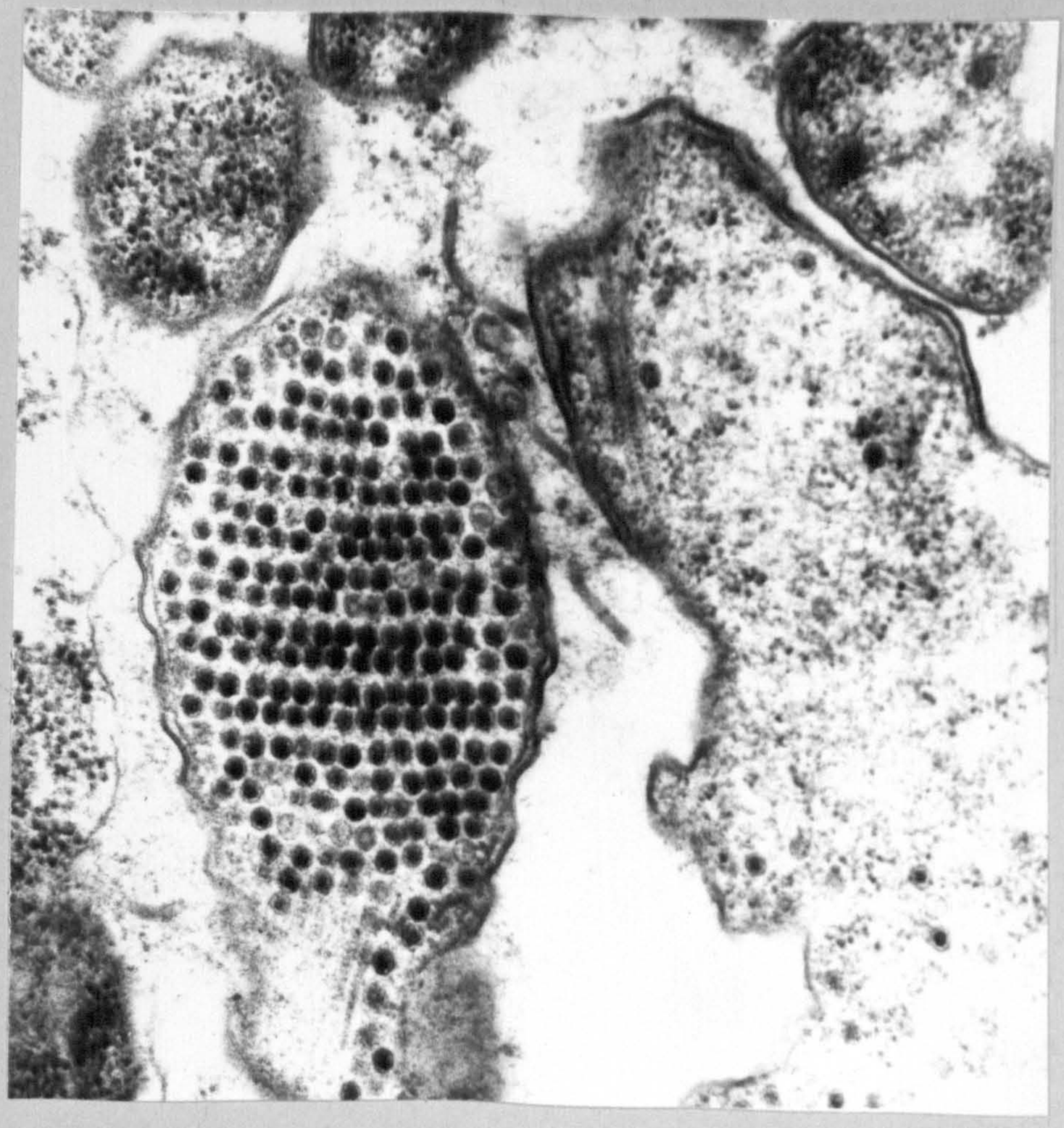

200 nm

Details of phage-virus replication in MLO from the secretory cells of Tellina collected at St. Andrews West Sands

Plates 126 and 127

Distinctive ordered arrays of phage-virus suggesting that many particles are formed nearly simultaneously at a circumscribed locus allowing crystallization to occur.

The electron-dense cores are surrounded by regularly repeating sub-units thought to be capsomeres.

Numerous striated rod-like structures are evident in these sections.

Elementary bodies (EB) lie between the MLO spherules.

Upper plate x 50,000

Lower plate x 70,000

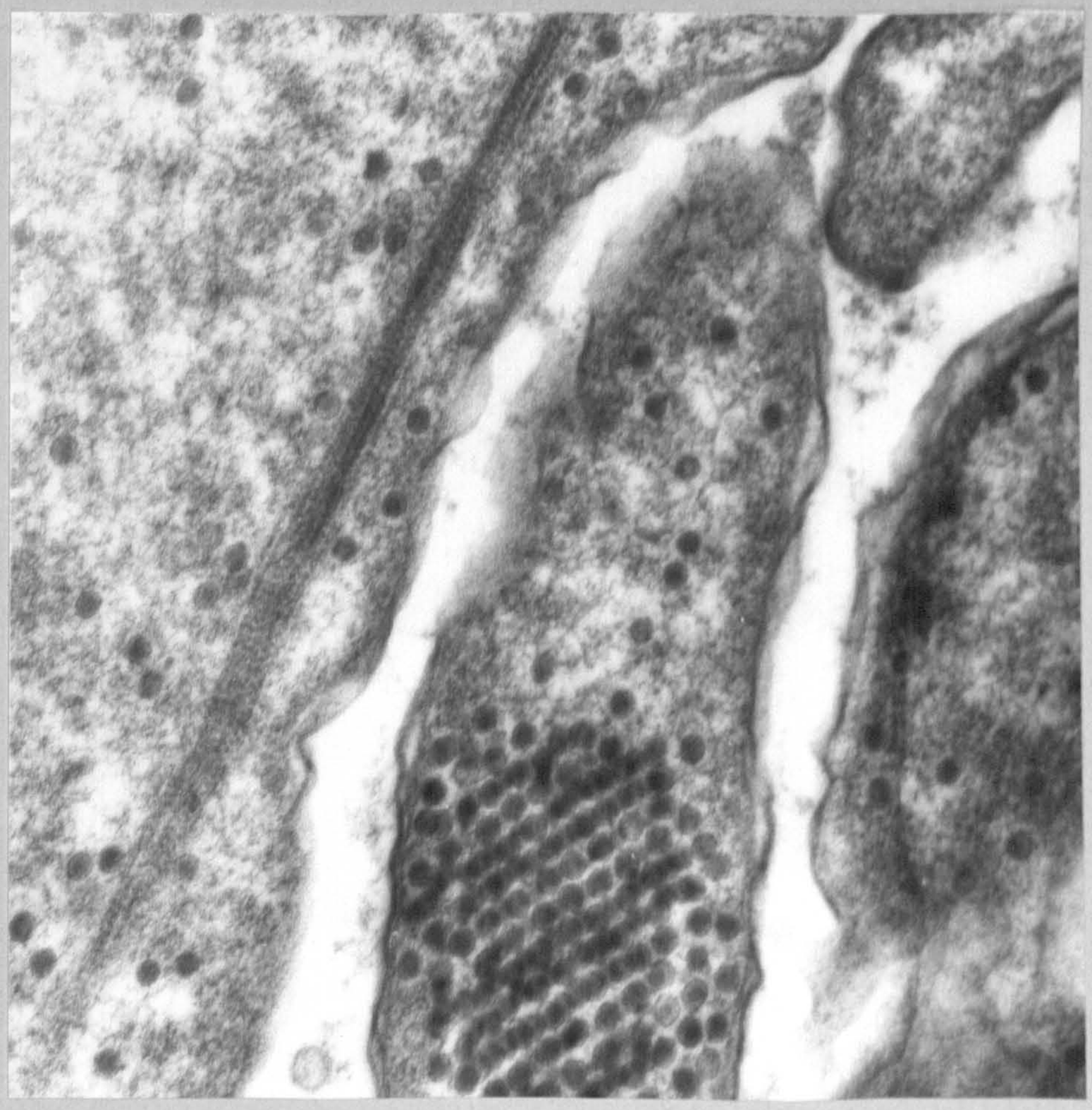

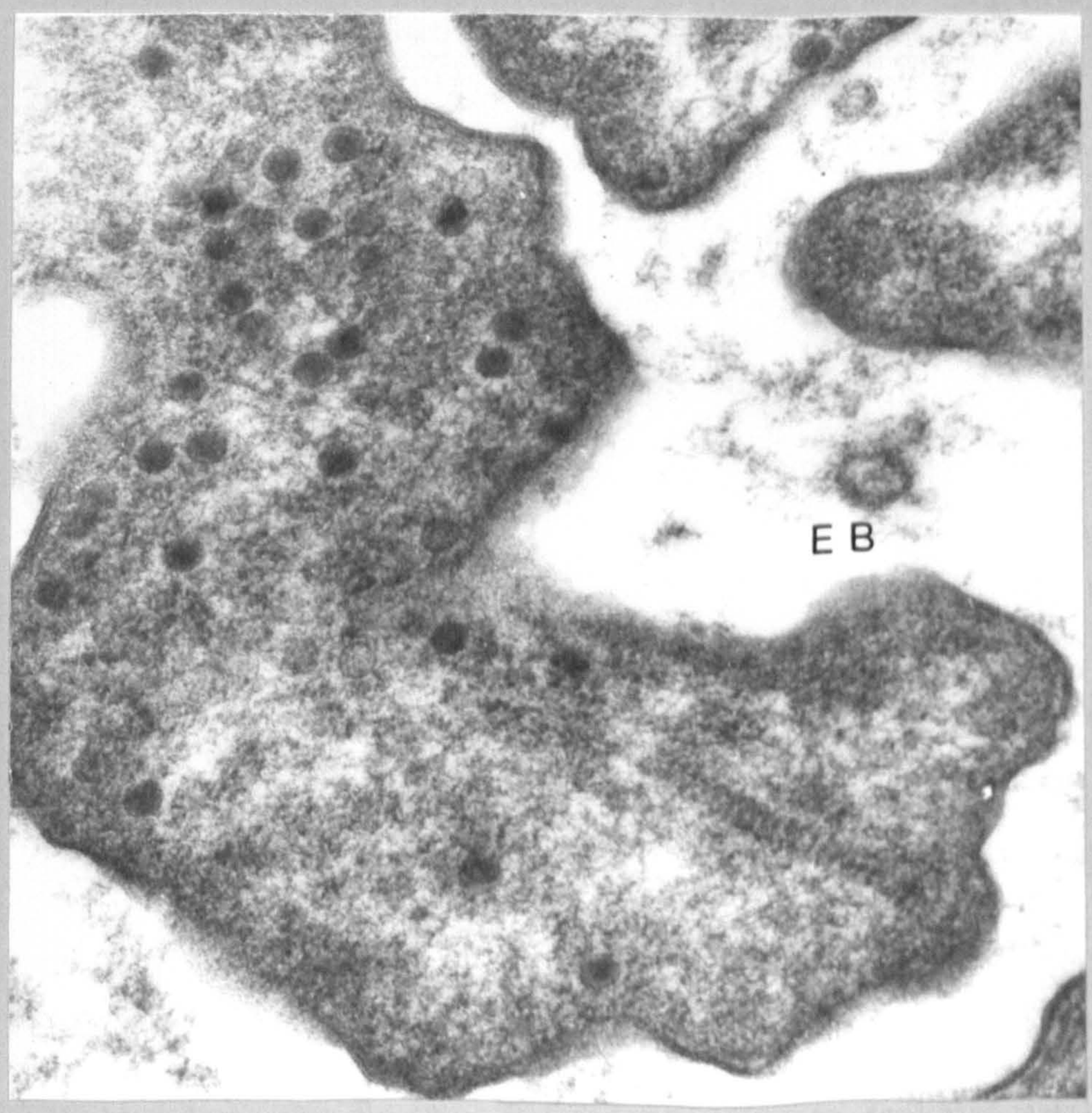
E B

On the presence of bacterial cells free in the lumen of digestive diverticula

Plate 128 and 129

This low power (x1,000) electron micrograph of the lumen of a tubule of the digestive diverticulum illustrates the presence of numerous spherules which have a definite cell wall. These are shown in greater detail in the lower micrograph.

The distal ends of the absorptive cells possess very numerous microvilli.

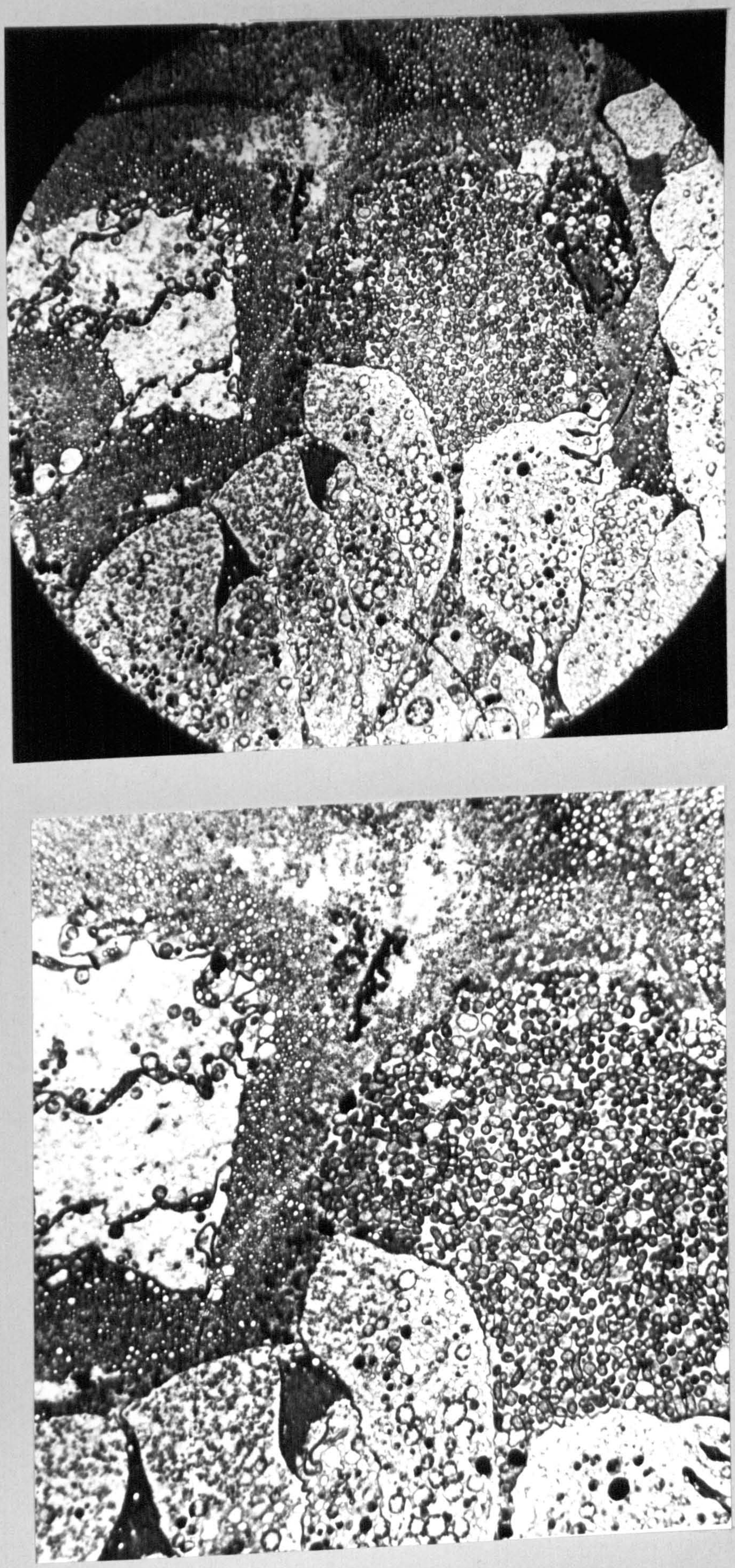

On the presence of bacterial cells in the lumen of the digestive diverticula

Plates 130 and 131

Sections serial to those of plates 128 and 129. It seems possible that these cells may originate from the lysis of an infected secretory cell as numerous inclusion bodies were found in the vicinity. However, these cells have a definite cell wall. This would indicate that these are free living bacteria rather than MLO.

Note the distal ends of absorptive cells characterised by numerous mitochondria profiles, microvilli and diffuse cytoplasm.

Upper plate x 4,000

Lower plate x 10,000

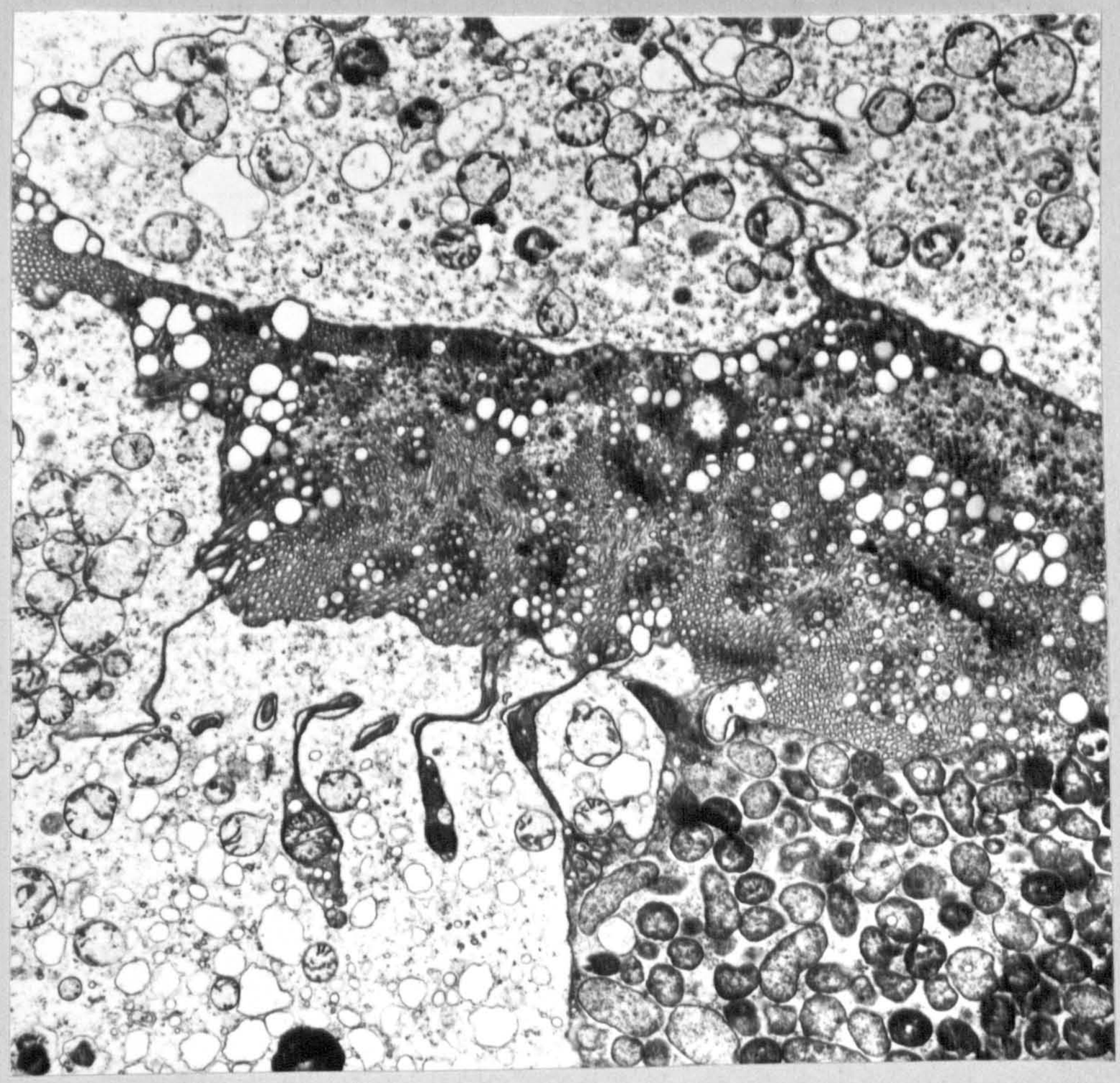

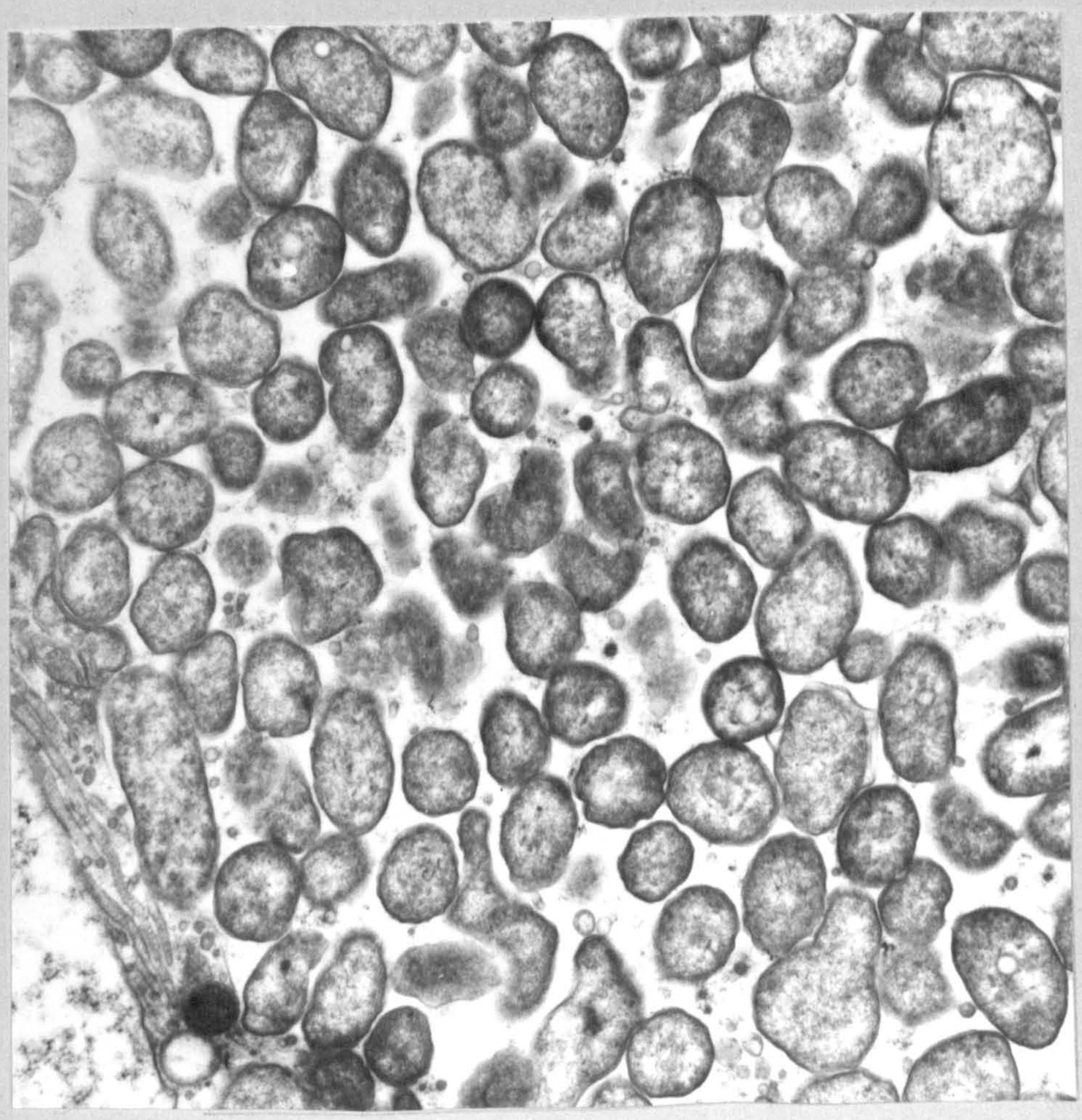

Early stages of secretory cell invasion by a mycoplasma-like organism

Plate 132

These electron micrographs (both X 10,000) are serial sections which serve to emphasize the multilobed nature of the MLO.

The host cell cytoplasm contains Golgi bodies with swollen vesicles.

Plate 133

The trilaminar membrane appears ruptured and the cytoplasm may be budding off to form a new individual. This form of cytoplasmic fragmentation is presumed to represent one type of reproduction.

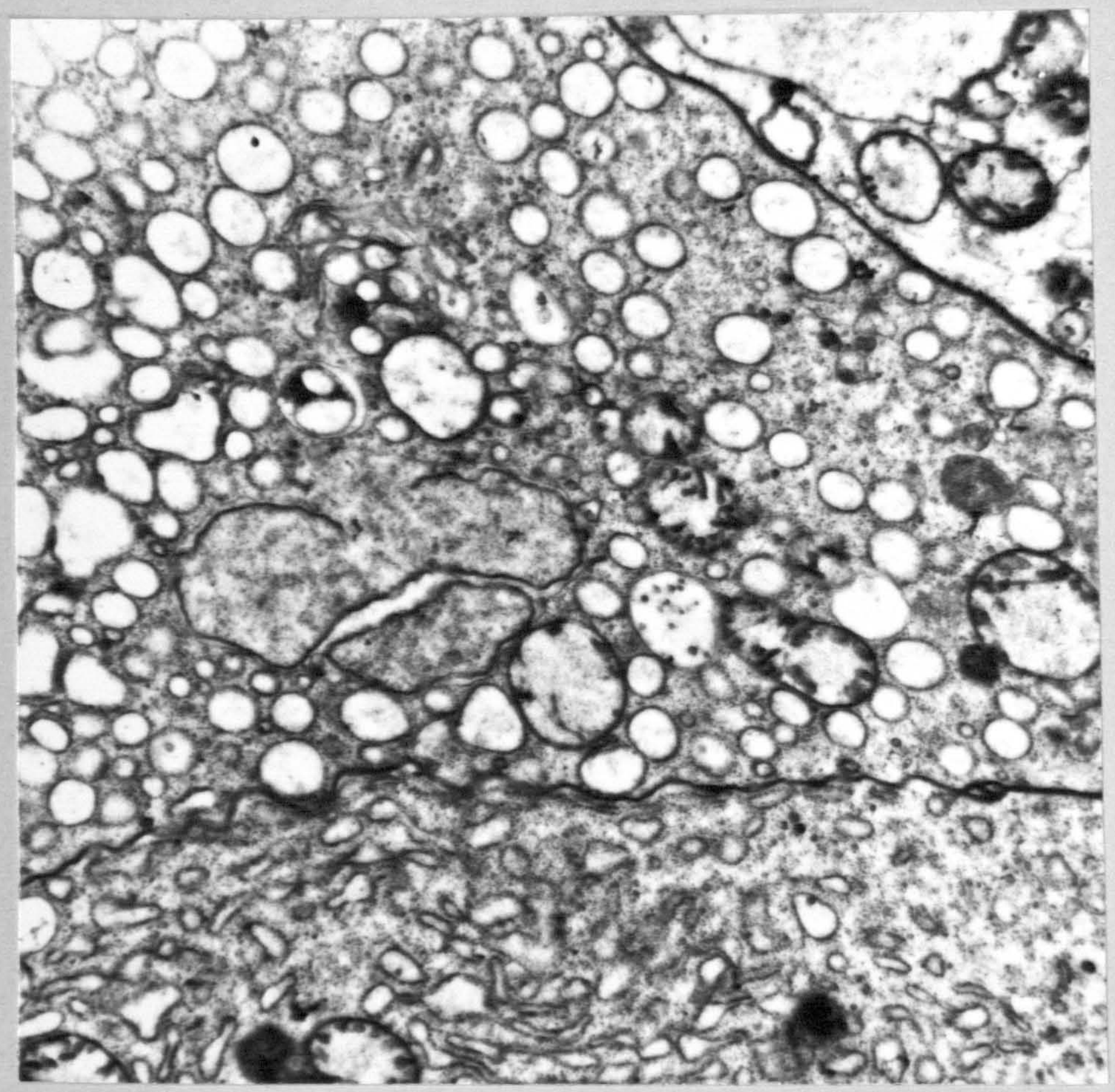

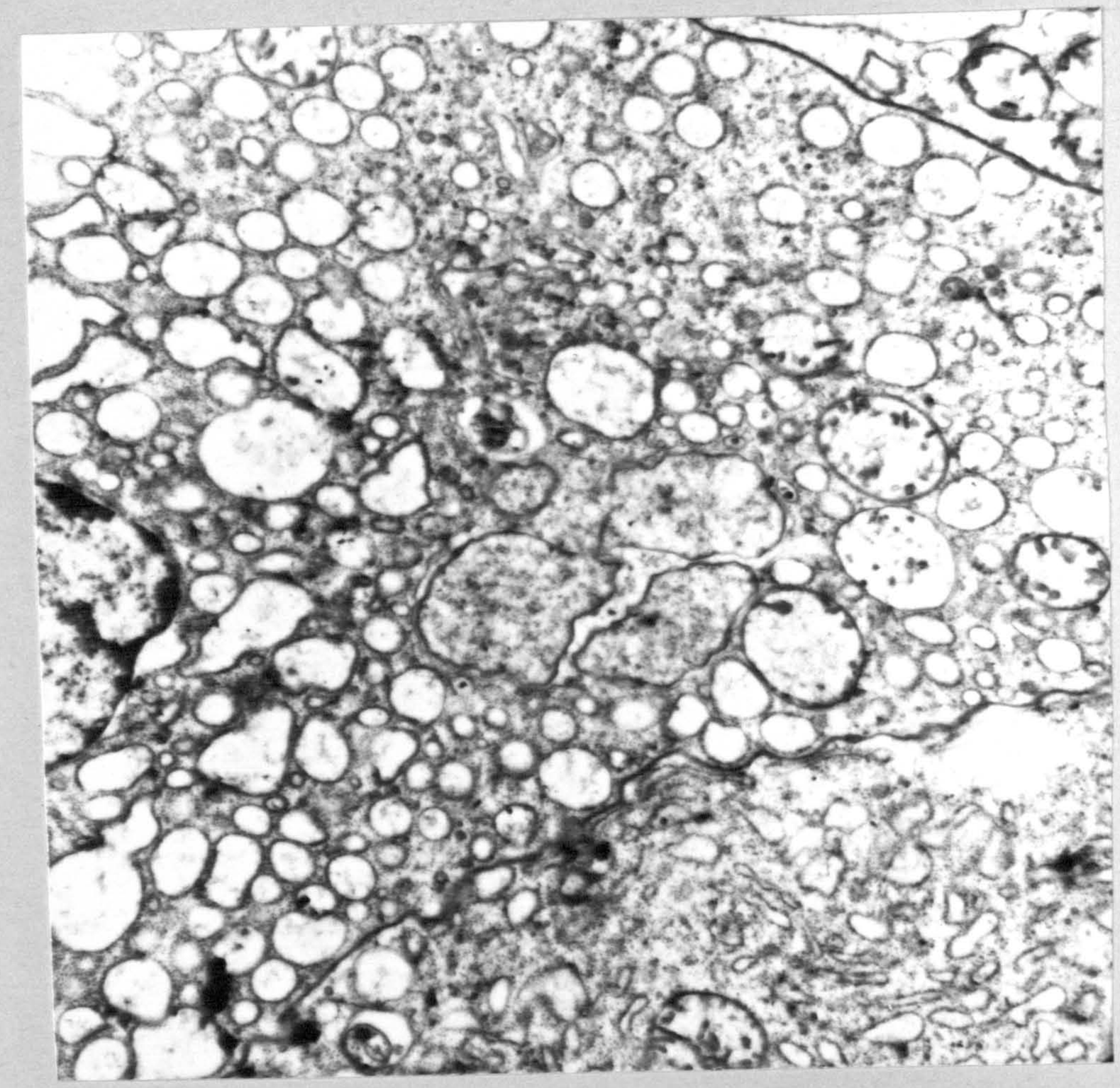

Reproduction in the MLO

Plate 134

An early membrane bound cytoplasmic inclusion containing MLO spherules. Note the presence of a'bleb' on one cell at centre (Magn. x 13,000)

Plate 135

Detail from the above plate showing the electron-dense nature of the contents of the 'bleb' which appear to have cut off from the parent cytoplasm by the formation of a plasma membrane. Note also the stellate nature of the DNA of this cell. This is characteristic of mycoplasmas. (magn. x 45,000)

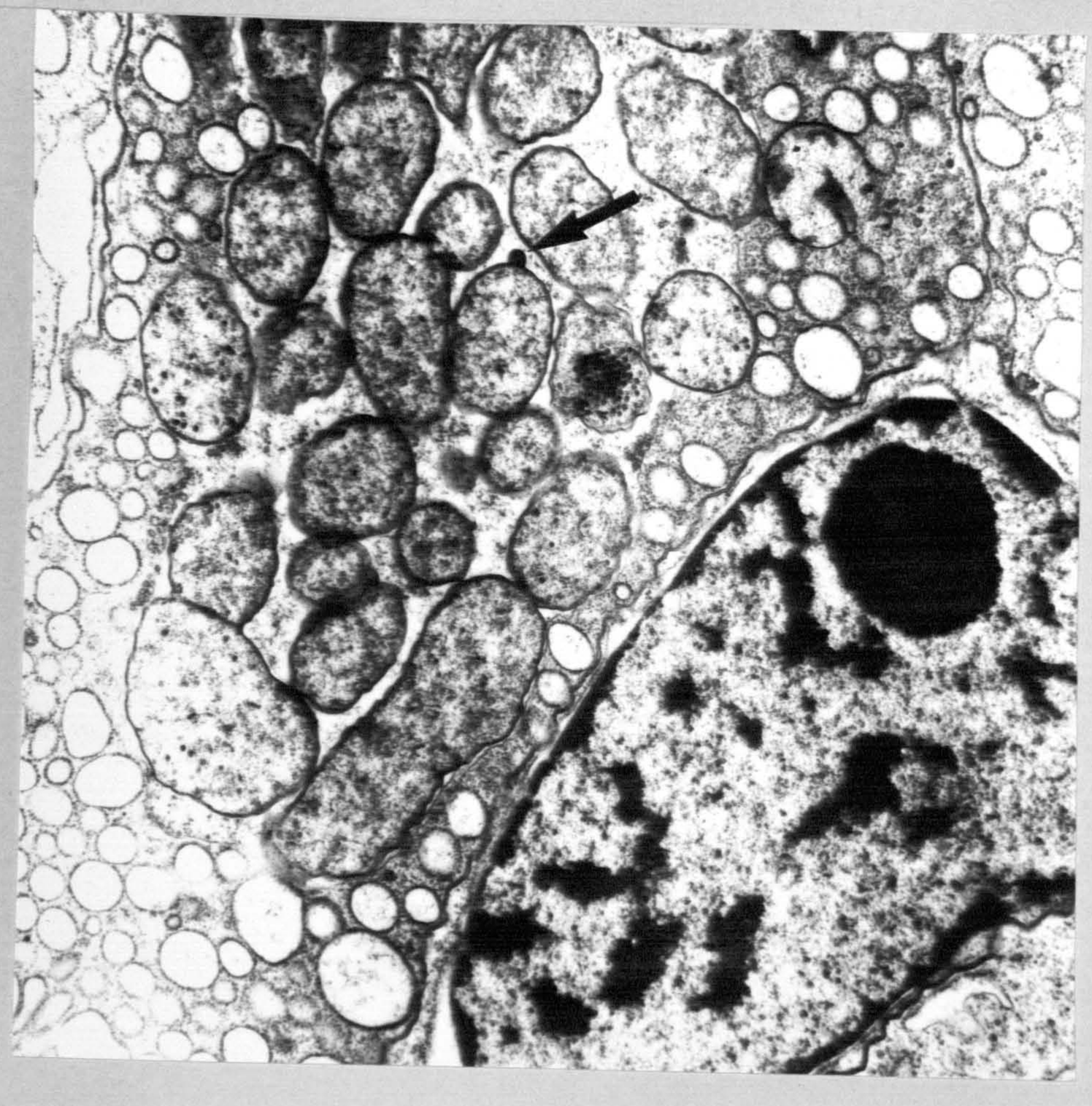

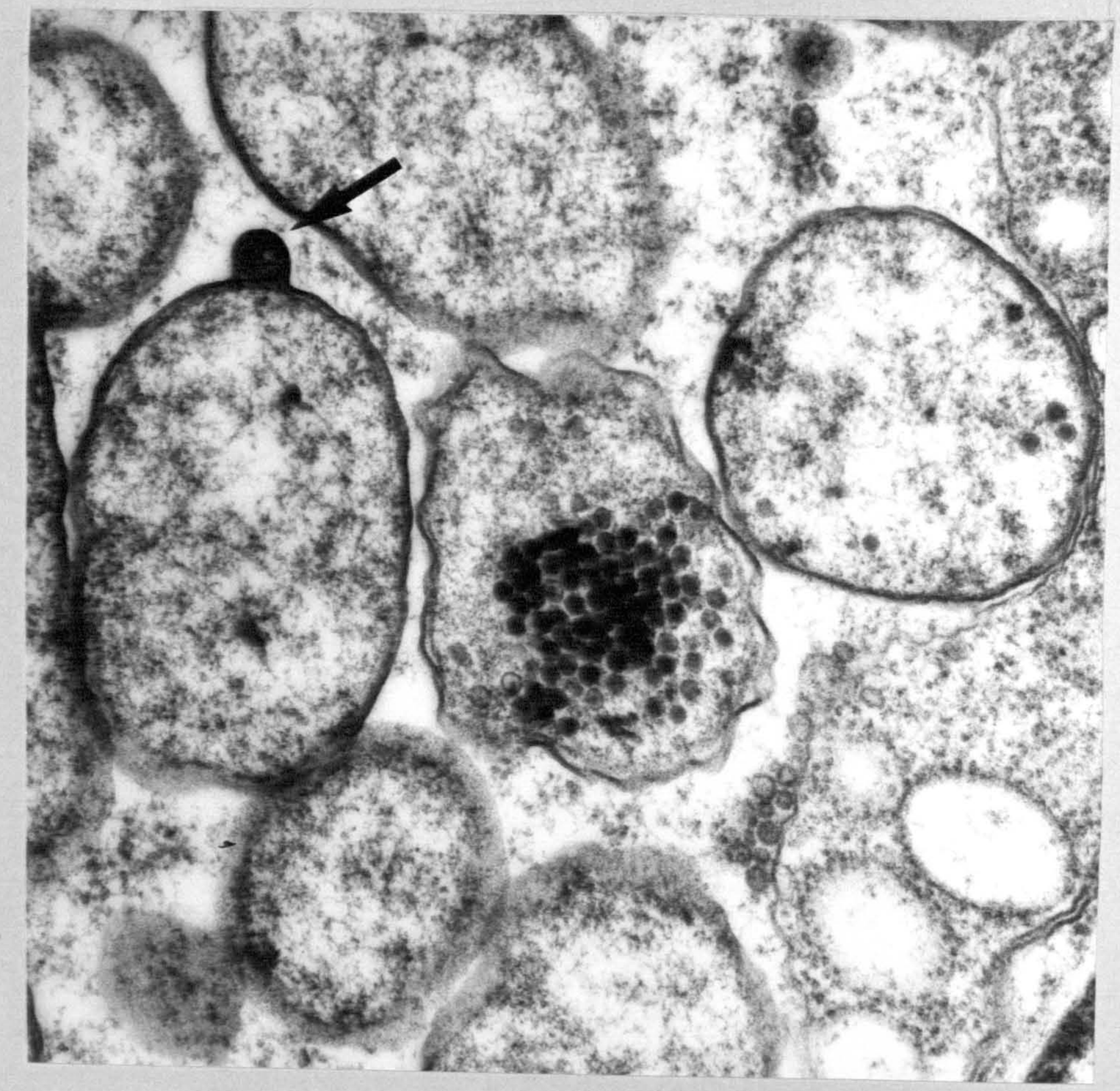

SECTION FOUR

The ultrastructure of Hill's Weymouth isolate of virus from <u>Tellina tenuis</u> collected at West Sands, St. Andrews (TV 1)

Plates 136 and 137

Phosphotungstic acid pH7 negatively staining virions from Bluefin fibroblast cell culture at Weymouth.

Photographed on an AEI Corinth electon microscope (x 100,000)

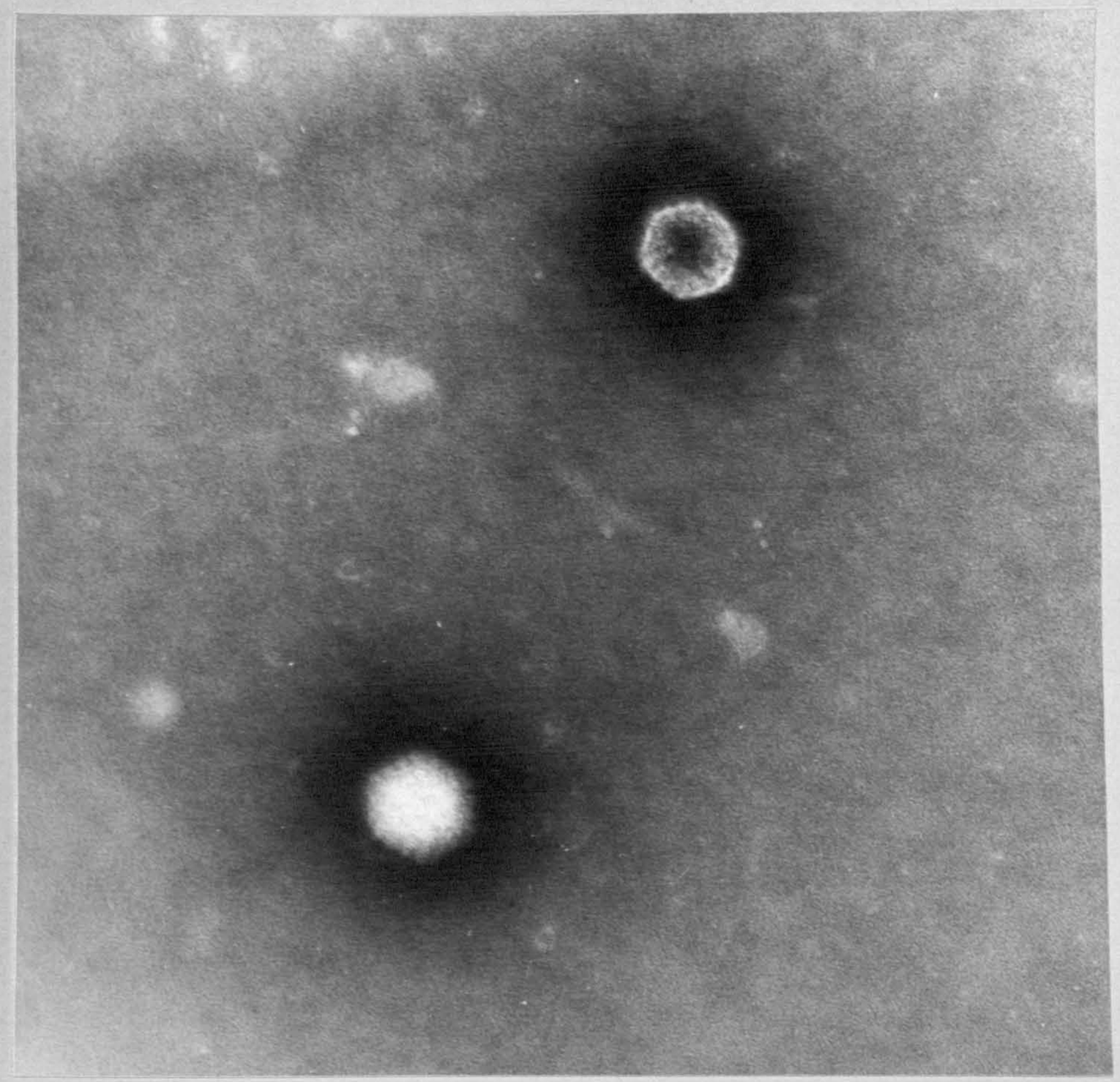

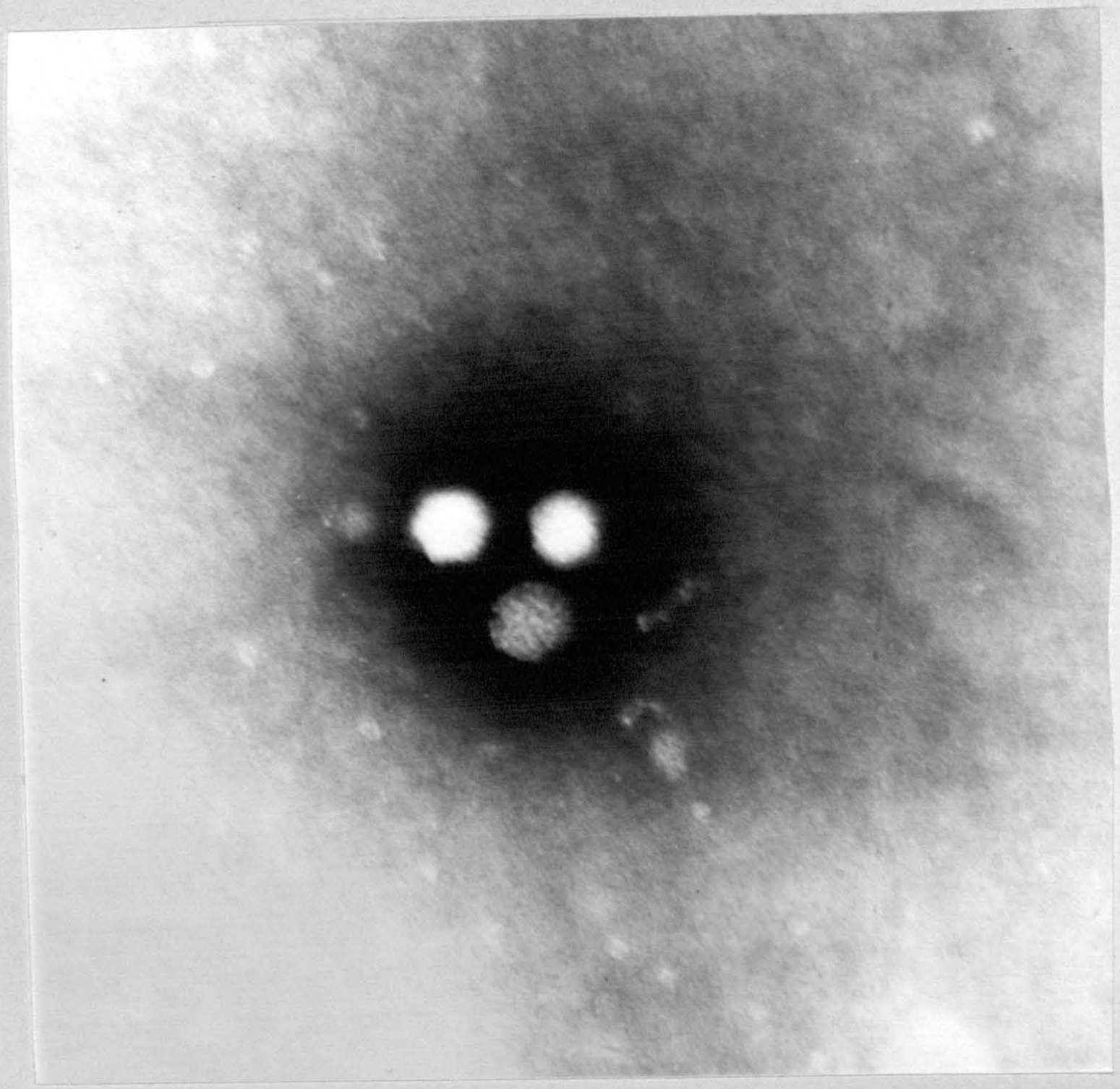

The ultrastructure of Hill's (Weymouth) virus isolate from *Tellina tenuis* collected at West sands, St. Andrews (TV 1).

Plate 138

TV 1 particles - magnification of 80,000 - negatively stained with phosphotungstic acid, pH 7. The virus capsid is composed of 92 capsomeres arranged in accordance with icosahdral symmetry. Two axes of 5-fold symmetry can be resolved.

Plate 139

The same isolate stained with uranyl acetate ph 4.5. Magnification of 80,000 x.

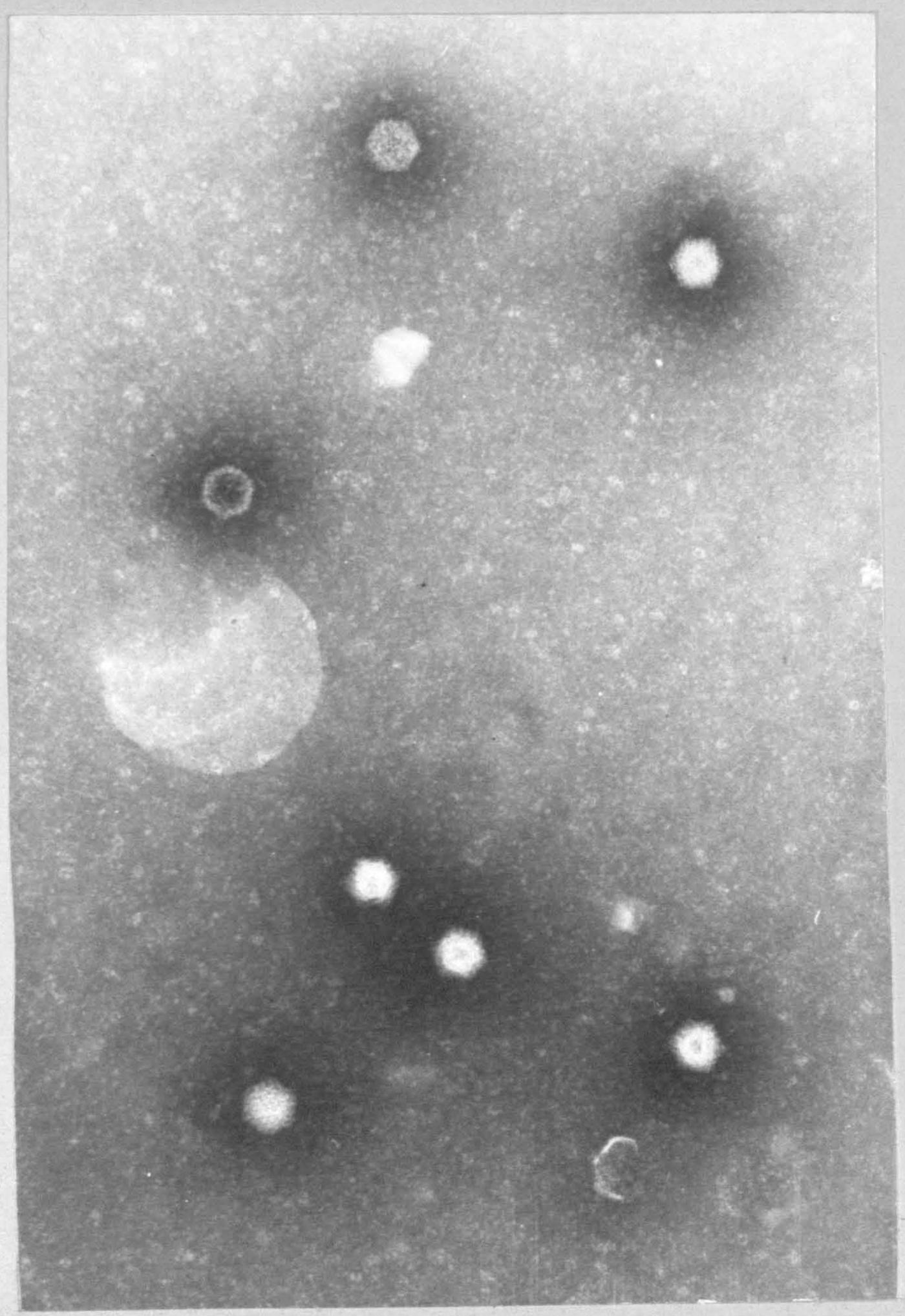

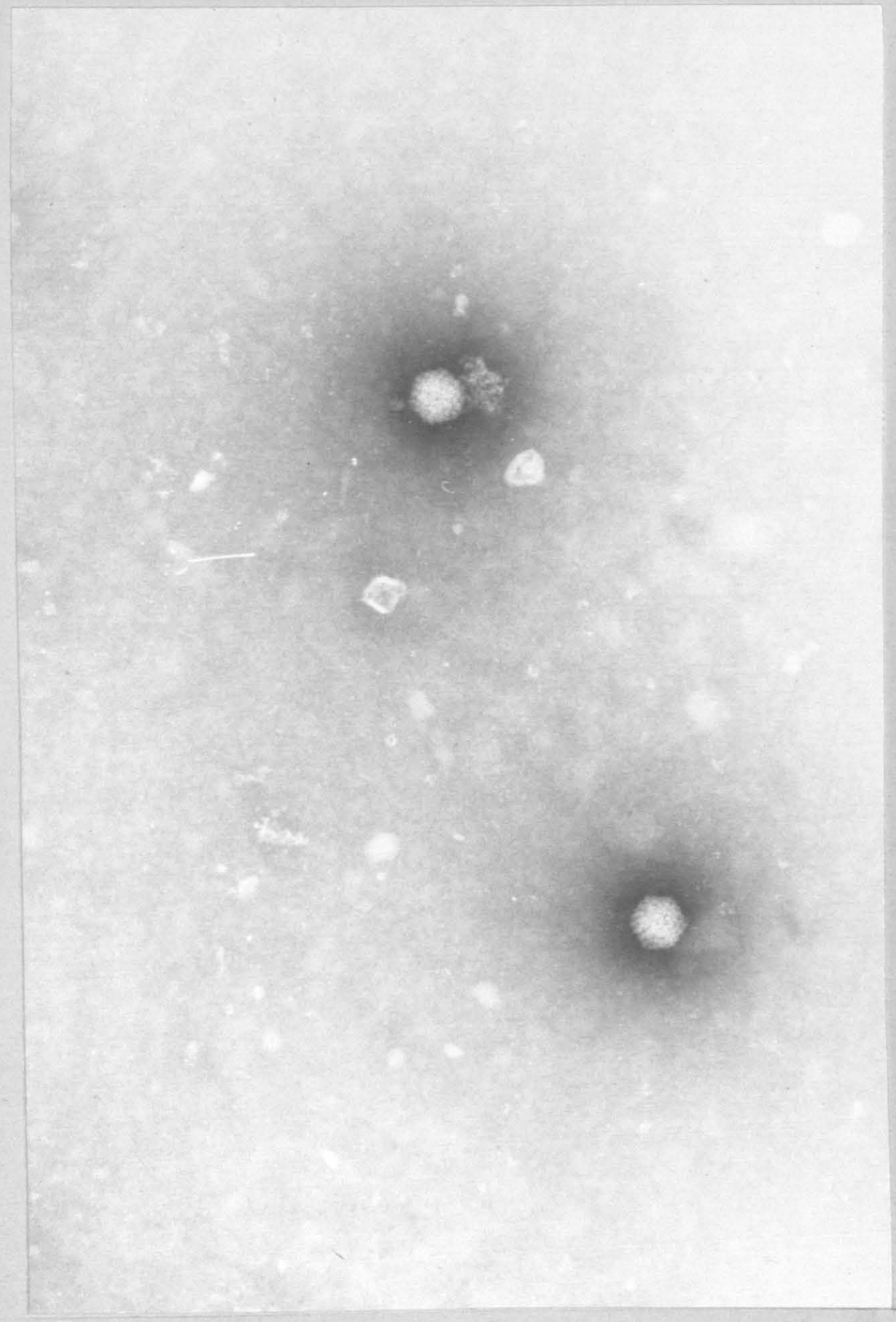

The ultrastructure of Hill's (Weymouth) isolate of virus from Tellina tenuis collected at West Sands St. Andrews (TV 1)

Plate 140

Preparation negatively stained with sodium silicotungstic acid pH 9. Two empty particles are visible where stain has penetrated the core of the particles. (Magn. x 80,000)

Plate 141

The same isolate negatively stained with potassium phosphotungstic acid pH 3. (Magn. x 80,000)

These electron micrographs were made on a Philips 300M electron microscope at the Regional Virus Laboratory, Ruchill, Glasgow.

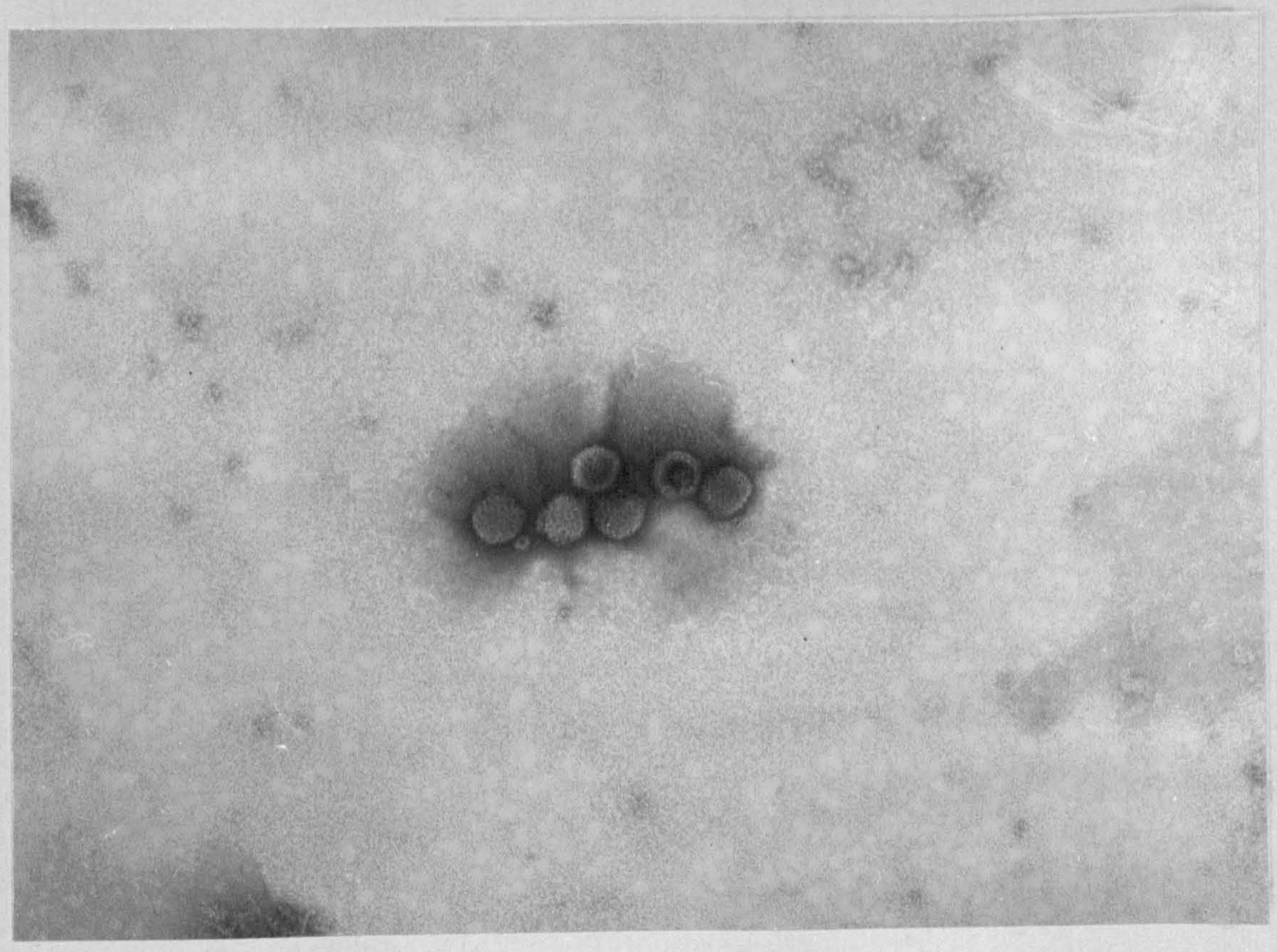

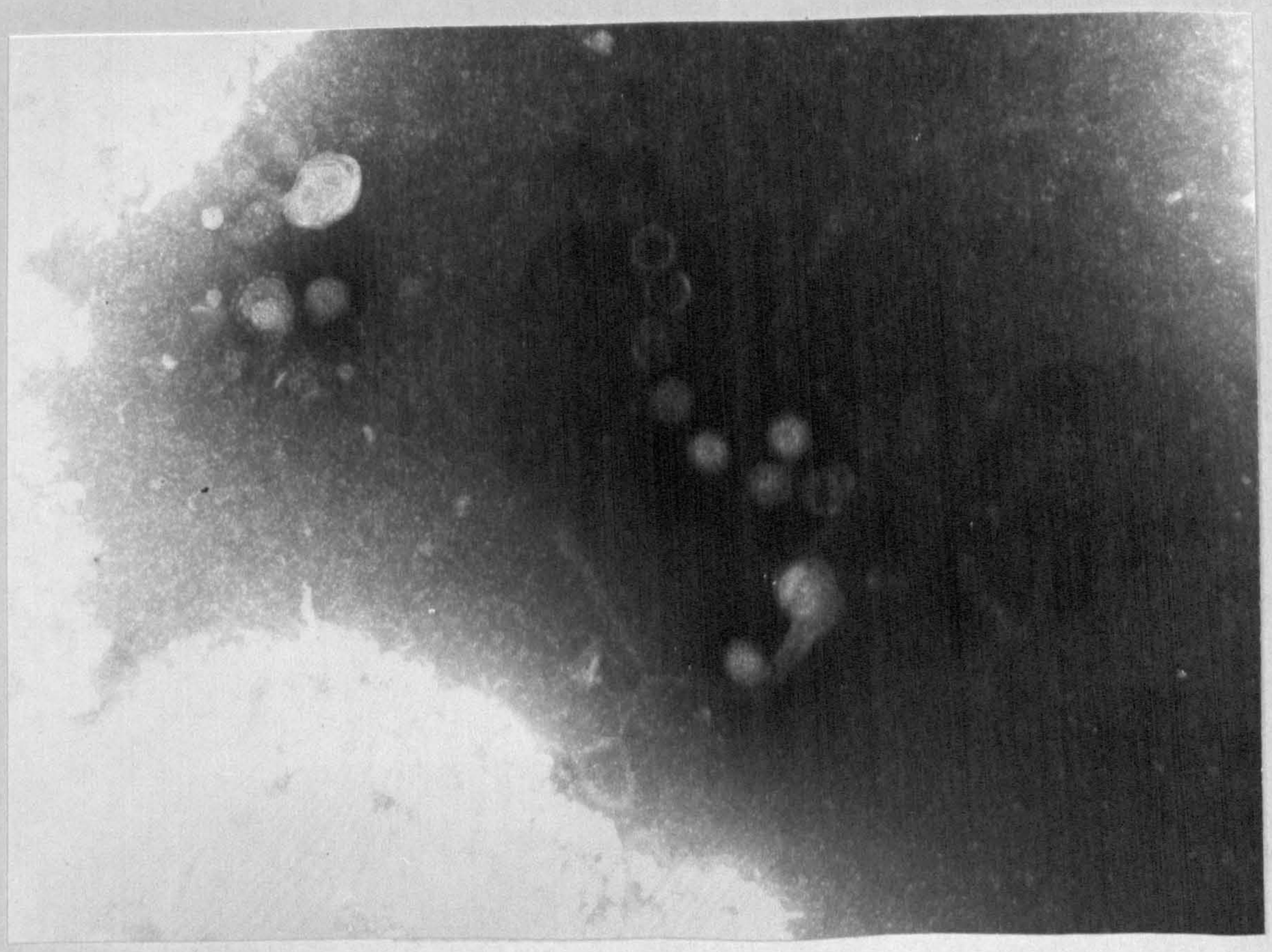

Atlantic salmon cells before inoculation with Tellina virus TV 1 (Weymouth isolate)

Plate 142, 143 and 144

These plates show the developing cell sheets from three different batches before inoculation. The cells appear healthy.

Magnification of x 150.

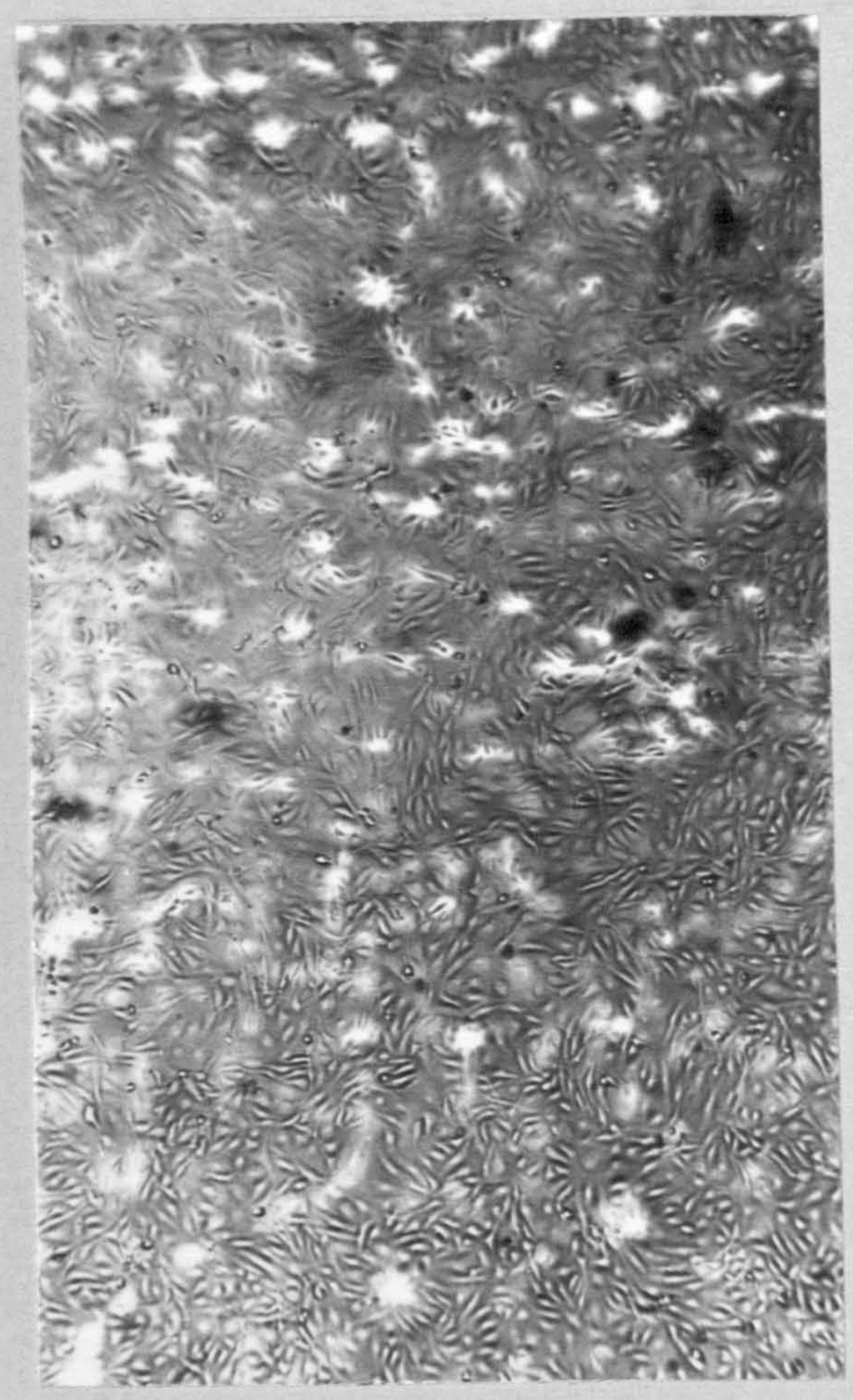

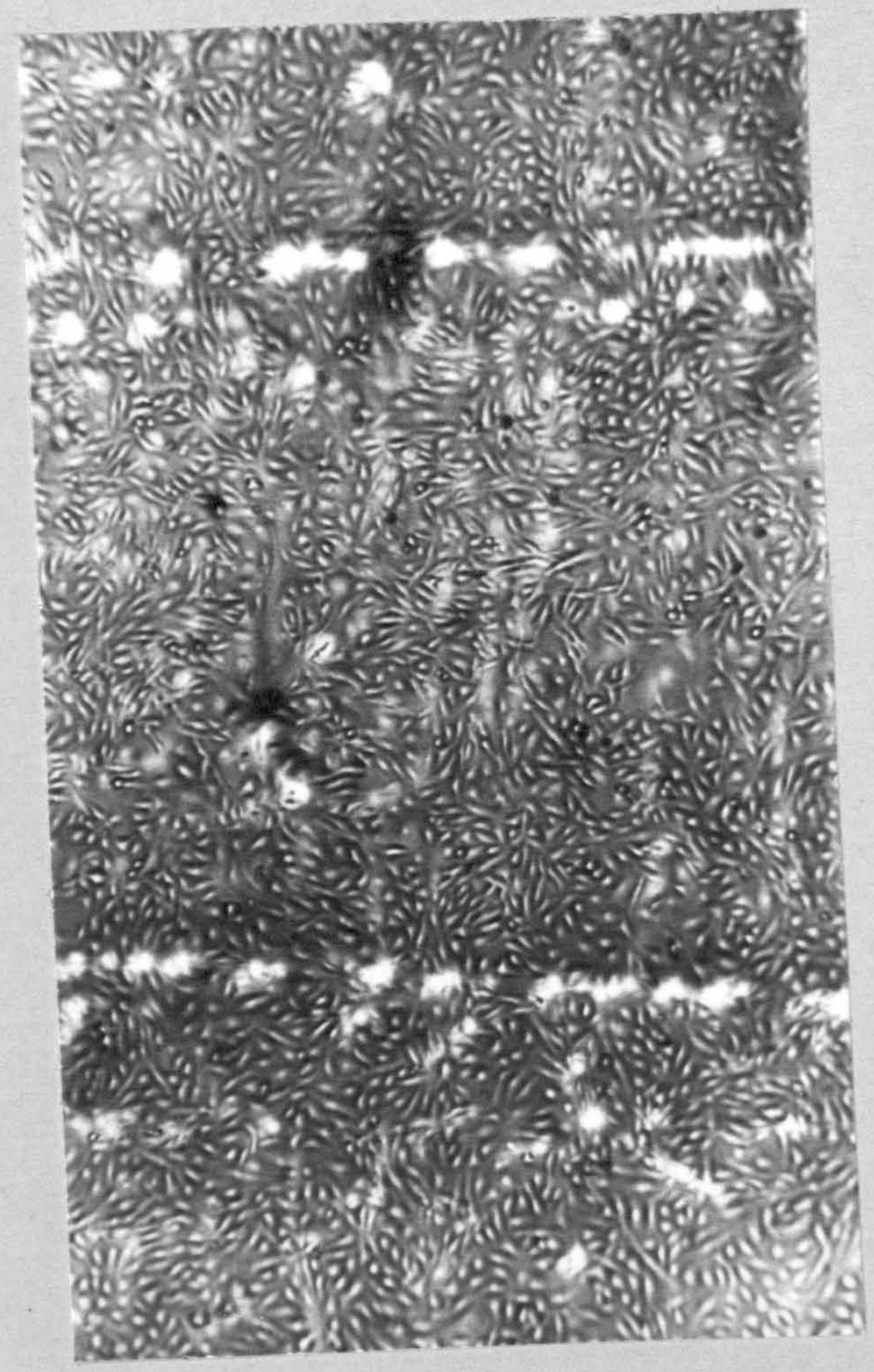

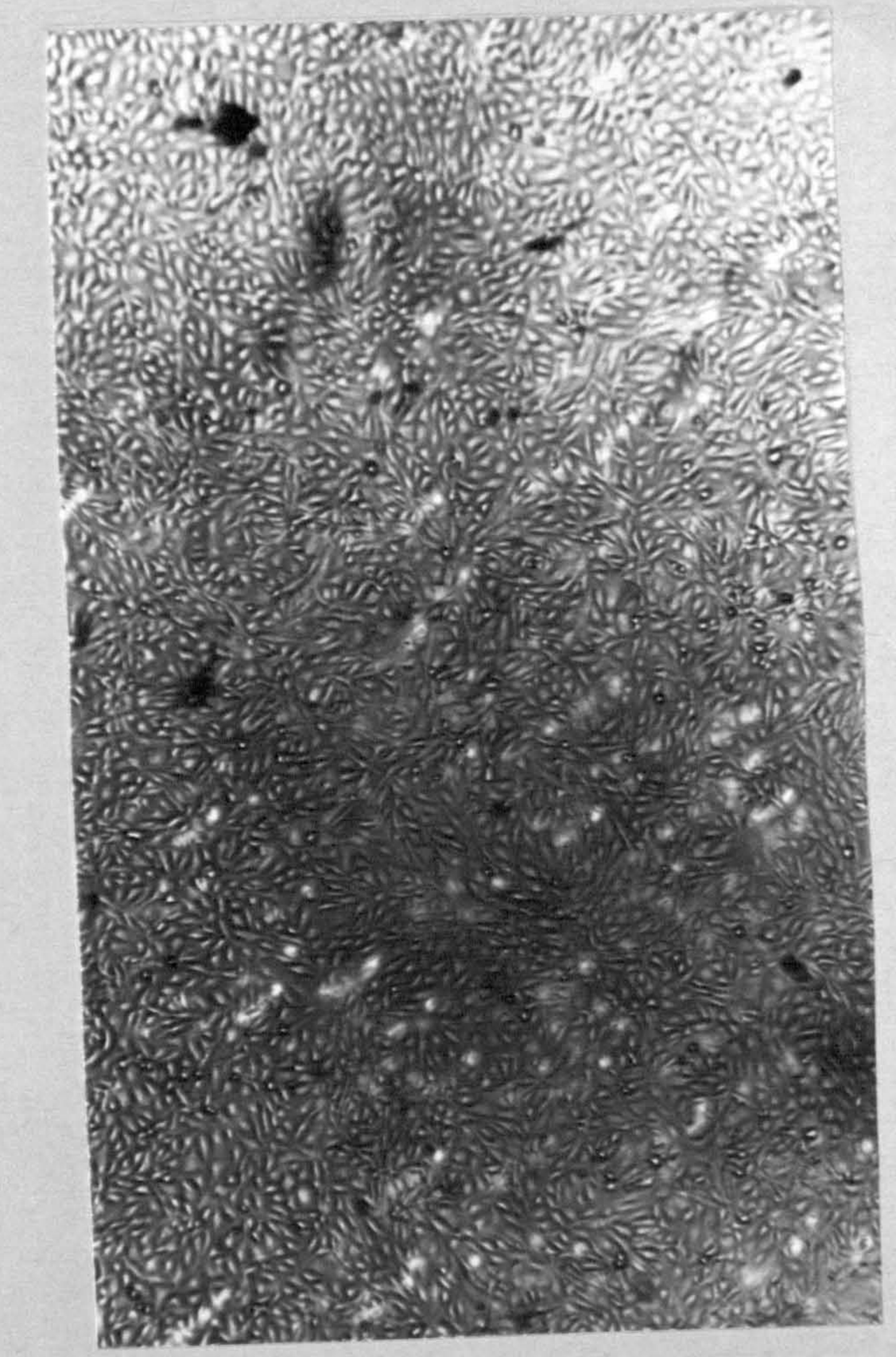

Atlantic salmon cells after inoculation with TV1, the Weymouth virus isolate.

Day 1. Plate 145

Day 2. Plate 146

Day 3. Plate 147

Magnification throughout x 150

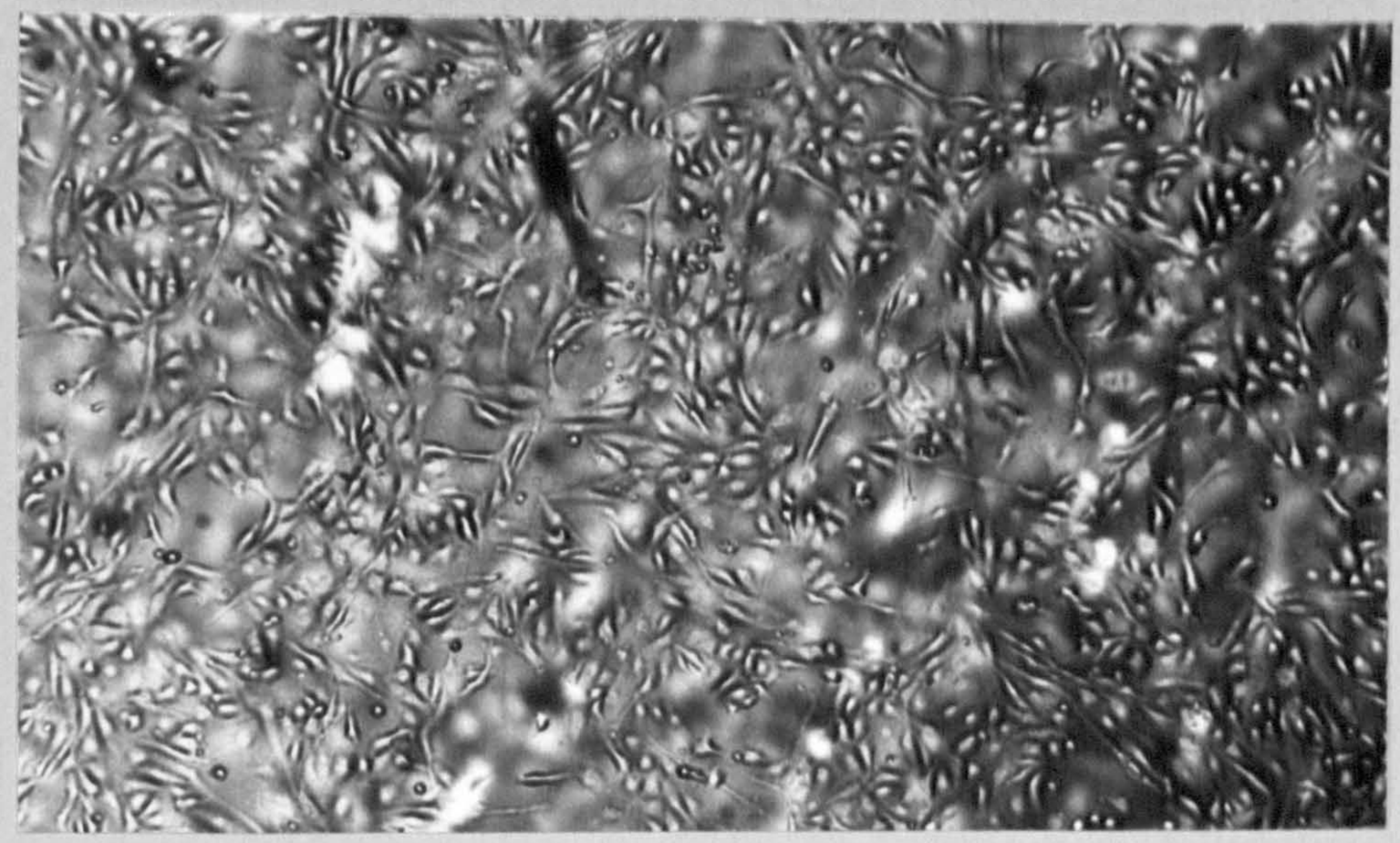

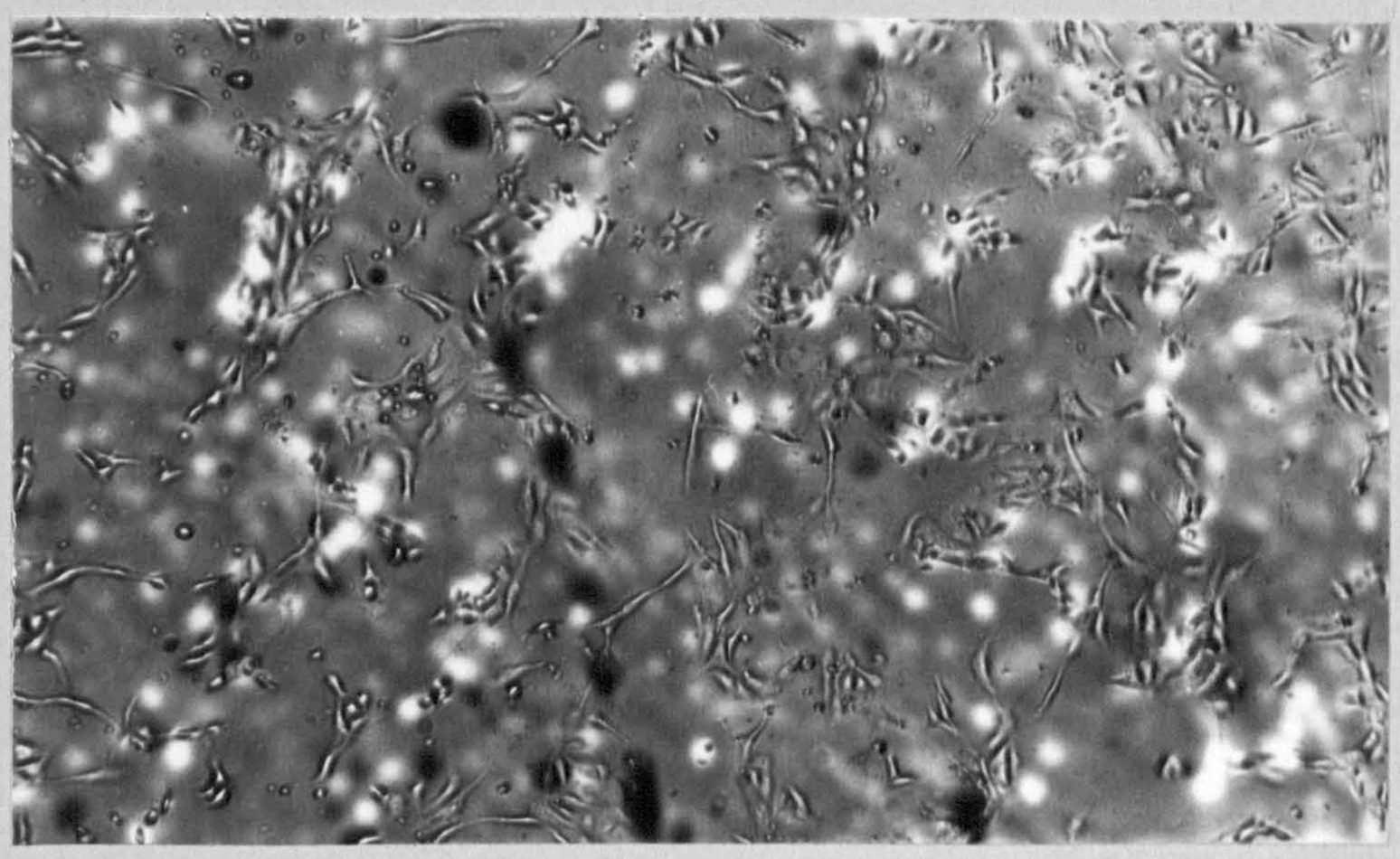

Atlantic salmon fibroblast cells artificially infected with TTV (Weymouth isolate)

Plate 148

Electron micrograph (X 3,000) of Atlantic salmon fibroblast cells from tissue culture. Note the progressive vacuolation at the centre of the cytoplasm and the numerous myelin-like configurations. Virus-like particles interdigitate with the myelin-like figures.

Plate 149

Detail of the above cell at a magnification of X15,000. Virus-like particles are estimated to be 60 nm in diameter corresponding with TV1 in size but without the regular hexagonal outline and definite core and coat. The rod-like structures are reminiscent of those seen by Moss and Gravell (1969) on the ultrastructure and sequential development of IPN virus.

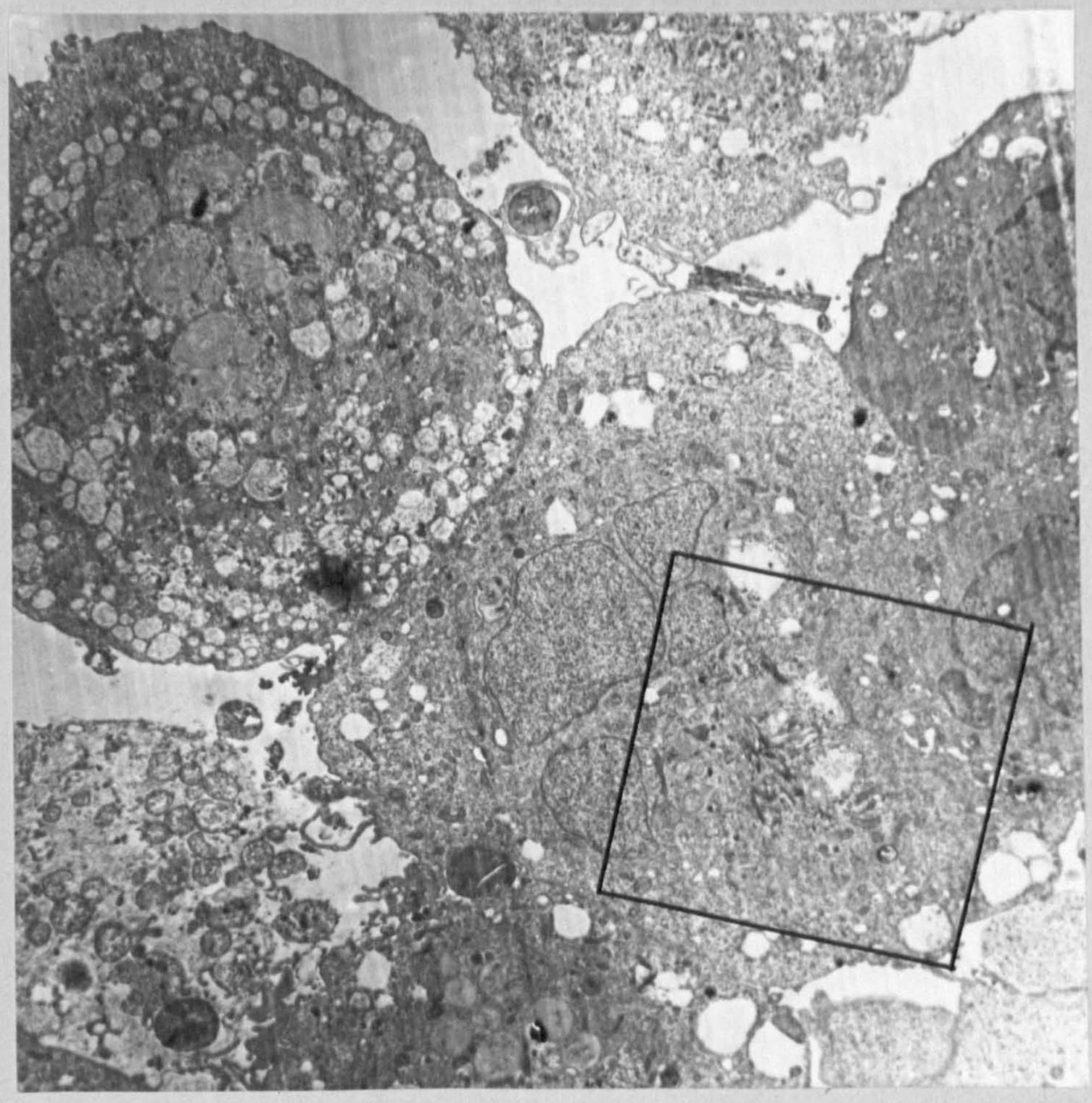

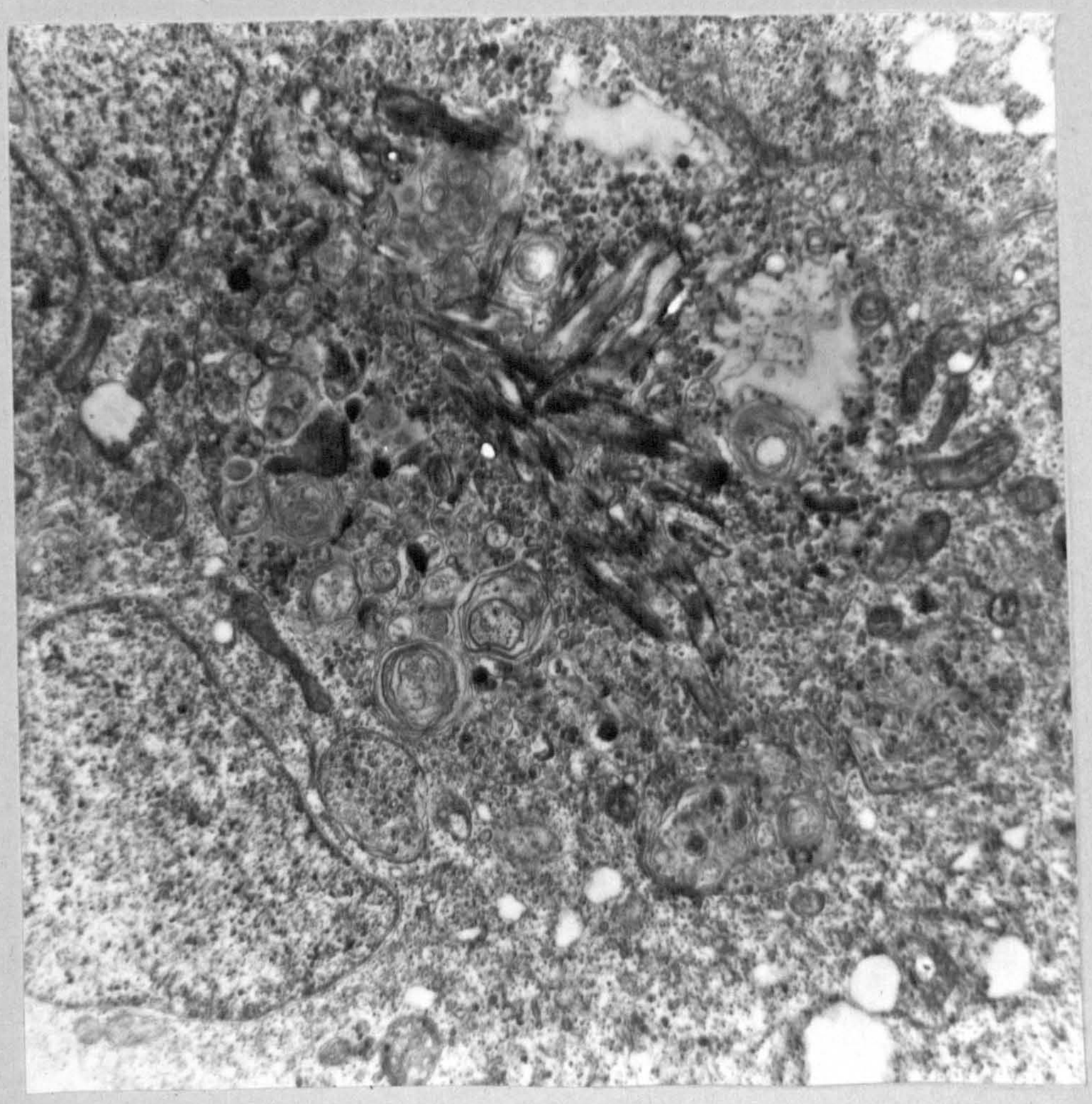

Atlantic salmon fibroblast cells artificially infected with TV1(Weymouth isolate)

Plate 150

Electron micrograph (X 10,000) of Atlantic salmon fibroblast cell. Note numerous myelin-like configurations, scattered ribosomes and virus-like particles within the membrane folds. These cells had been exposed to TV1 Weymouth isolate for 1 hour and then incubated at 12 degrees C for 3 days.

Pynocytosis of TV1 by the AS fibroblasts has resulted in caveola formation. The fusion of very numerous encytotic vesicles could account for the multiplicity of membrane profiles.

Plate 151

Detail of above cell showing virus-like particles of roughly hexagonal outline, approximately 60 nm in diameter. Magnification of X 80,000.

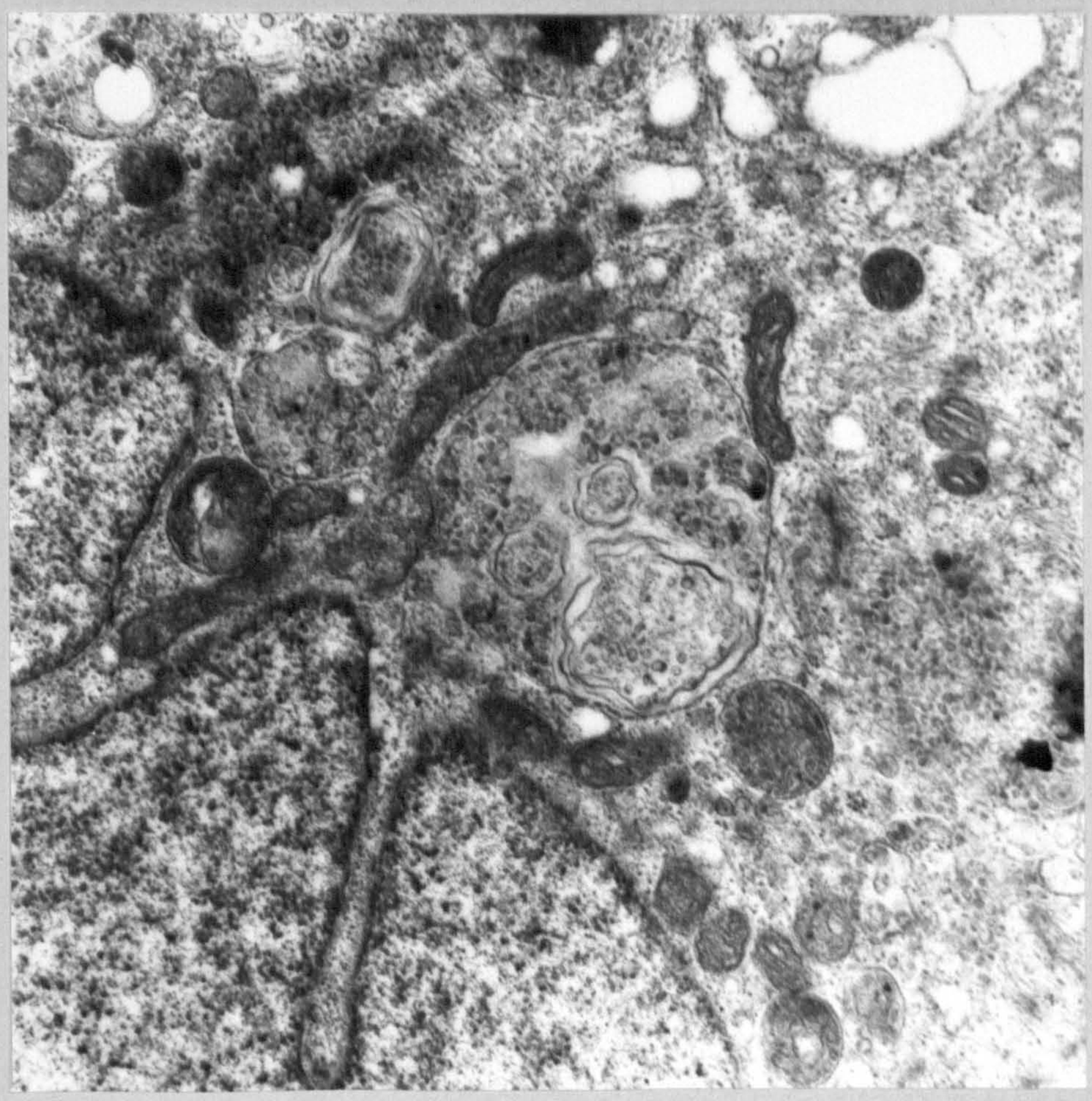

The MLO phage isolated from
Tellina tenuis digestive gland
by density gradient centrifugation
through sucrose

Plate 152 and 153

Negatively stained preparations
of virus using phosphotungstic
acid pH 7.2 as the stain.

These two micrographs were made
following two separate experiments
(1) using a homogenate from Kames
Bay, Millport Tellina and (2) using
West Sands, St. Andrews Tellina.

Top plate magnification of 85,000

Lower plate Magn. x 120,000

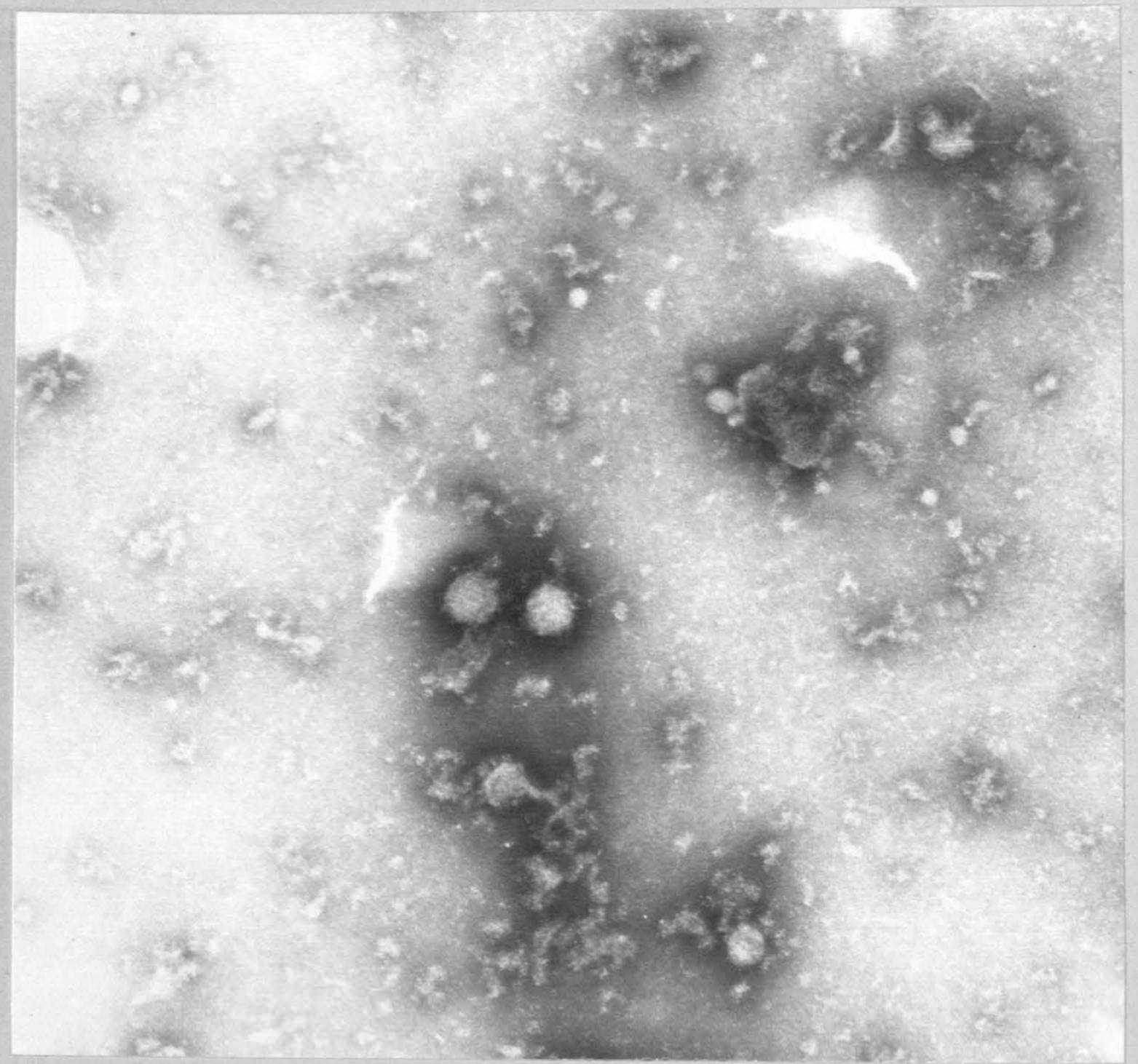

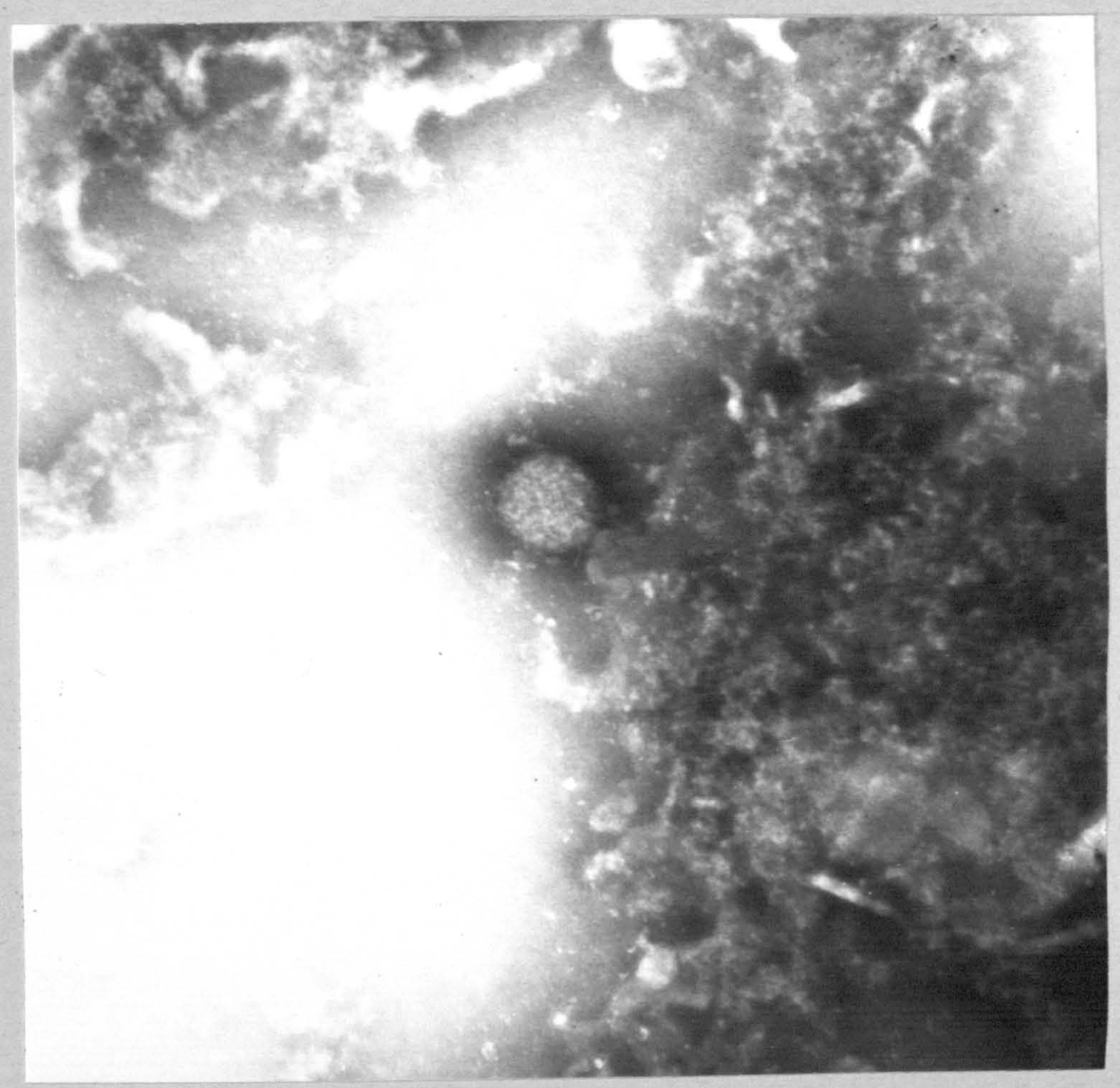

Isolation of MVT by Zonal Density Centrifugation in a Caesium Chloride Gradient

Plate 154

Tube A. The buoyant density of the lower band was 1.38, see also text figure 10. The Tellina extract was washed in this experiment with sodium deoxycholate, a detergent.

Plate 155

Tube B. The Tellina extract was unwashed. The buoyant density of the lower band was also 1.38 Particles seen by E.M. from the two, well defined bands are illustrated in Plates 156 and 157

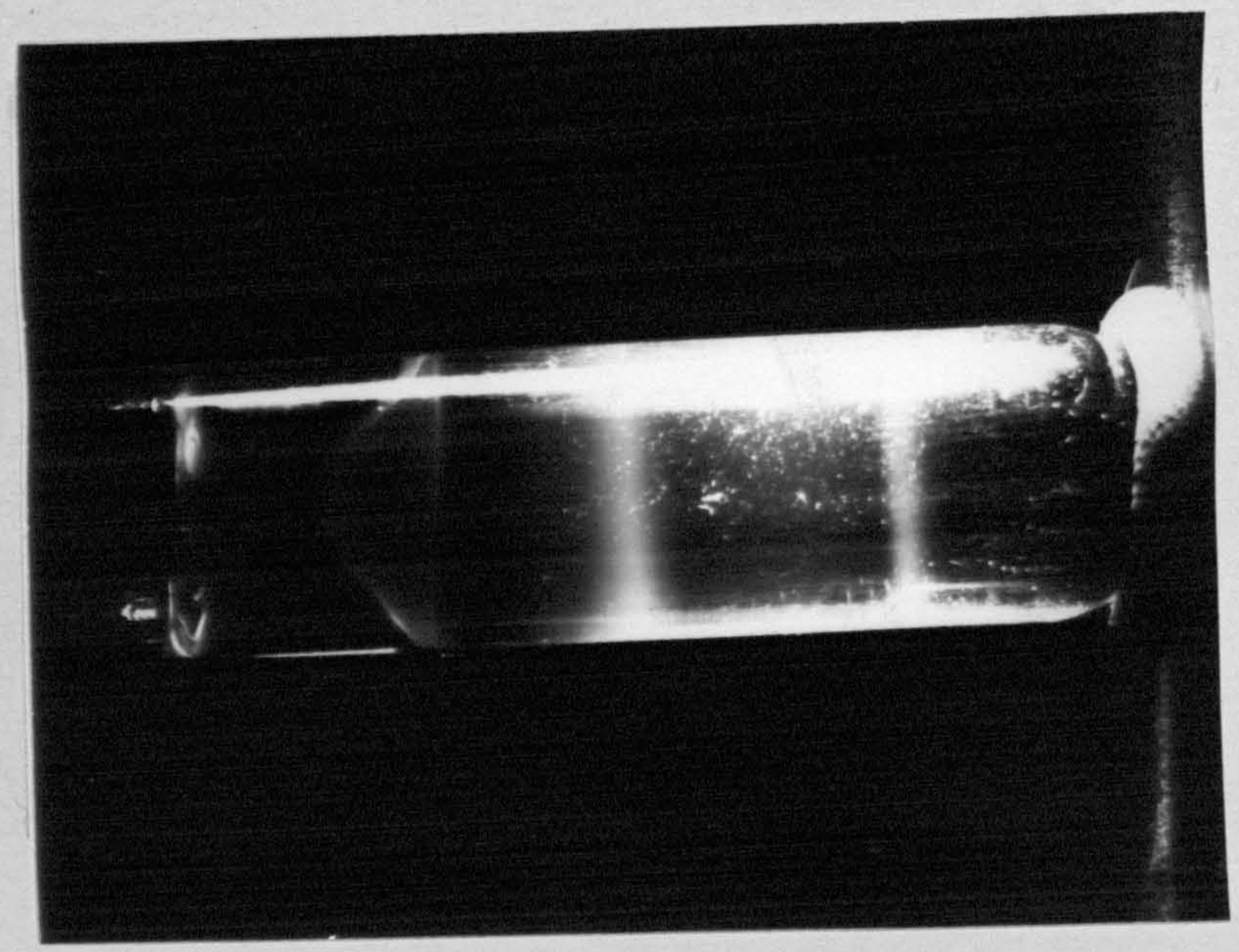

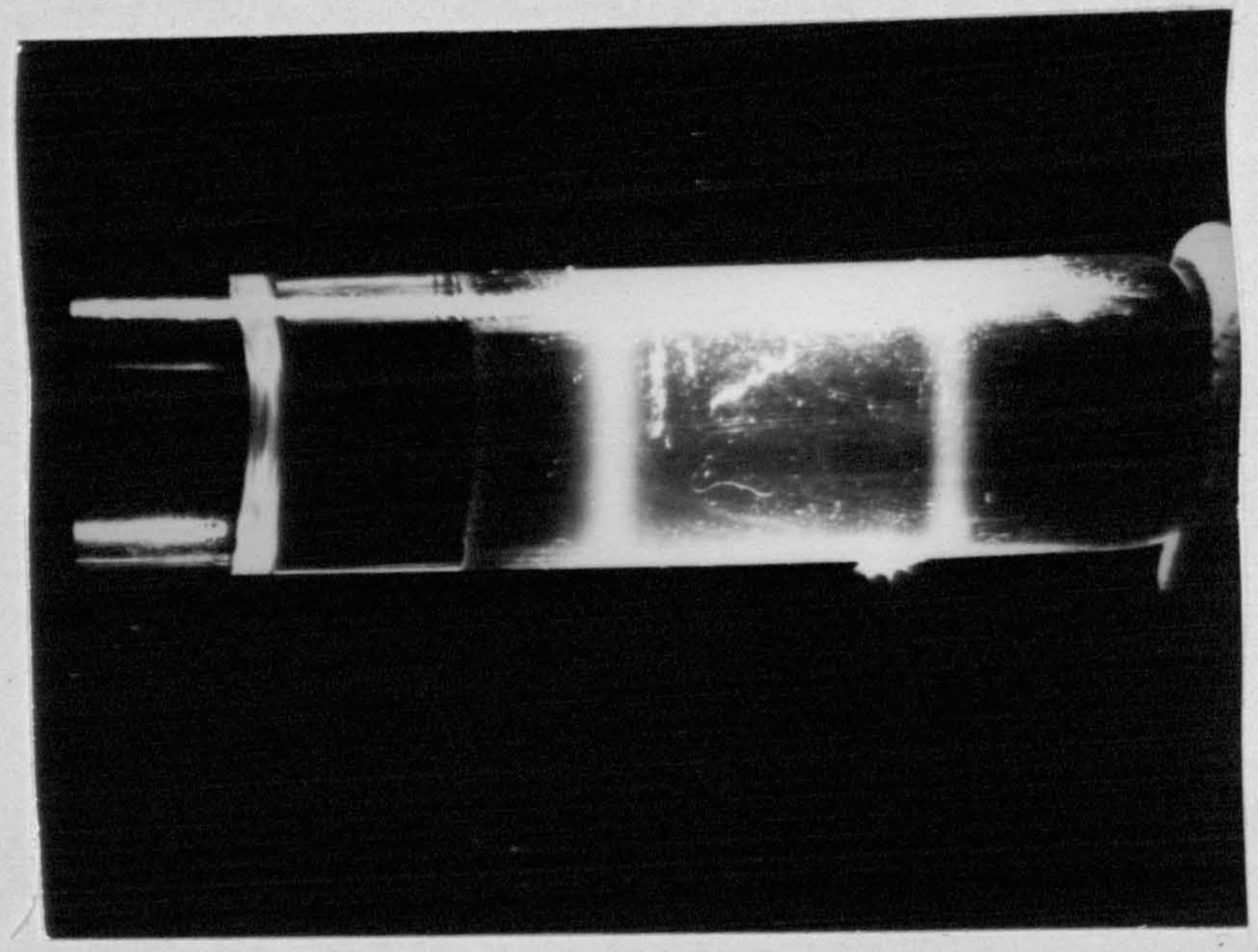

The centrifugation of digestive gland homogenates through CsCl gradients. Appearance of the bands after negatively staining

Plate 156

The previous plates illustrated the position of the bands within the tubes post centrifugation. This plate shows the top band and it appears to be made up of striated rod like structures having a diameter of 20-50 nm. Stained with PTA pH 7 Magn x 80,000

Plate 157

The particles forming the lower band appeared to be proteinaceous fragments of viral coat for the most part. Occassionally particles were found (inset) that were virus-like having a definite substructure and a diameter of 55 nm. Note the spherical nature of the particle. The buoyant density of these particles was estimated at 1.38
Stained with PTA pH 7, Magn. x 80,000
Inset magn. x 100,000

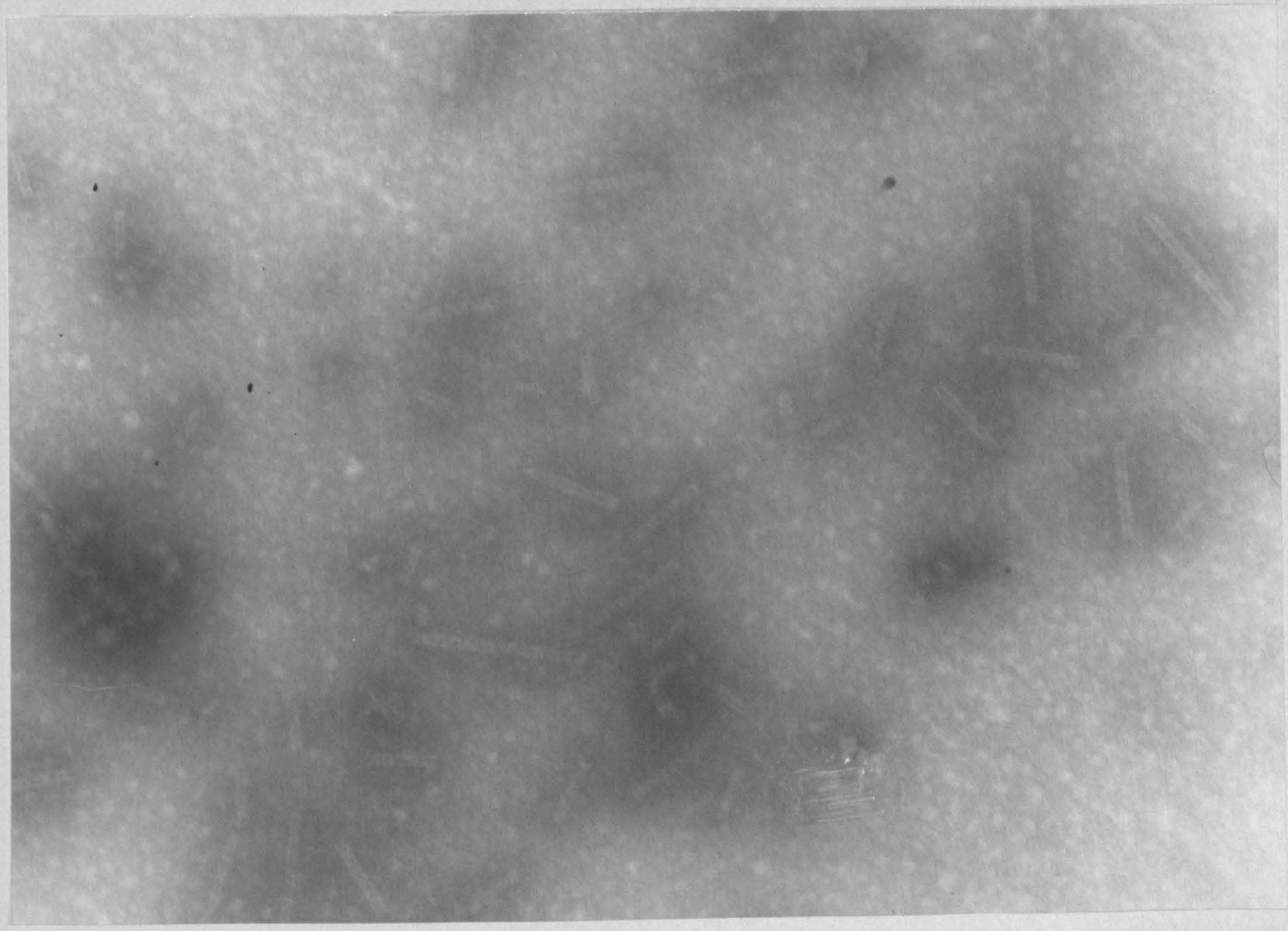

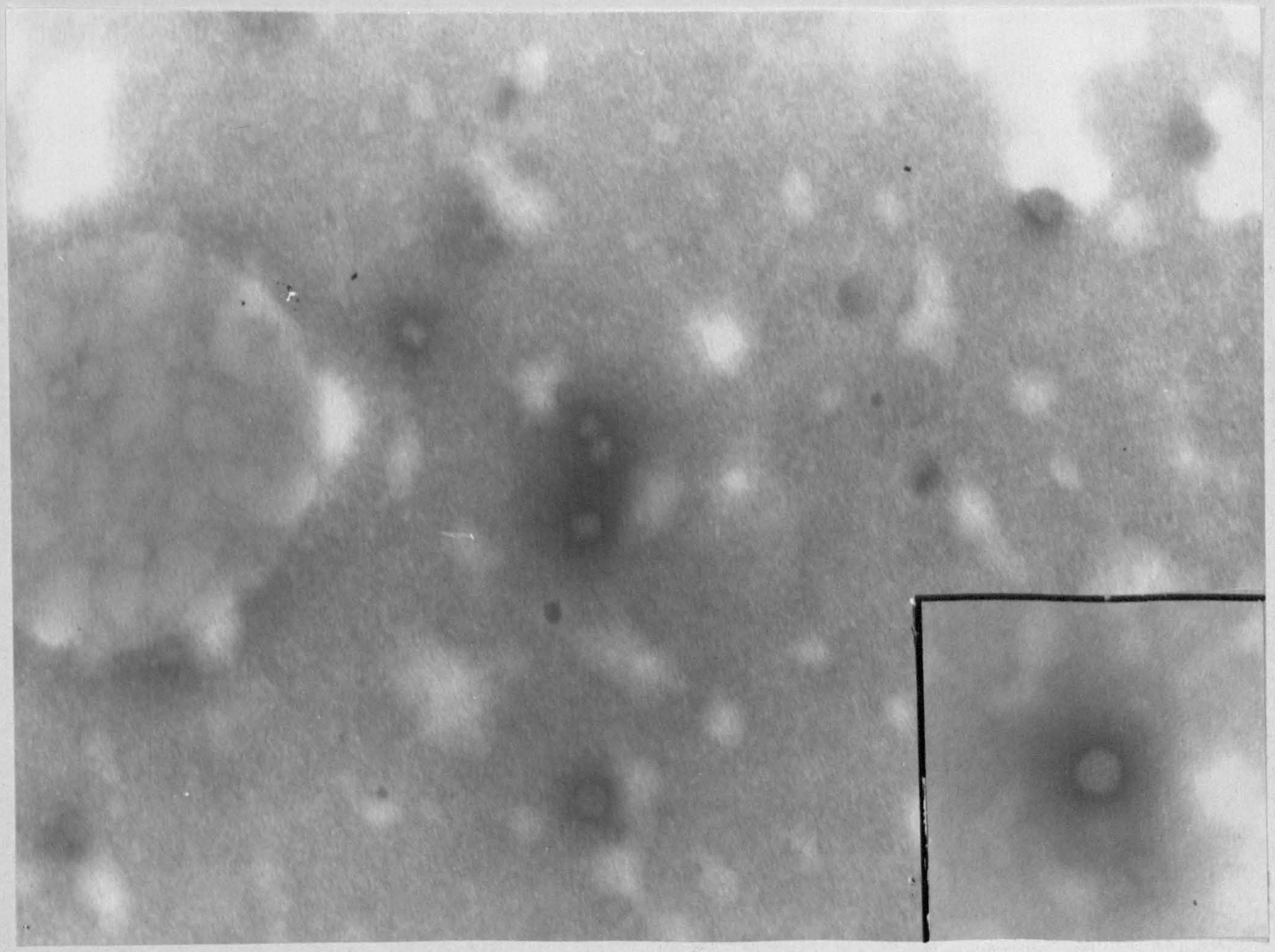

The appearance of the MLO as seen by negative staining

Plates 158 and 159

These spherules were frequently observed in preparations of the digestive gland post centrifugation through sucrose onto a caesium chloride "pad" (see also plates 160 and 161).

They closely resemble MLO prepared in a similar fashion (anderson, 1971) Hummeler et al (1965).

Note the capsular matrix composed of globular sub-units. The presence of striated rod like objects similar to those in plate 156 is also indicated.

Top plate Magn. x 80,000

lower plate Magn. x 100,000

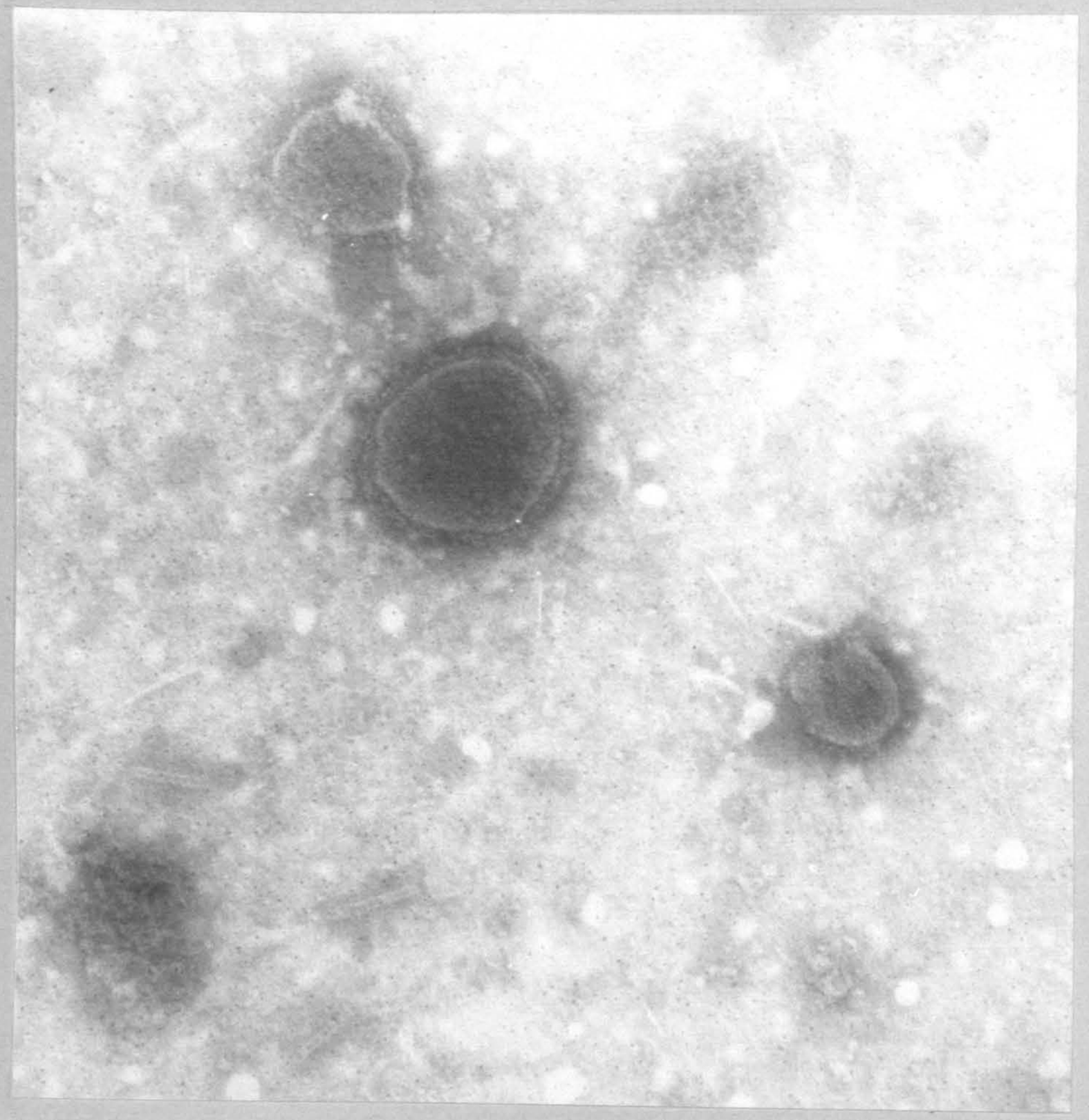

On the appearance of bands following centrifugation through sucrose density gradients of digestive gland extracts

Plates 160 and 161

Note the presence of an opalescent band at the interface between the sucrose solution and the caesium chloride "pad". This was extracted by puncturing the tube with a hypodermic needle and then examined by E.M. Particles of the type illustrated in Plate 152 and 153 were found.